EFFECTS OF NEUROMUSCULAR ACTIVITY COUPLED TO BDNF/TRKB SIGNALING ON THE EXOCYTOTIC PROTEINS MUNC18-1 AND SNAP-25 THROUGH NPKCE AND CPKCSSI

Anna Simó Ollé

UNIVERSITAT ROVIRA i VIRGILI

Effects of neuromuscular activity coupled to BDNF/TrkB signaling on the exocytotic proteins Munc18-1 and SNAP-25 through nPKCε and cPKCβI

ANNA SIMÓ I OLLÉ

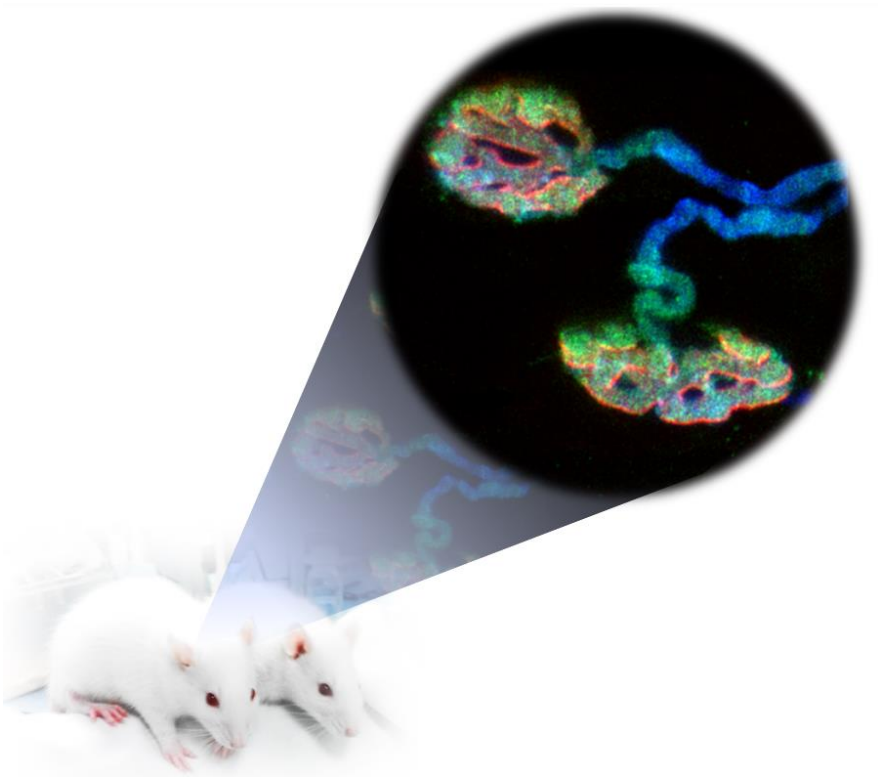

DOCTORAL THESIS 2017

Anna Simó i Ollé

Effects of neuromuscular activity coupled to BDNF/TrkB signaling on the phosphorylation of the exocytotic proteins Munc18-1 and SNAP-25 through nPKCε and cPKCβI

DOCTORAL THESIS

Thesis supervisors:
Dr. Maria Angel Lanuza
Dr. Neus Garcia
Prof. Josep Tomàs

Unitat d'Histologia i Neurobiologia
Departament de Ciències Mèdiques Bàsiques
UNIVERSITAT ROVIRA I VIRGILI
Reus 2017

UNIVERSITAT ROVIRA I VIRGILI
EFFECTS OF NEUROMUSCULAR ACTIVITY COUPLED TO BDNF/TRKB SIGNALING ON THE EXOCYTOTIC PROTEINS MUNC18-1 AND SNAP-25 THROUGH NPKCE AND CPKCSSI
Anna Simó Ollé

UNIVERSITAT ROVIRA I VIRGILI

UNITAT D'HISTOLOGIA I NEUROBIOLOGIA
DEPARTAMENT DE CIÈNCIES MÈDIQUES BÀSIQUES
FACULTAT DE MEDICINA I CIÈNCIES DE LA SALUT

Maria Angel Lanuza Escolano, professora titular del Departament de Ciències Mèdiques Bàsiques de la Universitat Rovira i Virgili.

Neus Garcia Sancho, professora titular del Departament de Ciències Mèdiques Bàsiques de la Universitat Rovira i Virgili.

Josep M. Tomàs Ferré, catedràtic del Departament de Ciències Mèdiques Bàsiques de la Universitat Rovira i Virgili.

FAIG CONSTAR que aquest treball, titulat ***"Effects of neuromuscular activity coupled to BDNF/TrkB signaling on the phosphorylation of the exocytotic proteins Munc18-1 and SNAP-25 through nPKCε and cPKCβI"***, que presenta Anna Simó i Ollé per a l'obtenció del títol de Doctor, ha estat realitzat sota la meva direcció al Departament de Ciències Mèdiques Bàsiques d'aquesta Universitat.

Reus, 7 de setembre de 2017

La directora i els codirectors de la tesi doctoral,

Dr. Maria Angel Lanuza Escolano | Dr. Neus Garcia Sancho | Prof. Josep Tomàs Ferré

UNIVERSITAT ROVIRA I VIRGILI
EFFECTS OF NEUROMUSCULAR ACTIVITY COUPLED TO BDNF/TRKB SIGNALING ON THE EXOCYTOTIC PROTEINS MUNC18-1 AND SNAP-25 THROUGH NPKCE AND CPKCSSI
Anna Simó Ollé

Agraïments

És difícil descriure els sentiments que m'envaeixen en aquests moments, ara que veig que estic al final d'aquesta etapa, i el que això significa. De fet, encara no en sóc conscient. Sentiments d'alegria, satisfacció, emoció, i d'alguna manera també de tristesa i nostàlgia, ara que sento que aquesta etapa és a punt d'arribar a la seva fi. M'enduc moltes coses bones d'aquests anys, ha sigut i encara està essent una etapa molt enriquidora, a tots nivells.

Des del primer moment aquest projecte ha estat un repte tant a nivell professional com personal. Ha esdevingut un camí ple de vivències, on els obstacles no han faltat, tant a dins com a fora del laboratori, però que mica en mica, i gràcies a l'ajuda i suport de totes les persones que m'envolten, s'han pogut anar superant, fins arribar al punt culminant d'aquest repte. Se'm fa difícil descriure el que ha significat per mi aquesta etapa, però el que sí tinc clar és que ha esdevingut un gran creixement personal, i que n'he tret moltíssimes coses bones, i sobretot a nivell humà. Em sento orgullosa de la feina feta, i encara més tenint en compte les condicions on sovint han incrementat els obstacles, que han fet el camí encara més distret. Al final tot se supera, sempre amb constància i sobretot paciència, aquests obstacles se superen i fan que al final del camí la sensació de satisfacció encara sigui més gran. Però sobretot el que tinc és una sensació d'infinit agraïment per moltes persones que m'han ajudat i acompanyat durant aquest camí, i que intentaré plasmar en les properes línies.

Començaré per aquelles persones que van confiar en mi des del primer moment, obrint-me les portes per iniciar aquest camí tant complex i meravellós que és la neurociència. Agraïda per tot el suport necessari que m'han proporcionat al llarg d'aquests anys i per l'ajut en poder convertir aquest projecte en un una realitat. Sempre els hi estaré agraïda per haver-me ensenyat, ajudat i guiat, per l'oportunitat de poder treballar i aprendre tant en aquesta unitat. Mil gràcies.

En primer lloc, agrair al Dr. Josep Tomàs per acceptar-me al seu grup i confiar en mi des de l'inici fins al final. Per estar sempre disposat a ajudar i escoltar quan ha fet falta. És un exemple a seguir de constància, de capacitat per afrontar i resoldre amb un rigor científic admirable tots els reptes que el camí va presentant.

A la Dra. Maria Àngel Lanuza, per confiar i obrir-me les portes des de l'inici en aquesta unitat, pel suport incondicional que m'ha proporcionat, pel coneixement que dia a dia ens ha transmès, pels consells, per guiar-me i ajudar-me durant tot aquest camí. Sobretot també per la relació que més enllà de l'àmbit professional ha esdevingut també a nivell personal.

A la Dra. Neus Garcia, per confiar i obrir-me les portes de de l'inici, sempre amb un somriure i on la relació tant personal com professional ha sigut impecable. Per ajudar-me en tot sempre que ho he necessitat, pel coneixement transmès i suport al llarg d'aquest camí.

A la Dra. Fenoll, pel somriure que ens ha regalat dia rere dia, per la seva amabilitat en tot moment, i per l'ajuda acompanyada de coneixement i bones paraules que sempre han sigut positives i ens han arrancat un somriure.

Al Dr. Manel Santafé, pel suport des de l'inici, pel coneixement que m'ha transmès, per les converses tingudes des de l'inici i ajut en tot el que he necessitat.

Al Dr. Nicolau Ortiz, per ajudar-me sempre en tot el que he necessitat, pels coneixements i debats enriquidors que hem compartit durant tots aquests anys.

A la Dra. Marta Tomàs, també pel suport sempre acompanyat d'un somriure i bones paraules cada moment que hem compartit, el qual sempre ha sigut positiu i enriquidor.

A la Teresa, que tot i malauradament haver compartit poc temps des del principi em va obrir les portes amb un somriure i oferir ajuda en tot.

A la resta de companys fisios, Marc, Ramon i Irina per la cooperació i alegria que heu aportat en aquest laboratori. Moltes gràcies!

A la Sílvia, per l'ajuda que en tot moment ens has donat, per les converses i la relació també immillorable tant a nivell professional com personal.

Agrair a tota la gent de l'estabulari, l'Amparo, la Celeste, el Juan i la Esperanza pel manteniment de les ratetes que han esdevingut una part tant important d'aquesta recerca. També agrair a tota la secretaria del Departament de ciències mèdiques bàsiques, la Montse, la Imma, l'Antonio i la Núria. Per tot l'ajut en la burocràcia que sovint per nosaltres se'ns fa tant pesada i insòlita, pel suport cada cop que hem pujat al vostre despatx.

Agrair infinitament a tot l'equip de companys de la unitat, l'Histoteam, on sense cap mena de dubte sense ells aquest camí hagués sigut molt diferent. Gràcies a vosaltres el bon record que m'enduc ara i sempre serà inoblidable, sou el millor grup que mai haguera pogut imaginar, mil gràcies a tots.

A l'Erica, absolutament per tot, per l'ajuda, pels consells, per la serenor i constància demostrats en cada moment per superar tots els entrebancs que ens han acompanyat, per ser la meva mestra des del principi. Per l'amistat, per les hores de riures, pels cafès acompanyats dels nostres croissants de xocolata blanca, per les tristeses i alegries compartides...mil gràcies per tot.

A la Laura, per l'alegria i electricitat que ens has aportat cada dia compartit. Ets una persona meticulosa, on dia a dia has demostrat que amb esforç i constància tot es pot fer, però sobretot amb un somriure i alegria. Per les excursions compartides, pel Montsant, pel Pedraforca, pels cims que ens queden!

Al Víctor, per la serenor que t'acompanya, pel teu coneixement, per la manera admirable d'afrontar els problemes, amb rigor científic, sempre positiu, per la calma que transmets i esdevé tant important en aquest món de la ciència on

la paciència hi té un paper clau. Per l'ajut i suport incondicional, pel teu somriure i les teves bones paraules que sempre ens han acompanyat. Mil gràcies per tot!

A la Laia, per tots els moments compartits en aquesta unitat, per l'ajuda també incondicional en tot moment des de la teva arribada, on ens vas portar aire fresc i ràpidament vas formar part de nosaltres. Gràcies per ajudar-me en tot sempre que ho he necessitat. Per la teva alegria, coneixement, positivisme i aquest punt àcid que tant m'agrada, no perdis aquest esperit!

Als Randoms, on sense ells tot haguera sigut molt diferent. Al Pablo, on des del inici em vas acollir amb els braços oberts i un gran somriure. Pel estar sempre disposat a donar un cop de mà, pel gran científic i millor persona, tant especial i bona en tots els sentits. A la Simona, per sempre ser-hi amb un somriure, disposada a ajudar, per l'amistat que des de l'inici m'has demostrat i poc a poc hem anat forjant. Per les hores compartides i les que queden, per cada moment que m'enduc i recordo amb alegria creuant-nos al passadís, mil gràcies. Al Jordi Blanco, per l'alegria que ens has aportat cada dia que entres per la porta, on des de lluny et sentim. Pel teu somriure, el teu positivisme, coneixement, rigor científic, el suport i ajut en tot moment des del primer dia. A la Nohora, Ivan, Cintia, Pia, Jose, Lucía, Gemma, Laia, Núria, Pol, Fiona, Laura, Guille, Albert, Jesús, Júlia... tots heu estat un pilar fonamental durant tot aquest temps. Pels dinars compartits, esmorzars, debats, alegries, somriures, festes, sopars compartits. Perquè compartim un mateix objectiu i m'heu fet sentir sempre acollida i com a casa. Gràcies a tots vosaltres aquesta etapa encara ha sigut més meravellosa del que mai haguera pogut imaginar, sou una gran família.

A la Dra. Anna Sanchez, Nita, per sempre ser-hi, encara que últimament ens separin milers de quilòmetres. Pel teu suport, per tot el que m'has aportat i m'aportes en aquesta vida. Has demostrat ser una gran científica i molt millor persona, infinitament agraïda.

A la Núria, què dir de tu...mil gràcies per tot, em sento molt afortunada de tenir-te aprop, des que en prou feines teníem força per aixecar la raqueta del terra. Ets un puntal importantíssim a la meva vida.

Al Guillem, per les hores de suport i acolliment fora del laboratori, als riures i mil moments compartits. A l'Alfons, per les hores i hores de tertúlies científiques tant enriquidores. Al Llem, Joanet, Ferri, Joan, Edu, Salvador, Laia, Sergi, Isabel, Víctor, Pere, Roger, Esteve, Mar, Àlex, Dani, Karpa, Padrí, Vicenç Pituka, Romà, David, Hèctor, al Fabi... perquè sou i sereu sempre un pilar clau a la meva vida, em sento molt orgullosa de tenir-vos aprop. A tot els Desgavellats, Iban, David, Jordi, Montse...les hores a l'escenari han ajudat molt! I finalment al David, on al final d'aquesta etapa t'he tingut dia a dia tant als bons com als mals moments, oferint sempre el millor de tu. Moltíssimes gràcies per tot.

Finalment agrair a la meva família tot el suport incondicional que sempre m'heu proporcionat. Sense vosaltres res haguera tingut sentit, ni haguera arribat on sóc ara. A la meva mare, per ser-hi sempre, oferint a canvi de res tota l'ajuda, suport, alegria, consells, bones paraules, ajudar-me a superar tots els entrebancs d'aquesta vida. Gràcies per aguantar-me en els bons i mals moments. Al meu germà Jordi i la Núria, també sense vosaltres res haguera tingut sentit ni haguera sigut tant fàcil. Gràcies per cada moment compartit, per les excursions, dinars, ajuda i suport incondicional, estic molt orgullosa de tenir-vos aprop. Gràcies per regalar-me el fillol més guapo que es pot imaginar, el petit Jan, que acaba d'arribar en aquest món, donant aire fresc i obrint un nou horitzó de somnis i il·lusions a la família. I finalment al Cim i a l'Idefix, per l'amor incondicional. Aquesta tesi us la dedico a tots vosaltres, mama, Jordi, Núria i Jan.

UNIVERSITAT ROVIRA I VIRGILI
EFFECTS OF NEUROMUSCULAR ACTIVITY COUPLED TO BDNF/TRKB SIGNALING ON THE EXOCYTOTIC PROTEINS MUNC18-1 AND SNAP-25 THROUGH NPKCE AND CPKCSSI
Anna Simó Ollé

"Nothing in life is to be feared, it is only to be understood. Now is the time to understand more, so that we may fear less".

Marie Curie

UNIVERSITAT ROVIRA I VIRGILI
EFFECTS OF NEUROMUSCULAR ACTIVITY COUPLED TO BDNF/TRKB SIGNALING ON THE EXOCYTOTIC PROTEINS MUNC18-1 AND SNAP-25 THROUGH NPKCE AND CPKCSSI
Anna Simó Ollé

INDEX

i. INDEX OF FIGURES

i. Index of figures

UNIVERSITAT ROVIRA I VIRGILI
EFFECTS OF NEUROMUSCULAR ACTIVITY COUPLED TO BDNF/TRKB SIGNALING ON THE EXOCYTOTIC PROTEINS MUNC18-1 AND SNAP-25 THROUGH NPKCE AND CPKCSSI
Anna Simó Ollé

ii. INDEX OF TABLES

iii. ABBREVIATIONS

aa	Amino acid
ACh	Acetylcholine
AChE	Acetylcholinesterase
AChR	Acetylcholine receptor
AL	Activation loop
ALS	Amyotrophic lateral sclerosis
AP	Action potential
aPKC	Atypical protein kinase C
APS	Ammonium persulfate
ARIA	AChR-inducing activity
ATP	Adenosine triphosphate
AZ	Active zone
BDNF	Brain-derived neurotrophic factor
BL	Basal lamina
BSA	Bovine serum albumin
Ca^{2+}	Calcium ion
CaMb	Calmodulin binding domain
CAPS	Calcium-dependent activator protein for secretion
CATCHR	Complex associated with tethering containing helical rod
CCP	Clathrin-coated pits
Cdk5	Cyclin-dependent kinase 5
ChAT	Choline acetyltransferase
CME	Clathrin mediated endocytosis
CMS	Congenital myasthenic syndrome
CNS	Central nervous system
cPKCβI	Classical protein kinase C beta I
Cplx	Complexin
Ctrl	Control
C1 - C2	Calcium-binding domains

DAG	Diacylglycerol
DMSO	Dimethyl sulfoxide
ECL	Enhanced chemiluminescence
EDTA	Ethylenediamine tetraacetic acid
EE	Early endosome
EI	Endocytic intermediates
EPP	End-plate potential
FGF	Fibroblast growth factor
GAPDH	Glyceraldehyde-3-Phosphate Dehydrogenase
H_{abc}	N-terminal regulatory domain with three α-helixes
HM	Hydrophobic motif
HRP	Horseradish peroxidase
Hz	Herz
Ig1 - Ig2	Immunoglobulin-like domain
IHC	Immunohistochemistry
IP_3	Inositol trisphosphate
K^+	Potassium ion
kDa	Kilodalton
LAL	Levator Auris Longus
LE	Late endosome
LRR	Leucine-rich repeat
M	Molar
mAChR	Muscarinic acetylcholine receptor
MAPK	Mitogen-activated protein kinase
MARCKs	Myristoylated alanine-rich C-kinase substrate
ml	Milliliter (10^{-3} l)
MMP-7	Matrix metalloproteinases
MN	Motoneuron
MSC	Myelinating Schwann cell
Munc13	Mammalian Unc-13
Munc18-1	Mammalian uncoordinated-18 protein

iii. Abbreviations

mV	Millivolt (10^{-3} v)
MVB	Multivesicular body
MW	Molecular weight
Na^+	Sodium ion
nAChR	Nicotinic acetylcholine receptor
NGF	Nerve growth factor
Nm	Nanometer (10^{-9} m)
NMJ	Neuromuscular junction
NMSC	Non-myelinating Schwann cell
nPKCε	Novel protein kinase C epsilon
NSF	N-ethylmaleimide-sensitive factor
NT	Neurotransmitter
NT-3 – NT-4	Neurotrophin-3 and 4
O/N	Overnight
PBS	Phosphate buffer saline
PC	Protein convertase
PDK1	3-phosphoinositide dependent kinase 1
PE	Phorbol ester
PHLPP	PH domain and leucine rich repeat protein phosphatase
PIP_2	Phosphatidylinositol 4,5-bisphosphate
PIP_3	Phosphatidylinositol 3,4,5-trisphosphate
PI3K	Phosphatidylinositol-4,5-bisphosphate 3-kinase
PKA	Protein kinase A
PKC	Protein kinase C
PLCγ	Phospholipase C gamma
PM	Plasma membrane
PMA	Phorbol 12-myristate 13-acetate
PMSF	Phenylmethanesulfonyl fluoride
PNS	Peripheral nervous system
PP2A	Protein phosphatase 2
PS	Phosphatidylserine

PVDF	Polyvinylidene difluoride
P75^{NTR}	p75 neurotrophin receptor
P-value	Level of statistical significance
RACK	Receptor for activated C-kinase
RIM	Rab3-interacting molecule
RRP	Readily releasable pool
SBL	Reduced sample buffer loading
SC	Schwann cell
SDS	Sodium dodecyl sulfate
SDS –PAGE	SDS-polyacrylamide gel electrophoresis
SEM	Standard error of the mean
Ser	Serine
SM	Sec1/Munc18 family of proteins
SMA	Spinal muscular atrophy
SNAP-25	Synaptosome associated protein of 25-kDa
SNARE	Soluble NSF Attachment Protein Receptor
SPSS	Statistical Package for the Social Sciences
St	Electrical stimulation without muscle contraction
St + contraction	Electrical stimulation with muscle contraction
SV	Synaptic vesicle
Syb	Synaptobrevin
Syt1	Synaptotagmin-1
TBE	Tribromoethanol
TBS	Tris-buffered saline
TBST	Tris-buffered saline 0.1% Tween 20
TEMED	N, N, N',N'-tetramethylethylenediamine
Thr	Threonine
TM	Turn motif
TMR	Terminal transmembrane region
TNF	Tumor necrosis factor
TRICT	Tetramethyl rhodamine iso-thiocyanate

iii. Abbreviations

Trk	Tropomyosin-related kinase receptor
TrkB.FL	TrkB full length receptor
TrkB.T1 – TrkB.T2	TrkB truncated isoforms
tSC	Terminal Schwann cell
Tyr	Tyrosine
t-SNARE	Target membrane –SNARE
v-SNARE	Vesicle SNARE
VAChT	Vesicular acetylcholine transporter
VAMP	Vesicle-associated membrane protein
VGCC	Voltage-gated calcium channel
VGSC	Voltage-gated sodium channel
vs	Versus
V1 - V5	PKC variable regions
v-SNARE	Vesicle-SNARE
v/v	volume/volume
w/v	weight/volume
α-BTX	α-bungarotoxin
βIV5-3	V5-containing cPKCβI inhibitor peptide
εV1-2	V1-containing nPKCε inhibitor peptide
µg	Microgram (10^{-6} g)
µl	Microliter (10^{-6} l)
µM	micromolar (10^{-6} M)
µ-CgTx- GIIIB	µ-conotoxin GIIIB
47/TrkB	TrkB receptor antagonist

ABSTRACT

At the neuromuscular junction (NMJ) synapse, several signaling pathways coordinate pre-, post-synaptic responses and associated glial cells. The relation between these signaling pathways modulates the pool of synaptic vesicles leading to neurotransmission. Moreover, PKC phosphorylates several molecules of synaptic vesicle exocytotic apparatus responsible to the regulation of neurotransmitter release. Munc18-1 and SNAP-25 are two PKC substrates that play a key role in the exocytotic machinery. In addition, PKC is modulated by presynaptic and postsynaptic activity in skeletal muscles. Nevertheless, it is still unknown which PKC regulates these key molecules in the NMJ. cPKCβI and nPKCε are exclusively located at the nerve terminal of the NMJ and are regulated by synaptic activity. In addition, muscle contraction through BDNF/TrkB has an important impact on these PKC isoforms. Therefore, this thesis is aimed to determine the expression, location and regulation by the PKC-activators calcium and phorbol esters (PMA) of Munc18-1 and SNAP-25 and their phosphorylated forms in the skeletal muscle. Also, to study whether Munc18-1 and SNAP-25 phosphorylation are affected by (1) synaptic activity and muscle contraction *per se*; and (2) nPKCε, cPKCβI and BDNF/TrkB signaling in a neuromuscular activity-dependent manner.

Main results, obtained by Western blot analysis and confocal microscopy, show that Munc18-1 and SNAP-25 are expressed and phosphorylated in basal conditions in the skeletal muscle, predominantly in the membrane fraction, with Munc18-1 being located at the nerve terminal. Munc18-1 and SNAP-25 phosphorylation are modulated by calcium, PMA, synaptic activity and enhanced by nPKCε. Otherwise, cPKCβI and BDNF/TrkB signaling pathway regulates Munc18-1 but not SNAP-25 phosphorylation. Finally, muscle contraction downregulates these proteins to reach a basal state.

In conclusion, these results provide a mechanistic insight into how Munc18-1 and SNAP-25 phosphorylation is regulated to achieve the extraordinary precision and plasticity of neurotransmission.

RESUM

A la sinapsis de la unió neuromuscular (NMJ), diverses vies de senyalització coordinen les respostes pre-/postsinàptiques i les cèl·lules glials associades. La relació entre aquestes vies modula les vesícules sinàptiques que regulen la neurotransmissió. A més, la PKC fosforila diverses molècules de l'aparell exocitòtic responsable d'aquesta regulació. Munc18-1 i SNAP-25 són substrats de PKC que juguen un paper clau en la maquinària exocitòtica. A més, la PKC està modulada per l'activitat pre-/postsinàptica al múscul esquelètic. No obstant això, encara es desconeix quines isoformes de PKC regulen aquestes molècules clau en la NMJ. cPKCβI i nPKCε es troben exclusivament en el terminal nerviós de la NMJ i estan regulades per l'activitat sinàptica. A més, la contracció muscular a través de BDNF/TrkB té un impacte important en aquestes isoformes. Amb tot, l'objectiu d'aquesta tesi és determinar l'expressió, localització i regulació pels activadors de PKC calci i èsters de forbol (PMA) de Munc18-1 i SNAP-25 i la seva fosforilació en el múscul esquelètic. A més, estudiar si aquestes fosforilacions estan afectades per (1) activitat sinàptica i contracció muscular *per se*; i (2) nPKCε, cPKCβI i la senyalització BDNF/TrkB de manera dependent d'activitat neuromuscular.

Els principals resultats, obtinguts mitjançant anàlisi Western blot i microscòpia confocal, mostren que Munc18-1 i SNAP-25 s'expressen i fosforilen en condicions basals en el múscul esquelètic, predominantment a la fracció membrana, essent Munc18-1 localitzat al terminal nerviós. La fosforilació de Munc18-1 i SNAP-25 és modulada per calci, PMA, activitat sinàptica i és promoguda per nPKCε. D'altra banda, cPKCβI i la senyalització BDNF/TrkB regulen la fosforilació de Munc18-1 però no la de SNAP-25. Finalment, la contracció muscular regula negativament aquestes proteïnes per assolir un estat basal.

En conclusió, aquests resultats proporcionen una visió mecànica de com Munc18-1 i SNAP-25 es regulen per aconseguir l'extraordinària precisió i plasticitat de la neurotransmissió.

RESUMEN

En la sinapsis de la unión neuromuscular (NMJ), varias vías de señalización coordinan las respuestas pre-/postsinápticas y las células gliales asociadas. La relación entre estas vías modula las vesículas sinápticas que regulan la neurotransmisión. Además, la PKC, modulada por actividad presináptica y postsináptica en el músculo esquelético, fosforila varias moléculas del aparato exocitótico responsable de esta regulación. Munc18-1 y SNAP-25 son sustratos de PKC que juegan un papel clave en la maquinaria exocitótica. Sin embargo, todavía se desconoce qué isoforma de PKC regula estas moléculas clave en la NMJ. cPKCβI y nPKCε se encuentran exclusivamente en el terminal nervioso de la NMJ y están reguladas por actividad sináptica. Además, la contracción muscular a través de BDNF/TrkB tiene un impacto importante en estas isoformas. Así mismo, el objetivo de esta tesis es determinar la expresión, localización y la influencia de los activadores de PKC calcio y ésteres de forbol (PMA) de Munc18-1 y SNAP-25 y su fosforilación en el músculo esquelético. Además, estudiar si dichas fosforilaciones están afectadas por (1) actividad sináptica y contracción muscular *per se*; y (2) nPKCε, cPKCβI y la señalización BDNF/TrkB de manera dependiente de actividad neuromuscular.

Los principales resultados, obtenidos mediante análisis Western blot y microscopia confocal, muestran que Munc18-1 y SNAP-25 se expresan y fosforilan en condiciones basales en el músculo esquelético, predominantemente en la fracción membrana, localizándose Munc18-1 en el terminal nervioso. La fosforilación de Munc18-1 y SNAP-25 se modula por calcio, PMA, actividad sináptica y es promovida por nPKCε. Por otra parte, cPKCβI y la señalización BDNF/TrkB regulan la fosforilación de Munc18-1 pero no de SNAP-25. Finalmente, la contracción muscular regula negativamente estas proteínas hacia un estado basal.

En conclusión, estos resultados proporcionan una visión mecánica de cómo Munc18-1 y SNAP-25 se regulan para lograr la extraordinaria precisión y plasticidad de la neurotransmisión.

UNIVERSITAT ROVIRA I VIRGILI
EFFECTS OF NEUROMUSCULAR ACTIVITY COUPLED TO BDNF/TRKB SIGNALING ON THE EXOCYTOTIC PROTEINS MUNC18-1 AND SNAP-25 THROUGH NPKCE AND CPKCSSI
Anna Simó Ollé

I. INTRODUCTION

UNIVERSITAT ROVIRA I VIRGILI
EFFECTS OF NEUROMUSCULAR ACTIVITY COUPLED TO BDNF/TRKB SIGNALING ON THE EXOCYTOTIC PROTEINS MUNC18-1 AND SNAP-25 THROUGH NPKCE AND CPKCSSI
Anna Simó Ollé

1. NEUROMUSCULAR JUNCTION AS A MODEL OF CHEMICAL SYNAPSES

The nervous system relies on the transmission of electrically or chemically encoded information, which propagates along an axon and is encoded as rapid changes of the membrane potential (action potentials, APs), through the synapses. In the nervous system, there are two major types of synaptic connections, the electrical and the chemical synapses. Although electrical synapses play several important roles in the nervous system, allowing the passive and direct flow of electrical current from one to another neuron, chemical synapses are far more numerous and provide the bulk of synaptic transmission.

Chemical synapses are specialized cell-to-cell junctions where nerve impulse is transmitted in one direction, from one neuron to another or from one neuron to a non-neuronal cell such as those in muscles or glands. Chemical synapses are made up of two domains or components: the presynaptic domain and the postsynaptic domain separated by an ultra-thin region known as the synaptic cleft (Palay and Palade, 1955). At such synapses, AP signal triggers the transmission mediated by neurotransmitters (NTs) that are rapidly secreted into the synaptic cleft from the presynaptic terminal to the postsynaptic cell (Burns and Augustine, 1995). Proteins in the presynaptic domain are geared towards the synthesis, storage and release of NT through synaptic vesicles (SVs) (Becherer and Rettig, 2006); while proteins in the postsynaptic domain are mainly oriented to detect and respond to the presence of NT (Kim and Sheng 2004). The presynaptic domain contains hundreds of SVs, early endosomal structures and other organelles (Südhof, 2004). Under electron microscopy, these SVs can be observed as small (40-50nm) electron dense rings which appear in clusters (Bodian, 1970; Südhof, 2004). Presynaptic domain is limited by the plasma membrane (PM) of the motoneuron (MN) in the nerve terminal; at the same time, the PM of the postsynaptic cell encloses the postsynaptic domain. Both are in close opposition to each other and separated by the synaptic cleft. The presynaptic PM has electron

dense bands named active zones (AZ) (Ahmari and Buchanan 2000), which have a high density of proteins that bind SVs to the presynaptic membrane to mediate synaptic vesicle fusion, allowing NTs to be released reliably and rapidly when an AP arrives. The AZs are in close opposition to another electron dense structure, the post synaptic density, bound to postsynaptic membrane, it contains receptors and kinases specialized in transducing signals received from the presynaptic domain (MacGillavry et al. 2011).

Neuromuscular junction (NMJ) is a specific peripheral tripartite synapse between motor nerve terminals, skeletal muscle fibers and terminal Schwann cells (tSCs) that cover the nerve-muscle contact. This kind of synapse is relatively simple and accessible to experimentation (Sanes and Lichtman, 2001). Much of the current understanding of the synaptic organization derives from studies of the vertebrate skeletal NMJ, which has a number of experimentally advantageous features. These include large size, relative isolation, robust transmission and possibility of accurate regeneration following injury (Patton 2003). Moreover, it is affected by several inherited and acquired neurological diseases (Kandel et al. 2012), being an ideal target to study and contribute to find new therapies related to muscular diseases.

The adult vertebrate skeletal NMJ has served as a model of the first rigorous scientific study where the chemical synaptic transmission was demonstrated (Dale et al. 1936). Soon thereafter, this synapse was used to show that the release of its NT, acetylcholine (ACh), is quantal and vesicular (Katz, 1996). Subsequently, the first NT receptor to be purified and then molecularly cloned was the nicotinic acetylcholine receptor (nAChR) (Duclert and Changeux, 1995). Since then, the NMJ has served as a model from which has emerged much of our understanding of the fundamental nature of synaptic transmission (Katz, 1996).

The NMJ is a highly specialized cholinergic synapse, allowing the signaling between muscle fiber and nerve cell, necessary for skeletal muscle function (Campanari et al., 2016). NMJs efficiently convert the electrical impulses of the

MNs into APs in the juxtaposed muscle fiber, a process that depends on (1) the release of large quantities of ACh molecules by the presynaptic MN as well as (2) the density of nAChRs clustering on the postsynaptic muscle membrane (Ogata, 1988; Slater, 2008; Zong and Jin, 2013).

Abnormalities in NMJ formation, maintenance, or function result in neurological disorders, including myasthenia gravis and related disorders (Keesey, 2004), congenital myasthenic syndromes (CMSs), (Engel et al. 2003), and MN diseases such as amyotrophic lateral sclerosis (ALS) and spinal muscular atrophy (SMA) (Murray et al. 2010). Therefore, a greater knowledge of the molecular mechanisms underlying the structure and function of NMJ will potentially contribute to the development of targeted therapeutic approaches.

2. STRUCTURE OF NEUROMUSCULAR JUNCTION

The NMJ is composed by three different cell types: motoneuron, muscle fiber and Schwann cell (Ogata, 1988) (**Figure 1**). At the same time, it is possible to distinguish between pre- and postsynaptic component, the space between both and the glial cell:

1. **Presynaptic component:** composed by the nerve terminal of the nerve fiber. It is responsible for the synthesis, storage and release of acetylcholine (ACh).
2. **Synaptic cleft:** is the space between pre- and postsynaptic membrane. It contains the synaptic **basal lamina** (BL) and is where ACh is released.
3. **Postsynaptic component:** composed by skeletal muscle fiber. It contains a high density of acetylcholine receptors (AChRs) and other molecules important for the function, establishment and maintenance of the NMJ.

4. **Glial cell:** the terminal Schwann cells (tSCs) which cover the nerve-muscle junction are directly involved in the regulation of neuronal activity and synaptic transmission (Castonguay et al. 2001).

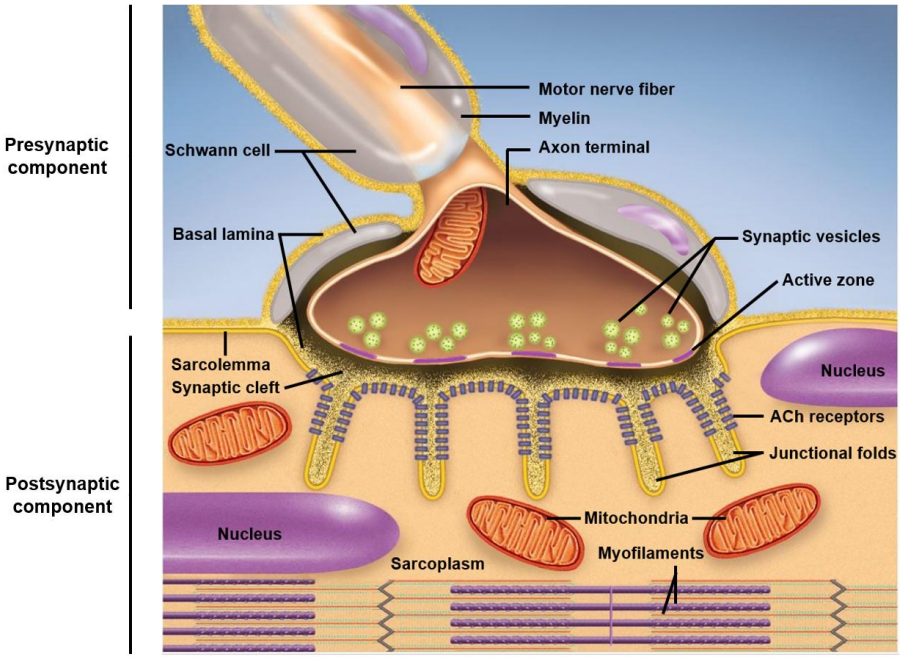

Figure 1. Neuromuscular junction structure. Cross-section diagram showing the three cell types of NMJ. The presynaptic component is composed (in brown) by the axon terminal of the motor nerve fiber, where active zones (in purple) and synaptic vesicles containing ACh (in green) are located. Surrounding the motor nerve and axon terminal are the Schwann cells (myelinogenic Schwann cell and the terminal Schwann cell respectively). The synaptic cleft is depicted by a space between the axon terminal and the synaptic folds of the muscle cell, and contains the basal lamina (in yellow). The postsynaptic component is composed by the muscle cell, where are located the nicotinic acetylcholine receptors (in blue). Adapted from McGraw Hill Companies.

2.1. Presynaptic component

The motoneuron is an excitable cell that has the property of responding to a stimulus by modifying its membrane potential. The MN is composed of a cellular body located at the ventral horn of the spinal cord and a long axon that projects to the peripheral nervous system (PNS) and innervates the muscle fiber. In mammals,

the axon ramifies intramuscularly in collateral axons, each of them form a nerve terminal that contacts a unique muscle fiber. Therefore, the presynaptic component of the NMJ corresponds to the nerve terminal of a MN. Nerve terminals are thin (approximately 2 µm), unmyelinated and split up into several small "twigs" when contacting a muscle fiber. The entire structure of nerve terminal branches is called motor endplate and covered by one or more tSCs.

Each MN and the entire set of muscle fibers that it innervates is called motor unit (Hirsch, 2007). To innervate a muscle, several motor units work together. The size of motor units and MN can differ from on muscle to another. The MN can be small, intermediate or large. Small MN innervate fewer muscle fibers and generate small forces while larger ones innervate more muscular fibers and generate more powerful forces.

The function of a nerve terminal is to convey the signals sent from the cellular body of the MN to the muscle fiber. These signals are propagated along the axon in form of electrical impulses. Axons transmit electrical signals over distances ranging from 0.1 mm to 2 m. To increase the speed by which nerve impulses are conducted, the axons of MNs are wrapped in an insulating sheath of a lipid substance called myelin, formed by Schwann cells. This sheath is interrupted at regular intervals by the nodes of Ranvier, separated spots on the axon where the action potential is regenerated creating a saltatory conduction. In addition, the nerve terminals receive from the axons a wide variety of chemical messages, organelles and molecules through anterograde soma transport.

The motor nerve terminal comprises a cluster of several specialized branches that contain high concentrations of SVs and proteins that regulate the timing, location, and depolarization-dependence of vesicle fusion (Patton 2003). At the synapse, almost all proteins are in some way associated with either the release or subsequent detection of NT (Jessell and Kandel, 1993; Burns and Augustine, 1995; Littleton and Bellen, 1995). To achieve that, neuromuscular synapses in mature vertebrates use the excitatory transmitter ACh, which triggers

muscle contraction. ACh is synthesized in motor nerve terminals from the chemical precursor choline and acetyl coenzyme A and it is degraded, by acetylcholinesterase (AChE), an enzyme that catalyzes the breakdown of ACh in the synaptic cleft (Quinn, 1987). ACh at the NMJ is released in small packets of thousands of ACh molecules, called quanta (Del Castillo and Katz, 1954). Each quantum of transmitter is packaged into SVs which are one of the most fundamental organelles involved in chemical neurotransmission (Heuser and Reese, 1973; Südhof, 2004). SVs are small lipid bilayer structures (about 50 nm), with a spherical shape. They can release their content upon presynaptic calcium ion (Ca^{2+}) entry by fusion with the PM at AZs. Each presynaptic button is densely packed with many vesicles, but only a small fraction of them are available for immediate release (Kaeser and Regehr, 2017). The subsequent docking, fusion, and release of NT (exocytosis) is a complex mechanism; the detail of which is the focus of the introduction chapter of this thesis. SVs also contain other compounds, such as adenosine triphosphate (ATP), which are co-released with ACh. Moreover, because ACh exocytosis is an energy-consuming process, the nerve terminal is rich in mitochondria in order to produce it when it is needed. A tightly controlled composition of proteins and lipids ensures the reliable neurotransmission at chemical synapses. Moreover, several proteins can be found in the membrane of the nerve terminal. Some of the most important are muscarinic acetylcholine receptors (mAChR) (Arenson 1989; Caulfield 1993; Ganguly and Das 1979; Garcia et al. 2010; Nadal et al. 2016, 2017; Santafé et al. 2006; Santafe et al. 2015), purinergic receptors (Garcia et al. 2013; Oliveira et al. 2015) and neurotrophin receptors such as Tropomyosin-related kinase receptor B (TrkB) (Hurtado et al. 2017a; Garcia et al. 2010; Gonzalez et al. 1999).

2.2. Synaptic cleft and basal lamina

Synaptic cleft is the space between pre- and postsynaptic membranes (50-100 nm wide), through which a nerve impulse is transmitted by the release of ACh (Wood and Slater, 2001) and it is occupied by a regular array of material of

moderate electron density. During development interactions occurring in the synaptic cleft are needed for the formation of pre- and postsynaptic specializations and therefore represent the starting point for signaling cascades that lead to synapse formation and stabilization (Craig 1998; Sanes and Lichtman 1999). Moreover, synaptic cleft can mediate some aspects of retrograde signaling, through which the activation of postsynaptic receptors may modulate the efficiency of the presynaptic compartment (Kandel et al. 2012).

At the vertebrate NMJ, within the synaptic cleft, and surrounding each nerve and muscle fiber, there are a thin layer called the basal lamina. It is composed of collagen and other extracellular matrix proteins, approximately 50 nm-thick, that contribute to tissue architecture and stability, form filtration barriers, and contain signaling molecules for cellular receptors (Patton 2003). In the NMJ, BL is also important because it covers the postsynaptic primary and secondary folds and allows contact with the opposing part of the synapse, the MN. In addition, the BL contains functionally specialized domains that support and regulate the specific cell types with which they come into contact. Thus, the molecular components of the BL function collectively as both general mechanical superstructure and specific cellular regulator (Patton 2000).

Associated with the synaptic portion of the BL are a number of proteins and glycoproteins that are not present in non-synaptic regions. These proteins includes AChE, laminin β2, which link the BL to the PM, agrin, AChR-inducing activity (ARIA), which are involved in the formation of the NMJ, and neurotrophic substances like fibroblast growth factor (FGF) (Falls et al., 1993; Sanes and Lichtman, 1999). Most relevant protein to considerer is AChE, the enzyme that rapidly cleaves ACh, thus limiting both the temporal and spatial extent of transmitter action (Wood and Slater, 2001; Rotundo, 2003). The enzyme is secreted from the muscle but remains attached to it by thin stalks of collagen fastened to the BL (Martyn et al. 2009). The efficiency of AChE ensures that transmission is restricted to a short time window

within an area near the transmitter release site, thus contributing to the temporal and spatial precision of skeletal muscle control.

2.3. Postsynaptic component

The postsynaptic component of the NMJ is formed by the muscle fiber membrane, which is called sarcolemma and is specialized to respond very quickly to the arrival of ACh, the cytoplasm below and the synaptic nuclei. The sarcolemma acts as a physical barrier against the external environment and facilitates signaling to the fiber.

Usually, the nerve terminal forms the synaptic contact at the center of the muscle fiber. Across the synaptic cleft, in the area where the contact takes place, the muscle "endplate'' surface forms a concavity named primary postsynaptic membrane, or primary fold. This shallow primary fold in turn is invaginated to form deeper folds, which increase the contact surface, called secondary folds (Liss and Salpeter 1987). At the top of the secondary folds are high concentrations of nAChRs in front of the nerve terminal. At the bottom of the secondary folds are concentrated voltage-gated sodium channels (VGSCs). Underneath the endplate, there are cytoskeleton fibers, microtubules and microfilaments, which maintain the structure of the folds and keep the nAChRs anchored to the membrane on the top of these. Secondary folds are unique to the NMJ and the high density of receptors that they allow is thought to enhance the safety factor for neurotransmission, which it refers to the ability of this to remain effective under various physiological conditions and stresses (Patton 2003; Sanes and Lichtman 1999) (**Figure 1**).

The nAChRs belong to the cys-loop superfamily of ligand activated ion channels that form pores or ionic channels. All members of this superfamily share a common structure and function. The crests of the folds are very defensibly packed with nAChRs at a density of about 10.000 receptors/μm^2 (Salpeter and Loring, 1985; Sine, 2012). Each nAChR is a protein comprised of five polypeptide

subunits surrounding a central, funnel-shaped pore, while on their synaptic surface they provide the binding sites for ACh. The mature adult receptor has two identical α subunits, one β, one δ and one ε subunit. In the absence of ACh, the central pore remains impermeable to the flow of cations. The pore opens in response to two molecules of ACh binding to the N-terminal domain of the junctions of the subunits αδ and αε promote the opening of the pore so that the sodium can get inside the fiber and it becomes depolarized. This procedure ends with a muscular contraction (Hirsch, 2007).

The aim of neuromuscular transmission is to cause muscle contraction. The muscle fibers that make up muscles are highly specialized to generate mechanical force under the control of the nervous system (Slater, 2008). A muscle fiber or myocyte is a long and cylindrical multinucleated cell (approximately 1-2 µm diameter) that contains myofibrils. The myofibrils are in turn composed of actin and myosin filaments. Muscle contraction results from the interaction between these filaments. Muscle fibers are organized into distinct thin (actin) and thick (myosin) filaments, corresponding to the light band (I-band) and dark band (A-band), which are further organized into overlapping arrays, the sarcomeres (**figure 2**). The sarcomere, the smallest functional unit of muscle fiber, is responsible for the striated appearance of skeletal muscle, and forms the basic machinery necessary for muscle contraction. The border between two neighboring sarcomeres is called the Z-line (also known as the Z-disc or Z-band). T-tubules are invaginations from the sarcolemma that communicate this outer membrane with the myocyte's sarcoplasmic reticulum. These structures are typically located at the junction overlap between the A and I bands of the sarcomere, and together with a pair of terminal cisternae (bulbous enlarged areas of the sarcoplasmic reticulum) form an arrangement called a triad (Padykula and Gauthier, 1970; Mitsui and Ohshima, 2012).

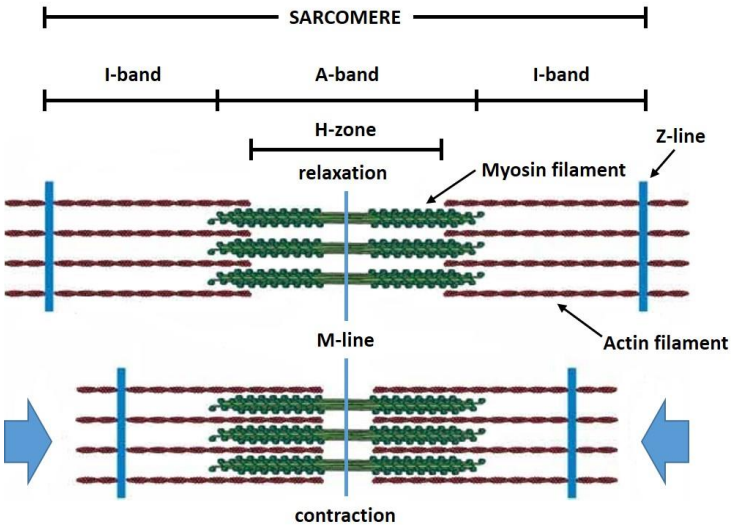

Figure 2. Longitudinal section of the basic organization of a sarcomere region. It shows of overlapping and crossed-over filament arrays created to generate the relative slip force between the filaments. Myosin (A-band) is represented in green, actin (I-band) in brown and the z-line in blue.

A motor unit is the MN and fibers of the skeletal muscle that it innervates. A single MN is able to innervate multiple muscle fibers, thereby causing the fibers to contract at the same time. Once innervated, the protein filaments within each skeletal muscle fiber slide past each other to produce a contraction. When AP arrives, it produces the release of Ca^{2+} influx. Then, actin filaments slide past myosin filaments; myosin heads become attached to actin filaments and form the protein complex actomyosin, which, thereby forms a cross-bridge between the two filaments and induces muscle contraction (**figure 2**) (Huxley, 2004; Mitsui and Ohshima, 2012).

2.4. Glial component

Schwann cells (SCs) are glial cells of the PNS and are closely associated with motoneurons. Further than only being passive supporters of the neurons, are directly related with the nervous transmission function. SCs are derived from neural crest cells, and come in two types either myelinating or non-myelinating SCs. Both play a pivotal role in the maintenance and regeneration of axons of the neurons in the PNS. In addition, they are related with the correct directionality of the axons and also help in the elimination of products of waste (Bhatheja and Field, 2006). Myelinating SCs (MSCs) are the most representative group and enclose one axon of about 1 µm of diameter and form myelin sheaths around, and are abundant in the axons of neurons. MSCs contribute to increase transmission velocity and improve stability of point-to-point connectivity decrease energy consumption for impulse transmission (Griffin and Thompson, 2008). Moreover, they are useful to avoid randomized polyinnervation due to the myelin sheaths capacity of secretion of replication inhibitory compounds. Non-myelinating Schwann Cells (NMSCs) are a minority and envelope several axons with a diameter of about 0,5 µm but do not recover them with myelin (Bhatheja and Field, 2006).

Terminal Schwann cells (tSCs) belongs NMSCs and are the glial cells of the PNS which cover the motor nerve terminals in NMJs (Sanes and Lichtman, 1999). There are especially important in the NMJ because they recover the terminal button and isolate the synapses from the environment and provide nutritive substances and an appropriate medium to the neuron cells. Although tSCs are similar to NMSCs in that they do not form multiple myelin wrappings around nerve terminals, they do wrap around single nerve terminals. TSCs plays a vital role in the synaptic transmission at the PNS, promoting stability of the NMJ, and are actively involved in modulating synaptic function (Auld and Robitaille 2003a,b; Feng and Ko 2008). In addition, they promote synapse elimination during the development process and synaptogenesis (Smith et al., 2013) and also help in the recovery after the nerve injury (Kang et al. 2014).

3. SYNAPTIC TRANSMISSION IN THE NEUROMUSCULAR JUNCTION

The electrical transmission in the nervous system occurs by the ability of a neuron to elicit AP firing in the neighboring neuron (Lisman et al. 2007). Synaptic transmission (or neurotransmission) is initiated when an AP triggers NT release from a presynaptic nerve terminal. The depolarization of PM of nerve terminal leads to Ca^{2+} influx through voltage-gated calcium channels (Katz and Miledi, 1967). The rise in the presynaptic calcium concentration increases the probability of SVs fusion with the PM at AZ and the subsequent vesicle exocytosis. Following fusion, SVs expel their NT content which diffuse over the synaptic cleft and bind to complementary ligand-gated ion channels at presynaptic cell, which transform the chemical signal back into an electrical signal (Südhof, 2004). To maintain the activity and integrity of a synapse, membranes and proteins are recycled and SVs are reacidified and refilled with NT (Südhof, 2004; Jahn and Scheller, 2006) to prepare them for a new round of exocytosis after arrival of another electrical impulse.

In the case of NMJ, impulse transmission takes place in a saltatory way along myelinated axons from one Ranvier node to the next. These involves the rapid release of quanta of ACh from the nerve, the binding of the ACh to nAChRs in the surface of the muscle fiber, the opening of those channels and the flow of current into the muscle fiber leading to depolarization and opening of VGSCs causing initiation of an AP and contraction of the muscle cell.

There are three primary modes of neurotransmitter release (Kaeser and Regehr, 2014):

- **Synchronous release** occurs within several milliseconds after an AP invades a presynaptic bouton. It is the main component in most synapses, whereby more than 90% of quanta can be released at low-frequency stimulation.

- **Asynchronous release** persists for tens of milliseconds to tens of seconds after an AP or series of APs.
- **Spontaneous release** occurs in the absence of presynaptic depolarization.

Neurons are electrically active by virtue of a potential difference that exists across their PM (Hodgkin and Katz, 1949). This gradient is maintained through the action of sodium/potassium ATPase (Na^+/K^+-ATPase) and unidirectional ion channels (Rakowski et al. 1989). Through the action of Na^+/K^+-ATPase, neurons contain a high intracellular concentration of potassium but a low intracellular concentration of sodium. At rest, this (typically) keeps the neuron below the threshold for firing APs, at -70 mV, but to start the neurotransmission a minimum level of depolarization called threshold action potential must be achieved. For this reason, changes in Na^+ and K^+ concentrations must be enough to throw the potential up to usually between -50 and +40 mV (varies depending on the situation and the stimuli). When the sodium channels open, the extracellular Na^+ gets in the cell and depolarizes it. Then, the potassium channels impulse the K^+ out of the cell and generate, this way, the repolarization. This procedure generates a change in the polarity among inside and outside the neuron that starts at the soma and travels by the axon until it reaches the nerve terminal. Once the AP arrives, it causes the opening of the presynaptic voltage-gated calcium channels (VGCCs) and provokes the Ca^{2+} influx, which allows the neurotransmission.

Neurotransmission at the presynaptic terminal involves synaptic vesicle exocytosis, endocytosis, and reuse of SVs. To enable these, apart from Ca^{2+} influx induced by depolarization, it is also necessary the SNARE (Soluble NSF Attachment Protein Receptor) complex assembly, which implies a number of proteins, found in the membranes and the cytoplasm of the nerve terminals of the MN. Moreover, neurotransmission has to deal with the amount of NT available and, to obtain an efficient response, postsynaptic receptors must be working correctly and so the postsynaptic cell.

4. SYNAPTIC VESICLES

Synaptic vesicles are the basic minimal units of membrane traffic in the presynaptic terminal, with a spherical shape and small diameter about 40 nm. SVs have been used as a classical example to illustrate the physico-chemical properties of a membrane trafficking organelle. The membrane of a single SV is composed of a large amount of phospholipid molecules, is enriched in cholesterol and numerous transmembrane and membrane-associated proteins. Detailed analysis of the protein composition of rat SVs revealed the presence of numerous integral membrane proteins among which the SNARE family (SNARE where NSF stands for N-ethylmaleimide-sensitive fusion protein, or factor) are the predominant proteins (Takamori et al., 2006). The membrane constituents of the organelle are ultimately responsible for orchestrating association of the complex, task execution, and complex disassembly. SVs proteins can either be classified as transport proteins, which are involved in NT uptake and storage, and as trafficking proteins involved in membrane fusion (Südhof, 2004). The most abundant SV trafficking proteins are Synaptobrevin-2 (Syb-2), synaptophysin and synaptotagmin-1 (Syt1) (**figure 3**) (Takamori et al., 2006; Wilhelm et al., 2014).

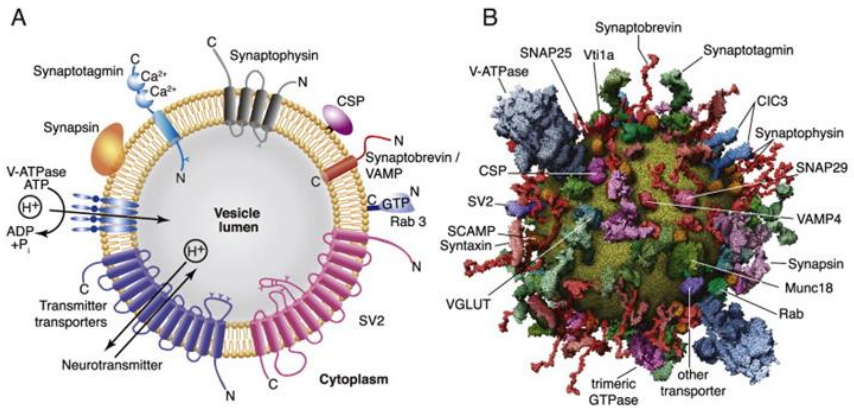

Figure 3. The protein composition of an average synaptic vesicle. A) Scheme of the structure and topology of the major synaptic vesicle (SV) membrane proteins. **B)** Molecular model of an average synaptic vesicle. SV proteins are displayed at near atomic resolution. SV surface is almost entirely covered with proteins. Source: Takamori et al., 2006.

4.1. Synaptic vesicle pools

In a typical synapse at rest, a small percentage of vesicles are attached to the AZs of the presynaptic membrane and the rest are distributed in nearby pools. Although the SVs all look alike under the electron microscope and no significant biochemical distinctions can be determined between them in a terminal at rest, there are distinct pools of vesicles with distinct functional properties. SVs are distributed in the presynaptic terminal in a specific way in order to favour their utilization and reutilization during maintained stimuli. Depending on the position where they are and the availability to be exocytated, vesicles can be classified in three different groups: the readily releasable pool (RRP), the recycling pool and the reserve/resting pool (Rizzoli and Betz, 2005; Alabi and Tsien, 2012).

- **The readily releasable pool (RRP):** This pool is constituted by vesicles which are docked at the synaptic AZ, available for immediate release, although not necessarily immediately releasable. This pool only constitutes about 1-5% of all vesicles and is the first to be released. For this reason, an intense or repetitive stimulus can exhaust it.
- **The recycling pool:** These vesicles are released during moderate (physiological) stimulation, and constitute about 5-20% of all vesicles. Physiological frequencies of stimulation cause it to recycle continuously and it is refilled by newly recycled vesicles, so that they can be used repeatedly during sustained activity (Harata et al., 2001; Kuromi and Kidokoro, 2003; Richards et al., 2003).
- **The reserve/resting pool:** These vesicles constitute about 80–90% of all vesicles in most presynaptic terminals**.** It is defined as a depot of SVs from which release is only triggered during intense stimulation. Interestingly, in the NMJ, intense stimulation results in fusion of all the vesicles in the terminal (Heuser and Reese, 1973), whereas in hippocampal neurons, a substantial proportion of the vesicles remain unused, even during strong nonphysiological stimulation. Both at central nervous system (CNS) and

NMJ synapses only 1-5% of all vesicles are recycled (Denker et al., 2011). Hence, the proportion the reserve pool vesicles that participate in synaptic transmission is still a matter of debate and await further investigations. It is possible that these vesicles are seldom or never recruited during physiological activity.

5. THE SYNAPTIC VESICLE CYCLE

The synaptic vesicle cycle resembles general membrane trafficking and can be divided into three phases: synaptic vesicle filling, exocytosis, and recycling. During filling, NTs are synthesized in the cytoplasm and are actively internalized into SVs via vesicular NT transporters and form a cluster or a reserve pool in the cytoplasm. Exocytosis of NT-filled SVs is a multistep pathway by which a SV fuses with the PM and releases its contents into the synaptic cleft and is triggered by calcium influx. After exocytosis, endocytosis recovers SVs from the PM and are recycled and refilled with NTs for a new round of exocytosis (**figure 4**) (Heuser and Reese 1973; Lisman et al. 2007; Südhof 2004).

5.1. Vesicular filling of acetylcholine

NTs are synthesized in the neuronal cytosol and are stored at high concentrations in the presynaptic nerve terminal into SVs by active transport, driven by a vesicular ATPase proton pump whose activity establishes an electrochemical gradient across the vesicle membrane. The neurotransmitter ACh is synthesized by the enzyme choline acetyltransferase (ChAT) in the cytoplasm of cholinergic neurons. Once synthetized, the vesicular acetylcholine transporter (VAChT) is responsible for loaded the ACh into the SVs in the terminals. VAChT works in coordination with another important enzyme, the vacuolar ATPase which pumps protons inside the vesicles and generates the gradient of protons needed to transport the ACh inside the vesicles (Gasnier, 2000; Südhof, 2004).

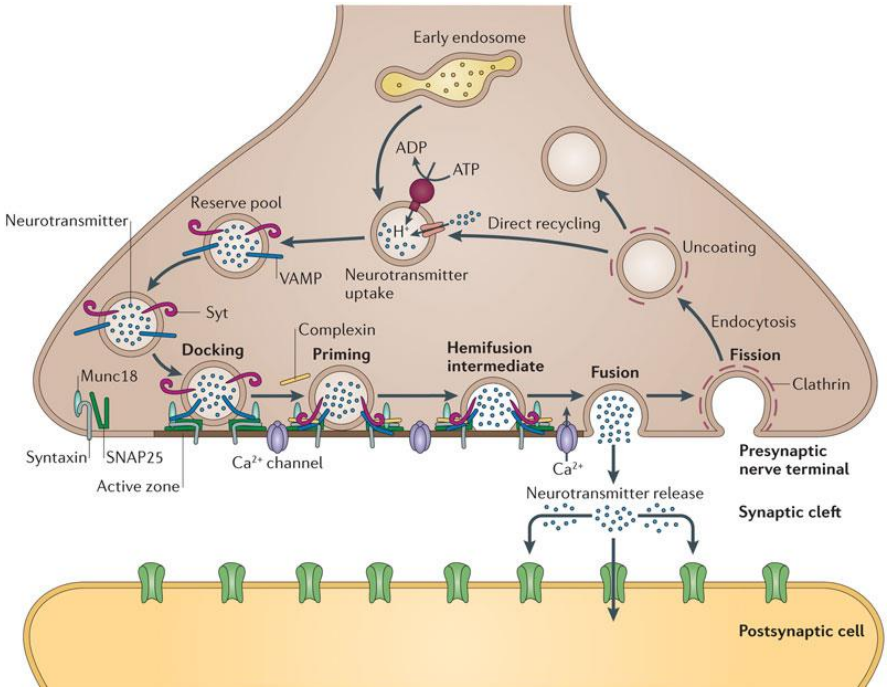

Figure 4. Synaptic vesicle cycle. Scheme of synaptic vesicle exocytosis and endocytic pathway. NTs are synthetized and stored into SVs at the presynaptic nerve terminal. SVs can form a reserve pool of NTs within the nerve terminal or bind to specialized sites of the presynaptic membrane called AZs, where they dock and release takes place. Priming involves all steps required to acquire fusion and release readiness of the exocytotic complex. NT diffuses out of the nerve terminal and binds to a postsynaptic receptor, which triggers signaling in the postsynaptic cell. In the case of the NMJ, ACh is released and binds to the ACh receptor, which results in depolarization of the muscle PM, leading to Ca^{2+} entry and muscle contraction. During NT release, the lumen of the SV is transiently opened to the outside, but it is later internalized into the nerve terminal by endocytosis. At the NMJ, SVs are mainly endocyted by a clathrin coat. After clathrin uncoating, SVs are internalized and regenerated through an endosomal intermediate. After that, SVs are refilled with NTs and the next cycle begins. ACh: acetylcholine; AZ: active zone; NMJ: neuromuscular junction; NT: neurotransmitter; PM: plasma membrane; SV: synaptic vesicle; Source: Rossetto et al. 2014.

5.2. Synaptic vesicle exocytosis

Exocytosis of NT-filled SVs is a multistep pathway. First, in order for SVs to mediate the rapid release of NT they must be first translocated, docked and primed at the AZs (Becherer and Rettig, 2006; Siksou et al., 2009). Then, when

calcium influx triggers the fusion of the membranes from the SVs, there are well placed to immediately NT release. This docked, primed and fusion of membrane is mediated and regulated by SNARE proteins that constitutes the basic fusion machinery (Brunger 2001; Chen and Scheller 2001) (**Figure 4 and 5**). SNARE proteins undergo conformational changes during SV cycle with structural interaction between SVs and the presynaptic membrane, leading the core complex formation and driving fusion and the subsequent NT release. The Ca^{2+} trigged NT release at synapses is regulated by the Sec1/Munc18 (SM) protein Munc18-1, the Syb-2, the Syntaxin-1A and SNAP-25 (synaptosome associated protein of 25-kDa molecular weight). The release takes place only one millisecond after the presynaptic membrane is excited.

Vesicle docking is a targeted reaction where SVs must attach to the AZ of the presynaptic PM. This step is essential for their fusion with the membrane and exocytosis of their NT to mediate synaptic impulse transmission. Unfortunately, there is still controversy in as to which molecular players constitute the functional docking machinery. It is required that the cytoplasmic domains of the three interacting proteins to form the SNARE complex contact and bridge the vesicular membrane and the PM (**Figure 4 and 5**). This docking appears also to require Munc18-1, which could serve as a membrane anchor on the PM. Syt1 is the calcium sensor for exocytosis, and SNAP-25 as an essential PM docking factor, which, together with a bimolecular Syntaxin/Munc18-1 complex, form the minimal docking machinery. Alternatively, SNAP-25 may interact directly with rabphilin and Syt1 to dock SVs (Mohrmann et al. 2013; Parisotto et al. 2012; Tsuboi and Fukuda 2005; Matthijs et al. 2008; de Wit et al. 2009).

Vesicle priming prepares the SV so that they are able to fuse rapidly in response to a calcium influx. This priming step is thought to involve the formation of partially assembled SNARE complexes. Importantly, only a fraction of vesicles located at or near the PM is competent to undergo AP induced fusion at any point in time. These are referred to as 'primed' vesicles and the total number of that is

referred to as the release competent or primed vesicle pool. CAPS (Calcium-dependent Activator Protein for Secretion) and Munc13 (Mammalian Unc-13) have been shown to be crucial for vesicle priming. These proteins are important for the initiation of SNARE complex formation and help to stabilize SVs in a fusion competent state (Südhof, 2004). The priming process is also regulated by Ca^{2+} (Neher and Sakaba, 2008). In priming, protein kinase C (PKC) activation of Munc13 probably acts via a direct or indirect interaction of the MUN-domain with SNARE and/or SM (Sec1/Munc18) proteins (Südhof and Rizo, 2011).

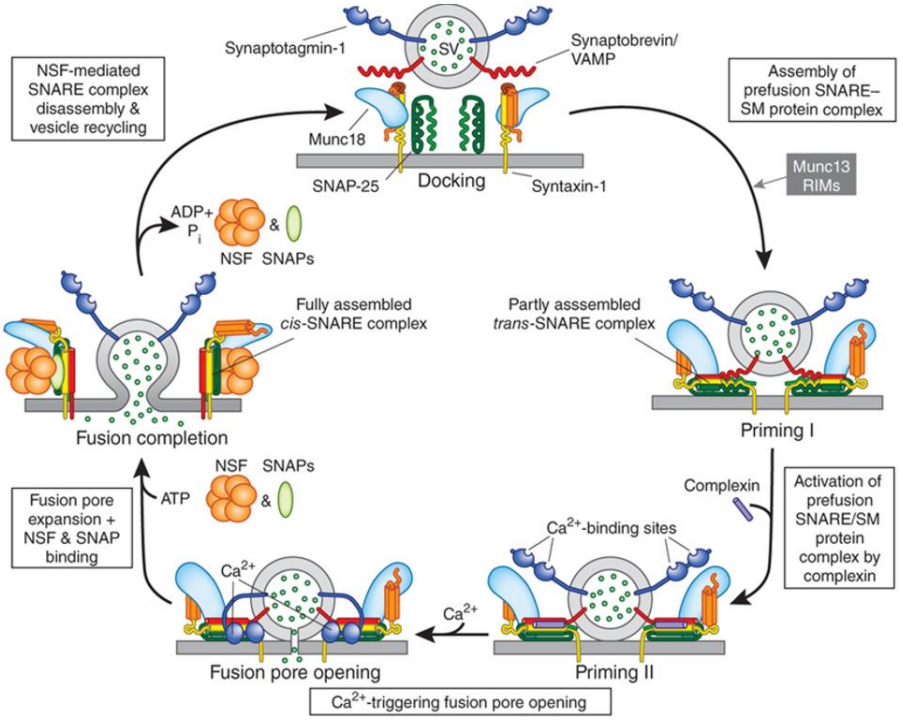

Figure 5. Synaptic vesicle exocytosis. Scheme model of the SNARE–SM protein and the points of action of their essential proteins involved in the synaptic vesicle cycle. The cycle illustrates the various transient stages of monomeric SNAREs and SNARE complexes bound to Munc18-1 and Synaptotagmin. Munc18-1 plays an essential role in guiding Syntaxin from its closed to open conformation associated with SNARE complexes. Complexin with partially assembled trans-SNARE complexes, which enhances vesicle priming for fusion, and the step of calcium triggering of fusion pore opening by synaptotagmin. NSF and α-SNAP are required for ATP dependent disassembly of SNARE complexes to bring the vesicles and the release site back to a state that allows for a new round of exocytosis. Source: Adapted from Südhof, 2013.

Vesicle fusion occurs when vesicular and PMs mixing and fusion pore open when SNARE complex zippered to the membrane proximal or transmembrane domain region (Chen and Scheller 2001; Pobbati et al. 2006). This process is leaded by SNARE complexes and Munc18-1, which controls this complex formation and may have a direct role in fusion. In addition, other SNARE complementary proteins such as Munc13 and RIMs (Rab3-interacting molecules), Complexin and Syt1 likely orchestrate SNARE-complex. Syt1 mediates triggering of release by Ca^{2+}, probably through interactions with SNAREs and both membranes, as well as through tight interplay with complexins. After SV collapse onto the PM companied by SNARE complex forming into *cis* conformation, SNARE complex will be disassembled by α-SNAP and NSF (Lin and Scheller, 2000). Due to the complexity of this step, it is fully explained in the follow section *The membrane fusion machinery*.

5.3. Synaptic vesicle endocytosis

Upon SV fusion, the neuronal membrane surface expands. The retrieval of SVs from the PM is crucial for keeping the size of the terminal constant by removing the excess membrane and permits a relatively small number of SVs to maintain synaptic transmission even during long periods of increased activity (Murthy and De Camilli, 2003). There are probably four different processes related with the recycling of the SVs: (1) clathrin mediated endocytosis (CME) of small SVs; (2) “kiss and run”, transient fusion with the PM; (3) bulk and (4) ultrafast endocytosis of large portions of membrane. These pathways differ in their timescales and molecular mechanisms (**Figure 6**).

Clathrin mediated endocytosis is an endocytic process via clathrin-coated pits, and occurs in response to a fully vesicle exocytosis outside the AZ, in the periactive zones, during normal synaptic transmission. Clathrin is a scaffold protein found on the inner surface of the PM which has a skelion shape. Clathrin with the aid of endocytic adaptors cover a membrane pit that by progressive membrane deformation driven by accessory endocytic proteins matures into a coated vesicle

(Fotin et al., 2004, 2006). Once the vesicle is fully formed, the clathrin complex is able to dissociate away before being recycled.

The **"kiss-and-run"** model operates during mild stimulation and describes the transient fusion of SVs with the PM without full vesicle collapse (Alabi and Tsien, 2013). The narrow fusion pores are closed rapidly within a time frame of only seconds to rejoin the AZ-bound SV pool without the need for endocytic sorting. In kiss-and-run, there is no need to sort proteins or lipids because the vesicle remains intact (Zhou et al. 2014).

Bulk endocytosis operates upon strong stimulation in the periactive zone. It is probably an emergency mechanism, when stimulation surpasses the ability of the synapse to recycle vesicles all vesicle pools are depleted and are only slowly regenerated. The vesicle membrane added into the PM either swells the nerve terminals or folds back onto itself, generating what has been termed “infoldings” or endosome-like vacuoles from which SVs eventually bud (Miller and Heuser, 1984; Rizzoli, 2014).

Recent studies (Watanabe et al., 2013a, 2013b) identify an **ultrafast** mode of endocytosis, occurring in the space between active and periactive zones which can quickly replenish the membrane surface are during intense stimulation. This spatial restriction is peculiar and interesting, as it may signify the existence of specialized membrane plates that prevent ultrafast membrane blebbing (Zhou et al. 2014). This process is very fast (about 50 – 100 ms after stimulation) and is clathrin-independent. Furthermore, it is unclear, whether ultrafast endocytosis retrieves exclusively lipids or the complete membrane including the SV proteins (Watanabe et al., 2013a, 2013b).

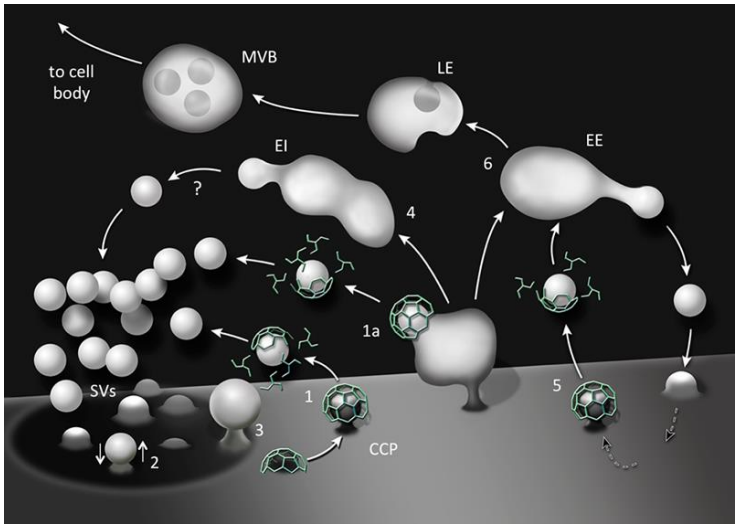

Figure 6. Pathways of synaptic vesicle recycling in nerve terminals. Scheme of membrane traffic in axon terminals illustrating established and putative pathways of endocytosis of synaptic vesicle (SV) membranes: clathrin-coated pits (CCP) from the PM and its deep infoldings **(1 and 1a)**,"kiss and run" **(2)**, ultrafast endocytosis **(3)**, and bulk endocytosis **(4)** followed by vesicle formation via yet unclear mechanisms **(?)** from endocytic intermediates (EI). This recycling traffic is interconnected with housekeeping membrane recycling **(5)** involving clathrin-mediated endocytosis and canonical early endosomes (EE) as well as with traffic to the cell body **(6)** via late endosomes (LE) and multivesicular bodies (MVBs). Source: Adapted from Saheki and De Camilli, 2012.

Bulk and ultrafast endocytosis involve large endocytic structures at the PM. Both kiss-and-run, bulk and ultrafast endocytosis do ensure instant membrane retrieval. While ultrafast recycling may be a default mechanism to maintain the surface area following vesicle fusion, CME and bulk endocytosis may impose different layers of regulation of synaptic vesicle function when neurons are being stimulated intensely. The dense body-plate region is packed with proteins specializing in vesicle fusion, while the periactive zone plate and associated cytoskeleton specialize in CME or bulk retrieval (Zhou et al. 2014).

No matter how the vesicles fuse, after release of NT, both newly formed and recycled vesicles have to be packed with NT, in order to be utilized in the subsequent responses. Thus, vesicular recycling is fundamentally controlling the synaptic efficacy.

6. THE MEMBRANE FUSION MACHINERY

Membrane fusion is the process by which two initially separated lipid bilayers merge to form a single unity. It is a universal biological process in life that is involved in many cellular events, and is essential for the communication between cells and between different intracellular compartments (Jahn et al. 2003). Repulsive forces between the approaching bilayers oppose spontaneous membrane fusion in living organisms. These forces result from electrostatic repulsion of equally charged membrane surfaces and from hydration repulsion. Moreover, the lateral tension of the bilayer interface has to be overcome (Kozlovsky et al. 2002). The energy required to overcome the energy barrier for the fusion of biological membranes is provided by specialized fusion proteins, like SNARE proteins in the exocytosis process, that forms a "rod-like" α-helical bundle, termed *trans*-SNARE complex (**figure 7**) (Jahn and Fasshauer 2012; Jahn et al. 2003).

6.1. The SNARE complex

Soluble N-ethylmaleimide-sensitive factor (NSF) attachment protein (SNAP) receptors, also known as SNARE complex, are known to be the core fusion machinery in neuro-exocytotic pathways (Rizo and Südhof, 2002; Jahn and Scheller, 2006). SNAREs make up an evolutionarily conserved superfamily of membrane-associated proteins that are differentially distributed among intracellular membranes (Jahn and Südhof, 1999; Bock et al., 2001; Jahn and Scheller, 2006). They are composed exclusively of alpha-helical segments, each protein with a 60–70 amino acid (aa) residues in length called the "SNARE motif", which tend to form a coiled coil structure (Terrian and White, 1997) (**figure 7**). The major proteins of the SNARE family that plays an essential role in fusion especially during neuronal exocytosis are Syb, SNAP-25 and Syntaxin-1A. SNAREs can be divided into two categories based on their primary localization in the cell. With only a few exceptions, a single SNARE family protein resides on the vesicle and is

called the "v-SNARE." The other three SNARE motifs reside on the target membrane and are called "t-SNAREs" (Fasshauer et al., 1998). Both sequence analysis and X-ray crystallography studies of the SNAREs have allowed for their classification into Q-SNAREs and R-SNAREs (Fasshauer et al., 1998), depending upon the amino acid, either glutamine or arginine, present at the ionic layer of the SNARE complex (Sutton et al., 1998). Syb-2 and Syntaxin-1A each have one SNARE motif, whereas SNAP-25 contains two SNARE motifs. Syntaxin-1A and SNAP-25 are mainly located in the presynaptic PM whereas Syb-2 is expressed in a SV membrane (Takamori et al., 2006). SNARE motifs zipper together to form a parallel four-helix bundle called the "core complex" (**Figure 7**).

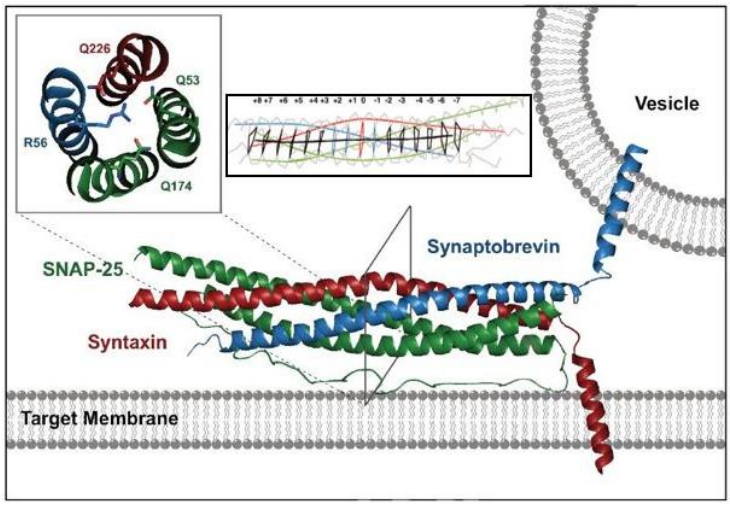

Figure 7. The SNARE core complex machinery. The SNARE complex forms a parallel four-helix bundle to bridge the vesicle and target membranes. Syntaxin (red) is inserted into the plasma membrane by a transmembrane domain. SNAP-25 (green) is associated with the target membrane by palmitoylation and contributes two alpha-helices to the complex. Inset displays the four residues that define the 0 layer.

The SNARE core complex is highly stable and requires boiling with sodium dodecyl sulfate (SDS) for disassembly (Chen et al. 1999). The stability of SNAREs can be attributed to strong hydrophobic interactions between "layer residues" that run the length of the core complex. The centre bundle of the helical domain contains 16 layers of interface including 15 hydrophobic interface among the side

chain from each SNARE motif, and one highly conserved electrostatic "0" layer which contains 3 glutamine (Qa, Qb, Qc) and 1 arginine (R) residues (**Figure 7**). Accordingly, the SNARE proteins whose SNARE motif contributes these residue was classified as Qa-(Syntaxin), Qb-(SNAP), Qc-(SNAP) and R-SNARE (Syb-2) (Fasshauer et al., 1998; Bock et al., 2001). The conservation of the 0 layer residues provides an effective evolutionary categorization for classifying the relatedness of SNAREs in evolution (Kloepper et al. 2007).

The zippering process of membrane fusion results in a structural transition of the loose *trans*-SNARE complex to a tight *trans*-SNARE complex and identified by the formation of four α-helical bundles (**Figure 7**). The states between loose and tight *trans*-SNARE complexes are thought to be reversible and reach equilibrium (Xu et al. 1999). The bilayers of the target and vesicular membranes merge the *trans*-SNARE complex into *cis*-complex, which results in release of vesicle content. After the fusion, the *cis*-SNARE complex binds to NSF trough α-SNAP, which destabilizes the zippering and allows the recycle mechanisms of the cell to start working. Only the conformed SNARE complex can bind α-SNAP and NSF and because of this specificity has this name (Jahn and Fasshauer, 2012).

6.2. SNARE proteins: Synaptobrevin-2, SNAP-25 and Syntaxin-1a

SNARE complex integrates Synaptobrevin, SNAP-25 and Syntaxin-1A, which are the essential core in SVs exocytosis. Nevertheless, after many studies, it has been confirmed that the SNARE itself is not enough for the fusion to take place; instead, some more proteins are needed to allow the synaptic membrane fusion. The best known of this "complementary proteins" are Synaptotagmin, Complexin, Munc13 and Munc18-1 (Jahn and Fasshauer, 2012). Proteins explained in the following sections are represented graphically in **Figure 8**.

6.2.1. Synaptobrevin

Synaptobrevin (Syb, also called VAMP or v-SNARE) is a small integral membrane protein that belongs to vesicle-associated membrane protein (VAMP) family. The isoforms I and II (Syb-1 and Syb-2) are widely distributed in both CNS (Raptis et al., 2005) and PNS (Li et al., 1996), being Syb-2 the most studied isoform. It is a protein of about 18 kDa and is anchored into the membrane of the SVs, which have to be exocytated. It works by identifying the target membrane because it has associated with both Syntaxin-1A and SNAP-25 (together called t-SNARE) (Pobbati et al. 2006).

Syb-2, has one SNARE domain, which is connected by a linker domain to the C-terminal transmembrane region (TMR) (**Figure 8**). It has been proved that the TMRs, together with the linkers add stability to the SNARE complexes and resistance versus denaturalization procedures. TMR domain being free reduces the stability of the SNARE complex because it makes interferences in the conformation of the quadruple helix.

6.2.2. Syntaxin-1A

Syntaxin family members are t-SNAREs and share three common features: an NH_2- terminal regulatory domain composed of three α-helixes called the H_{abc} domain, a SNARE motif, and a COOH-terminal transmembrane anchor (**Figure 8**). In those syntaxins involved in exocytosis, the H_{abc} domain folds back on the central helix of the SNARE motif to generate a closed and inactive conformation (Dulubova et al. 1999; Munson et al. 2000).

Syntaxin isoform in the PNS, Syntaxin-1A, weights about 33 kDa and contains only one SNARE domain located just before the linker and C-terminal TMR domain. In the N-terminal extreme Syntaxin-1A has a triple helix bundle known as H_{abc} domain or N-peptide which can form a tight complex with the neuronal SM proteins (Fernandez et al., 1998). Munc-18-1 is a SNARE regulator proposed to maintain mammalian Syntaxin-1A in a closed conformation. Syntaxin-

1A in conjugation with Munc18-1, fold back onto the SNARE motif, forming a "closed conformation" that prevents Syntaxin-1A from forming the core complex with Syb-2 and SNAP-25. Thus, Syntaxin-1A must have a conformational change to switch between its complex with Munc18-1 and the core complex.

6.2.3. SNAP-25

SNAP-25 (synaptosomal-associated protein of 25 kDa) is a component of the SNARE complex, which is involved in the exocytotic release of NTs during synaptic transmission (Südhof, 2004; Milovanovic and Jahn, 2015). When SNAP-25 is absent, it has been shown that vesicle docking at the presynaptic AZs persists, but the pool of primed vesicles for release is empty, and fast calcium-triggered exocytosis is abolished (Sørensen et al., 2003). In addition, SNAP-25 has an important role in the vesicle docking and priming, provided by the calcium-dependent interaction with Syt1, as well as in triggering fast exocytosis (Mohrmann et al. 2013). It is unique among the other SNAREs as it contributes two 70 aa SNARE motifs linked by a loop with palmitate-modified cysteine residues to be attached to the terminal (or target) membrane (Gonzalo et al. 1999). Its two SNARE domains (**figure 8**) interact with the SNARE domains from the Syb-2 and Syntaxin-1A (**Figure 9**). SNARE motifs are largely unstructured but spontaneously assemble into helical SNARE complexes. SNAP-25 is about 206 aa residues long and does not carry any other domain (Stein et al., 2009).

SNAP-25 is a PKC substrate *in vivo* (Shimazaki et al., 1996; Kataoka et al., 2000). The PKC phosphorylation site in SNAP-25 has been mapped to the serine 187 (Ser-187), in a region of critical importance in calcium-triggered exocytosis (Weinberger and Gerst, 2004). It seems that the level of phosphorylated SNAP-25 in resting cells is low but a partial phosphorylation is seen when [Ca^{2+}] is increased (Nagy et al., 2002). Several results support the hypothesis that PKC phosphorylation of SNAP-25 is required for fast vesicle pool refilling in response to synaptic activity or elevated intracellular calcium concentration. It has been proposed that vesicle refilling and pool size would be coordinately controlled by

phosphorylation of SNAP-25 via two different signal pathways. Protein kinase A (PKA) phosphorylation of SNAP-25 at threonine-138 (Thr-138) controls the size of the releasable vesicle pools, whereas PKC phosphorylation of SNAP-25 at Ser-187 is involved in regulating refilling after the pools have been emptied (Nagy et al., 2002; Leenders and Sheng, 2005a). In addition, SNARE complex formation by purified recombinant SNAP-25, Syntaxin-1A, and Syb-2 *in vitro* is inhibited or promoted as a result of the phosphorylation on Thr-138 by PKA or at Ser-187 by PKC, respectively. Thus suggest that SNAP-25 phosphorylation by PKA or PKC contributes differentially to the control of exocytosis by regulating SNARE complex formation (Gao et al. 2016).

6.3. The complementary SNARE proteins: SNARE regulators

Although SNARE proteins can provoke the release of NTs *in vitro* by their own (Weber et al., 1998), additional protein are required for vesicle transport and fusion, regulation of the speed and the precision of the Ca^{2+} dependent NT release *in vivo* (Guo et al., 2000). These "accessory proteins" are many, but Synaptotagmin, Complexin, Munc18-1 and Munc-13 are especially significant, and the set of all of them confer onto synaptic exocytosis its uniquely exquisite regulation (reviewed in (Brunger, 2005; Rizo and Rosenmund, 2008; Sørensen, 2009; Südhof and Rothman, 2009). Munc18-1 belongs to SM family of proteins which are proposed the essential proteins for activation of SNARE-complex assembly at the vesicle-fusion step (Waters and Hughson, 2000). Hence, these SM proteins will be extensively explained in the next chapter.

6.3.1. Synaptotagmin-1

Synaptotagmin-1 is a 65 kDa vesicular membrane protein, also known as Syt1, which is believed to be the key regulator for the temporal control of SNARE-dependent SV fusion (Chapman, 2002; Südhof, 2004; Rizo and Rosenmund, 2008). Syt1 belongs a family of fifteen membrane-trafficking proteins that are characterized by an N-terminal TMR, which serves as a vesicular anchor and two

calcium-binding domains (C2A and C2B) (**Figure 8**). These domains contains the loop region in the C-terminal ending which permits the regulation of its activity trough calcium binding, which are connected by a flexible linker and able to bind three and two Ca^{2+} ions, respectively (Rizo and Südhof, 2002). Syt1 changes conformation upon Ca^{2+} binding and triggers the fast fusion and subsequent NT release (Lee et al. 2010; Yoshihara and Littleton 2002). The two C2 domains are homologous to the C2 regulatory region of PKC (Perin et al., 1991).

It is activated by calcium dependent PKCs through specific phosphorylation at Thr-112 residue. Then, Syt1 binds the Ca^{2+} through its C2 domains. The C2 domains can bind PIP_2 (Phosphatidylinositol 4,5-bisphosphate, a minor phospholipid component of cell membranes in PM) in both a Ca^{2+} -independent manner, through a stretch of polybasic amino acids, and in a Ca^{2+} -dependent manner at the Ca^{2+} - binding pocket (Araç et al., 2006; Radhakrishnan et al., 2009; van den Bogaart et al., 2011). This interaction provokes a conformational change that makes the protein to bend inside the target membrane and it gets linked to the SNARE proteins, which favours the merge of the target and vesicular membranes (Caccin et al. 2015; Chapman 2008; Choi et al. 2010; Kim et al. 2012).

Overall, Syt1 participates in most steps of membrane fusion process via interacting with SNARE proteins and membrane. Syt1 largely enhanced vesicle docking via interacting with t-SNARE and PIP_2 (Hui et al. 2009; Kim et al. 2012; Lai and Shin 2012). In the step of vesicle priming and lipid mixing, Syt1/Ca^{2+} penetrates into membrane, generate positive curvature, and bring two opposition membrane closer (Hui et al., 2009). Accordingly, SNARE zippering is facilitated by Syt1 shorten the distance between two membranes (van den Bogaart et al., 2011). In the final fusion pore opening step, Syt1/Ca^{2+} initiate the process and expand that with Complexin.

6.3.2. Complexin

Complexins, (Cplxs), constitute a family of cytosolic proteins of about 15-20 kDa, which bind the SNARE complex and have the capacity of promoting and clamping the exocytosis depending on their spatial conformation, which changes subjected to the environment. They positively regulate a late, post-priming step in Ca^{2+} -triggered synchronous NT release, but the underlying molecular mechanisms are unclear. In mammals, the Cplx family consists of four members (Cplx-1 to -4) which are ubiquitous in the organisms and have a highest presence in the CNS (Xue et al., 2008). The Cplx-1 isoform is the one that binds tightly to the SNARE both if it is in a partial assembled form to help stabilize the structure or in its complete form to regulate the level of exocytosis accomplished. Other isoforms have less affinity and because of that their function is minor (Mohrmann et al. 2015; Xue et al. 2007).

Complexin 1 (Cplx-1), also called synaphin-2, contains 134 aa and consists of four domains (**Figure 8**). The N-terminal domain, which is required for activation of synchronous Ca^{2+} -triggered release. The α-helical motif, which is located near the center of the protein and bind to the SNARE complex, contains two domains: the central helix domain ($Cplx_{cen}$) and the accessory α-helix domain ($Cplx_{acc}$) (Chen et al. 2002). The $Cplx_{cen}$ binds the SNARE complex independently of its conformation is partial or complete, and is required for all functions of Cplx-1. The $Cplx_{acc}$ are entirely dispensable for activation of Ca^{2+} -triggered SV fusion and is essential for regulation of spontaneous release. $Cplx_{acc}$, initially (when exocytosis is clamped) is in an angle that positions it distant of the SNARE complex. When, through calcium binding, Syt1 gets activated and changes its conformation, it provokes a conformational change in the Cplx-1 protein which drives $Cplx_{acc}$ to a parallel position in relation with the SNARE complex, and this possibilities an interaction that is thought to trigger the exocytosis (Krishnakumar et al., 2011). Finally, the C-terminal domain is involved in vesicle priming and binds to anionic membranes with curvature sensitivity (Xue et al., 2007; Brose, 2008; Choi et al.,

2016). In all, Cplx-1, together with Syt1, regulates spontaneous and synchronized fast SV fusion (Yoon et al., 2008).

However, numerous studies have shown apparent discrepancies of the physiological role of Cplx in the NT release, demonstrating a differential function between species. The extensive analysis of their different domains in several species has shown that Cplxs have both inhibitory and facilitative functions (Brose, 2008; Xue et al., 2008; Trimbuch and Rosenmund, 2016). Most of the recent discussion has focused mainly on two questions. On the one hand, to understand the physiological relevance of a multiple role for Cplxs in SV priming, as well as the facilitation and inhibition of NT release. On the other hand, resolve the complex molecular interactions of Cplxs with the SNARE complex and with the Ca^{2+} -sensor Syt1 (Brose, 2008; Sørensen, 2009; Südhof and Rothman, 2009; Trimbuch and Rosenmund, 2016).

In summary, the functional role of Cplxs in mammalian neurons is still heavily debated. It seems clear the idea that Cplx has evolved differently in different species to optimize coding at synapses. Surely once the subtle structural variations in these individual domains are better studied, the general function of this molecule in different organisms can be determined more accurately (Trimbuch and Rosenmund, 2016).

6.3.3. Munc13

Munc13 (Mammalian Unc13) is an exocytosis involved protein of about 200 kDa from presynaptic AZs that also have a crucial function in NT release. Detailed physiological and morphological studies have shown that Munc13 is involved in docking and priming of SVs, suggesting that Munc13 acts as a key switch that acts on the release machinery. It works by modulating the action of important exocytotic proteins such as Munc18-1 through its most C-terminal domain called MUN. The proteins that contain the MUN domain are members of the CATCHR (Complex Associated with Tethering Containing Helical Rod) family of proteins and

work in various trafficking steps (James and Martin, 2013). Next to MUN domain proteins, this family consists of the Dsl1 complex, Conserved Oligomeric Golgi complex, Golgi-associated retrograde protein complex and exocytotic complexes that help tether the vesicle to the membrane. Munc13 proteins have two principal functions at the AZ: to prime the SNARE/SM protein fusion machinery for exocytosis, thus rendering SVs fusion competent, and to mediate short-term plasticity by regulating this priming activity (Südhof, 2012). Crystallized structures have shown that Munc13 has multiple domains (**Figure 8**): MUN, which integrates four different subdomains named from A to D and is the one which gives the principal function to the protein; in the N-terminal it has two C2 domains (C2A and C2B) and also in the C-terminal there is another C2 domain (C2C) which bind calcium. The first C2A domain provides a link to Rab3-interacting molecules (RIMs), large Rab3 effectors that have multiple roles in additional forms of presynaptic plasticity (Rizo and Südhof 2012). Between the two N-terminal C2 domains there is a CaMb domanin (Calmodulin binding domain) and a C1 domain which binds diacylglycerols (DAGs) in this order. This makes us think this protein is highly regulated by calcium. These additional domains probably controls diverse forms of regulation of release during presynaptic plasticity, likely by modulating the key function of the MUN domain (Rizo and Xu, 2015). In reference to the MUN domain it has been found to interact with membrane-anchored SNARE complexes and Syntaxin-1A–SNAP-25 heterodimers (Guan et al. 2008; Weninger et al. 2008), and also to bind weakly to Munc18-1 and to the Syntaxin-1A SNARE motif (Ma et al., 2011). Thus, these recent studies have proposed that MUN domain is the responsible of accelerating the conformational change of Munc18-1 which permits the modification of Syntaxin-1A from the closed form to the open one to complete SNARE complex formation and possibilities the triggering of exocytosis (Yang et al. 2015).

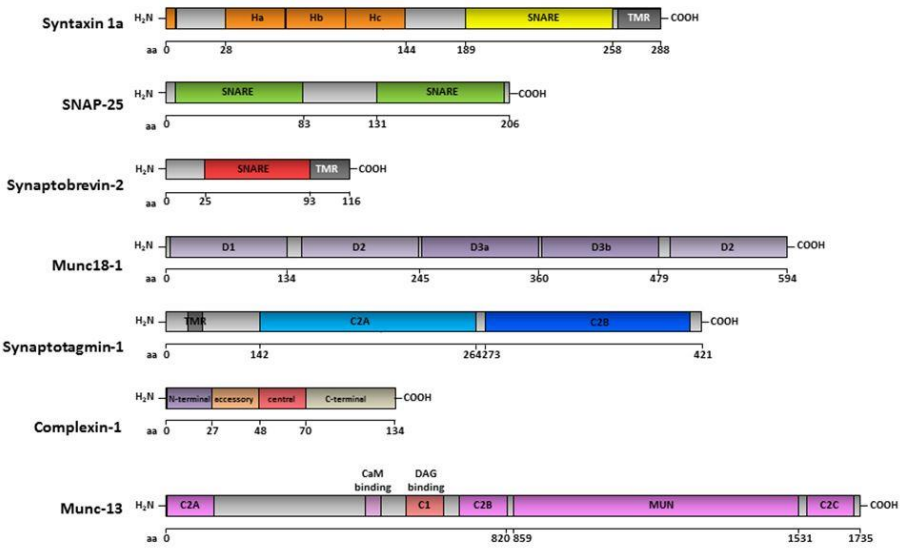

Figure 8. Domains of the SNAREs and the principal proteins implicated in the synaptic vesicles exocytosis.

7. SEC1/MUNC18 (SM) FAMILY OF PROTEINS

All types of intracellular membrane fusion that are controlled by SNAREs also depend on SM proteins, and the absence of the respective SM proteins generally leads to a block in membrane fusion (Toonen and Verhage, 2007; Südhof and Rothman, 2009; Carr and Rizo, 2010). The members of the SM family of proteins are essential component of the vesicle fusion machinery and exert their function at the post-docking step prior to fusion. Different family members participate in different vesicle trafficking steps. The family is composed of proteins that are soluble, but are also found on the membrane where they work in close collaboration with the SNARE proteins, in particular the syntaxins (Qa-SNARE) (Rizo and Südhof, 2002; Toonen and Verhage, 2007; Carr and Rizo, 2010). Their importance has been reported in numerous studies and their absence observed in Munc18-1 knockout mice leads the total abrogation of NT release (Verhage et al.

2000), and multiple studies have suggested that Munc18-1 is involved in synaptic vesicle docking, priming, and fusion (Toonen and Verhage, 2007; Südhof and Rothman, 2009; Carr and Rizo, 2010). Multiple types of interactions between Munc18-1 and the neuronal SNAREs, particularly Syntaxin-1A, mediate these diverse functions, at least in part. Thus, Munc18-1 binds tightly to Syntaxin-1A folded in the closed conformation (Misura et al. 2000), to the Syntaxin-1A N-terminal region through both the N-peptide and the H_{abc} domain and to the four-helix bundle of the SNARE complex (Deák et al. 2009; Rizo and Xu 2015; Xu et al. 2010).

Munc18-1 (mammalian uncoordinated-18) was the first SM protein to be found (Dulubova et al. 1999; Misura et al. 2000) and has been confirmed as an essential protein for the neurotransmission to take place and that together with the SNARE proteins forms the essential machinery of fusion for synaptic exocytosis. It is a cytosolic protein of about 70 kDa (~600 aa residues) that in the PNS can be found in the entire axonal route. It has five functional domains (d1, d2a and d2b and d3a and d3b) which give to the entire protein its concrete functions (**Figure 8**).

7.1. Molecular role of SM proteins: Munc18-1/SNARE complex assemblies

Despite many years of intensive research there is still some controversy over the molecular mechanism of SM proteins (Rizo and Südhof, 2002; Toonen and Verhage, 2007; Südhof and Rothman, 2009; Carr and Rizo, 2010). Loss-of-function mutations for all different SM protein members show comparable phenotypes as they lead to very severe impairment of vesicle docking and fusion. This strongly suggests that all types of SM proteins are essential for the last step in vesicle trafficking. As outlined earlier, the core fusion machinery is through to consist of SNARE proteins that assemble between vesicle and target membrane, a reaction that eventually leads to membrane merger. The neuronal SM protein Munc18-1 was discovered as a binding partner of Syntaxin-1A, and when the

crystal structure of Munc18-1/Syntaxin-1A complex was solved, it was discovered that Munc18-1 arrests Syntaxin-1A in a tight closed conformation (Misura et al. 2000). Then this interaction was investigated in more detail. These studies revealed that Munc18-1 has been wrapped in a functionality paradox because of its interaction with Syntaxin-1A closed form. On the one hand, *in vitro* studies revealed that the binding of Munc18-1 to Syntaxin-1A prevented Syntaxin-1A from forming a SNARE complex with its partner SNAREs SNAP-25 and Syb-2 (Dulubova et al. 1999; Pevsner et al. 1994; Yang et al. 2000). On the other hand *in vivo* Munc18-1 knock-out mice studies revealed the SNARE doesn't form and the neurotransmission is completely omitted (more than even in SNAP-25 or Syb-2 knock-outs) (Gulyás-Kovács et al. 2007; Verhage et al. 2000). It was speculated that the true activity of Munc18-1 is to bind to the ensemble SNARE complex in order to help this process or to directly participate in membrane fusion (Shen et al., 2007; Rizo and Rosenmund, 2008; Deák et al., 2009; Südhof and Rothman, 2009).

The interactions between some of its domains result in an arch shape, which has been conserved through evolution. Domain 1 and 3a form a cavity that allows Syntaxin-1A closed form to bind in a tightly way as it is in contact with the N-peptide. At the same time, the N-peptide is also capable of binding the opposite surface (which strengthens the union). On the other side, when the SNARE complex binds Munc18-1, it does it through the 3a external surface or the same cavity. These multiple possibilities of union are thought to regulate different precise functions that can be either stimulatory or inhibitory (Rizo and Südhof, 2012; Rizo and Xu, 2015).

Moreover, several studies have converged on the conclusion that the essential stimulating function of Munc18-1 in secretion involves domain 3a (Boyd et al. 2008; Han et al. 2013, 2014; Hu et al. 2011; Parisotto et al. 2014). This is further supported by the effect of PKC phosphorylation of residues within the domain 3a, which promotes vesicle priming (Nili et al., 2006). This 3a domain may

undergo a conformational change from a folded-back "closed" helical hairpin to an extended "open" helical hairpin where the aa stretch from 324 to 339 extends helix 12. Thus, these conformational change in domain 3a can coincide with the transition from the closed to the open Syntaxin-1A and promote SNARE complex assembly (Parisotto et al. 2014) and vesicle priming (Munch et al., 2016). Moreover, helix 12 contains residues that interact with part of the syb-2 SNARE domain (Baker et al. 2015; Xu et al. 2010), raising the possibility that the extended helix forms a template to structure syb-2 (Parisotto et al. 2014).

It has been determined by multiple studies that Munc18-1 is implied in exocytosis by interacting with proteins basically in two ways. Different experiments have proposed many models to explain how Munc18-1 works. Nowadays is accepted a compilation of several of them (Rizo and Südhof, 2012; Rizo and Xu, 2015) which proposes that Munc18-1 has two principal roles. On the one hand, it clamps the NT release because it binds to closed Syntaxin-1A by its N-terminal domain H_{abc}. This stabilizes that protein but also inhibits the assembly of the SNARE complex and vesicle docking. On the other hand, when Ca^{2+} triggers neurotransmission, it also provokes an effect on Munc13, which causes the opening of Syntaxin-1A. Because of that, Munc18-1, which initially was bound to Syntaxin-1A, translocates itself to bind the heterodimer Syntaxin/SNAP-25 so, it binds to vesicle and terminal membranes implicated in the merge to help in the assembly of the complete SNARE complex. The translocation may be helped by interactions with the membranes or by allosteric activation and phosphorylations derived from PKCs activation (Dulubova et al. 2007; Südhof and Rothman 2009; de Vries et al. 2000). As a result, Munc18-1 is essential to permit the exocytosis by favoring the correct formation of SNARE but, at the same time, is a mechanism which permits an accurate regulation of the synaptic exocytosis by preventing the premature SNARE formation as it establishes an energy barrier (Dulubova et al. 2007; Jahn and Fasshauer 2012; Khvotchev et al. 2007; Shen et al. 2007).

Due to the importance of Munc18-1 in the modulation of synaptic exocytosis, it is necessary to guarantee the correct regulation of itself. To enable this regulation, Munc18-1 has two consensus sites that correspond to Serine residues (Ser-306 and Ser-313) which are a phosphorylation point for PKCs. It is thought that this phosphorylation procedure takes place during the depolarization of the membrane when the transmission impulse arrives at the terminal button. It is important to take into account that PKCs not only phosphorylate Munc18-1; instead, they also phosphorylate SNAP-25 and Syt1 and ion channels like voltage-gated K^+ and Ca^{2+} channels (Genc et al., 2014a).

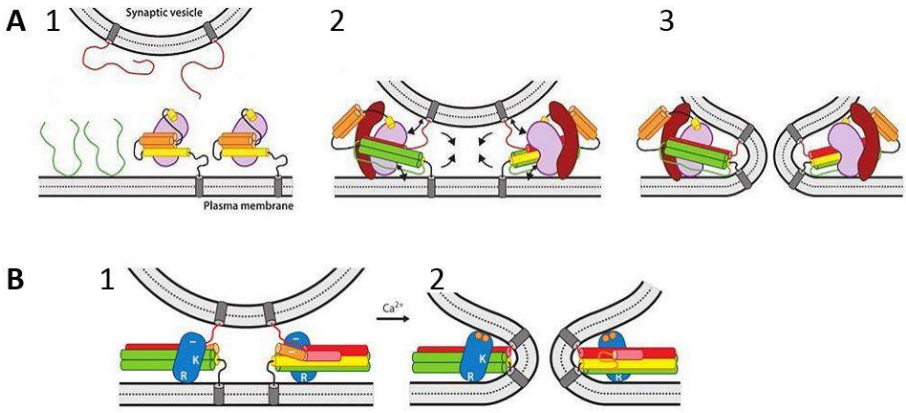

Figure 9. Schematic representation of membrane fusion machinery. Munc18-1 (purple), Syntaxin (yellow and orange), Synaptobrevin-2 (Syb-2, red), SNAP-25 (green), Munc-13 (dark red), Synaptotagmin-1 (Syt1, blue) and Complexin (Cplx, orange and pink). **A) 1.** Syb-2 and SNAP-25 are in a coiled coil form while Syntaxin is closed because of being associated with Munc18-1. **2.** Munc18-1 bound the partially assembled SNARE complexes while Munc13 permits the membranes to be closed together. **3.** The complete SNARE formation permits the fusion pore to open. **B) 1.** Syt1 and Cplx are linked to the SNARE complex. **2.** Once calcium influx arrives Cplx and Syt1 change their conformation and favour membranes fusion. Source: Adapted from Rizo and Xu 2015.

8. REGULATION OF EXOCYTOSIS: ROLE OF PROTEIN KINASES C

SNARE proteins themselves are not capable to complete neurotransmitter release; instead, other molecules are involved. Firstly, cytoskeleton and motor proteins have to be bound to SVs to transport them to the AZs (Bombardier and Munson, 2015). Moreover, it has been shown that the regulation of exocytosis and various forms of synaptic plasticity is mediated by different proteins such as protein kinases A and C, as protein phosphorylation has a key role in exocytosis (Morgan et al., 2005).

PKCs affect exocytosis through the phosphorylation of different proteins as voltage-gated K^+ channels and Ca^{2+} channels (Zamponi et al., 1997), maintaining vesicle pools and phosphorylating the SNARE complex proteins SNAP-25, Syntaxin-1A, Syt1 (Shimazaki et al., 1996; Hilfiker et al., 1999) and the complementary proteins. One of those complementary proteins that is especially important is Munc18-1 (introduced before), which has to be phosphorylated by PKC *in vitro* on Ser-306 and Ser-313 to permit NT release (Tanaka and Nishizuka, 1994; Majewski and Iannazzo, 1998; Barrett and Rittenhouse, 2000; Leenders and Sheng, 2005a).

8.1. Protein kinase C

8.1.1. PKC structure and function

Protein kinases C are members of the superfamily serine/threonine (Ser/Thr) protein kinase enzymes, the AGC kinases, which are widely distributed in all cells (Lanuza et al. 2014; Obis et al. 2015a; Santafé et al. 2007). These proteins can exist both in a soluble state in the cytosol and as a membrane-anchored protein. PKC members play a key role in the regulation of multiple cellular pathways including proliferation, migration, differentiation, apoptosis, platelet activation, rearrangements of the actin cytoskeleton, ion channel modulation, secretion, neurotransmission and neuronal plasticity (Antal and Newton 2014;

Lanuza et al. 2014; Tanaka and Nishizuka 1994; Tomàs et al. 2014). Given its relevant role to cellular signaling mechanisms, the study of the intracellular pathways in where they are involved is particularly important. Moreover, PKCs are remarkable targets to provide pharmacological tools for fighting against pathologies (Blumberg, 1988) due to the fact that they are activated by tumor-promoting phorbol esters such as phorbol 12-myristate 13-acetate (PMA) which mimics their activation mechanism (Castagna et al., 1982; Ashendel, 1985; Steinberg, 2008).

PKCs were originally defined as proenzymes needed to be proteolitically cleaved to acquire its kinase activity and the ability to phosphorylate substrates. Then, it was shown that PKCs could be activated by DAG in a Ca^{2+} -dependent manner (Inoue et al., 1977; Takai et al., 1979). Subsequently, it was established that PKCs consists of 10 isozymes divided into three sub-families based on their second messenger mode of regulation (Steinberg, 2008).

- **Classical PKC (cPKC) sub-family (or conventional)**: comprises PKCα, βI, βII and γ isoforms that require DAG as the primary activator along with phosphatidylserine (PS) and Ca^{2+} as cofactors of activation.
- **Novel PKC (nPKC) sub-family:** comprises PKCδ, PKCε, PKCθ and PKCη and are regulated by DAG and PS but do not require Ca^{2+} for activation.
- **Atypical PKC (aPKC) sub-family:** comprises PKCζ and PKCι (PKCλ in mouse) and their activity is stimulated only by PS and not by DAG and Ca^{2+}.

All protein kinases share a similar structure. In the C-terminal part, there is a highly conserved catalytic kinase domain with a motif for ATP/substrate-binding and catalysis. In the N-terminal there is the regulatory domain which contains the C1 and C2 motifs that bind to a pseudosubstrate (a mimetic peptide which resembles a PKC substrate but that contains an alanine inset of the Ser/Thr phosphoacceptor site). The regulatory domain is isoform-specific and allow PKCs to assemble specific responses to different stimuli. It takes part in maintaining the enzyme in an inactive conformation and serves as a target identifier for cellular

locations. Moreover, it mediates protein-protein interactions. These two domains bind together by a hinge region, which is composed of five variable regions (termed V1-V5) which are also isoform-specific.

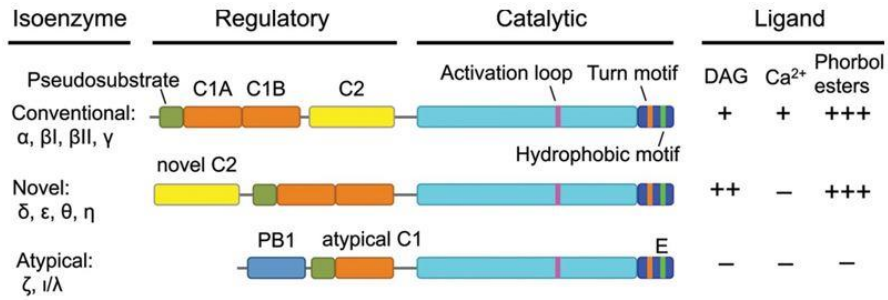

Figure 10. Primary structure and relative ligand-responsiveness of PKC family proteins. Domain structure of PKC family members, showing autoinhibitory pseudosubstrate segment (olive green), C1 - domain (orange), C2 domain (yellow), kinase core (cyan) and C-terminal tail (dark blue); the activation loop (pink), turn motif (orange) and hydrophobic motif (green) phosphorylation sites are also indicated. The ligands that bind to each subfamily, along with their relative affinities, are indicated. Source: Wu-zhang and Newton, 2013.

8.1.2. Signal propagation

In order for PKC achieve full catalytic competency to effectively transduce extracellular signals to downstream targets, PKC must be properly primed and positioned for optimal signaling. Perturbation of the phosphorylation state, conformation, or localization of PKC can disrupt these signaling events, leading to altered physiological states found in some diseases (Blumberg, 1988).

Before PKC responds to lipid second messengers the enzyme must undergo a multi-step maturation process (priming), corresponding to three properly ordered phosphorylations. These priming phosphorylations correspond to different regions of the catalytic domain: the activation loop (AL), turn motif (TM), and hydrophobic motif (HM) in cPKCs and nPKCs. For aPKC, only AL and TM phosphorylations are required, as the HM contains a phosphomimetic glutamate (Keranen et al. 1995; Newton 2001). AL phosphorylation is catalyzed *in vivo* by 3-

phosphoinositide dependent kinase 1 (PDK1) and is required for maximal PKC catalytic activity (Dutil et al. 1998; Le Good et al. 1998). Autophosphorylation of the TM and HM is triggered after PDK1 phosphorylation of AL. Priming phosphorylations contribute to the formation of a catalytically competent kinase structure, ready to be activated through the modulation of its regulatory domain. Loss of one priming phosphorylation sensitizes other priming sites, which triggers a general destabilization of the fold of the kinase domain (Bornancin and Parker, 1996). Once PKC is fully primed, the pseudosubstrate keeps PKC inhibited until required. In summary, PKC catalytic activity is dependent on two main factors: the priming of the AL, TM and HM phosphorylation sites and the release of the autoinhibitory pseudosubstrate from the substrate-binding cleft.

The activation mechanism of PKCs in cells occurs when they are translocated from the cytosol (where they are inactive with the pseudosubstrate docked in the substrate binding cleft) to cellular membranes (Dutil and Newton, 2000). PKC activation is triggered by the union of different ligands to their receptors that resulted in phospholipase C (PLC) activation. These enzyme hydrolyzes PIP_2 to generate the membrane-bound second messenger DAG and inositol trisphosphate (IP_3) (Nishizuka, 1988). IP_3 mobilizes intracellular Ca^{2+}. These second messengers, Ca^{2+} and DAG, initiate the membrane translocation and activation of PKC (König et al. 1985; Newton 1993). High [Ca^{2+}] affect numerous intracellular processes including the migration of some PKC isoforms to the PM, where DAG can activate them. Many PKCs are also pharmacologically activated by tumor-promoting phorbol esters such as PMA, which are potent analogues of DAG, that anchor PKCs in their active conformations to membranes (Sharkey et al. 1984; Steinberg 2008)

cPKC and nPKC isoforms contain two C1 domains (C1A and C1B) in their regulatory domain. These domains bind the second messenger DAG, promoting their association with hydrophobic lipids in the PM (Kazanietz et al., 1995; Mosior and Newton, 1995). Phorbol ester (PE) compounds bind the C1 domain in a similar

manner to DAG (Sharkey et al. 1984). The aPKC also contains a C1 domain, referred to as an atypical C1 domain because it does not respond to either DAG or PE (Ono et al., 1989; Ways et al., 1992).

The cPKC and nPKC isoforms also contain a C2 domain. The C2 domain of the cPKCs associates with the acidic phospholipid PS at the PM in a Ca^{2+}-dependent manner (Bazzi and Nelsestuen, 1990; Luo et al., 1993). The nPKC C2 domain also associates with acidic phospholipids in the PM, though the nPKC C2 domain lacks a Ca^{2+} -binding site and its affinity for PS is therefore Ca^{2+}-independent (Ponting and Parker, 1996).

In both cPKC and nPKC isozymes, the second messenger-bound C1 and C2 domains co-operate in localizing PKC to the PM. This results in the release of the pseudosubstrate from the substrate-binding cleft. The pseudosubstrate then likely associates with acidic phospholipids in the PM, stabilizing the active PKC conformation (Mosior and McLaughlin, 1991).

For cPKC and nPKC isozymes, once DAG is metabolized, the PKC regulatory domains can be released from the PM and once again allow autoinhibition of PKC in the cytosol (Bazzi and Nelsestuen, 1989). PKC is also susceptible to proteolytic cleavage when membrane-bound, which produces a constitutively active PKC kinase domain (Inoue et al., 1977). Additionally, the PKC kinase domain phosphorylations are susceptible to phosphatase attack by PP2A (Hansra et al., 1996) and PHLPP (Gao et al. 2008) at the membrane.

In summary, in the case of cPKCs, Ca^{2+} binds the C2 domain and pretargets PKC to the membrane, allowing the C1 domain to more effectively find its membrane-embedded ligand, DAG. The coordinated engagement of both the C1 and C2 domain on membranes provides the energy to release the autoinhibitory pseudo-substrate (Xu et al. 2004). Thus, when PKC has an open conformation binds its substrates and initiates downstream signaling events. The nPKCs, due to not having a calcium-binding C2 domain, and therefore lacking the membrane

mechanism of pretarget, these isoforms compensate it by having a C1 domain that binds to membranes containing DAG with higher affinity than the C1 domain of cPKCs, being the C1B domain the main determinant of membrane binding. Finally, the aPKCs have only a single C1 domain that binds PIP_3 or ceramide, but not DAG or calcium (Antal and Newton 2014; Newton 2009).

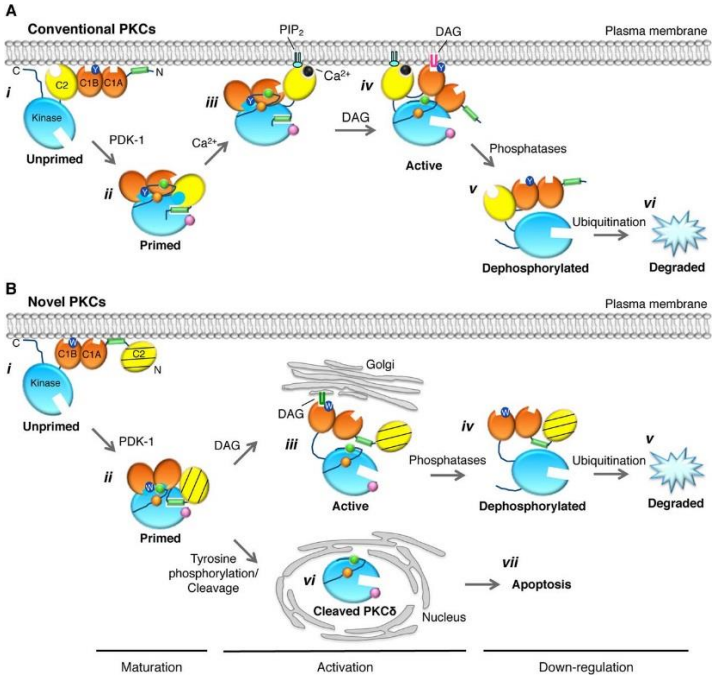

Figure 11. Regulation of conventional and novel protein kinase C. A) Life cycle model of cPKC. (i) Unprimed cPKC is in a membrane-associated, open conformation in which C1A, C1B and C2 domains are fully exposed. **(ii)** Upon priming phosphorylation (P) at its AL (pink circle) by PDK-1, followed by P at the TM (orange circle) and the HM (green circle), cPKC adopts a closed conformation in which the C2 domain interfaces with the kinase domain and traps the pseudosubstrate into the substrate-binding site, both C1 domains become masked, and the primed enzyme localizes to the cytosol. This ensures efficient suppression of activity in the absence of appropriate stimuli. **(iii)** In response to agonists that promote PIP_2 hydrolysis, cPKC is recruited to the PM in a Ca^{2+} -dependent manner. **(iv)** Membrane-targeted PKC binds DAG, predominantly via the C1B domain, thereby activating PKC. **(v)** Dephosphorylation of activated cPKC allows it to regain the open conformation of unprimed PKC. **(vi)** cPKC-ubiquitination leads to its degradation. **(B) Life cycle model of nPKC. (i)** Unprimed nPKC is also in an open conformation that associates with membranes. **(ii)** Priming Ps induce a closed conformation with both C1 domains masked. **(iii)** In response to agonists that produce DAG, nPKC is recruited to and activated at the DAG-rich Golgi via its

C1B domain. **(iv)** Activated nPKC is dephosphorylated, **(v)** ubiquitinated and degraded. **(vi)** PKCδ can also be activated by tyrosine P and caspase cleavage. **(vii)** Nuclear-localized PKCδ can induce apoptosis. (Activation loop (AL), turn motif (TM), and hydrophobic motif (HM)). Source: Antal and Newton 2014.

8.1.3. Scaffolding proteins: RACKs

Given the large overlap in potential PKC isoform substrates, the functional specificity in PKC signaling is achieved by proper spatial localization (Yedovitzky et al., 1997). Some isoforms of the PKC family are specifically related with the release of neurotransmitters in the presynaptic terminal while others are commonly found in the postsynaptic component regulating AChRs stability (Lanuza et al. 2014; Obis et al. 2015b). This specific distribution is achieved by scaffolding proteins, which position PKC near its activators and substrates or at a particular cellular compartment, which allow for isozyme-specific signaling. The proteins responsible for binding to activated PKC and thus regulating its activity are RACKs (receptors for activated C-kinase) (Morgan et al. 2005; Snyder et al. 2006). This interaction is mediated by the C2 domain (Kheifets and Mochly-Rosen, 2007).

RACKs are very important for distribution and classification of the PKCs, and also are the molecules which permit the binding of phosphorylated PKC to the membrane so they can be active and do their function. Once PKCs are mature and activated, phosphorylated PKCs can bind to the membrane through these RACK proteins and, from there, they can phosphorylate their different target proteins. Different PKC isozymes bind to specific RACKs to target them to their proper location for cellular function. Mutation of the RACK binding site alters PKC activation in cells (Kheifets and Mochly-Rosen, 2007). RACKs not only bind PKC but also other signaling molecules such as PLCγ, Src, and integrins (Schechtman and Mochly-Rosen, 2001). By serving as adaptors for other proteins, RACKs facilitate signaling by bringing enzymes in close proximity with their substrates or their activators.

The understanding how the interaction between PKC and RACK is mediated, and due to the importance of the therapeutic potential of PKC in different diseases, has allowed designing different activators and inhibitors of PKC over the years. In order to achieve a better understanding of the specific function of each PKC isoform object of study, different inhibitors have been widely used in this thesis (see subsection *Reagents* in *Material and Methods* section).

8.2. PKCs in the neurotransmission

Nowadays, the exocytosis process in the NMJ is quite well established (Rizo and Xu, 2015). It is also well documented that presynaptic protein phosphorylation by PKCs is an important mechanism that regulates NT release (Genc et al. 2014; Hilfiker and Augustine 1999; Katayama et al. 2017; Korogod et al. 2007; Leenders and Sheng 2005; Santafé et al. 2005, 2006; Vaughan et al. 1998) but there are still doubts in the precise steps of these pathways. At the NMJ, whereas PKA is tonically coupled to potentiate ACh release, PKC couples in a regulated manner when several activity demands are imposed (Besalduch et al. 2010; Santafé et al. 2005, 2006, 2009). The fine regulation of neurotransmission in the motor nerve terminals is modulated by presynaptic mAChRs (Garcia et al. 2005; Nadal et al. 2016; Santafé et al. 2006) adenosine receptors (Correia-de-Sá and Ribeiro 1994; Garcia et al. 2013; Santafe et al. 2015) and neurotrophin receptors (Hurtado et al. 2017a; Pitts et al. 2006; Tomàs et al. 2014). In addition, the way that a synapse works is largely the logical outcome of the confluence of these metabotropic-signaling pathways on PKC (Catterall 1999; Obis et al. 2015a,b; Tanaka and Nishizuka 1994; Tomàs et al. 2014). As a consequence, it is sure that PKC family is highly involved in the regulation of neurotransmission and because of that it is crucial to know which PKC isoforms are involved in it, how do they work and where are located at the nerve terminal.

In the NMJ, synaptic activity depends on the influx of calcium among other molecules. Because of that and despite of the remaining doubts in the precise

steps, it has been proved that neurotransmission is regulated by presynaptic classical and novel PKC isoforms (Besalduch et al. 2010; Santafé et al. 2006; Santafé et al. 2005). These isoforms are cPKCβI and nPKCε, which are exclusively located in the presynaptic terminal of the NMJ. Their presence and function are regulated by postsynaptic contractile activity induced by presynaptic activity, due to a neurotrophic feedback through BDNF/TrkB signalling from the postsynaptic component (Besalduch et al. 2010; Hurtado et al. 2017a; Obis et al. 2015a,b).

8.3. Roles of cPKCβI and nPKCε at the NMJ

The protein kinase C beta I (cPKCβI) isozyme belongs to the family of classical PKC which require PS, DAG, and Ca^{2+} for their activation. It has been shown that increased synaptic activity is associated with an increase in the activation of classical PKCs and their phosphorylation and that muscle contraction is a necessary condition to increase cPKC isozymes in the nerve terminal. It has been shown that cPKCβI is exclusively located in the presynaptic terminal (Besalduch et al., 2010), and under synaptic activity condition increases its phosphorylation in the membrane fraction, where is active (Hurtado et al. 2017b). Once that, cPKCβI is able to enhance neurotransmission, being directly involved in modulation of calcium-depending ACh release at the NMJ.

The protein kinase C epsilon (nPKCε) belongs to the novel PKC isozyme family, characterized for being Ca^{2+}-independent and DAG-sensitive Ser/Thr kinases. nPKCε is highly expressed in the brain and is the most abundant PKC in the presynaptic terminal, where it has been identified to modulate NT release (Shirai et al. 2008). This PKC isoform is involved in regulating several cellular functions like proliferation, differentiation, gene expression, muscle contraction, adaptation to mechanical force, inflammatory and immune response. Because of this widespread functionality, nPKCε can be found in most tissues but its presence is greater in neuronal, hormonal and immune cells (Akita 2002), being especially important in the brain and in the PNS. The nPKCε is exclusively located in the

presynaptic component of the NMJs, regulated by synaptic activity involving muscle contraction through TrkB function to enhance phosphorylation of MARCKs (myristoylated alanine-rich C-kinase substrate) and is involved in ACh release (Akita, 2002).

To be able to respond to second messengers, both cPKCβI and nPKCε have to be phosphorylated at three points. If they are not or are under-phosphorylated, it is immature and remains anchored via its catalytic domain to proteins that keep it inactivated. When the isoform is mature, it can be activated by different second messengers including DAG, PIP_3 or Ca^{2+} by physiological stimuli (Akita 2002). In the case of cPKCβI, it has to be translocated to the membrane and be phosphorylated by the PDK1 under synaptic activity conditions to be able to respond to second messengers (Akita, 2002) and then to trigger its function that is to enhance neurotransmission.

Therefore, we suggest both nPKCε and cPKCβI isozyme are good PKC isoform candidates that could be related with the phosphorylation of Munc18-1, SNAP-25 and Synaptotagmin in the presynaptic terminal. Because of this, they would have an effect on their activity and, consequently, would have an important role in regulating the formation of the SNARE complex and, therefore, modulating transmitter release.

9. RETROGRADE NEUROTROPHIC CONTROL

Nerves and skeletal muscles interact via two modes of communication: electrical activity and neurotrophic regulation (Baldwin et al. 2013; Cisterna et al. 2014). Nerve impulses generated in the CNS trigger muscle contraction via electromechanical coupling. On the other hand, neurotrophic control acts via the release of neurotrophic factors, including neurotrophins, and regulates the

development, differentiation, survival and function of the nerve terminal (Wang et al. 1995; Mantilla et al. 2004; Pitts et al. 2006).

Neurotrophins are a family of closely related proteins that were identified initially as survival factors for sensory and sympathetic neurons, and have since been shown to control many aspects of survival, development and function of neurons in both the PNS and CNS (Lewin and Barde 1996; Reichardt 2006). Nerve growth factor (NGF), brain-derived neurotrophic factor (BDNF), neurotrophin-3, and neurotrophin-4 (NT-3, NT-4) constitute the protein family of mammalian neurotrophins. They are initially synthesized as precursor forms, or proneurotrophins, that are cleaved to release C-terminal mature forms (Maisonpierre et al., 1991; Mowla et al., 2001). Neurotrophins interact with two distinct classes of transmembrane receptors: the smaller low affinity $p75^{NTR}$ neurotrophin receptor and the tropomyosin-related kinase (Trk) receptor, often with opposite functional outcomes. These two classes of receptors are activated preferentially by proneurotrophins and mature processed neurotrophins, respectively. However, both types of receptors also possess neurotrophin-independent signaling functions (Hempstead, 2006). $P75^{NTR}$ receptor belongs a tumor necrosis factor (TNF) superfamily that binds all neurotrophins. Trk receptors belongs a superfamily of three high affinity receptor tyrosine (Tyr) kinases (TrkA, TrkB and TrkC) which constitutes the second major class of neurotrophin receptors in mammals and are well-known, each of which can be activated by one or more of four neurotrophins (**Figure 12**). NGF preferentially binds TrkA, BDNF and NT4 bind TrkB, and NT-3 binds TrkC (and TrkA to a lesser extent) (Bothwell, 2016).

Over the years, it has been shown that neurotrophic signaling plays a key role in the structural and functional properties of motor units. Moreover, it is well-known that BDNF/TrkB signaling pathway acutely regulates essential aspects of the synaptic transmission at the adult NMJs (Mantilla et al. 2014; Mantilla and Ermilov 2012) including NT release through PKC activity (Garcia et al. 2010; Obis et al. 2015b; Santafé et al. 2014).

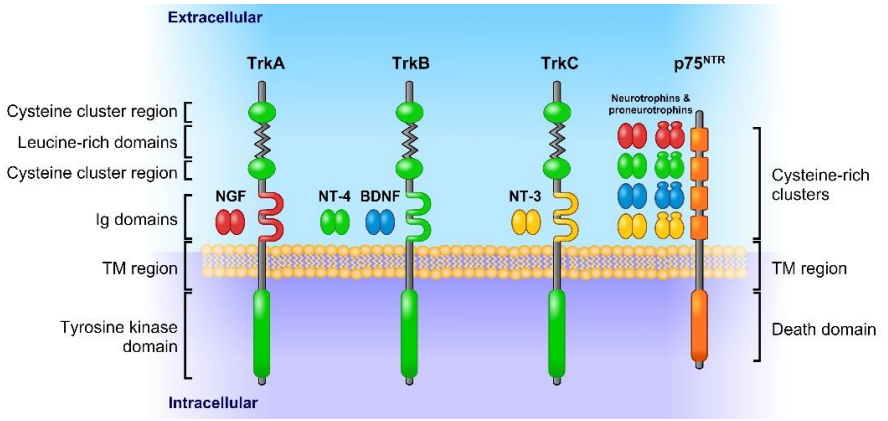

Figure 12. Neurotrophins and their receptors. Scheme showing the common structure and ligands of Trk and $p75^{NTR}$ receptors. Trk: Tropomyosin-Related Kinase; NGF: Nerve Growth Factor; BDNF: Brain-Derived Neurotrophic Factor; NT: Neurotrophin; Ig: Immunoglobulin; TM region: Transmembrane region.

9.1. Brain derived neurotrophic factor

Brain-derived neurotrophic factor (BDNF) is a member of the neurotrophic factor family that plays a key role in regulating survival, growth and maintenance in a variety of neurons including dorsal root ganglion cells (Acheson et al. 1995) hippocampal and cortical neurons (Acheson et al., 1995), and motoneurons (Kishino et al. 1997). Moreover, BDNF is known to play an important role in synaptic function. BDNF is secreted in an activity- and Ca^{2+}-dependent manner. The activity-dependent secretion of BDNF may be critically involved in controlling synaptic transmission and long-term synaptic plasticity and may represent an important mechanism underlying local and synapse-specific modulation by BDNF (Kishino et al., 1997). BDNF can induce its own release *via* a positive feedback loop including stimulation of TrkB receptors, activation of PLCγ and mobilization of intracellular calcium stores (Canossa et al. 2001). Stimulation of metabotropic glutamate receptors can also activate PLCγ and induce calcium release from intracellular storages via IP_3 resulting in BDNF release (Canossa et al., 2001).

BDNF exerts its biological effects as a non-covalently linked homodimer with a molecular weight of approximately 30kDa (Canossa et al., 2001). It is synthesized as pre-proBDNF, a precursor protein that is further processed in the endoplasmic reticulum to proBDNF (Greenberg et al. 2009). The proBDNF isoform is then N-glycosylated and glycosulfated (Greenberg et al., 2009). The glycosylation increases the stability of proBDNF during processing and subcellular trafficking. The pro-domain participates in the proper folding and intracellular sorting of BDNF (Mowla et al., 2001). The translated protein is transported to the Golgi for sorting into either constitutive or regulated secretory vesicles. ProBDNF is subsequently cleaved to produce the mature monomeric form (mBDNF) of approximately 13 kDa (Blum and Konnerth 2005), inside the cell in *trans*-Golgi network or post-Golgi compartments by pro- convertases and furin, or outside the cell by matrix metalloproteinases (MMP-7) or plasmin (Blum and Konnerth, 2005). The processing enzymes in the regulated and constitutive secretion pathways are different and the cleavage of BDNF occurs in different subcellular compartments. This post-secretory proteolytic processing is essential for efficient TrkB receptor activation. The two isoforms induce different and even opposite functions by binding the two cell surface receptors, the low-affinity $p75^{NTR}$ or TrkB receptor. Specifically, proBDNF has more affinity for $p75^{NTR}$ receptor and mBDNF binds preferentially TrkB receptor (Seidah et al., 1996; Pang et al., 2004).

In vivo BDNF is co-expressed with the cleaved pro-peptide in dense core vesicles presynaptically in the hippocampus, indicating that BDNF is cleaved inside the vesicles and possibly released together with the cleaved pro-domain (Dieni et al. 2012). Since there are enzymes that are able to cleave proBDNF to mBDNF also extracellularly, it has been debated whether proBDNF can be released from the neurons or if it is processed to mature BDNF in secretory vesicles before release.

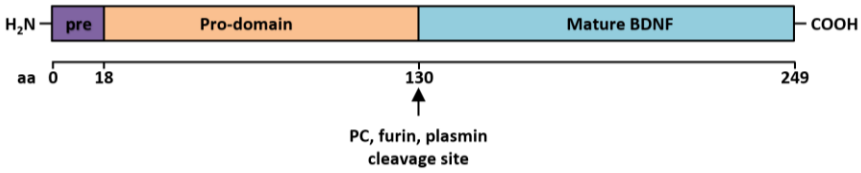

Figure 13. Brain-derived neurotrophic factor. Scheme of the different domains of BDNF along the length of its amino acid (aa) sequence (overall 249 aa; pre-domain: 18 aa; pro-domain: 112 aa; mature BDNF: 119 aa). Different types of intracellular protein convertases (PCs), furin, and plasmin can cleave at position 130 to pro- into the mature form, respectively.

9.2. Tropomyosin receptor kinase B

TrkB receptor is widely expressed in both the peripheral and central nervous systems. It is essential for normal function of the mammalian brain. It has three isoforms generated by alternative splicing: TrkA, TrkB and TrkC. All Trk receptors have three main parts: extracellular, transmembrane and intracellular domains, and are distinguished among other receptor tyrosine kinases by their extracellular domain. The intracellular domains of TrkB include a tyrosine kinase domain and tyrosine motifs. Tyrosine phosphorylation controls the kinase activity of TrkB receptors and can regulate the binding of adaptor molecules to the receptor. The catalytic domain inside the tyrosine kinase domain is highly conserved among all the receptor tyrosine kinases (Dieni et al., 2012). The extracellular domain is composed by an array of three leucine-rich repeats (LRRs), flanked by two cysteine-rich domains (C1 and C2) and two immunoglobulin-like domains (Ig1 and Ig2). The IgG-like domain adjacent to the transmembrane domain acts as a binding site for neurotrophins and determines the ligand specificity of the receptor (Urfer et al. 1995). Neurotrophin binding to this domain can induce activation of the catalytic tyrosine kinase domain of the receptor. The other IgG domain and the leucine- and cysteine-rich repeats also seem to participate in ligand binding either directly or by inducing conformational changes (Urfer et al., 1995). The LRRs are thought to participate in protein-protein interactions. Specifically the second LRR of TrkB seems to bind BDNF (Windisch et

al. 1995). Co-expression of $p75^{NTR}$ can alter the extracellular sites of TrkB required for BDNF binding (Windisch et al., 1995). In the absence of $p75^{NTR}$, BDNF binds to the IgG-C2 domain of TrkB but when $p75^{NTR}$ and TrkB are expressed together, BDNF binding requires the LRR and the cysteine 2 domains. Juxtamembrane domain (short sequence of about 80 aa located between the transmembrane and tyrosine kinase domain) of TrkB regulates the internalization of the receptor after ligand binding (Zaccaro et al., 2001). The extracellular domain of TrkB can be N-glycosylated, and this glycosylation is required for the localization of the Trk receptors to the cell membrane and can inhibit ligand-independent activation of the receptor (Sommerfeld et al., 2000).

There are several alternatively spliced isoforms of TrkB with the same affinity to neurotrophins, the full length receptor (TrkB.FL) which contains an intracellular tyrosine kinase domain and two truncated TrkB isoforms lacking it (TrkB.T1 and TrkB.T2) (Watson et al., 1999). TrkB.FL transduces the crucial effects of BDNF signal via Ras-ERK, PI3K, and PLCγ. TrkB.T2 is a variant mainly predominant in the brain tissue and does not appear to have individual signaling ability (Stoilov et al. 2002). TrkB.T1 form can bind to neurotrophins and is internalized upon ligand binding (Biffo et al. 1995) but due to the lack of a kinase domain cannot signal to the cytoplasm (Biffo et al., 1995). In addition, TrkB.T1 is the main truncated isoform in the skeletal muscle and some studies suggest unique signaling roles for TrkB.T1, for example, by modulating Ca^{2+} signaling mechanisms (Rose et al. 2003). Other evidence suggests that TrkB.T1 acts in a dominant negative fashion to decrease signaling through TrkB.FL (Rose et al., 2003). Recent studies demonstrate that the ratio between TrkB.FL and TrkB.T1 determines the net effect of BDNF signaling at neuromuscular system (Eide et al., 1996; Gonzalez et al., 1999; Haapasalo et al., 2001; Dorsey et al., 2012).

TrkB receptor can be quickly translocated to the membrane from intracellular pools by BDNF stimulation or as a result of increased neuronal activity. TrkB can also be inserted to the cell membrane after intracellular

transactivation (Puehringer et al. 2013). In addition to the insertion of TrkB into the cell membrane, neuronal activity and increase in intracellular calcium concentration regulate the internalization of TrkB receptors (Puehringer et al., 2013). The kinetics of the receptor insertion to the membrane and its subsequent internalization can define the signaling pathways and other downstream actions of the receptor. Inserting more TrkB receptors to the cell membrane compensates for the endocytosis occurring after ligand binding, and the TrkB signaling shifts from a transient event to sustained state (Du et al., 2003).

9.3. BDNF/TrkB downstreaming signaling pathway

Activation of downstream signaling pathways via TrkB starts by BDNF binding to the Ig domain (Ig2) closest to the *trans*-membrane domain of TrkB. The BDNF homodimer binding to the TrkB extracellular region promotes receptor dimerization, which activates the intrinsic tyrosine kinase domain, leading to autophosphorylation on specific tyrosine residues in the activation loop (Y701, Y706 and Y707, accordingly to the sequence of TrkB in rat) (Du et al., 2003; Zhao et al., 2009). Phosphorylation of these residues can leads to an open conformation of the receptor resulting in transphosphorylation and allowing the access of substrates to the kinase. The active tyrosine kinases in turn phosphorylate two additional phosphorylation sites: Y515 and Y816 (Middlemas et al. 1994; Segal et al. 1996). These two activated sites induce conformational changes and serve as docking sites for different cytoplasmic molecules and signaling enzymes triggering various parallel signal transduction cascades with distinct functions. Three main pathways are regulated by the activation of TrkB through these two activated sites (**figure 14**): (i) phosphatidylinositol-3 kinase – Akt (PI3K/Akt) (Atwal et al. 2000), (ii) Ras-mitogen-activated protein kinase (Ras/MAPK) (Atwal et al., 2000), and (iii) PLCγ (Thomas et al., 1992), being phosphorylated Y516 (pY516) which actives the two first pathways and phosphorylated Y817 (pY817) which activates PLCγ pathway. These downstream signaling pathways mediate neuron outgrowth, neuronal differentiation or survival (Vetter et al., 1991).

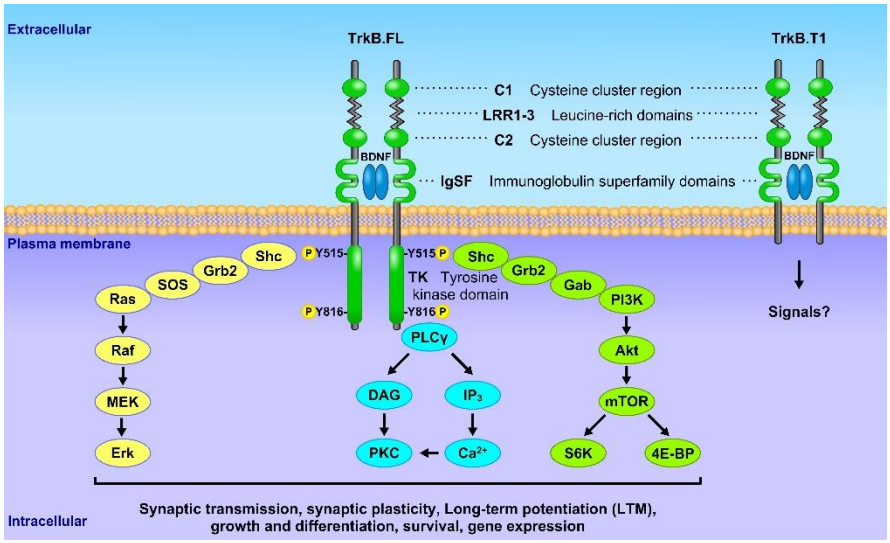

Figure 14. The major signaling pathways elicited by brain-derived neurotrophic factor (BDNF) through TrkB receptor. TrkB.FL receptor has an extracellular ligand-binding domain, a singular transmembrane region, and an intracellular region. BDNF binds to the extracellular domain of TrkB forming homodimers to activate downstream intracellular signaling cascades. In concrete, TrkB.FL triggers Shc-Ras-MAPK, phospholipase C gamma (PLCγ)- protein kinase C (PKC) and phosphatidyl inositol-3 kinase (PI3K)-AKT pathways. On the right, TrkB.T1 is depicted and lacks an intracellular tyrosine kinase domain.

9.4. Exercise modulation of BDNF/TrkB neuromuscular signaling

Nowadays there are strong evidence that suggests the exercise training provides many benefits to CNS health, including the improvement of synaptic function (Pattarawarapan and Burgess, 2003). In this context, it is well accepted that BDNF plays a key role in mediating the benefits of exercise (Gomez-Pinilla and Hillman 2013; Gomez-Pinilla et al. 2008; Neeper et al. 1995; Vaynman et al. 2006; Zoladz and Pilc 2010). Although BDNF is secreted in an activity-dependent manner (Lu 2003) and its expression in rodent spinal cord and skeletal muscle increases after exercise are required basal levels of neuromuscular activity to maintain normal levels of BDNF in the neuromuscular system (Gomez-Pinilla et al. 2001; Gomez-Pinilla et al. 2002; Gomez-Pinilla et al. 2012). Recent studies of cultured myotubes have shown to produce BDNF after contraction, suggesting a postsynaptic origin of this neurotrophin (Matthews et al. 2009). Recently, it has

been clarified that in the neuromuscular system *in vivo* BDNF is enhanced by presynaptic activity and by the resulting muscle contraction itself (Matthews et al., 2009). Furthermore, exogenous BDNF increases evoked ACh release at the NMJ and the TrkB receptor is normally coupled to this process (Garcia et al. 2010; Mantilla et al. 2004; Santafé et al. 2014). Together, this and other findings support that neuromuscular activity promotes BDNF/TrkB signaling to regulate neuromuscular function (Dorsey et al. 2012; Hurtado et al. 2017a; Kulakowski et al. 2011).

UNIVERSITAT ROVIRA I VIRGILI
EFFECTS OF NEUROMUSCULAR ACTIVITY COUPLED TO BDNF/TRKB SIGNALING ON THE EXOCYTOTIC PROTEINS MUNC18-1 AND SNAP-25 THROUGH NPKCE AND CPKCSSI
Anna Simó Ollé

II. HYPOTHESIS AND OBJECTIVES

UNIVERSITAT ROVIRA I VIRGILI
EFFECTS OF NEUROMUSCULAR ACTIVITY COUPLED TO BDNF/TRKB SIGNALING ON THE EXOCYTOTIC PROTEINS MUNC18-1 AND SNAP-25 THROUGH NPKCE AND CPKCSSI
Anna Simó Ollé

1. HYPOTHESIS

Preceding this study, other studies have described the relation between neurotransmission and PKC activity, which, at the same time, are thought to be modulated by pre- and postsynaptic activity in the neuromuscular junction of skeletal muscles. From that premise, we hypothesize that presynaptic and postsynaptic activity regulate the phosphorylation of Munc18-1 and SNAP-25, which play a key role in synaptic vesicle exocytosis. We also hypothesize that this modulation takes place through PKC activity, giving special attention to the exclusively presynaptic isoforms nPKCε and cPKCβI. Moreover, the last one has been related with BDNF/TrkB signaling pathway and, therefore, these could also be involved in Munc18-1 and SNAP-25 regulation.

In order to determine this hypothesis, our first objective is to determine the presence of Munc18-1 and SNAP-25 in the peripheral nervous system and their location in the presynaptic terminal to reaffirm their function in the neurotransmission. Then, we will determine if Munc18-1 and SNAP-25 levels are affected after electrical stimulation resulting, or not, in muscle contraction. This will allow us to determine whether Munc18-1 and SNAP-25 are modulated by both synaptic activity and muscle contraction.

Furthermore, because Munc18-1 and SNAP-25 have to be phosphorylated to be active, we will determine whether the presynaptic and/or postsynaptic activity regulates their phosphorylation. Next, we will determine whether Munc18-1 and SNAP-25 phosphorylation depends on Ca^{2+} and if they are enhanced when PKC family is activated by phorbol esters in the NMJ. Additionally, we will identify whether Munc18-1 and SNAP-25 phosphorylation is related with the PKC isoforms nPKCε and or cPKCβI, which have been demonstrated to be essential for neurotransmission at the NMJ.

Finally, we will determine whether BDNF/TrkB signaling pathway, which is enhanced by synaptic activity and directly related with the cPKCβI isoform in the neuromuscular system, regulates the phosphorylation levels of Munc18-1 and SNAP-25 proteins and whether they are related or not with synaptic activity induced in the skeletal muscle.

2. OBJECTIVES

General objective

The main objective of this thesis is to determine how the phosphorylation of the exocytotic proteins Munc18-1 and SNAP-25 is modulated by synaptic activity and muscle contraction through the cPKCβI and nPKCε isoforms and TrkB signaling at the neuromuscular junction.

Specific objectives

1. To determine the expression, location and regulation by the PKC-activators calcium and PMA of Munc18-1 and SNAP-25 and their phosphorylated forms in the skeletal muscle.

2. To determine whether the synaptic activity modulates Munc18-1, SNAP-25 and their phosphorylation levels in the skeletal muscle through nPKCε and cPKCβI isoforms and BDNF/TrkB signaling pathway.

2.1. To determine whether synaptic activity regulates Munc18-1, SNAP-25 and their phosphorylation levels.

2.2. To determine whether nPKCε and cPKCβI isoforms and their interaction regulate the phosphorylation of Munc18-1 and SNAP-25, related or not,

with the synaptic activity, and whether nPKCε and cPKCβI are interdependent.

2.3. To determine whether BDNF/TrkB signaling pathway regulates the phosphorylation of Munc18-1 and SNAP-25 related with the synaptic activity.

3. To determine whether the synaptic activity resulting in muscle contraction has repercussion on Munc18-1, SNAP-25 and their phosphorylation levels in the skeletal muscle through nPKCε and cPKCβI isoforms and BDNF/TrkB signaling pathway.

3.1. To determine whether nerve-induced muscle contraction regulates Munc18-1, SNAP-25 and their phosphorylation levels.

3.2. To determine whether nPKCε and cPKCβI isoforms regulate the phosphorylation of Munc18-1 and SNAP-25 under nerve-induced muscle contraction condition and the dependence between nPKCε and cPKCβI.

3.3. To determine whether BDNF/TrkB signaling pathway regulates the phosphorylation of Munc18-1 and SNAP-25 under nerve-induced muscle contraction condition.

UNIVERSITAT ROVIRA I VIRGILI
EFFECTS OF NEUROMUSCULAR ACTIVITY COUPLED TO BDNF/TRKB SIGNALING ON THE EXOCYTOTIC PROTEINS MUNC18-1 AND SNAP-25 THROUGH NPKCE AND CPKCSSI
Anna Simó Ollé

III. MATERIAL AND METHODS

UNIVERSITAT ROVIRA I VIRGILI
EFFECTS OF NEUROMUSCULAR ACTIVITY COUPLED TO BDNF/TRKB SIGNALING ON THE EXOCYTOTIC PROTEINS MUNC18-1 AND SNAP-25 THROUGH NPKCE AND CPKCSSI
Anna Simó Ollé

1. ANIMALS

To perform this thesis young adult male *Sprague-Dawley* rats from 30 to 45 days old has been used (purchased from Charles River, Criffa, Barcelona). Levator Auris Longus (LAL) and diaphragm muscles from were used to perform the stimulation and immunohistochemistry (IHC) experiments. All animals were maintained on the animal facility in a standard cage of Makrolon^{R} (23x46x14 cm^{3}) and were housed in a room equipped under standards conditions: constant temperature (22° ± 2°C), relative humidity (50 ± 10%) and automatic light cycles (12-h light/dark). Food (*Panlab* rodent chow, Barcelona, Spain) and tap water were offered *ad libitum* throughout the study. The use and treatment of animals has been aproved by the *Comitè Ètic d'Experimentació Animal de la Facultat de Medicina i Ciències de la Salut de la Universitat Rovira i Virgili* in accordance with *Llei 5/1995* and *Decret 214/1997 de la Generalitat de Catalunya* and *RD español 53/2013* (published in *BOE 34, 08/02/13*) which establishes the basic norms applicable for the protection of animals used in experimentation and other scientific purposes.

The animals were anesthetized with tribromoethanol (TBE) 2% injected via intraperitoneal (0.15 ml/10g body weight). Once deeply anesthetized were sacrificed with exsanguination immediately and the needed muscles were obtained for further use in accordance with the guidelines of the European Community's Council Directive of 24 November 1986 (86/609/EEC) for the humane treatment of laboratory animals.

2. STUDY MODEL: SKELETAL MUSCLE

In this thesis, to perform immunohistochemistry (IHC) it has been used as a skeletal muscle study model a Levator auris longus (LAL) muscle, which allows moving the ears in rodents. It is a good model for IHC localization studies due to its morphological characteristics. To perform Western blot techniques were used the diaphragm muscle. It is a dome-shaped muscle divided in two hemi-diaphragms, which are innervated separately, what permits to stimulate separately each one of them.

2.1. Levator auris longus (LAL)

Levator auris longus (LAL) is a superficial muscle located under the dorsal skin in the area of the head and neck of the mammals. It has a cranial and caudal part. The fibers in the cranial region were originated in the spines of the fourth cervical vertebra and goes towards anterior part of the pinna base, where it inserts. The fibers in the caudal region were extended from the fourth and fifth cervical vertebra to the back of the pinna base. It consists of fast-twitch muscle fibers (Erzen et al. 2000) which are arranged in five or six layers of cells (5.25 ± 0.78) in the cranial portion (Erzen et al., 2000), while in the caudal part could be more (Angaut-Petit et al. 1987).

The LAL muscle is an excellent model to study the NMJ morphology through IHC experiments (see below). This is because it is a very thin muscle, and therefore, the antibodies can penetrate and immunolabel the target proteins allowing the visualization of the nerve terminal and the nAChRs. Moreover, that it is possible to visualize complete innervation of the muscle without cutting it into slices (Angaut-Petit et al., 1987). Due to these technical and morphological features, thin, flat shape and few layers, LAL muscle is an ideal model for IHC studies.

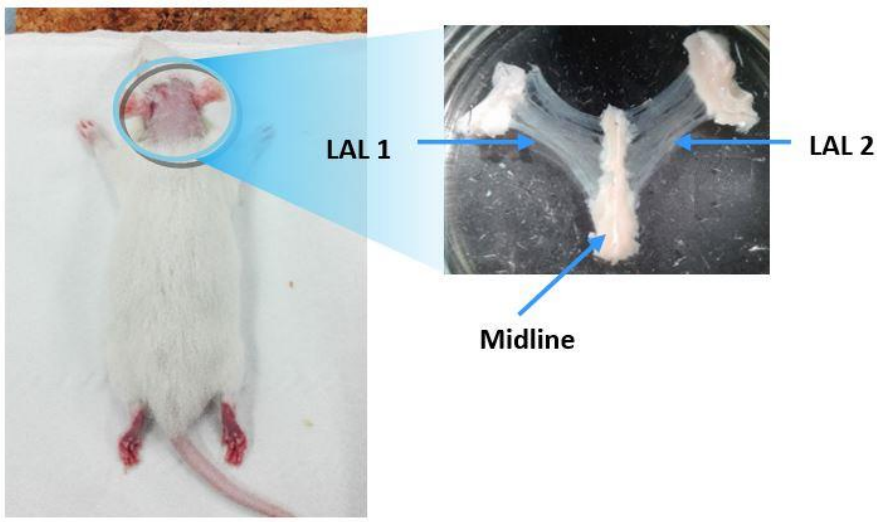

Figure 15. Levator auris longus (LAL) muscle structure. LAL muscle of adult rat. It is located under the dorsal skin in the area of the head and neck and consists in two parts: the left muscle (LAL 1) and the right muscle (LAL 2), between them there is a midline, which separate the two LALs.

2.2. Diaphragm skeletal muscle

The **diaphragm** skeletal muscle is thin and flat, it has the innervation zone very well defined, and whose function is to produce respiratory movements. It is an ideal model for electrophysiology studies because of the easy location of individual muscle fibers and isolated synapses, for this reason it has been described as a useful model to study synaptic function (Besalduch et al. 2010; Chand et al. 2015; Obis et al. 2015b; Rosato et al. 1999; Urbano et al. 2003). Accessibility to the phrenic nerve helps to dissect and stimulate it and thus enhance independently synaptic activity and muscle contraction. The pattern of innervation allows separating the synaptic areas of extrasynaptic with relative ease. It forms a wall between the thorax and the abdomen and consists of a peripheral muscular region (costal part) and a central aponeurotic in the shape of a clover (Pickering and Jones 2002; De Troyer et al. 1981). The anterior part has its insertion at the costal end. It is innervated by the phrenic nerve, which proceeds from the cervical segments C3-C5 of the spinal cord. It descends through the

thorax to the diaphragm, where it divides to innervate the two hemidiaphragms that form it. The innervation of each hemidiaphragm begins in the central and inner part and is divided into three branches: one towards the anterior part and two towards the posterior part. From each of the branches come different smaller branches, innervating in a massive form, in the form of a tree, the external part where the different synapses are formed, defining a zone of innervation well limited. Diaphragm is in a way unusual because only a subset of muscle fibers is active with a prolonged duty cycle as compared to other skeletal muscles (De Troyer et al., 1981; Pickering and Jones, 2002). However, nerve stimulation simultaneously recruits all motor units and uniforms the heterogeneous level of activity of the fibers.

3. SKELETAL MUSCLE EXTRACTION PROCEDURE

As previously described (see section 1, *Animals*), the animals were anesthetized with TBE 2% by intraperitoneal injection. Unconsciousness is assured by assessing lack of ocular, patellar and caudal reflexes. Sacrifice was performed by exsanguination. For the muscle dissection was required a stereoscopic microscope and surgical equipment. The dissections were performed on a Petri dish covered with a silicone elastomer (Sylgard®) to pin the muscles with dissecting needles in order to facilitate the extraction. LAL muscles was used for IHC analysis. Diaphragm muscles were used to biochemical studies using Western blot techniques.

3.1. LAL muscle extraction for IHC analysis

Once the animals are anesthetized, the coat is shaved from the neck and head area, where the LAL muscle lays underneath. After sacrifice by exsanguination, rats are pinned down in a support, dorsal side up with one pin in each paw and one pin through the nose. Then, the first T-shaped incision is

performed only through the skin, using small spring scissors to cut from the beginning of the neck to reach the eyes. The skin is removed in this region, avoiding the sides closer to the ears as these are the attachment points of the LAL muscle. Afterwards, the preparations undergo a step of fixation. In concrete, the muscle pack that contains the LAL muscle is fixed using a collection vessel with 4% paraformaldehyde (PFA) during 90 minutes. The following steps of the dissection are performed on a Sylgard® coated Petri dish to allow clamping and stretching of the muscle exposing its ventral side with dissecting needles. Muscles are rinsed with 1X PBS (phosphate buffered saline, composed by 140 mM NaCl, 2.7 mM KCl, 1.5 mM KH_2PO_4 and 8.1 mM Na_2HPO_4 adjusted pH at 7.4) to keep them hydrated in a physiological solution. Once the ventral side of the muscle is exposed, they are pinned to facilitate the removal of the connective and muscular tissues that cover the LAL. The identification of the LAL midline is important to differentiate it from other muscles and distinguish its left and right sides (LAL1 and LAL2, **figure 15**). After three washes of 5 minutes, the muscle is turned over and re-pinned in order to remove the tissues covering the dorsal surface. It is necessary to take special care to remove the connective tissue from both dorsal and ventral surfaces of the muscles, which may hinder the penetration of the antibodies into the sample.

3.2. Diaphragm muscle extraction for biochemical studies

Once the animals are anesthetized and sacrificed by exsanguination, rats are pinned down in a support, ventral side up with one pin in each paw. Then, using small scissors, the first T-shaped is performed only through the skin, by the ventral part, leaving the rib cage in sight. Then, the same procedure is performed with the musculature but this time until the sternum. The viscera are removed carefully to avoid damage the diaphragm and cut off the excess skin on the sides. Then, midway between the neck and the apex of the sternum, a cut is made to separate the rib cage from the rat. With the help of clamps, it is holding by the xiphoid process of the sternum to cut the spinal column below the diaphragm. Until this step, because the manipulation of the tissues is performed without

keeping the physiological conditions, it is very important to go as fast as possible to keep the muscles alive. Diaphragm is pinned by the xiphoid process upwards and the sides of the rib cage, keeping the organs up, to a Petri dish with Sylgard®. In order to keep the tissues alive and in perfect condition they must remain constantly submerged in oxygenated Ringer. Then, cut the column and the ribs on both sides from the front (sternum) to the column. The remaining organs (lungs, heart and thymus) are cut with the help of spring scissors and under the magnifying glass, very carefully to maintain intact the phrenic nerves that innervate each hemidiaphragm. Afterwards, with the help of scissors the rests of ribs are cut, leaving only the diaphragm insert attached to them. The column is then cut and removed, separating the two hemidiaphragms on its dorsal side. Once both hemidiaphragms are separated, maintaining that pinned and well extended in the Sylgard® dish, the remaining viscera are cut keeping intact the phrenic nerves, using a spring scissors and under the magnifying glass. Finally, the connective tissue that envelops the nerves is removed, taking special care to the end of these where the suction will be performed, and be careful not to pinch them to avoid damaging them.

Nerve suction is performed in repetitive stimulation experiments. To do this, the preparation is transferred to a rectangular chamber, only with Sylgard® floor to hold the muscle to the base and raised with Ringer or with the correspondently reagent. The dissection of both hemidiaphragms is performed for biochemical studies (see section 4, S*keletal muscle stimulation*).

3.3. Spinal cord and brain extraction for biochemical studies

To extract the spinal cord, once the rats have been anesthetized and sacrificed by exsanguination, they are T-shaped pinned with needles on support. Using scissors, an incision is performed in the dorsal side above the spine until it is exposed. Then the spinal bones are cut carefully until the spinal cord is shown. The ventral region of the spinal cord is selected and placed in an Eppendorf tube

containing cold PBS. Then freezes at -30°C. Specifically, of the spinal cord the ventral region is used which is where the cell bodies of motoneurons that innervate skeletal muscles.

To perform brain extraction, after sacrifice by exsanguination, the rats are pinned down in a support, dorsal side up with needles on each paw and through the nose. Using bone cutting spring scissors, a cut is performed from both sides of the mouth to the surface of the skull. Pressure is then exerted to open the cranial surface and access the brain which is removed with a spatula and frozen immediately in an Eppendorf tube with 1X PBS at -30°C.

4. SKELETAL MUSCLE STIMULATION

Biochemical activity-dependent protein expression studies were performed using skeletal muscle samples (see section 2, *Study model: skeletal muscle*). For this, a protocol of continuous stimulation of the diaphragm muscle from the rats was followed imposing moderate activity. In all the experimental protocols, the diaphragm muscles were removed surgically maintaining the phrenic nerve intact and were pinned in a Sylgard Petri dishes containing normal Ringer solution continuously bubbled with 95% O_2/5% CO_2 at room temperature to simulate the physiological conditions of the muscle *in vivo*. The *ex vivo* stimulation method allowed describing the regulation mechanisms involved in the NMJ by showing the effect of presynaptic stimulation and how the muscle responds to it. To obtain real and extrapolable results it was very important to maintain the conditions as similar as *in vivo* as possible.

The electric stimuli were transmitted from an A-M Systems 2100 isolated pulse generator (Carlsborg, WA) to the muscle by a platinum electrode connected to the phrenic nerve. To stimulate the muscle, the phrenic nerve was subjected to a 30 minutes period of stimulation connected by an electrode to a stimulator unit

at 1Hz. In order to study separately the effect of presynaptic stimulation (and synaptic transmission) from the effect of the muscle cell contraction in response to stimuli, we performed experiments in which contractions were prevented. Muscle contraction was blocked by using 1.5 µM µ-conotoxin GIIIB (µ-CgTx- GIIIB), a contraction blocker that selectively inhibits sarcolemmal VGSCs without affecting synaptic ACh release (Favreau et al. 1999) (see section 5, *Reagents*).

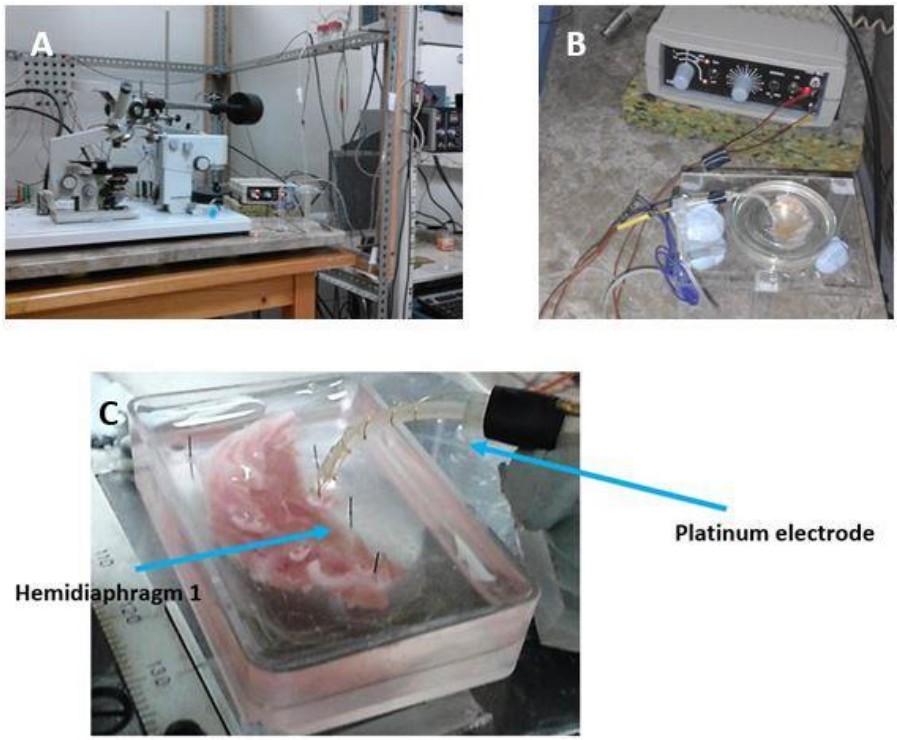

Figure 16. Electrophysiology equipment. A) Cibertec stimulator cs-20. **B)** Cibertec ISU connected to a hemidiaphragm through the suction of the phrenic nerve. **C)** Detail of the platinum electrode from the stimulator unit connected by suction to the phrenic nerve. The muscle rests pinned in a Sylgard dish, submerged in a normal Ringer solution.

To study the differences of the effect of the stimuli or the contraction towards themselves or towards a control without stimuli we performed experiments in which the contraction was restricted *(St)* or not *(St + Contraction)*. Three main experiments were designed in order to distinguish presynaptic effects form postsynaptic effects of muscular activity. Each of these were composed by a treatment and its particular control treatment, using for that both hemidiaphragms from the same rat respectively:

- **Stimulation experiment (Ctrl *vs* St)** permits to study the differences between the basal conditions and the stimuli product of the stimulator.

- **Contraction experiment (St *vs* St + Contraction)** is useful to study the differences between the stimuli, which are product of the stimulator and the stimuli together with the contraction generated by the muscle in response.

- **Stimulation and contraction experiment (Ctrl *vs* St + Contraction)**, permits the study of the differences between the basal stimuli and the stimuli, which are product of the stimulator and the contraction generated by the muscle in response.

Once the experiments were completed, both hemidiaphragms are immediately frozen in liquid N_2 and stored at -80 °C.

Table 1. Summary of electrophysiological treatments applied to extracted rat diaphragms. **Stimulation experiment** *(Ctrl vs St)* compares (1) the stimulation of muscles with contraction blocked by µ-conotoxin GIIIB with (2) muscles that were not stimulated but incubated with µ-conotoxin GIIIB, to discard side-effects of the blocker. **Contraction experiment** *(St vs St + contraction)* compares (1) the stimulation of muscles with contraction unaltered with (2) stimulated muscles with contraction blocked. Finally, **stimulation and contraction experiment** *(Ctrl vs St + contraction)* compares (1) the stimulation of muscles with contraction unaltered with (2) muscles that were not stimulated and their contraction unaltered.

Experiment	Control Treatment	Treatment	Final outcome
Presynaptic stimulation (Ctrl *vs* St)	**No stimulation, blocked contraction** 1. Hemidiaphragm extraction. 2. µ-conotoxin GIIIB preincubation. t=30 min 3. Incubation in Ringer solution without stimulation. t=30 min 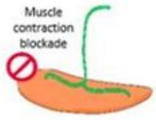	**Stimulation, blocked contraction** 1. Hemidiaphragm extraction. 2. µ-conotoxin GIIIB preincubation. t=30 min 3. Phrenic nerve stimulation (1 Hz) with contraction blocked. t=30 min 	**Effect of presynaptic stimulation** 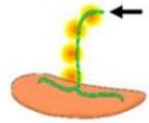
Contraction (St *vs* St + Contraction)	**Stimulation, blocked contraction** 1. Hemidiaphragm extraction. 2. µ-conotoxin GIIIB preincubation. t=30 min 3. Phrenic nerve stimulation (1 Hz) with contraction blocked. t=30 min 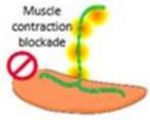	**Stimulation, contraction** 1. Hemidiaphragm extraction. 2. Preincubation in Ringer solution. t=30 min 3. Phrenic nerve stimulation (1 Hz) with contraction. t=30 min 	**Effect of muscle contraction** 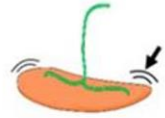
Presynaptic stimulation with contraction (Ctrl *vs* St + Contraction)	**No stimulation, not blocked contraction** 1. Hemidiaphragm extraction. 2. Incubation in Ringer solution without stimulation. t=30 min 	**Stimulation, contraction** 1. Hemidiaphragm extraction. 2. Phrenic nerve stimulation (1 Hz) with contraction. t=30 min 	**Effect of presynaptic stimulation with contraction** 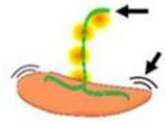

5. REAGENTS

Normal Ringer

Normal Ringer solution was used to incubate the diaphragms during all stimulation/contraction treatments, as well as throughout the muscle extraction process to keep it alive. It contains (in mM): NaCl 137, KCl 5, $CaCl_2$ 2, $MgSO_4$ 1, NaH_2PO_4 1, $NaHCO_3$ 12 and glucose 12,1 mM, it is bubbled constantly with 95% O_2, 5% CO_2.

Dimethyl sulfoxide (DMSO)

DMSO (dimethyl sulfoxide; Tocris, Ellisville, MO, USA) facilitates the penetration of additional components into the muscle tissues. The final concentration of DMSO in control and drug-treated preparations was 0.1% (v/v). It has been shown that the use of solutions containing this DMSO concentration does not affect neurotransmission in the studied parameters attributable to this solvent (Favreau et al., 1999). It was added 1ml/l of DMSO to the normal Ringer.

μ-conotoxin GIIIB

In presynaptic stimulation treatments and electrophysiological experiments, muscle contraction was blocked using μ-conotoxin GIIIB (μ-CgTx-GIIIB, Alomone Labs Ltd, Jerusalem, Israel). This peptide was made up as lyophilized powder of >99% purity. Blocker reconstitution was made with MQ distilled water to reach 150M and it was stored at 4°C for periods up to one week or at -20°C for periods always minor than three months. Working solution: 1.5 μM diluted in normal Ringer solution (Favreau et al. 1999).

High and low calcium levels

In order to study whether phosphorylation of target proteins were modulated by Ca^{2+} in the NMJ, it was used high and low calcium levels. In some experiments, it was increased the content of calcium of the normal Ringer to 5mM or decreased it to 0.25 mM. To accomplish this, the amount of $CaCl_2$ (0.1 M stock) added to the normal Ringer was changed.

TrkB receptor antagonist

47/TrkB (clone 47/TrkB; cat. no. 610102; 250µg/ml, from BD Transduction Laboratories (Lexington, KY)) is an anti-TrkB antibody from mouse. It recognizes the human TrkB sequence between the aa 156 and 322 (extracellular) encompassing the second cysteine-rich domain and the two Ig-like C2 domains. This antibody inhibits BDNF binding to TrkB receptors. Because the receptor final conformation is not the same as with its natural ligand, 47/TrkB effectively inhibits autophosphorylation residues Y670, Y674 and Y675 of TrkB (Favreau et al., 1999). Working solution: 10µg/ml (Balkowiec and Katz, 2000a).

Exogenous BDNF

BDNF (*Human Brain-derived neurotrophic factor,* from Alomone Labs Ltd; Jerusalem, Israel) is a specific TrkB agonist. It was prepared in MQ distilled water (0.37 µM). Working solution: 10nM. Previous experiments demonstrated that this concentration was the most accurate one after trying 1, 10 and 100 nM.

Phorbol 12-myristate 13-acetate (PMA)

PMA (Phorbol 12-myristate 13-acetate) from Sigma-Aldrich (St. Louis, MO) is a non-specific agonist of PKC. It was made up for the stock solution as 10 mM in DMSO and stored at -20°C. Working solution: 10 nM.

nPKCε inhibitor peptide

εV1-2 (myristoylated nPKCεV1-2 peptide, EAVSLKPT) from Calbiochem (Merk, Germany) is a nPKCε specific translocation inhibitor peptide to block nPKCε activity. It is an 8-residue peptide fragment contained in the εV1 region (Cazorla et al., 2011), which is the binding domain to its RACK receptor. It was made up for the stock solution as 1mM in normal Ringer and stored at -80 °C. Working solution: 100 µM. Previous experiments demonstrated that this concentration was the most accurate after trying 1, 10 and 100 µM (Johnson et al., 1996b).

cPKCβI inhibitor peptide

βIV5-3 (aa 646-651; kindly provided by Dr. Mochly-Rosen from Stanford University) is a specific translocation inhibitor peptide to block cPKCβI activity. It is derived from the V5 domain of cPKCβI and binds to the anchoring protein βI-RACK, disrupting the interaction between cPKCβI and its specific βI-RACK (Stebbins and Mochly-Rosen 2001). This inhibits its translocation to the membrane and so its activation. It was made up for the stock solution as 10 mM in normal Ringer and stored at -80 °C. Working solution: 10 µM. Working concentrations were 1, 5 and 10 µM.

These PKC inhibitor peptides impossibilities the translocation of these PKCs to the membrane and, therefore, they cannot do their normal function. This inhibition of function revealed that cPKCβI and nPKCε have essential roles in ACh release regulation (Stebbins and Mochly-Rosen, 2001). Then these PKC isoforms may be essentials for the regulation of the signal transmission in NMJ.

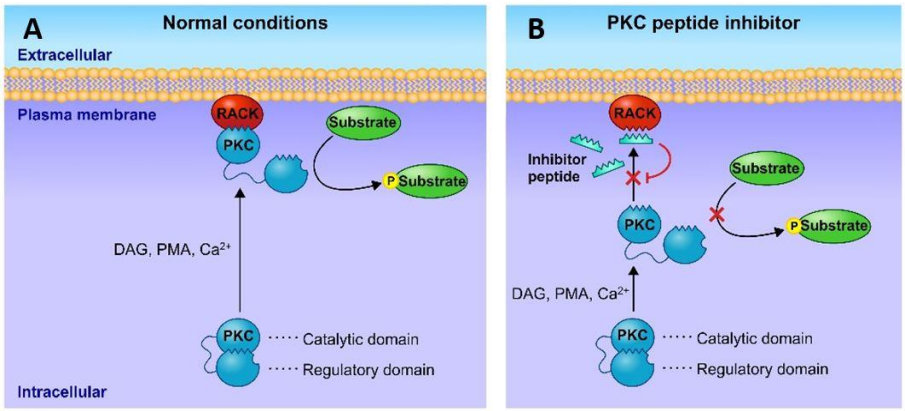

Figure 17. Protein kinase C peptide inhibitor. (A) Protein kinase C (PKC, in blue) changes from an inactive to active state when diacylglycerol (DAG) or PMA increases, in which both the RACK binding site and the active site are exposed. The active PKC binds to RACK (red), anchoring it near its substrate (green), which once phosphorylated (P) triggers the physiological responses of the isoenzyme. **(B)** The inhibitor peptide binds to the RACK and blocks the binding of the activated isozyme to that RACK. Therefore, the physiological responses mediated by that isozyme are blocked.

6. TISSUE PREPARATION FOR BIOCHEMICAL STUDIES

6.1. Muscles homogenization

For biochemical studies, total skeletal tissue protein was obtained from previously extracted diaphragm muscle samples, frozen in liquid nitrogen and stored at -80°C before use. The muscles were homogenized using a high-speed homogenizer (overhead stirrer, VWR International, Clarksburg, MD) in lysis buffer containing 150 mM NaCl, 50 mM Tris–HCl pH 7.4, 1 mM EDTA (Ethylenedinitrilo-tetraacetic acid), 50 mM NaF (sodium fluoride), 1 mM PMSF (phenylmethanesulfonyl fluoride), 1 mM sodium orthovanadate from Sigma, (St. Louis, MO), 1% IGEPAL CA-630 (Octylphenoxy poly(ethyleneoxy)ethanol) from Sigma, (St. Louis, MO), 0.1% Triton X-100 and a 1% protease inhibitor cocktail (P8340, Sigma-Aldrich, St. Louis, MO). The ratio followed was of 1 ml of lysis buffer per 0.5 g of tissue (20% w/v). Tissue preparation is done at cold temperatures

(4°C) to avoid protein denaturing and degradation. In order to separate extracellular matrix components from non-lysed cell moieties, the insoluble material was removed by centrifugation at 1000 g for 10 minutes at 4°C, discarding the precipitate. The supernatants were collected and centrifuged at 15000 g for 20 minutes at 4°C. Finally, the resulting supernatants (total protein lysates) were collected, aliquoted and stored at -80 °C before use.

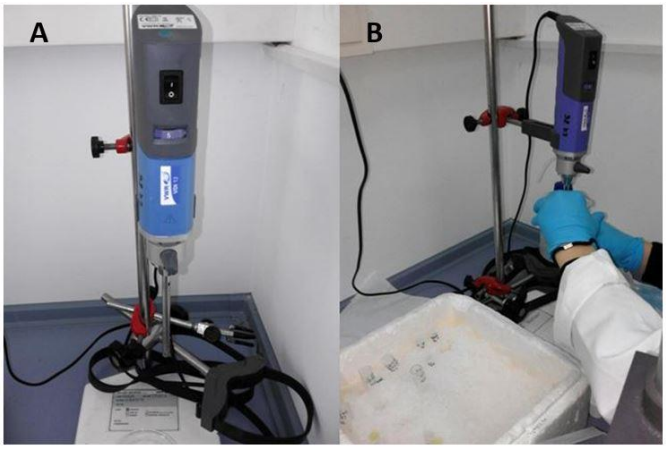

Figure 18. Homogenizer. A) High-speed homogenizer (overhead stirrer, VWR International, Clarksburg, MD). **B)** Process of muscle homogenization.

Membrane and cytosol separation

In order to isolate the membrane and cytosolic fractions, diaphragm muscles were dissected and homogenized using a high-speed homogenizer in ice-cold lysis buffer without detergents (in mM: NaCl 150, Tris-HCl (pH 7.4) 50, EDTA 1, NaF 50, PMSF 1, sodium orthovanadate 1 and protease inhibitor cocktail (1/100)). The homogenized samples were cleared at 1000 g for 15 minutes at 4°C, and the resulting supernatant was further centrifuged at 130000 g for 1 hour at 4°C. The supernatant corresponded to the cytosolic fraction and the pellet, to the membrane fraction. The latter, was resuspended in lysis buffer (in mM: NaCl 150, Tris-HCl (pH 7.4) 50, EDTA 1, NaF 50, PMSF 1, sodium orthovanadate 1; NP-40 1%, Triton X-100 0.1% and protease inhibitor cocktail (1/100)). Protein concentrations

were determined in the same way as total protein lysates (see above). Validation of the purity of the subcellular fractionation was determined by examining the presence fraction-specific housekeeping proteins like GAPDH (Glyceraldehyde 3-phosphate dehydrogenase) for cytosol and Na/K-ATPase for membrane by Western blotting. GAPDH immunoreactivity was never observed in the membrane fraction.

6.2. Protein concentration

Protein concentrations of each hemidiaphragm were determined by using the Bio-Rad DC protein assay (Bio-Rad, Hercules, CA). Experimental procedures were performed to determine the linear and quantitative dynamic range for each target protein, using a standard curve of bovine serum albumin (BSA) (Sigma-Aldrich, St. Louis, MO) at concentrations of 0, 0.1, 0.2, 0.4, 0.8 and 1 mg/ml. The appropriate dilutions of samples were used for the accurate and normalized quantitation by densitometric analysis. Absorbance determination was performed on a spectrophotometer (CECIL, CE2030) at a wavelength of 750 nm. Protein concentration of each hemidiaphragm was determined to adjust and load the same amount of protein for each sample in the electrophoresis (see below).

7. ANALYSIS TECHNICHES

7.1. Electrophoresis SDS-page and Western blot

In order to study the effect caused by the different treatments used, to the target proteins and their phosphorylations, a Western blot analysis was used. Western Blot is an analytical technique widely used to detect specific proteins in a tissue homogenate sample. To distinguish the proteins of a sample, they are first separated by their molecular weight through electrophoresis. For this, an electric field with constant voltage of 90-120 V is applied through an acrylamide gel and

the proteins are driven across the mesh of the gel under denaturation conditions to avoid the influence of the 3D conformation on their migration. Then, the proteins are transferred on a synthetic membrane of PVDF (polyvinylidene difluoride) to immobilize them. Finally, the target proteins are detected by immunoblotting. The specificity of the antibody-antigen interaction enables a target protein to be identified in the midst of a complex protein-mixture. The combined use of electrophoresis and Western blot technique allows the quantitative detection of the presence of a protein and even its post-modified-transcriptional state (expression changes, phosphorylation state, etc.). It is the most commonly used method to measure the expression of a protein in cell signaling experiments. To perform and evaluate each experiment, at least five independent animals (n> 5) were used.

Sample preparation

Samples were prepared to have a final volume of 15 µl. Each sample contained 30-40 µg of protein (calculated previously with the DC assay) in reducing loading buffer (SBL1X). This buffer was stored at -20°C at 5X concentration to dilute it in the samples to 1X. The final concentrations were 40 mM Tris HCl pH 6.8, 5% (m/v) SDS, 8.4% (v/v) Glycerol, 16% (v/v) β-mercaptoethanol and 0.01% (v/v) bromophenol blue in MQ water. β-mercaptoethanol was used to break disulfide bonds and SDS, which is a negative charged detergent, was used to solubilize the proteins. Then, samples were submitted to a thermic shock (5 minutes at 100°C and freezing them immediately after) to denaturalize the proteins. Altogether, with this protocol, proteins could only migrate depending on their molecular weight in the acrylamide gel.

SDS-PAGE gel electrophoresis

SDS-polyacrylamide gel electrophoresis (SDS-PAGE) is one of the most widely used techniques for the separation of proteins according to their molecular weight (Laemmli 1970). It separates denaturized proteins in the presence of a

perpendicular electric field to a gel composed by Acrylamide/Bis-acrylamide, which forms a reticular mesh. The technique applies a negative charge so proteins move towards a positive charge. A variable proportion of Acrylamide/Bis-acrylamide, Tris buffer, SDS, ammonium persulfate (APS) and TEMED (N, N, N',N'-tetramethylethylenediamine) (the last two were used to polymerize the gel) composed the gel. The gel acts as a physical filter so that larger proteins travel relatively slower than smaller proteins. A single gel integrated two percentages of acrylamide. The top portion known as stacking gel was of a lighter percentage and lower pH (6.8). Under it, there was the running gel with a higher percentage (usually between 8% and 15%) and pH (8.8). The stacking gel concentrated the proteins so that they migrate in equal conditions and the running gel had the specific function of separating them depending on the weight as they were negatively charged. The gels were included in a cassette with electrode assembly and were submerged in a tank filled with SDS-PAGE 1X running buffer and the samples were loaded to the gel wells. Then, the electric field was applied in a constant voltage of 90-120 V by a Mini-Protean 3 electrophoresis system and a PowerPac™ Basic Power Supply (Bio-Rad, Hercules, CA). Molecular weight standards were used to control the separation of proteins during electrophoresis (Precision Plus Protein™ Dual Xtra, Bio-Rad, Hercules, CA).

Transfer

Once the gel had run, the proteins were transferred to a polyvininylidene difluoride (PVDF) membrane (Hybond™-P; Amersham, GE Healthcare) utilizing a perpendicular electric field to the gel by a Trans-Blot® Turbo™ Transfer System with its Transfer Buffer (Bio-Rad, Hercules, CA) to immobilize them and allow immunodetection. After the transference, it is important to check the quantity of protein loaded. It was used the SYPRO Ruby Protein Gel Stain kit by Bio-Rad as a loading control to normalize the changes of the studied proteins within pairs of samples as actins are not a housekeeping control in our working model.

Blocking and immunolabeling

For immunodetection the membranes were blocked with the wash solution Tris-buffered saline 0.1% Tween 20 (TBST) containing 5% (W/V) phosphoblocker reagent (PhosphoBLOCKER™ Blocking Reagent, Cell Biolabs, inc. CA, USA) or BSA for phosphorylated proteins or nonfat dry milk or BSA for total proteins during 1 hour at room temperature. After this time, membranes were incubated in primary antibody (specific for the interest protein) overnight at 4°C. Afterwards, the membranes were washed three times with TBST (5 minutes) and incubated during 90 minutes with a secondary antibody linked to horseradish peroxidase (HRP). Before detection and visualization, membranes were washed three times with TBST and one with TBS. During all incubations and washes, membranes were in constant shake.

In order to analyze the phosphorylation ratio of a protein, it is convenient to immunoblot both proteins in the same membrane. The process of stripping removes the primary and secondary antibodies from the first detection and allows the re-probing of the following protein without interferences. The antibody against the phosphorylated protein is incubated before the antibody against the non-phosphorylated total protein. This is because the phosphorylated form is a subset of the total form of a protein. After membranes were visualized (see below) they were incubated with stripping solution (Tris HCl 1M pH=6.8; SDS 20 % (v/v); β-mercaptoethanol 100 mM) at 50 °C during 30 minutes with constant shaking. Once the stripping solution was removed, the membranes were washed six times with TBST during 5 minutes each. Finally, the process of blocking and immunolabeling were performed as stated above.

Detection, visualization and data analysis

Membranes were visualized by chemiluminiscence with the ECL kit (Amersham Life Science, Arlington Heights, IL) which provides the substrate to the HRP. The blots were imaged with a ChemiDoc XRS+ (Bio-Rad, Hercules, CA)

associated with Imaging System ImageLab software. The densitometry of the resultant bands was analyzed with the ImageJ software (ImageJ, RRID: SCR 003070). GAPDH and Na/K-ATPase proteins were used as loading controls, as well as total protein staining (Sypro Ruby protein blot Stain, Invitrogen). The integrated optical density of the bands was normalized with respect to (1) the background values and to (2) the total protein transferred on PVDF membranes, measured by total protein analysis. All protein phosphorylation was determined as the ratio of phosphorylated protein versus total protein content, respectively. The relative variations between the experimental samples and the control samples were calculated from the same membrane image. The data were taken from densitometry measurements made in at least five separate experiments, plotted against controls. Data are mean values ± SEM. Statistical significance of the ratios between groups was evaluated with the SPSS (Statistical Package for the Social Sciences; IBM) software under the paired Wilcoxon test or the Student's t-test and the normality of the distributions was tested with the Shapiro-Wilk test. The criterion for statistical significance was $p<0.05$ versus the control.

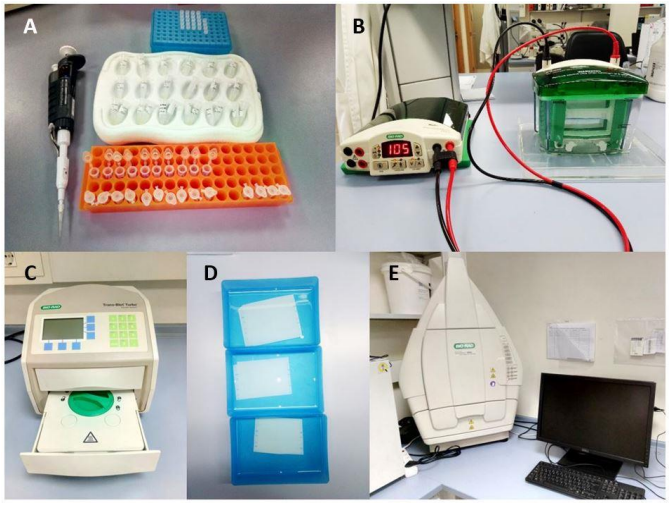

Figure 19. Western Blot equipment. A) Micropipette used for sample preparation and ice-cold support to maintain the samples at 4°C. **B)** SDS-PAGE electrophoresis. **C)** Trans-Blot® Turbo™ Transfer System. **D)** Compartments used to perform membrane blocking and immunolabeling. **E)** ChemiDoc XRS+ (Bio-Rad, Hercules, CA).

7.2. Immunohistochemistry

In order to study the localization of Munc18-1 in the NMJ it was used fluorescent immunohistochemistry. To perform and evaluate each IHC, at least five independent animals (n> 5) were used.

Basis of the technique

Fluorescent Immunohistochemistry (IHC) combines histological, immunological and biochemical techniques to identify the tissue distribution and localization of specific cellular components such as proteins or biomarkers with high precision using specific antibodies labeled with a visible label. The classic IHC assay involves the detection of antigens expressed in a tissue sample using a primary antibody capable of binding to such target antigens with high specificity. Once antigen-antibody binding has occurred, a secondary antibody coupled with a fluorophore is added which has the ability to bind to the primary antibody. These fluorophores are molecules capable of emitting light from a given spectrum when excited at the appropriate wavelength. Many fluorophores have different properties of excitation and emission. For this reason, it is possible to label different proteins in different colors and display them together. By this conventional technique, the proteins present in the three elements of the NMJ (nerve terminal, acetylcholine receptors and Schwann cell) were labeled so that they could be visualized together, or in the desired combination, in addition to the target protein Munc18-1.

IHC procedure

Once the immunoreactivity of Munc18-1 was found to be identical in both LAL and diaphragm muscles, subsequent IHC were performed only in LAL muscles. After LAL muscles from rats were removed, fixed and washed (see subsection *LAL muscle extraction for IHC analysis*), the IHC protocol was performed. First, the muscles were incubated overnight at 4°C with a permeation solution of 1% Triton

X-100 in PBS and 4% BSA to block the unspecific bindings. Then, muscles were incubated overnight at 4°C in mixtures of primary antibodies raised in different species, depending on the number of proteins to be labeled (anti-Munc18-1, anti-Syntaxin, and anti-S-100) in 1% Triton 4% BSA. To remove the antibody residues, three washes of 5 minutes with 1X PBS and constant shake at room temperature were performed. Thereafter, the muscles were also incubated overnight at 4°C in mixtures of the corresponding secondary antibodies. Finally, muscles were washed three times more with PBS. Whole muscles were mounted in Mowiol® medium (0.2 M Tris-HCL pH 8.5 and glycerol; Calbiochem) with 0.1% (g/ml) of p-phenylenediamide (Sigma-Aldrich) to be ready to visualize.

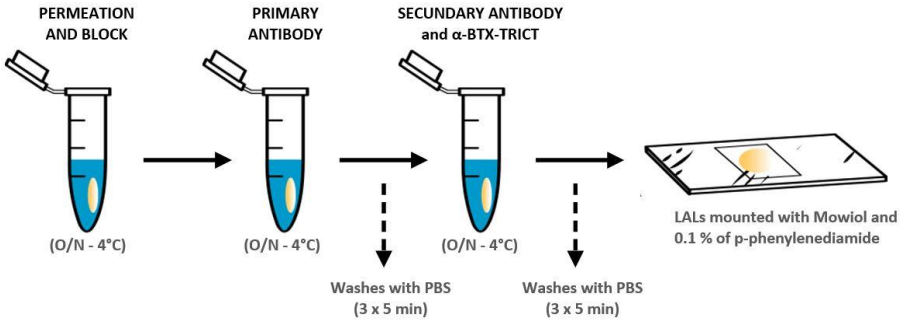

Figure 20. Scheme of Immunohistochemistry process performed in rat LAL muscle. The first step is to permealize and block the unspecific bindings with 1% Triton X-100 and 4% BSA overnight (O/N) at 4 °C. LAL muscle is incubated with primary antibody or mixture of these. To remove the antibody residues, wash them three time with 1X PBS (5 minutes per wash) and then incubate with the corresponding secondary antibodies conjugated to different fluorophores (O/N at 4 °C). Wash three times of 5 minutes with PBS to remove the excess of antibody and mount the sample on a microscope slide with Mowiol® medium and 0.1 % of p-phenylenediamide and covered with a coverslip.

Detection of NMJ

To detect the three components of the NMJ different antibodies were used. The nerve terminal was detected by Syntaxin. It is a SNARE protein located in synaptic membrane, so that it labels more precisely the terminal buttons. The Schwann cell was labelled with S-100, which is a protein that belongs to a

superfamily of calcium-binding proteins. The post-synaptic component was labelled by α-BTX (α-bungarotoxin) conjugated with TRICT (1 µg/ml tetramethyl rhodamine iso-thiocyanate, in red), which joins irreversibly nAChRs and allows us to identify the synaptic area. The anti-Munc18-1 antibody was recognized by the secondary antibody Alexa-fluor 488 donkey anti-rabbit (in green), which is against the specie which were obtained the primary antibody. Alexa-fluor 647 donkey anti-mouse was used to recognize the anti-S-100 antibody (in blue) so the Schwann cell was detected (**Figure 25**). Some muscles were used as a control to demonstrate that antibodies had specificity. The secondary antibody specificity was tested by incubation in the absence of primary antibody. All antibodies and dilutions used are shown in the follow section, *Antibodies*.

7.3. Visualization by fluorescence and confocal microscopy

The preparations were observed firstly with an inverted Nikon TE-2000 fluorescent microscope (Nikon, Tokyo, Japan) connected to a personal computer running image analysis software (ACT-1, Nikon). It allows to see the different proteins of NMJ labeled previously and make a first screening of whether there is a positive or negative mark. In addition, the filters and the dichroic beamsplitter were chosen depending on the spectral excitation and the emission of the fluorophore used to label the sample which permits to visualize each one in different colors. The labeled NMJ visualized with fluorescent microscopy permits to identify each protein in a specific color: the target protein Munc18-1 in green, the Schwann cell in blue and the nAChRs in red. To see the colocalization of all proteins labeled the images were merged.

High-resolution confocal images were obtained with a 60x oil objective (1.4 numerical aperture) on a laser scanning Confocal Nikon TE2000-E microscope. Z stacks were obtained and additional optical sections above and below each junction were collected to ensure that the entire synapse was included.

With the scanned of various thin sections through the sample, confocal maximal projections of labelled components were permitted to obtain representative images to demonstrate the morphology of the neuromuscular synapses in young adult rat.

8. ANTIBODIES

To detect by Western blot the interest proteins for this study, which are Munc18-1, SNAP-25, cPKCβI, nPKCε, their phosphorylated forms phospho-Munc18-1, phospho-SNAP-25, phospho-cPKCβI and phospho-nPKCε, different specific primary antibodies from different commercial manufacturers were used, which are specified in the **Table 2**. The secondary antibodies used in Western Blot were donkey anti-rabbit and rabbit anti-mouse conjugated to HRP (Horseradish Peroxidase) and are specified in **Table 3**.

For immunolabeling the muscles for immunohistochemistry techniques (IHC), primary antibodies commonly used as markers to differentially detect the components of the NMJ (Syntaxin for the nerve terminal and S-100 for the terminal Schwann cell) were utilized together with their corresponding secondary antibody and a widely used toxin to label acetylcholine receptors, α-BTX conjugated with TRICT. Moreover, a specific antibody was used to localize Munc18-1 protein, which is the key protein in this thesis. For further information about the antibodies used, see **Table 2 and 3.**

As a control, primary antibodies were omitted from some muscles during the immunohistochemical and Western blot procedures. These control muscles never exhibited positive staining or revealed bands of the appropriate molecular weight with the respective procedures. In double-staining protocols, omitting either one of the two primary antibodies completely abolished the corresponding staining and there was no cross-reaction with the other primary antibody. Pre-

treatment of a primary antibody with an excess of the appropriate blocking peptide (between three- and eightfold by weight) in skeletal muscle tissue prevented immunolabeling.

Table 2. Summary of primary antibodies for Western blot and IHC.

Primary antibody	Manufacturer	Host	Dilution for WB	Dilution for IHC
Munc18-1 (D406V)	#13414 Cell Signaling Technologies	Rabbit mAb	1:1000	1:5000
pMunc18-1 (Ser 313)	Ab138687 Abcam	Rabbit pAb	1:1000	
SNAP-25 (D9A12)	#5309 Cell Signaling Technologies	Rabbit mAb	1:1000	
pSNAP-25 (Ser 187)	PA5-35406 Thermo Fischer Scientific	Rabbit pAb	1:1000	
nPKCε (C-15)	sc-214 Santa Cruz Biotechnology	Rabbit pAb	1:1000	
pnPKCε (Ser 729)	sc-12355 Santa Cruz Biotechnology	Rabbit pAb	1:1000	
cPKCβI (C-16)	sc-209 Santa Cruz Biotechnology	Rabbit pAb	1:1000	
pcPKCβI (Thr 641)	Ab75657 Abcam	Rabbit pAb	1:1000	
Syntaxin	S0664 Sigma-Aldrich	Mouse pAb		1:1000
S-100	Acris	Mouse pAb		1:100
GAPDH	sc-20358 Santa Cruz Biotechnology	Goat pAb	1:200	
Na/K-ATPase	Developmental Studies Hybridoma Bank	Mouse mAb	1:100	

Table 3. Summary of secondary antibodies and neurotoxins for Western blot and IHC.

Secondary antibody	Manufacturer	Host	Dilution for WB	Dilution for IHC
Anti-rabbit conjugated HRP	711-035-152 Jackson Immunoresearch	Donkey pAb	1:10000	
Anti-mouse conjugated HRP	A9044 Sigma-Aldrich	Rabbit pAb	1:10000	
Alexa-fluor 488 anti rabbit	A21206 Invitrogen	Donkey pAb		1:300
Alexa-fluor 647 anti mouse	A31571 Invitrogen	Donkey pAb		1:300
TRITC-α-BTX (neurotoxin)	T1175 Invitrogen	*Bungarus multicinctus* venom		1:800

UNIVERSITAT ROVIRA I VIRGILI
EFFECTS OF NEUROMUSCULAR ACTIVITY COUPLED TO BDNF/TRKB SIGNALING ON THE EXOCYTOTIC PROTEINS MUNC18-1 AND SNAP-25 THROUGH NPKCE AND CPKCSSI
Anna Simó Ollé

IV. RESULTS

UNIVERSITAT ROVIRA I VIRGILI
EFFECTS OF NEUROMUSCULAR ACTIVITY COUPLED TO BDNF/TRKB SIGNALING ON THE EXOCYTOTIC PROTEINS MUNC18-1 AND SNAP-25 THROUGH NPKCE AND CPKCSSI
Anna Simó Ollé

CHAPTER I. MUNC18-1 PHOSPHORYLATION IS REGULATED BY SYNAPTIC ACTIVITY INDUCED BDNF/TrkB/PKC SIGNALING IN THE SKELETAL MUSCLE

1. Munc18-1 and pMunc18-1 in the adult skeletal muscle: expression, location and regulation by calcium and PMA

1.1. Expression and location of Munc18-1 and pMunc18-1

Western blot analysis using an antibody raised against Munc18-1 was carried out to determine the presence of this protein in the diaphragm skeletal muscle of young adult rats (P30-P40). We also immunoblotted samples with an anti-phospho-Ser-313-specific Munc18-1 antibody to identify the specific PKC phosphorylation of Munc18-1 that is a requisite for exocytosis (Laemmli, 1970).

The antibody anti-phospho-Munc18-1 was raised against the amino acids 160-340 of Munc18-1 which include Ser-313, the phosphorylation site for PKC *in vitro* (Fujita et al. 1996). The antibodies were tested also in spinal cord and brain. In all tissues, the antibodies only recognized the corresponding protein, labeling a 70 kDa band for Munc18-1 and a 67.5 - 68.7 kDa band for pMunc18-1, corresponding to the predicted molecular weights provided by the manufacturer's data sheets (**figure 21**). The Western blot experiments revealed significant amounts of Munc18-1 in the diaphragm muscle with a high fraction phosphorylated on Ser-313 under basal conditions (isolated muscle that does not receive action potentials from the motor neuron soma). Spinal cord and brain showed high amounts of Munc18-1 but pMunc18-1 was barely detected in agreement with published data (Garcia et al. 1994; Hata et al. 1993; Pevsner et al. 1994). Specifically, the ventral region of the spinal cord was used, which is where the cell bodies of MN innervating the skeletal muscles are located.

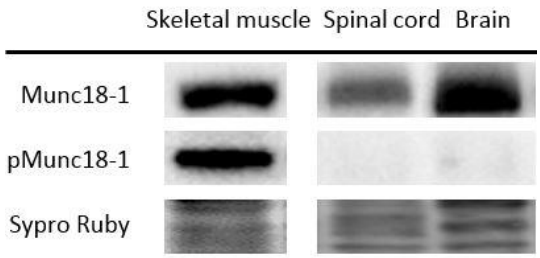

Figure 21. Munc18-1 and pMunc18-1 distribution in different tissues. Western blot bands of Munc18-1 and pMunc18-1 from adult rat skeletal muscle (diaphragm), spinal cord and brain under basal conditions. Munc18-1 is expressed in the three tissues but the phosphorylated form is only abundant in muscle while it is not appreciable in spinal cord and brain.

Although Munc18-1 is a soluble protein, it has important intracellular dynamics depending on its phosphorylation state. Because it has been described that in the synapses Munc18-1 can interact with Syntaxin-1 or with other binding partners in the membrane or can dissociate from them increasing free Munc18-1 concentration (Cijsouw et al., 2014), we analyzed Munc18-1 and pMunc18-1 in the cytosol and membrane fractions under basal conditions (**figure 22**).

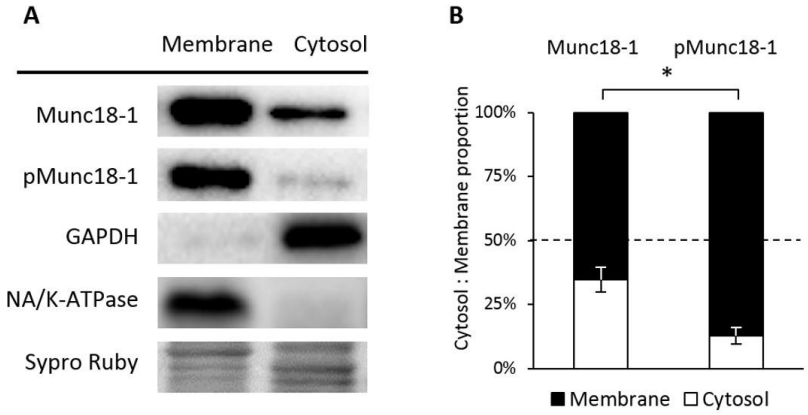

Figure 22. Membrane and cytosol distribution of Munc18-1 and pMunc18-1 under basal conditions. A) Western blot bands of membrane and cytosol distribution of Munc18-1 and pMunc18-1 in basal conditions. **B)** Western blot bands of Munc18-1 and pMunc18 quantified as optical density corresponding to A. Results show that, in basal conditions, Munc18-1 is located in both cytosol and membrane fractions with a higher presence in the

membrane while pMunc18-1 is mainly anchored to the membrane and it is barely detectable in the cytosolic fraction. Moreover, glyceraldehyde 3-phosphate dehydrogenase (GAPDH) is found in the cytosol fraction and undetectable in the membrane fraction. As expected, the membrane protein Na^+/K^+-ATPase is highly enriched in this cellular component, and undetectable in the cytosol fraction. Data are mean percentage ± SEM, * $p < 0.05$ ($n = 5$). Values obtained from Western blot quantification have been normalized in relation with the total protein blotted in the membranes.

Results show that in basal conditions Munc18-1 is located in both, the membrane and the cytosol fractions, with a higher presence in the membrane. Munc18-1 phosphorylation is highly located in the membrane and it is barely detectable in the cytosol. We used GAPDH and ATPase controls to check the correct separation between fractions. Results showed that the cytosolic protein GAPDH was in the cytosol fraction and essentially undetectable in the membrane fraction. In concordance, the membrane protein Na/K-ATPase was highly enriched in this cellular component, and undetectable in the cytosol fraction, confirming the successful protein extraction.

1.2. Calcium and PMA promote Munc18-1 phosphorylation

As it is known that Ser-313 phosphorylation of Munc18-1 occurs in response to PKC stimulus *in vitro* (Fujita et al. 1996) and in synaptosomes (de Vries et al., 2000; Barclay et al., 2003), we investigated whether activation of PKC in the isolated muscle alters pMunc18-1 in the skeletal muscle. **Figure 23** shows that both Munc18-1 and phosphorylation of Munc18-1 is markedly increased by phorbol 12-myristate 13-acetate (PMA¸ the pan-activator of PKC isoforms) treatment (10 nM, 30 minutes) although the ratio pMunc18-1/Munc18-1 is decreased (-23.45 % ± 8.06; $p<0.05$) similarly as it happens in electrically stimulated muscles (*St*) (see later).

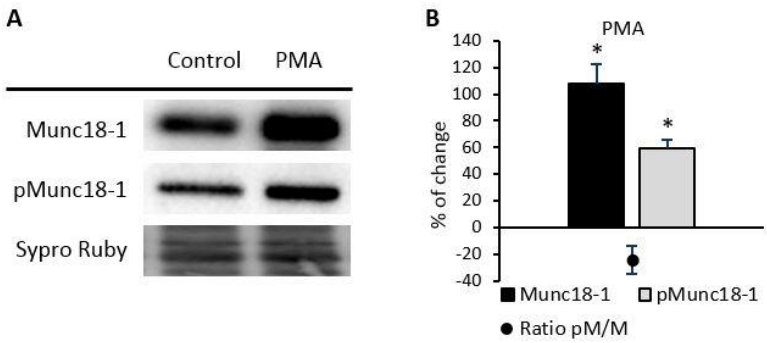

Figure 23. Phorbol 12-myristate 13-acetate (PMA) treatment increases Munc18-1 and pMunc18-1 levels in skeletal muscle. A) Western blot bands of Munc18-1 and pMunc18-1 from rat diaphragm under basal condition before and after PMA treatment. **B)** Western blot bands of Munc18-1 and pMunc18 quantified as optical density corresponding to A. The analysis of percentage of change values confirms the Munc18-1 and pMunc18 statistically significant increase after PMA treatment. Data are mean percentage ± SEM, * $p < 0.05$ (n = 5). Values obtained from Western blot quantification have been normalized in relation with the total protein blotted in the membranes.

It has been shown previously that Ca^{2+} (the primary intracellular trigger of exocytosis), induces phosphorylation of Munc18-1 on Ser-313 in chromaffin cells (Craig et al. 2003). In order to determine whether the phosphorylation is also modulated by Ca^{2+} at the NMJ, muscles were incubated with a Ringer solution of 0.25mM of Ca^{2+} or 5mM of Ca^{2+} for 30 minutes. **Figure 24** shows that phosphorylation of Ser-313 was markedly increased by high (5mM) Ca^{2+} Ringer whereas the total amount of Munc18-1 decreased. Accordingly, the ratio pMunc18-1/Munc18-1 was increased (76.68 % ± 12.04; $p<0.05$). On the contrary, incubation in low Ca^{2+} Ringer (0.25mM) did not result in any change of pMunc18-1 level though, in this case, total Munc18-1 was greatly increased (47.89 % ± 5.81; $p<0.05$). Therefore, although the interpretation of these results is complex, the data show that the changes in expression and phosphorylation of Munc18-1 on Ser-313 depend on Ca^{2+} at the NMJ in a similar way than in other synapses.

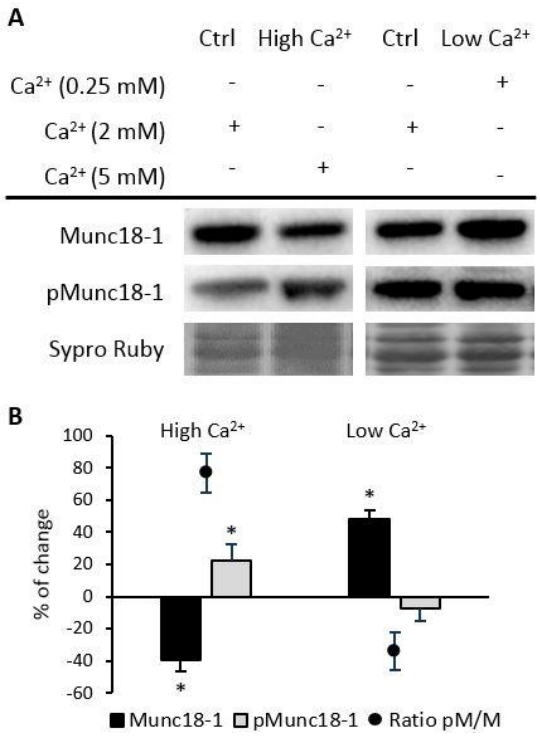

Figure 24. Calcium modulates total Munc18-1 and its phosphorylation at the neuromuscular junction. A) Western blot bands of Munc18-1 and pMunc18-1 from rat diaphragm under basal conditions incubated with different calcium concentrations (30 minutes). **B)** Western blot bands of Munc18-1 and pMunc18 quantified as optical density corresponding to A. High Ca^{2+} concentration (5mM) provokes an increase in pMunc18-1 levels while Munc18-1 significantly decreases. Accordingly, the ratio pMunc18-1/Munc18-1 is significantly increased. Low Ca^{2+} concentration (0.25mM) does not modify pMunc18-1 levels but significantly increases Munc18-1 levels in relation with normal Ringer Ca^{2+} concentration. Therefore, the ratio is significantly decreased. The analysis of percentage of change values confirmed the pMunc18-1 increase to be statistically different when treated with high Ca^{2+} Ringer while there is no significant change when treated with low Ca^{2+}. Data are mean percentage ± SEM, * $p < 0.05$ ($n = 5$). Values obtained from Western blot quantification have been normalized in relation with total protein in the membranes.

In conclusion, Munc18-1 is expressed and phosphorylated in basal conditions in the skeletal muscle with a predominant location in the membrane fraction. Furthermore, phosphorylation of Munc18-1 at Ser-313 occurs in response to pharmacologic PKC stimulus and changes in extracellular calcium. However, in these two last conditions, expression and phosphorylation are not produced in the same manner (see *Discussion*).

Subsequently, immunohistochemical analyses were performed to identify the cellular localization of Munc18-1 at the adult neuromuscular junction.

1.3. Munc18-1 is located in the nerve terminal at the NMJ

Immunofluorescence staining coupled with confocal microscopy analysis was performed to determine the presence and localization of Munc18-1 at the adult NMJ. Immunofluorescence experiments were performed in the diaphragm and LAL muscles and immunoreactivity for Munc18-1 was identical in both muscles. All pictures in **figure 25** show intense immunoreactivity for Munc18-1 in the synaptic area identified with AChR labeling. A-B shows two NMJs with double labeling: AChRs in red and Munc18-1 in green. The *en face* (25A) and the *en side* (25B) images show Munc18-1-positive green immunolabeling concentrated at the presynaptic position, over the red postsynaptic gutters (asterisks in 25B). It can be also observed that Munc18-1 label has stronger concentration in some areas (arrows). C-G shows NMJs with triple labeling: AChRs in red, the nerve terminal (Syntaxin; C-E) or the Schwann cell (S-100; F-G) in blue and Munc18-1 in green. C and F show low magnification images reflecting an abundant Munc18-1-positive green immunolabeling concentrated at the synapses. D-E show detailed Munc18-1-positive green immunolabeling concentrated at the presynaptic position over the red postsynaptic gutters and colocalized with Syntaxin (E, *en side* NMJ, asterisks). F-G shows that there is not colocalization between Munc18-1 and the Schwann cell. In C, D and F it appears that pre-terminal axon is also Munc18-1-positive. The muscle cell has not been labeled.

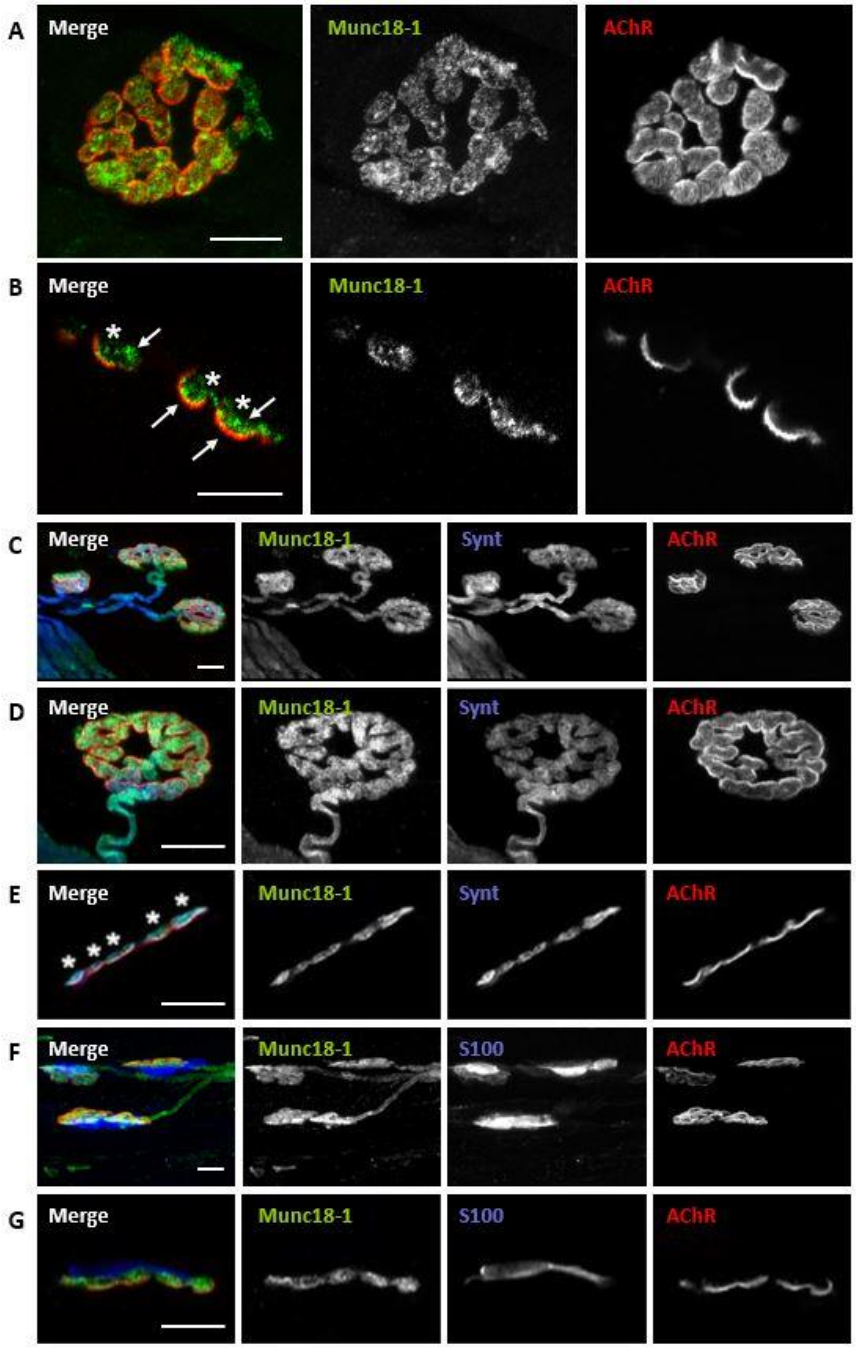

Figure 25. Munc18-1 is exclusively located in the presynaptic component of the neuromuscular junction. Multiple-immunofluorescence-stained muscles visualized at the confocal microscope. **A)** Munc18-1 colocalizes with AChR from a NMJ *en face* view. **B)**

Munc18-1 colocalizes with AChR from a NMJ *en side* view. **C-D)** Munc18-1 colocalizes with Syntaxin and AChR from *en face* view. **E)** Munc18-1 colocalizes with Syntaxin and AChR from *en side* view. **F)** Munc18-1 colocalizes with S-100 and AChR from *en face* view. **G)** Munc18-1 colocalizes with S-100 and AChR from a NMJ *en side* view. To obtain A-B images, the staining labelled Munc18-1 in green and postsynaptic AChRs in red. For C-E images, the staining labelled Munc18-1 in green, postsynaptic AChRs in red and nerve terminals marked by Syntaxin in blue. For F-G images, the staining labelled Munc18-1 in green, postsynaptic AChRs in red and perisynaptic Schwann cells marked by S-100 in blue. Scale bars = 10 µm.

2. Synaptic activity modulates Munc18-1 and pMunc18-1 through nPKCε, cPKCβI and BDNF/TrkB signaling pathway

2.1. Synaptic activity increases Munc18-1 phosphorylation

Neuronal activity regulates transmitter release at synapses and it has been recently established that presynaptic PKC isoforms (whose activity may be related with the phosphorylation of Munc18-1) are differently regulated at the NMJ by nerve activity and by its resulting muscle activity (Besalduch et al. 2010; Hurtado et al. 2017a). Therefore, we first isolated the effect of the presynaptic stimulation (and synaptic transmission) from the effect of the muscle cell contraction, by performing experiments in which contraction was inhibited. Specifically, synaptic activity includes the presynaptic events related with nerve stimulation (1 Hz, 30 minutes), synaptic transmission and endplate potential generation due to ACh signaling (referred to as the *Stimulation (St)* condition in the figures). Muscle contraction includes membrane depolarization of the muscle fiber involving voltage-gated sodium channels and the resulting myofiber contraction (referred to as the *Contraction* condition in the figures). In particular, muscle contraction was inhibited using µ-CgTx-GIIIB (Obis et al. 2015a,b) that preserves the full functionalism of neurotransmission. We performed Western blot analysis and a quantitative study (see *Analysis techniques* in *Material and Metho*ds section) to analyze the density of the bands and evaluate the relative amount of Munc18-1 and its phosphorylated form in different conditions of stimulation. The results show that the nerve stimulation (1 Hz for 30 minutes) significantly increased Munc18-1 (45.06 % ± 9.26; $p<0.05$) and pMunc18-1 (32.89 % ± 8.3; $p<0.05$) levels

(**figure 26**). In concordance, the ratio pMunc18-1/Munc18-1 remained the same (8.52% ± 7.02; p>0.05).

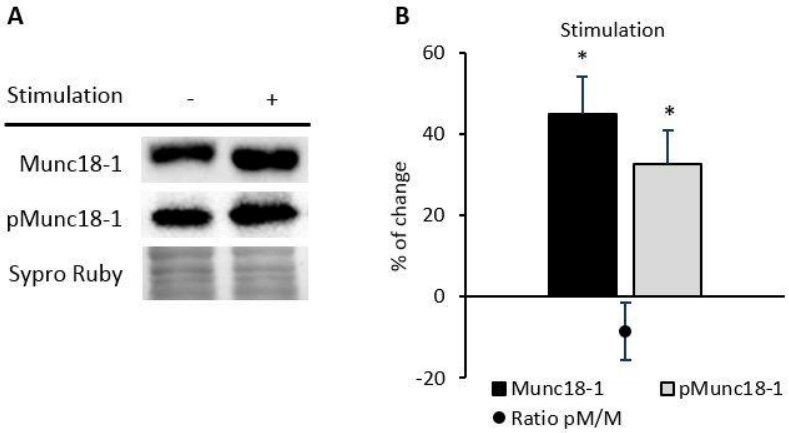

Figure 26. Synaptic activity increases Munc18-1 and pMunc18-1 levels in skeletal muscle. A) Western blot bands of Munc18-1 and pMunc18-1 from rat diaphragm under basal and stimulated conditions (*Stimulation* treatment at 1 Hz for 30 minutes). **B)** Western blot bands of Munc18-1 and pMunc18 quantified as optical density corresponding to A. Results show a statistically significant increase of Munc18-1 and pMunc18-1 proteins in stimulated samples without contraction in comparison with basal condition samples. Data are mean percentage ± SEM, * $p < 0.05$ (n = 5). Values obtained from Western blot quantification have been normalized in relation with total protein blotted in the membranes.

This effect is similar to the previously described effect of the incubation with the activator of PKC, PMA. As it will be showed in the following pages, Munc18-1 phosphorylation may be directly modulated by the increased PKC activity observed during synaptic activity. Altogether, the results show that nerve stimulation increases phosphorylation of Munc18-1 on Ser-313. Moreover, we analyzed pMunc18-1 protein level in cytosol and membrane fractions under nerve electrical stimulation. Results show that in this condition of activity pMunc18-1 is significantly increased in the cytosol fraction (53.91 % ± 3.07; p<0.05; **figure 27**), indicating that the increased amount of Munc18-1 phosphorylated after stimulation involves a disconnection of the molecule from the membrane. The increase induced by synaptic activity of total levels of Munc18-1 could be explained by an increase of its synthesis or, alternatively, by a decrease in its degradation.

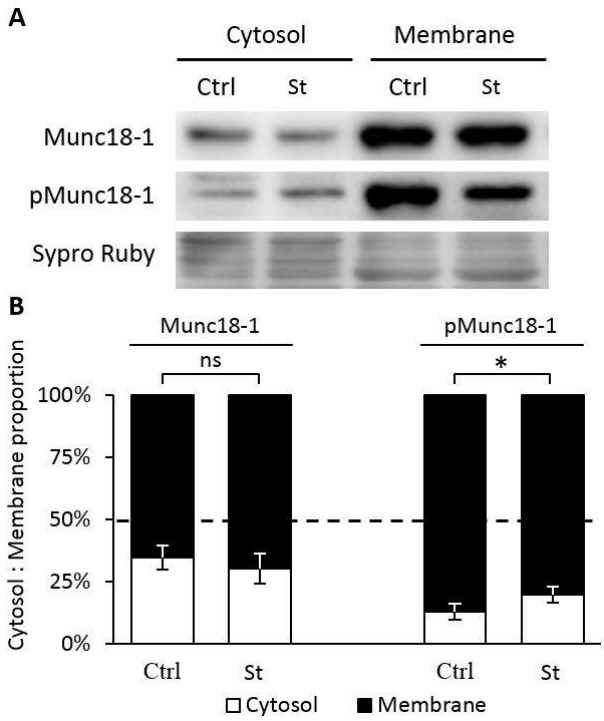

Figure 27. Synaptic activity increases pMunc18-1 levels in the cytosol fraction of skeletal muscle while Munc18-1 does not change. A) Western blot bands of membrane and cytosol distribution of Munc18-1 and pMunc18-1 both in basal and synaptic activity conditions (corresponding to a stimulated (*St*) treatment). **B)** Western blot bands of Munc18-1 and pMunc18 quantified as optical density corresponding to A. Results show that in synaptic activity condition pMunc18-1 increases in the cytosol fraction while total levels of Munc18-1 do not change. Data are mean percentage ± SEM, * $p < 0.05$ ($n = 5$). Values obtained from Western blot quantification have been normalized in relation with total protein blotted in the membranes.

Moreover, because the Munc18-1 phosphorylation may be a rapid process to facilitate the exocytosis mechanism, we analyzed pMunc18-1 and Munc18-1 at shorter times of stimulation (1 min and 10 min, 1Hz). Surprisingly, presynaptic stimulation for 1 minute did not modify significantly the pMunc18-1 protein level while presynaptic stimulation for 10 minutes significantly increased Munc18-1 phosphorylation (30.81 % ± 4.41; $p<0.05$). This value was not different from that observed after 30 minutes of stimulation (**figure 28**). Munc18-1 protein level

gradually increased until 30 minutes (**figure 28**). In concordance, the ratio pMunc18-1/Munc18-1 was significantly increased after 10 minutes of nerve electrical stimulation (34.53 % ± 6.62; $p<0.05$). These results suggest that activation of Munc18-1 induced by synaptic activity can be relatively fast and remains unchanged for a period of time.

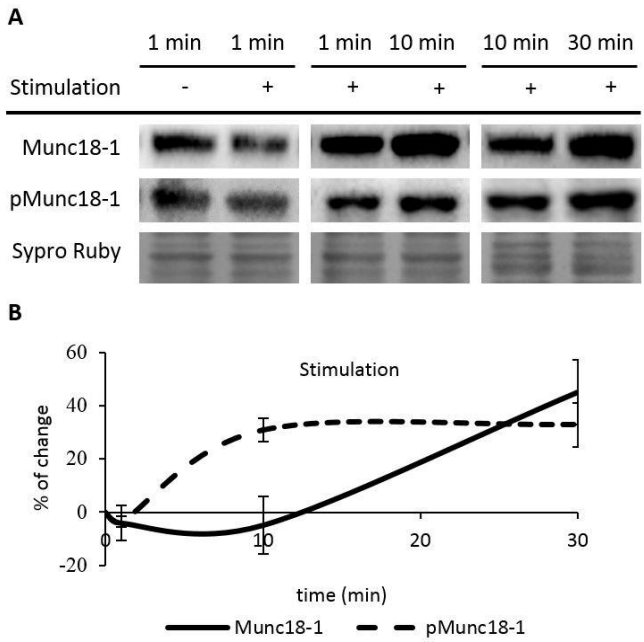

Figure 28. Time course of the modulation of Munc18-1 and pMunc18-1 by synaptic activity A) Western blot bands of Munc18-1 and pMunc18-1 at 1, 10 and 30 minutes after presynaptic stimulation treatment at 1 Hz. **B)** Western blot bands of Munc18-1 and pMunc18 quantified as optical density corresponding to A. Each time-point has been compared to its previous time-point. Presynaptic stimulation significantly increases pMunc18-1 at 10 minutes. Both Munc18-1 and pMunc18-1 gradually increase until 30 minutes after electrical stimulation. Data are mean percentage ± SEM, * $p < 0.05$ ($n = 5$). Values obtained from Western blot quantification have been normalized in relation with total protein blotted in the membranes.

However, because Munc18-1 phosphorylation does not increase after 1 minute of stimulation, we next analyzed whether the unchanged pMunc18-1 protein level at shorter times (1 minute) could be modified by inhibiting the action of phosphatases, because several of these enzymes regulate the effects of synaptic activity at the NMJ, see Hurtado et al., 2017a (**figure 29**). Preincubation with a cocktail of phosphatase inhibitors significantly increases the pMunc18-1 level (35.68 % ± 8.13; $p<0.05$). This indicates that phosphatase activity regulates Munc18-1 phosphorylation-dephosphorylation at short stimulation times. It may be possible that synaptic activity induces a quick and transient phosphorylation of Munc18-1 (maybe related to the immediate fast exocytotic process) whereas during continuous nerve stimulation, the level of pMunc18-1 continuously increases and is finally sustained for a long period.

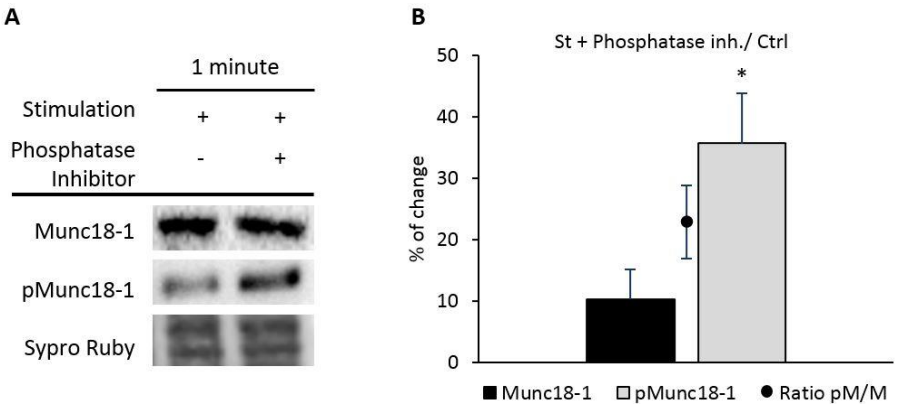

Figure 29. Nerve stimulation with preincubated phosphatase inhibitors significantly increases pMunc18-1 levels at 1 minute. A) Western blot bands of Munc18-1 and pMunc18-1 of skeletal muscle after 1 minute of presynaptic stimulation treatment (1 Hz stimulation) preincubated with phosphatase inhibitors. **B)** Western blot bands of Munc18-1 and pMunc18 quantified as optical density corresponding to A. Phosphatase inhibition significantly increases pMunc18-1 under presynaptic stimulation treatment at 1 minute. In accordance, the pMunc18-1/Munc18-1 ratio significantly increases. Data are mean percentage ± SEM, * $p < 0.05$ ($n = 5$). Values obtained from Western blot quantification have been normalized in relation with total protein blotted in the membranes.

2.2. Both nPKCε and cPKCβI regulate synaptic-induced Munc18-1 phosphorylation

PKC has been involved since many years ago in the control of neurotransmitter release (Genc et al. 2014; Hilfiker and Augustine 1999; Katayama et al. 2017; Korogod et al. 2007; Leenders and Sheng 2005; Santafé et al. 2005, 2006; Vaughan et al. 1998) and Munc18-1 is one of its substrates (Fujita et al., 1996). In particular, nPKCε and cPKCβI isoforms are good candidates to regulate the phosphorylation of Munc18-1 because are exclusively located in the nerve terminal of the NMJ, regulated by synaptic activity and involved in neurotransmitter release (Besalduch et al. 2010; Hurtado et al. 2017a; Obis et al. 2015b). In order to test whether these two isoforms are involved in the phosphorylation of Munc18-1, muscles were exposed to the nPKCε-specific translocation inhibitor peptide, epsilon V1-2 (εV1-2; Johnson et al. 1996), and to the cPKCβI-specific translocation inhibitor peptide, beta I V5-3 (βIV5-3; Liu et al. 1999; Zhang et al. 2015) to block the isoform activities. We previously demonstrated that the peptides εV1-2 and βIV5-3 inhibit the presence of pnPKCε and pcPKCβI respectively in the synaptic membrane of the diaphragm muscle cells (Hurtado et al. 2017a; Obis et al. 2015a,b). Accordingly, **figure 30.A and B** shows that incubation with the peptide εV1-2 (100 μM) produces a significant decrease in nPKCε and pnPKCε protein levels. In addition, cPKCβI and pcPKCβI levels also decrease after incubation with the peptide βIV5-3 (10 μM) (**figure 30.C and D**). These decreases in PKC ε and βI isoforms suggest that these isoforms may be tonically involved in some nerve terminal processes.

Next, we determined how nPKCε and cPKCβI activities affect the level and the phosphorylation of Munc18-1 in basal conditions and after presynaptic stimulation.

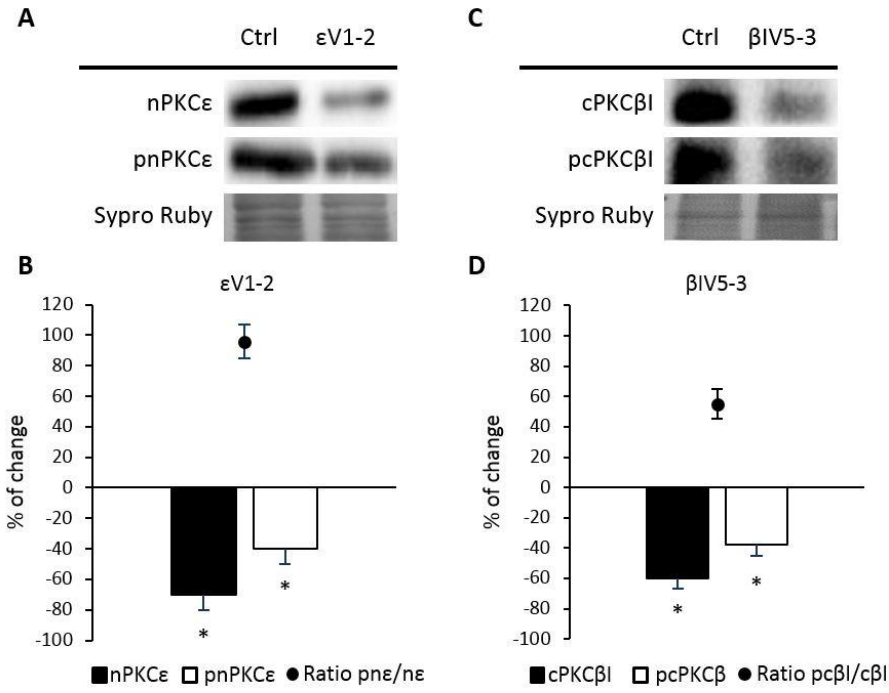

Figure 30. The εV1-2 and βIV5-3 peptides inhibit the presence of nPKCε and cPKCβI respectively and their phosphorylation levels under basal conditions. A-C) Western blot bands of nPKCε and cPKCβI of skeletal muscle under basal conditions preincubated with their respective εV1-2 and βIV5-3 peptides. **B-D)** Western blot bands of nPKCε and cPKCβI and their phosphorylation quantified as optical density corresponding to A and C respectively. The inhibitor peptides εV1-2 and βIV5-3 significantly decrease both PKC isoforms and their phosphorylations under basal conditions. Data are mean percentage ± SEM, * $p < 0.05$ ($n = 5$). Values obtained from Western blot quantification have been normalized in relation with total protein in the membranes.

2.2.1. nPKCε positively modulates Munc18-1 phosphorylation

Figure 31 shows that incubation for 30 minutes of the muscles with the peptide εV1-2 produces a significant decrease in Munc18-1 and pMunc18-1, indicating that in basal conditions nPKCε is regulating the Munc18-1 protein level and, maybe consequently, its phosphorylation, suggesting that nPKCε could have a tonic effect positively regulating pMunc18-1. The ratio pMunc18-1/Munc18-1 in basal conditions was slightly but not significantly decreased (-16.71 % ± 9.82; $p>0.05$).

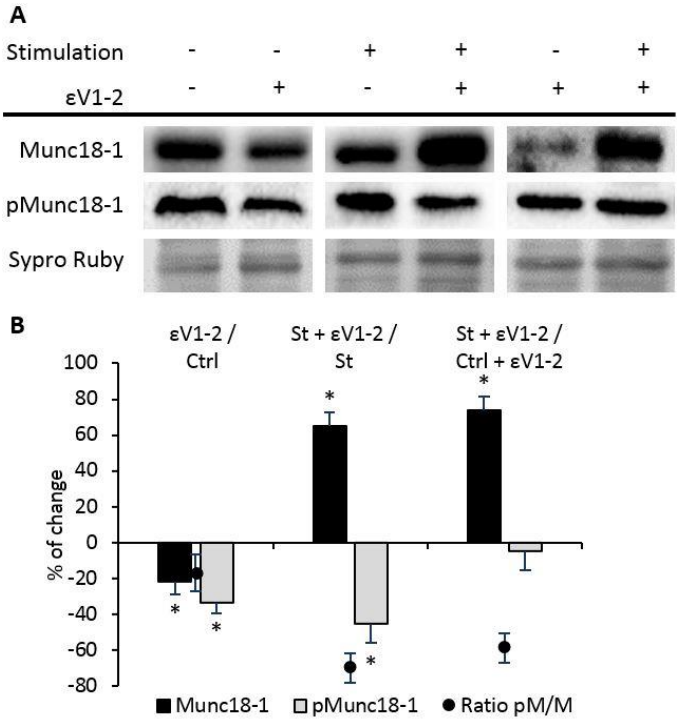

Figure 31. The nPKCε inhibitor εV1-2 peptide modulates Munc18-1 and pMunc18-1 levels under basal and synaptic activity conditions. A) Western blot bands of Munc18-1 and pMunc18 in skeletal muscle under basal and nerve stimulation conditions (1 Hz stimulation for 30 min) preincubated with the nPKCε inhibitor peptide εV1-2. **B)** Western blot bands of Munc18-1 and pMunc18-1 quantified as optical density corresponding to A. The analysis of percentage of change values shows that under basal conditions both Munc18-1 and its phosphorylation significantly decrease (*εV1-2/Ctrl:* muscles in basal conditions versus preincubated with εV1-2 peptide). Moreover, in both *St + εV1-2/ St* (synaptic activity compared with the εV1-2 peptide) and *St + εV1-2/ Ctrl + εV1-2* conditions (basal conditions compared with stimulated samples; both treated with εV1-2 peptide) pMunc18-1/Munc18-1 ratios significantly decrease. Data are mean percentage ± SEM, * $p < 0.05$ ($n = 5$). Values obtained from Western blot quantification have been normalized in relation with total protein blotted in the membranes.

To relate the effects of synaptic activity and nPKCε activity we stimulated (1 Hz, 30 minutes) phrenic nerve of muscles previously incubated with the blocking peptide (100 µM, 30 minutes). We found a significant decrease in pMunc18-1 level (-44.96 % ± 10.8; $p<0.05$) and a significant increase in total Munc18-1 level (65.32 % ± 7.6; $p<0.05$) (**figure 31**). In concordance, the ratio pMunc18-1/Munc18-1 was significantly decreased (-69.82 % ± 8.03; $p<0.05$) indicating that nPKCε specifically enhances phosphorylation of Munc18-1 in conditions of increase of synaptic activity.

Furthermore, to know whether nPKCε is responsible of the increase of Munc18-1 phosphorylation induced by the nerve stimulation we compared Munc18-1 and pMunc18-1 protein levels in control and stimulated samples in which nPKCε had been blocked with the inhibitor peptide (*St + εV1-2 vs Ctrl + εV1-2*) (**figure 31**). We found a significant increase of Munc18-1 (73.63 % ± 7.9; $p<0.05$) with a no significant change on pMunc18-1 level (-4.49 % ± 10.74; $p>0.05$). These results show that the inhibitor peptide is able to completely avoid the phosphorylation induced by the synaptic activity indicating that nPKCε regulates the increase of Munc18-1 phosphorylation induced by the nerve stimulation and suggest that this isoform could phosphorylate Munc18-1 at the NMJ. Moreover, the inhibitor peptide did not avoid the increase in Munc18-1 that synaptic activity caused, but enhanced even more the levels of Munc18-1. This result reinforces the idea that nPKCε is not regulating Munc18-1 protein levels induced by the nerve stimulation.

Together, these results emphasize the specific role of nPKCε enhancing Munc18-1 phosphorylation in presence of synaptic activity. According it was previously reported that the same condition of activity significantly decreased pnPKCε (Obis et al. 2015a), indicating that the nPKCε-induced increase of pMunc18-1 after synaptic activity is accompanied by a significant decrease of the total and phosphorylated nPKCε. Probably, these outcomes are reflecting the well-known process of the downregulation that PKC undergoes after activation (Gould

et al. 2009; Gould and Newton 2008; Kang et al. 2000; Lee et al. 1996; Lu et al. 1998). Moreover, it should be noted that nPKCε auto-phosphorylation is not induced by synaptic activity and that its reduction due to degradation does not affect its kinase function at least on the Munc18-1 substrate. It seems that there is a pool of signaling-competent nPKCε ready to phosphorylate the amount of substrate available at the start of the synaptic activity (and even at basal conditions).

2.2.2. cPKCβI inhibits Munc18-1 phosphorylation

We also analyzed the effect of blocking the membrane translocation of cPKCβI with the peptide βIV5-3 on Munc18-1 phosphorylation in the skeletal muscle. **Figure 32** shows that the peptide βIV5-3 decreased total Munc18-1 levels but did not change pMunc18-1 in basal conditions (ratio pMunc18-1/Munc18-1: 40.92 % ± 5.68; $p<0.05$). However, when the βIV5-3 was preincubated during synaptic activity, a significant increase in pMunc18-1 level was observed with no change in total Munc18-1. In concordance, the ratio pMunc18-1/Munc18-1 was significantly increased (52.35 % ± 7.21; $p<0.05$), indicating that the role of the cPKCβI isoform during synaptic activity contributes to reduce Munc18-1 phosphorylation. As with nPKCε above, we compared Munc18-1 and pMunc18-1 protein level in control and stimulated samples in which cPKCβI had been blocked with the inhibitor peptide (**figure 32**). We found a significant increase of Munc18-1 (26.01 % ± 5.41; $p<0.05$) with a non-significant change of pMunc18-1 level (-1.2 % ± 3.35; $p>0.05$), being the ratio pMunc18-1/Munc18-1: -21.18 % ± 6.74; $p<0.05$. This indicates that, cPKCβI activity is somehow necessary (see discussion) for the increase of Munc18-1 phosphorylation induced by the nerve stimulation (**figure 32**, last column). By the contrary, cPKCβI activity seems not involved in the nerve-induced increased of the Munc18-1 total protein levels (second last column).

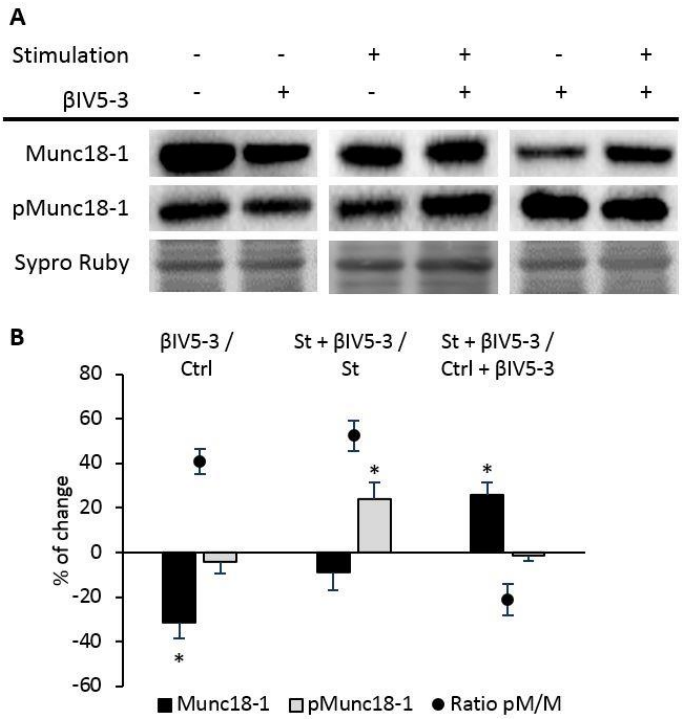

Figure 32. The cPKCβI inhibitor βIV5-3 peptide modulates Munc18-1 and pMunc18-1 levels under basal and synaptic activity conditions. A) Western blot bands of Munc18-1 and pMunc18 in skeletal muscle under basal and nerve stimulation conditions (1 Hz stimulation for 30 min) preincubated with the cPKCβI inhibitor peptide βIV5-3. **B)** Western blot bands of Munc18-1 and pMunc18 quantified as optical density corresponding to A. The analysis of percentage of change values shows that in both *βIV5-3/Ctrl* (muscles in basal conditions versus preincubated with βIV5-3 peptide) and *St + βIV5-3/St* (synaptic activity compared with the βIV5-3 peptide) conditions, the ratio of pMunc18-1/Munc18-1 significantly increases. Moreover, in *St + βIV5-3/Ctrl + βIV5-3* (basal conditions compared with stimulated samples; both treated with βIV5-3 peptide) pMunc18-1/Munc18 ratio is significantly decreased. Data are mean percentage ± SEM, * $p < 0.05$ ($n = 5$). Values obtained from Western blot quantification have been normalized in relation with total protein blotted in the membranes.

We previously reported that pPKCβI increases in the membrane fraction while total cPKCβI is downregulated during synaptic activity (Hurtado et al. 2017a,b). This indicates that the synaptic activity induces cPKCβI phosphorylation and its activation, being functionally maintained in the membrane. Therefore, and in opposition with nPKCε phosphorylation, synaptic activity increases cPKCβI auto-

phosphorylation suggesting that it promotes cPKCβI competence. In relation with the regulation of Munc18-1 phosphorylation, the synaptic activity-induced cPKCβI activity would promote a negative effect on pMunc18-1 protein level (not detected in basal conditions). Interestingly, Munc18-1 protein levels are influenced by PKCβI activity. In concrete, this isoform promotes Munc18-1 levels in basal conditions. However, synaptic activity can increase Munc18-1 without PKCβI action, as stimulus without cPKCβI keeps increasing Munc18-1 levels (**figure 32**, last column).

Altogether, our results indicate that both, nPKCε and cPKCβI isoforms contribute to regulate Munc18-1 phosphorylation during synaptic activity at the NMJ, although nPKCε and cPKCβI work in opposite directions in relation with Munc18-1 phosphorylation: cPKCβI seems to reduce phosphorylation while nPKCε increases it. Therefore, a balance between the activities of the two isoforms can be a relevant cue in the regulation of the exocytotic apparatus.

2.2.3. Interdependence between nPKCε and cPKCβI isoforms

Having established that phosphorylation of Munc18-1 is regulated by the opposite action of nPKCε and cPKCβI, we next further investigated whether cPKCβI signaling regulates nPKCε and whether nPKCε signaling regulates cPKCβI. First, we used the cPKCβI-specific translocation inhibitor peptide (βIV5-3) to block the corresponding isoform activity. Muscles were then immunoblotted to detect nPKCε protein levels and its phosphorylated form in the diaphragm muscle. As mentioned above, the peptide decreased the level of the corresponding isoform in the synaptic membrane. **Figure 33** shows that βIV5-3 was able to significantly increase pnPKCε protein levels (with a significant decrease in nPKCε) in both basal and synaptic activity conditions. In particular, the ratio pnPKCε/nPKCε significantly increased (basal conditions: 106.06 % ± 8.69; $p<0.05$; synaptic activity: 101.84 % ± 10.45; $p<0.05$). Moreover, in *St + βIV5-3/Ctrl + βIV5-3* (basal conditions compared with stimulated samples; both treated with βIV5-3 peptide) both nPKCε and

pnPKCε significantly increased. These results indicate that the cPKCβI isoform negatively regulates pnPKCε phosphorylation and maybe its activity. Together, the data indicate that as a result of the increase of synaptic activity pnPKCε enhances phosphorylation of Munc18-1 and cPKCβI decreases it, maybe through negatively regulating the action of pnPKCε.

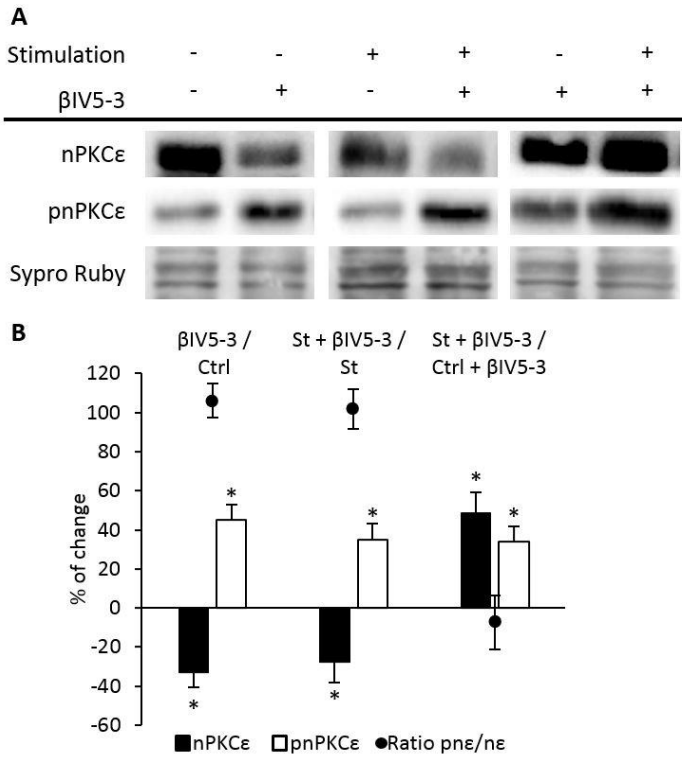

Figure 33. The cPKCβI inhibitor βIV5-3 peptide modulates nPKCε and pnPKCε levels under basal and synaptic activity conditions. A) Western blot bands of nPKCε and pnPKCε in skeletal muscle under basal and nerve stimulation conditions (1 Hz stimulation for 30 min) preincubated with the cPKCβI inhibitor peptide βIV5-3. **B)** Western blot bands of nPKCε and pnPKCε quantified as optical density corresponding to A. The analysis of percentage of change values shows that in both *βIV5-3/Ctrl* (muscles in basal conditions versus preincubated with βIV5-3 peptide) and *St + βIV5-3/St* (synaptic activity compared with the βIV5-3 peptide) conditions, the ratio pnPKCε/nPKCε significantly increases. Moreover, in *St + βIV5-3/Ctrl + βIV5-3* (basal conditions compared with stimulated samples; both treated with βIV5-3 peptide) both nPKCε and pnPKCε significantly increase. Data are mean percentage ± SEM, * $p < 0.05$ ($n = 5$). Values obtained from Western blot quantification have been normalized in relation with total protein blotted in the membranes.

On the contrary, **figure 34** shows that εV1-2 was able to significantly decrease cPKCβI without changing pcPKCβI protein levels in both basal and synaptic activity conditions. These results indicate that pnPKCε isoform enhances cPKCβI levels but does not affect its activity. Together, these results demonstrate the mutual regulatory influence between nPKCε and cPKCβI. Thus, a hypothesis could be formulated on the existence of a finely regulated feedback between these two PKC isoforms to properly modulate relevant molecules of the exocytotic apparatus.

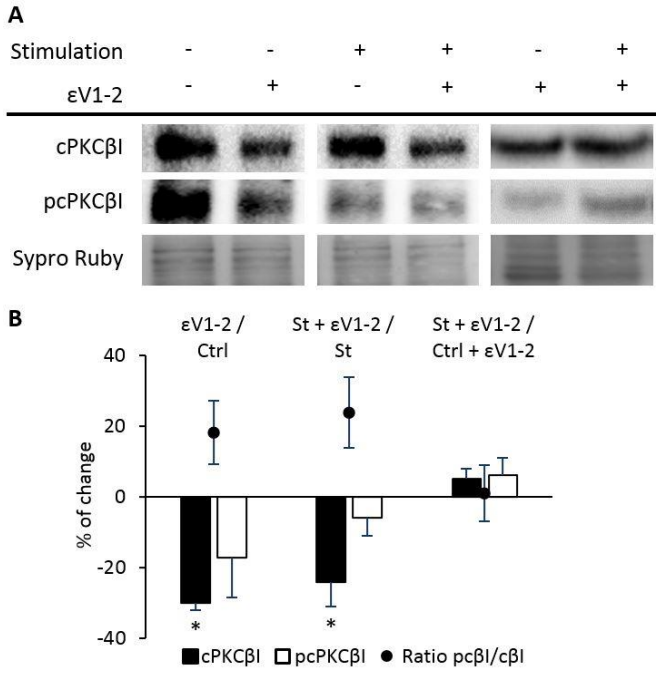

Figure 34. The nPKCε inhibitor εV1-2 peptide decreases cPKCβI protein levels without changing its phosphorylation levels under basal and synaptic activity conditions. A) Western blot bands of cPKCβI and pcPKCβI in skeletal muscle under basal and nerve stimulation conditions (1 Hz stimulation for 30 min) preincubated with the nPKCε inhibitor peptide εVI-2. **B)** Western blot bands of cPKCβI and pcPKCβI quantified as optical density corresponding to A. The analysis of percentage of change values shows that in both εVI-2/Ctrl (muscles in basal conditions versus preincubated with εVI-2 peptide) and St + εVI-2/St (synaptic activity compared with the εVI-2 peptide) the cPKCβI total levels significantly decreased, being the ratio pcPKCβI/cPKCβI in this last condition significantly increased. Data are mean percentage ± SEM, * $p < 0.05$ ($n = 5$). Values obtained from Western blot quantification have been normalized in relation with total protein blotted in the membranes.

2.3. BDNF/TrkB pathway regulates Munc18-1 phosphorylation

We recently described that synaptic activity enhances BDNF/TrkB signaling pathway to increase cPKCβI activity (Hurtado et al. 2017a). To demonstrate whether the activation of TrkB is critical to affect pMunc18-1 level, we selectively suppressed TrkB activity in electrically nerve-stimulated diaphragm muscles using a selective TrkB inhibitor. We used the anti-TrkB antibody 47/TrkB which effectively inhibits endogenous BDNF from binding to TrkB receptors (Balkowiec and Katz 2000). We measured resultant Munc18-1 and pMunc18-1 levels and found that in electrically stimulated muscles, TrkB blockade resulted in a significant increase in pMunc18-1 without affecting Munc18-1 level (**figure 35**). In concordance, the ratio pMunc18-1/Munc18-1 significantly increased (99.69 % ± 14.04; $p<0.05$). This result suggests that, in conditions of synaptic activity, a TrkB-mediated tonic effect partly reduces the pMunc18-1 increase, which is produced during nerve stimulation. This result reinforces the idea of a negative role of the endogenous BDNF-TrkB pathway on Munc18-1 phosphorylation, without affecting Munc18-1 protein levels. Surprisingly, however, preincubation with exogenous BDNF (10nM, 30 minutes) in nerve-stimulated muscles (*St*) did not modify the pMunc18-1 protein level (**figure 35**).

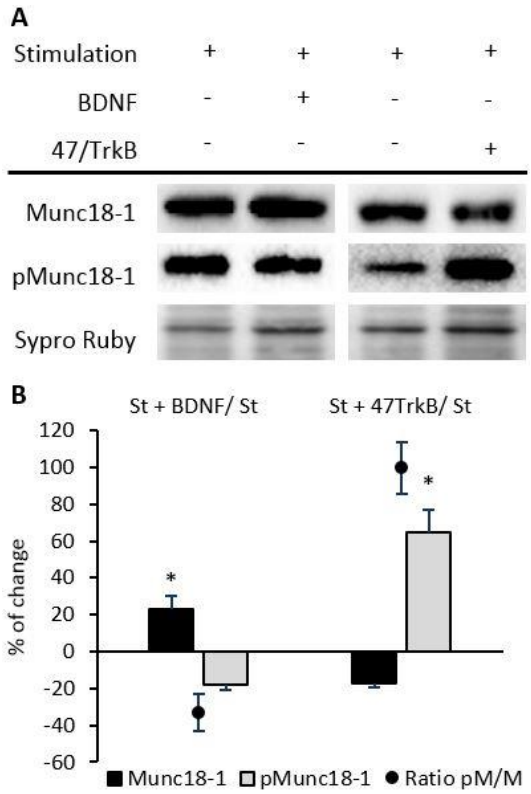

Figure 35. BDNF/TrkB signaling modulates Munc18-1 and pMunc18-1 levels under synaptic activity conditions. A) Western blot bands of Munc18-1 and pMunc18-1 in skeletal muscle under presynaptic nerve stimulation treatment (1 Hz stimulation for 30 min) preincubated with exogenous BDNF and the sequestering antibody 47/TrkB respectively. **B)** Western blot bands of Munc18-1 and pMunc18-1 quantified as optical density corresponding to A. The analysis of the percentage of change values shows that after the treatment with BDNF, the ratio of pMunc18-1/Munc18-1 significantly decreases while after the 47/TrkB treatment, the ratio significantly increases. Data are mean percentage ± SEM, * $p < 0.05$ ($n = 5$). Values obtained from Western blot quantification have been normalized in relation with total protein blotted in the membranes.

These results show that, even though exogenous BDNF cannot affect the phosphorylation of Munc18-1, endogenous BDNF could act through TrkB to negatively regulate the phosphorylation of Munc18-1. On the contrary, exogenous BDNF slightly but significantly increased the Munc18-1 protein level and it seems to positively regulate the increase of Munc18-1 protein levels perhaps inducing its

synthesis or alternatively decreasing its degradation. We chose the BDNF dose based in a previous dose–response and time-course study in the same muscle model to determine its effect on the size of the evoked end-plate potential (EPP) (Garcia et al. 2010). Interestingly, exogenous BDNF decreases also Munc18-1 and pMunc18-1 levels in basal conditions.

Altogether, these results show that TrkB signaling negatively regulates Munc18-1 phosphorylation. Interestingly, the synaptic activity-induced TrkB effects are similar to those of cPKCβI suggesting that cPKCβI and TrkB work coordinately to regulate the phosphorylation of Munc18-1 in this condition.

In summary, our results indicate that the phosphorylation of Munc18-1 at the NMJ is increased in response to a signaling mechanism initiated with synaptic activity and directly mediated by nPKCε. It seems however, that cPKCβI and TrkB activities work to prevent this synaptic activity/nPKCε-induced Munc18-1 phosphorylation.

It is not known whether synaptic activity-induced nPKCε activity is also regulated by BDNF/TrkB signaling pathway (as it is the cPKCβI activity). Therefore, we next performed experiments to assess how the BDNF-sequestering antibody 47/TrkB affects nPKCε and pnPKCε, when synaptic activity is increased. **Figure 36** shows that pnPKCε level significantly increased (without change of nPKCε) after blocking endogenous BDNF under *Stimulation* condition, indicating that TrkB activity decreases the phosphorylation of nPKCε (ratio pnPKCε/nPKCε 147.88 % ± 10.12; $p<0.05$) and probably its activity. In concordance, we showed previously that blocking TrkB also highly increases pMunc18-1 levels. These results, together, are good evidence that pnPKCε activity and pMunc18-1 level are positively related and negatively modulated by TrkB in presynaptic stimulation condition. TrkB would enhance pcPKCβI activity to prevent the synaptic activity-induced Munc18-1 phosphorylation mediated by pnPKCε.

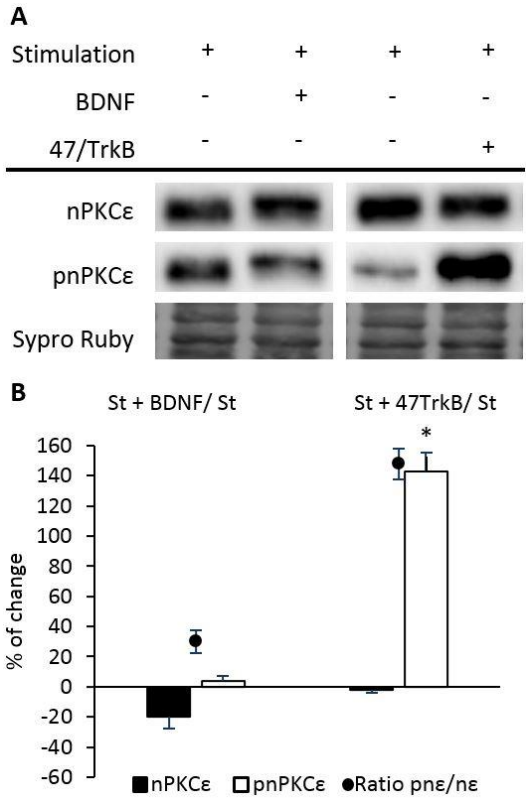

Figure 36. BDNF/TrkB signaling modulates nPKCε phosphorylation levels under synaptic activity conditions. A) Western blot bands of nPKCε and pnPKCε in skeletal muscle under presynaptic nerve stimulation treatment (1 Hz stimulation for 30 min) preincubated with exogenous BDNF and the sequestering antibody 47/TrkB respectively. **B)** Western blot bands of Munc18-1 and pMunc18-1 quantified as optical density corresponding to A. The analysis of the percentage of change values shows that after the 47/TrkB treatment, pnPKCε significantly increases without change in the nPKCε total levels. In accordance, the ratio is significantly increased. Data are mean percentage ± SEM, * $p < 0.05$ ($n = 5$). Values obtained from Western blot quantification have been normalized in relation with total protein blotted in the membranes.

3. Muscle contraction prevents Munc18-1 phosphorylation against the activity of nPKCε, cPKCβI and BDNF/TrkB

3.1. Muscle contraction prevents the synaptic activity-induced Munc18-1 phosphorylation

In previous studies, it has been established that the presynaptic PKC isoforms ε and βI are differently regulated by nerve activity and by its resulting muscle activity in the NMJ (Besalduch et al. 2010; Hurtado et al. 2017a; Obis et al. 2015a). Specifically, muscle activity *per se* has a critical role to enhance presynaptic nPKCε and cPKCβI protein levels. Therefore, we next investigated the role of muscle contraction over Munc18-1 protein level and its phosphorylation, and also the relationship with these PKC isoforms. In our experimental design, we can distinguish the effects of synaptic activity from those of muscle contraction (**Table 1**). Synaptic activity includes the presynaptic events related with nerve stimulation (1 Hz, 30 minutes), synaptic transmission and endplate potential generation due to ACh signaling (referred to as the *Stimulation (St)* condition in the figures). Muscle contraction includes membrane depolarization of the muscle fiber involving voltage-gated sodium channels and the resulting myofiber contraction (referred to as the *Contraction* condition in the figures). Finally, presynaptic *Stimulation with Contraction* treatment comprises the effects of synaptic activity and muscle contraction, showing complete neuromuscular activity.

Figure 37 shows that the electrical stimulation of synaptic inputs to the diaphragm muscle followed by the resulting muscle contraction (contrary to what happens in the condition of only stimulation without contraction previously described) did not change the amount of Munc18-1 and pMunc18-1 (although a non-significant decrease is detected). Interestingly, when the effect of muscle contraction was itself analyzed by comparing stimulated muscles with unaltered contraction (*Stimulation with Contraction*) with stimulated muscles that were

preincubated with μ-CgTx-GIIIB (*Stimulation*), we found that the concurrence of muscle contraction with electrically stimulated synaptic activity prevented the Munc18-1 increase and even promoted a slightly significant reduction in pMunc18-1 level (-22.85 % ± 6.5; $p<0.05$). In concordance, the ratio of pMunc18-1/Munc18-1 was maintained (-15.48 % ± 2.4; $p>0.05$). These results indicate that muscle contraction *per se* prevents (or reverts to control values) the nerve activity-induced Munc18-1 and pMun18-1 increase (showed in **figure 26**).

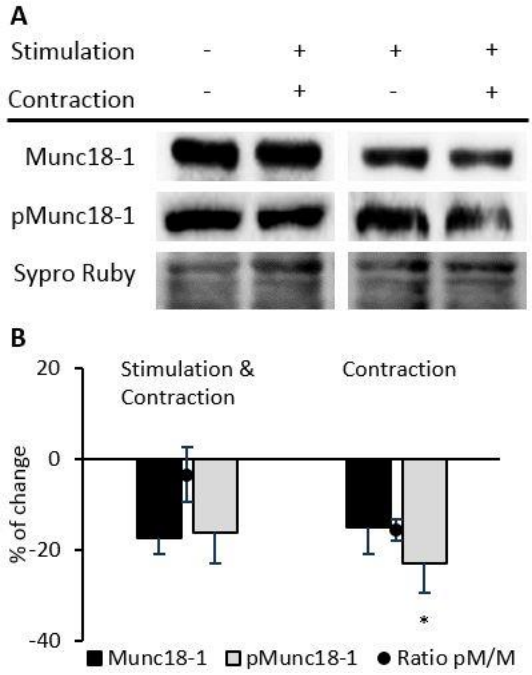

Figure 37. Muscle contraction downregulates pMunc18-1 levels in the skeletal muscle. A) Western blot bands of Munc18-1 and pMunc18-1 from rat diaphragm treated with electrical stimulation at 1 Hz for 30 minutes with contraction and only contraction. **B)** Western blot bands of Munc18-1 and pMunc18 quantified as optical density corresponding to A. *Contraction* results show a statistically significant decrease of pMunc18-1. Data are mean percentage ± SEM, * $p < 0.05$ ($n = 5$). Values obtained from Western blot quantification have been normalized in relation with total protein blotted in the membranes.

We next wanted to know whether muscle contraction prevents the nerve-induced phosphorylation of Munc18-1 even a short times of stimulation. Therefore, we performed experiments at 1, 10 and 30 minutes with nerve-electrical stimulation resulting in muscle contraction. Results showed that 10 minutes of stimulation resulting in muscle contraction slightly increased Munc18-1 phosphorylation (18.06 % ± 8.52; $p>0.05$) but declined under baseline at 30 minutes of electrical stimulation (**figure 38**). On the contrary, stimulation for 1 minute with muscle contraction significantly decreased total Munc18-1 protein levels (-34.41 % ± 3.74; $p<0.05$) (**figure 38**), further decreased after 10 minutes of stimulation (-49.19 % ± 7.02; $p<0.05$) and raised back to near baseline by 30 minutes of electrical stimulation (-17.43 % ± 3.35; $p>0.05$, compared with a non-stimulated control) (**figure 38**). The time course evolution of pMunc18-1 between 1-10 minutes is similar during stimulation with and without contraction although lower in contraction. However, the effect of muscle contraction when the stimulation is longer (10-30 minutes) is to significantly decrease pMunc18-1 protein levels. Together, these results indicate that muscle contraction prevents phosphorylation of Munc18-1 only when a continuous stimulation is performed.

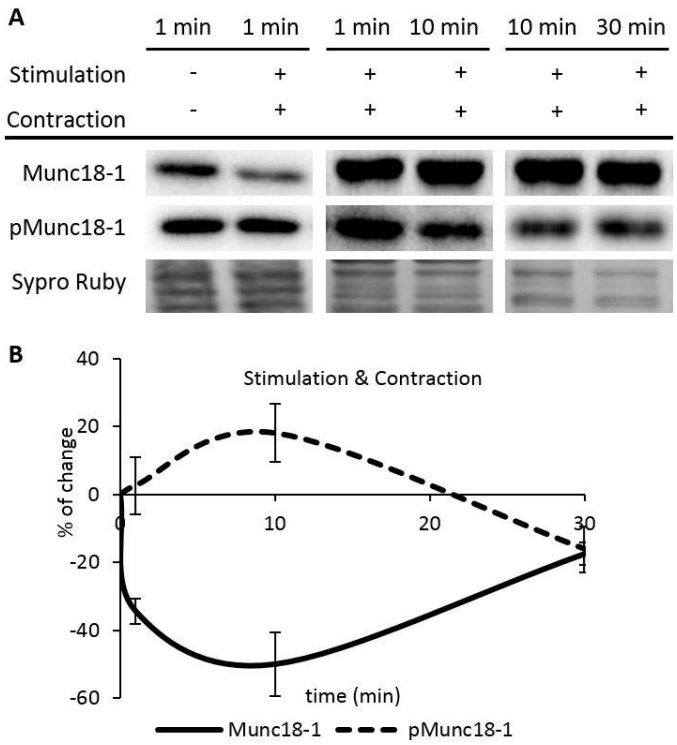

Figure 38. Time course of the modulation of Munc18-1 and pMunc18-1 by muscle contraction. A) Western blot bands of Munc18-1 and pMunc18-1 at 1, 10 and 30 minutes after presynaptic stimulation with contraction treatment at 1 Hz. **B)** Western blot bands of Munc18-1 and pMunc18 quantified as optical density corresponding to A. Each time-point has been compared to its previous time-point. Muscle contraction significantly increases pMunc18-1 at 10 minutes. Moreover, Munc18-1 significantly decreases at 1 minute and is maintained until 30 minutes. Data are mean percentage ± SEM, * $p < 0.05$ ($n = 5$). Values obtained from Western blot quantification have been normalized in relation with total protein blotted in the membranes.

3.2. Both nPKCε and cPKCβI promote Munc18-1 phosphorylation in muscle contraction conditions

To test whether nPKCε is related to Munc18-1 phosphorylation when nerve stimulation results in muscle contraction, we analyzed pMunc18-1 level in nerve stimulated contracting muscles preincubated with the peptide εV1-2. We found a

slight but significant decrease in pMunc18-1 levels with unchanged levels of total Munc18-1 (**figure 39**). In concordance, the ratio of pMunc18-1/Munc18-1 significantly decreased (-20.59 % ± 5.1; $p<0.05$). This result indicates that nPKCε positively regulates Munc18-1 phosphorylation in nerve stimulated contracting muscles.

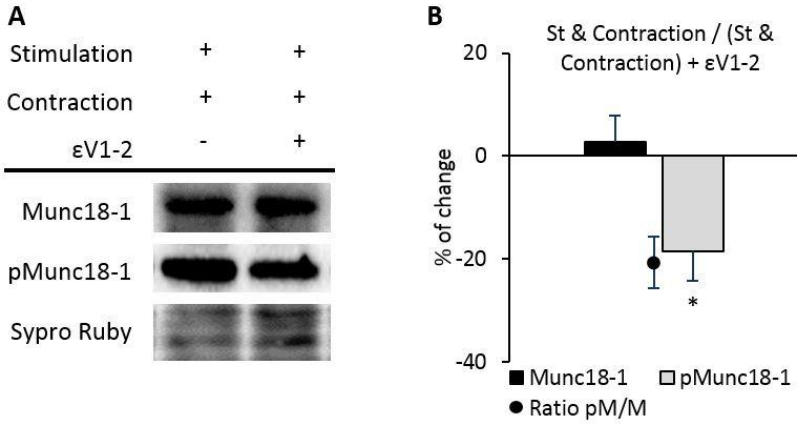

Figure 39. nPKCε modulates Munc18-1 phosphorylation levels under synaptic activity with muscle contraction conditions. A) Western blot bands of Munc18-1 and pMunc18-1 in skeletal muscle under nerve stimulation conditions (1 Hz stimulation for 30 min) resulting in contraction preincubated with the nPKCε inhibitor peptide εV1-2. **B)** Western blot bands of Munc18-1 and pMunc18-1 quantified as optical density corresponding to A. The analysis of the percentage of change values shows that the phosphorylation of Munc18 as well as the ratio of pMunc18-1/Munc18-1 significantly decrease. Data are mean percentage ± SEM, * $p < 0.05$ ($n = 5$). Values obtained from Western blot quantification have been normalized in relation with the total protein blotted in the membranes.

When the βIV5-3 peptide is preincubated in muscles in which nerve stimulation results in muscle contraction, there is a significant decrease in pMunc18-1 level accompanied with a significant increase of total Munc18-1 protein level (**figure 40**). The ratio of pMunc18-1/Munc18-1 significantly decreased (-48.55 % ± 10.1; $p<0.05$). This result indicates that during the full activity of the NMJ including muscle contraction, the role of the cPKCβI positively contributes to increase pMunc18-1. The increased levels of Munc18-1 observed

when the peptide βIV5-3 is incubated under muscle contraction conditions could be explained because cPKCβI negatively regulates the synthesis of Munc18-1 and/or because Munc18-1 is accumulated as a result of the drop in its phosphorylation.

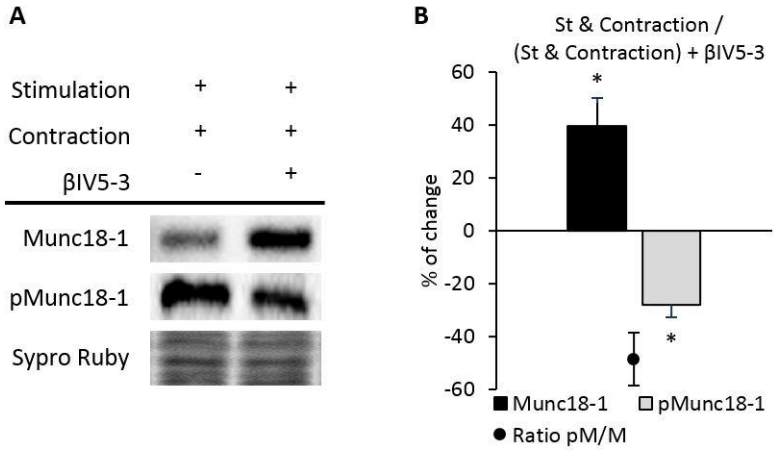

Figure 40. cPKCβI modulates Munc18-1 phosphorylation levels under synaptic activity with muscle contraction conditions. A) Western blot bands of Munc18-1 and pMunc18-1 in skeletal muscle under nerve stimulation conditions (1 Hz stimulation for 30 min) resulting in contraction preincubated with the cPKCβI inhibitor peptide βIV5-3. **B)** Western blot bands of Munc18-1 and pMunc18-1 quantified as optical density corresponding to A. The analysis of the percentage of change values shows that the ratio of pMunc18-1/Munc18-1 significantly decreases. Data are mean percentage ± SEM, * $p < 0.05$ ($n = 5$). Values obtained from Western blot quantification have been normalized in relation with the total protein blotted in the membranes.

Figure 41 shows that βIV5-3 significantly enhances pnPKCε protein level and a diminution of nPKCε in synaptic activity resulting in muscle contraction condition. The ratio pnPKCε/nPKCε significantly increased (102.96 % ± 9.65; $p<0.05$). These results indicate that cPKCβI isoform negatively regulates pnPKCε phosphorylation activity. This effect is the same as doing cPKCβI on nPKCε under synaptic activity conditions.

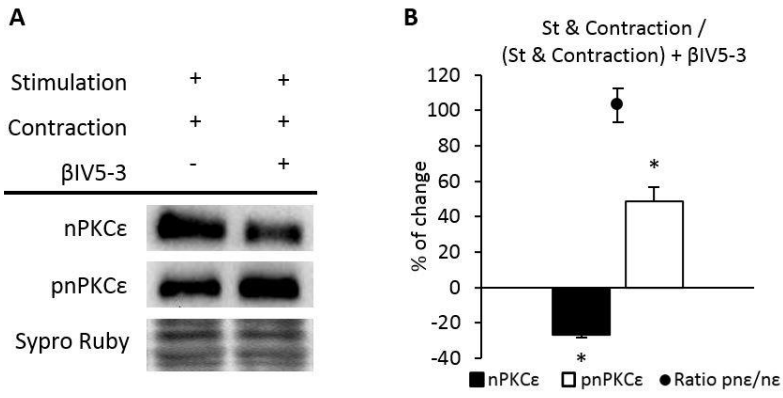

Figure 41. cPKCβI modulates nPKCε and pnPKCε levels under synaptic activity with muscle contraction conditions. A) Western blot bands of nPKCε and pnPKCε in skeletal muscle under nerve stimulation conditions (1 Hz stimulation for 30 min) resulting in contraction preincubated with the cPKCβI inhibitor peptide βIV5-3. **B)** Western blot bands of nPKCε and pnPKCε quantified as optical density corresponding to A. The analysis of the percentage of change values shows that the ratio of the phosphorylation of nPKCε as well as pnPKCε/nPKCε significantly increases. Data are mean percentage ± SEM, * $p < 0.05$ ($n = 5$). Values obtained from Western blot quantification have been normalized in relation with the total protein blotted in the membranes.

Altogether, the results show that nerve stimulation increases phosphorylation of Munc18-1 on Ser-313 and that the resulting nerve-induced muscle contraction induces an important change that prevents the effect of nerve stimulation by itself on Munc18-1 and pMunc18-1 levels when a continuous stimulation is performed. Moreover, nPKCε positively regulates Munc18-1 phosphorylation both in basal and synaptic activity conditions (with and without contraction), being higher the effect of nPKCε in synaptic activity without contraction. The cPKCβI isoform negatively regulates pnPKCε phosphorylation activity in all the studied activity conditions. However, during the full activity of the NMJ, including muscle contraction, the role of the cPKCβI shifts to increase pMunc18-1.

3.3. BDNF/TrkB pathway promotes Munc18-1 phosphorylation in muscle contraction conditions

Because the BDNF/TrkB is a key pathway that affects nPKCε and cPKCβI isoforms and it is influenced by muscle contraction (Hurtado et al. 2017a; Obis et al. 2015a), we next analyzed the regulation of Munc18-1 and pMunc18-1 protein levels by the BDNF/TrkB in muscle contraction conditions. Moreover, we described above that the continued occurrence of neurotransmission and contractile activity causes an important drop of pMunc18-1 after 30 minutes. Blocking TrkB with 47/TrkB in the *Stimulation and Contraction* condition, did not change Munc18-1 (**figure 42**) indicating that endogenous BDNF does not affect Munc18-1 protein level. However, pMunc18-1 significantly decreased when TrkB was blocked with 47/TrkB (**figure 42**), a result which suggests that phosphorylation of Munc18-1 seems produced dependently of the TrkB signaling. Surprisingly, exogenous BDNF in the *Stimulation and Contraction* condition significantly decreased pMunc18-1 and Munc18-1 protein levels (**figure 42**). This result indicates that exogenous BDNF and endogenous BDNF act differently, suggesting that the first one could be binding a different receptor. The result also reinforces the idea that exogenous BDNF has the same effect as contraction, both reducing pMunc18-1 level. This could have two explanations, BDNF could have an additional effect over the muscle contraction through an independent pathway or BDNF could be part of the same pathway that muscle contraction triggers. Evidence support that muscle contraction induces BDNF synthesis (Hurtado et al. 2017a). In this regard, the present results could indicate that the pathway triggered by postsynaptic contraction is not saturated at the moderate frequency of stimulation of 1 Hz and can be enhanced adding exogenous BDNF. Altogether, these results show that TrkB signaling regulates Munc18-1 phosphorylation without affecting total Munc18-1 protein levels. Synaptic activity enhances Munc18-1 phosphorylation while the resulting muscle contraction decreases it. Interestingly, the synaptic activity and the muscle contraction induced similar effects on TrkB and on cPKCβI,

suggesting that both molecules work coordinately to regulate the phosphorylation of Munc18-1 under these conditions.

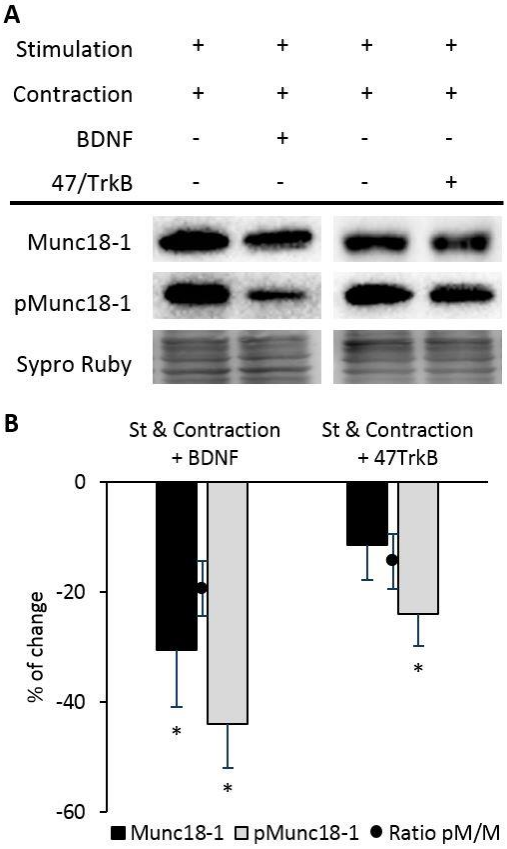

Figure 42. BDNF/TrkB signaling modulates Munc18-1 and its phosphorylation levels under synaptic activity with contraction conditions. A) Western blot bands of Munc18-1 and pMunc18-1 in skeletal muscle under presynaptic nerve stimulation with contraction treatment (1 Hz, 30 min) preincubated with exogenous BDNF and the sequestering antibody 47/TrkB respectively. **B)** Western blot bands of Munc18-1 and pMunc18-1 quantified as optical density corresponding to A. The analysis of the percentage of change values shows that both treatments significantly decrease pMunc18-1 levels. Moreover, in BDNF treatment Munc18-1 total levels significantly decrease. Data are mean percentage ± SEM, * $p < 0.05$ ($n = 5$). Values obtained from Western blot quantification have been normalized in relation with total protein in the membranes.

Thus, these results demonstrate that muscle contraction prevents the synaptic activity–induced Munc18-1 phosphorylation against the activity of nPKCε, cPKCβI and TrkB.

CHAPTER II. SNAP-25 PHOSPHORYLATION IS INDUCED BY SYNAPTIC ACTIVITY AND MEDIATED BY THE nPKCε ISOFORM IN THE SKELETAL MUSCLE

1. SNAP-25 and pSNAP-25 in the adult skeletal muscle: expression, location and regulation by calcium and PMA

1.1. Expression and location of SNAP-25 and pSNAP-25

Western blot analysis using an antibody raised against SNAP-25 was carried out to determine the presence of this protein in the diaphragm skeletal muscle of young adult rats (P30-P40). We also immunoblotted samples with an anti-phospho-Ser-187-specific SNAP-25 antibody to identify the specific phosphorylation of SNAP-25 (Shimazaki et al., 1996). This antibody is a synthetic phosphopeptide that was raised against the amino acid residues surrounding the phospho Ser-187 of rat SNAP-25, the phosphorylation site for PKC *in vitro* (Kataoka et al. 2000; Leenders and Sheng 2005; Nagy et al. 2002). The antibodies were tested also in spinal cord and brain. In all tissues, the antibodies only recognized the corresponding protein, labelling a 28 kDa band for pSNAP-25, which corresponded to the predicted molecular weight in accordance with the manufacturer's data sheets (**figure 43**). The Western blot experiments revealed significant amounts of SNAP-25 in the diaphragm muscle with a high fraction phosphorylated on Ser-187 under basal conditions (**figure 43**). The ventral part of the spinal cord and the brain showed also higher amounts of SNAP-25 than pSNAP-25 in agreement with published data (Oyler et al., 1992; Mandolesi et al., 2009).

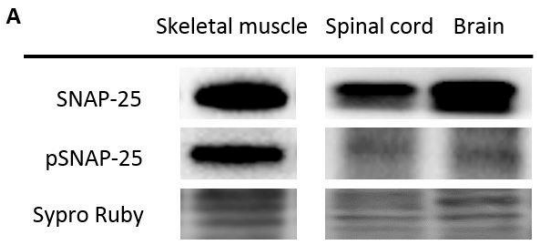

Figure 43. SNAP-25 and pSNAP-25 distribution in different tissues. Western blot bands of SNAP-25 and pSNAP-25 from adult rat skeletal muscle (diaphragm), spinal cord and brain under basal conditions. Both SNAP-25 and pSNAP-25 are expressed in the three tissues with a higher presence in the skeletal muscle.

We analyzed SNAP-25 and pSNAP-25 in the cytosol and the membrane fractions in basal conditions (**figure 44**). Results show that SNAP-25 and pSNAP-25 are located in both the membrane and the cytosol fractions, being predominant in the membrane. We used GAPDH and ATPase controls to check for the correct separation between membrane and cytosol fractions. Results showed that the cytosolic protein GAPDH was in the cytosol fraction and essentially undetectable in the membrane fraction. In concordance, the membrane protein Na^+/K^+-ATPase was highly enriched in this cellular component, and undetectable in the cytosol fraction, confirming the successful protein extraction.

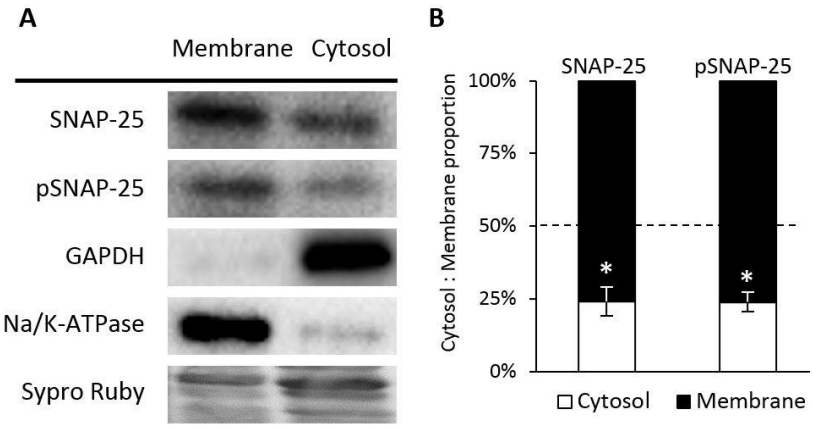

Figure 44. Membrane-cytosol distribution of SNAP-25 and pSNAP-25 under basal conditions. A) Western blot bands of membrane and cytosol distribution of SNAP-25 and pSNAP-25 in basal conditions. **B)** Western blot bands of SNAP-25 and pSNAP-25 quantified

as optical density corresponding to A. Results show that in basal conditions, both SNAP-25 and pSNAP-25 are located predominantly in the membrane fraction. Moreover, glyceraldehyde 3-phosphate dehydrogenase (GAPDH) is found in the cytosol fraction and undetectable in the membrane fraction. As expected, the membrane protein Na^+/K^+-ATPase is highly enriched in this cellular component, and undetectable in the cytosol fraction. Data are mean percentage ± SEM, * $p < 0.05$ ($n = 5$). Values obtained from Western blot quantification have been normalized in relation with the total protein blotted in the membranes.

1.2. PMA and calcium modulates SNAP-25 protein levels

As it is known that Ser-187 phosphorylation of SNAP-25 occurs in response to PKC stimulus (Shimazaki et al., 1996; Nagy et al., 2002; Lau et al., 2010), we investigated whether activation of PKC in the isolated muscle alters pSNAP-25. **Figure 45** shows that SNAP-25 is markedly increased by the pan-activator of PKC isoforms, the PMA treatment (10nM, 30 minutes). Surprisingly, PMA did not affect the phosphorylation of SNAP-25. The ratio pSNAP-25/SNAP-25 decreased (-30.16 % ± 4.81, $p<0.05$). Thus, PMA did not affect the phosphorylation of SNAP-25, but only its total level.

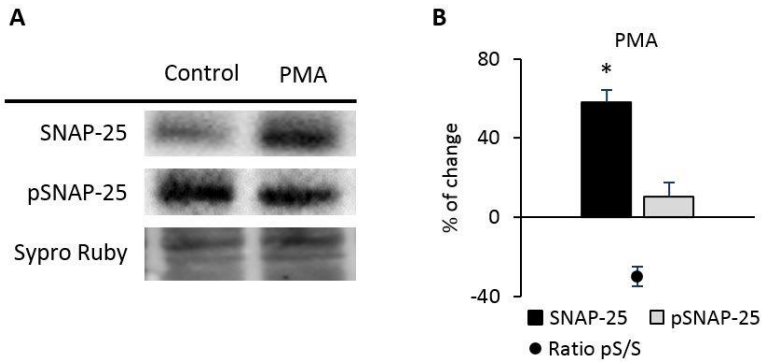

Figure 45. Phorbol 12-myristate 13-acetate (PMA) treatment increases SNAP-25 total levels in skeletal muscle. A) Western blot bands of SNAP-25 and pSNAP-25 from rat diaphragm under basal condition without and with PMA treatment. **B)** Western blot bands of SNAP-25 and pSNAP-25 quantified as optical density corresponding to A. The analysis of the percentage of change values shows a significant increase of SNAP-25 after PMA treatment without affecting pSNAP-25. In accordance, the pSNAP-25/SNAP-25 ratio is significantly decreased. Data are mean percentage ± SEM, * $p < 0.05$ ($n = 5$). Values obtained from Western blot quantification have been normalized in relation with the total protein blotted in the membranes.

Previously, intracellular Ca^{2+} (the primary intracellular trigger for exocytosis) has been shown to induce the phosphorylation of SNAP-25 on Ser-187 in neural and chromaffin cells (Shimazaki et al., 1996; Yang et al., 2007; Pozzi et al., 2008). In order to ascertain whether the phosphorylation is also modulated by Ca^{2+} at the NMJ, muscles were incubated with a Ringer solution of 0.25mM or 5mM of Ca^{2+} for 30 minutes. **Figure 46** shows that both, expression and phosphorylation on Ser-187 was decreased by high (5mM) Ca^{2+} Ringer. Accordingly, the ratio pSNAP-25/SNAP-25 was maintained. On the contrary, incubation in low Ca^{2+} Ringer (0.25mM) significantly increased pSNAP-25 level though, in that case, total SNAP-25 decreased. Therefore, although the interpretation of these results is complex, it seems that changes in the expression and phosphorylation of SNAP-25 on Ser-187 depend somehow on Ca^{2+} at the NMJ. It is interesting that high calcium concentrations decrease the phosphorylation of SNAP-25 while increase the phosphorylation of Munc18-1 and more details have been provided in the discussion.

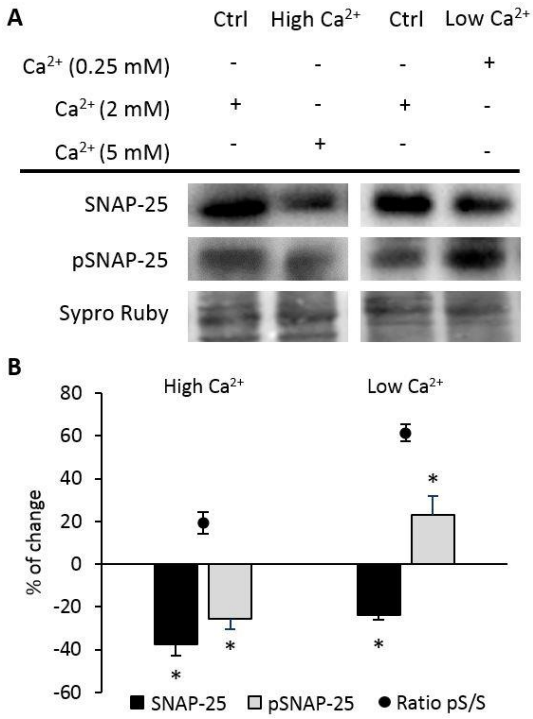

Figure 46. Calcium modulates total SNAP-25 and pSNAP-25 at the neuromuscular junction. A) Western blot bands of SNAP-25 and pSNAP-25 from rat diaphragm under basal conditions incubated with different calcium concentrations (30 minutes). **B)** Western blot bands of SNAP-25 and pSNAP-25 quantified as optical density corresponding to A. The analysis of the percentage of change values confirms that a high Ca^{2+} concentration (5mM) provokes a significant decrease in both SNAP-25 and pSNAP-25 levels. Low Ca^{2+} concentrations (0.25mM) significantly decreased SNAP-25 levels and increased in pSNAP-25 with resect to normal Ringer Ca^{2+} concentration. Therefore, the ratio is significantly increased. Data are mean percentage ± SEM, * $p < 0.05$ ($n = 5$). Values obtained from Western blot quantification have been normalized in relation with the total protein blotted in the membranes.

2. Effects of synaptic activity over SNAP-25 and pSNAP-25 and through nPKCε, cPKCβI and BDNF/TrkB signaling pathway

2.1. Synaptic activity increases SNAP-25 phosphorylation

Next, we analyzed whether synaptic activity regulates SNAP-25 protein levels. We separated the effect of the presynaptic stimulation (and synaptic transmission) from the effect of the muscle cell contraction, by performing experiments in which contraction was inhibited. As previously described, muscle contraction was inhibited using μ-CgTx-GIIIB (Favreau et al., 1999) that preserves the full functionalism of neurotransmission. We performed Western blot analysis and a quantitative study to analyze the density of the bands and evaluate the relative amount of SNAP-25 and its phosphorylated form in different conditions of stimulation. The results showed that the nerve stimulation (1 Hz for 30 minutes) significantly increased pSNAP-25 levels (46.12 % ± 6.31; $p<0.05$), without change SNAP-25 levels. In concordance, the ratio pSNAP-25/SNAP-25 significantly increased (51.99 % ± 9.91; $p<0.05$) (**figure 47**).

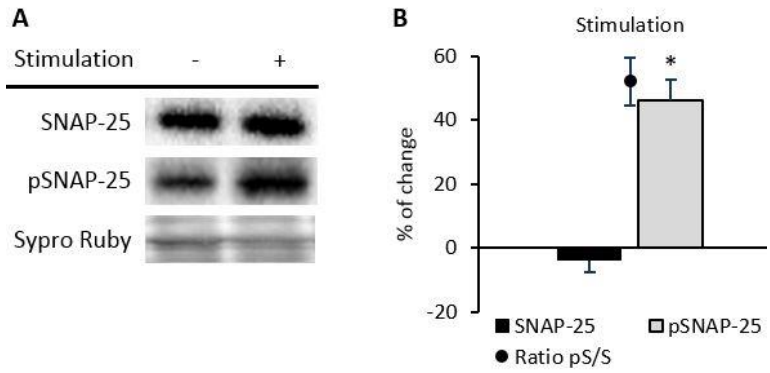

Figure 47. Synaptic activity increased pSNAP-25 levels in skeletal muscle. A) Western blot bands of SNAP-25 and pSNAP-25 from rat diaphragm under basal and stimulated conditions (*Stimulation* treatment at 1 Hz for 30 min). **B)** Western blot bands of SNAP-25 and pSNAP-25 quantified as optical density corresponding to A. Results show a statistically significant increase of pSNAP-25 in stimulated samples without contraction in comparison with basal condition samples. Data are mean percentage ± SEM, * $p < 0.05$ ($n = 5$). Values obtained from Western blot quantification have been normalized in relation with the total protein blotted in the membranes.

Moreover, we analyzed SNAP-25 and pSNAP-25 protein level in cytosol and membrane fractions under electrical stimulation through the nerve. Results showed that in this condition of activity pSNAP-25 was significantly increased in the membrane fraction (20.92 ± 4.32, $p<0.05$; **figure 48**), indicating that the increased amount of pSNAP-25 after stimulation involves an enhanced association of the molecule to the membrane.

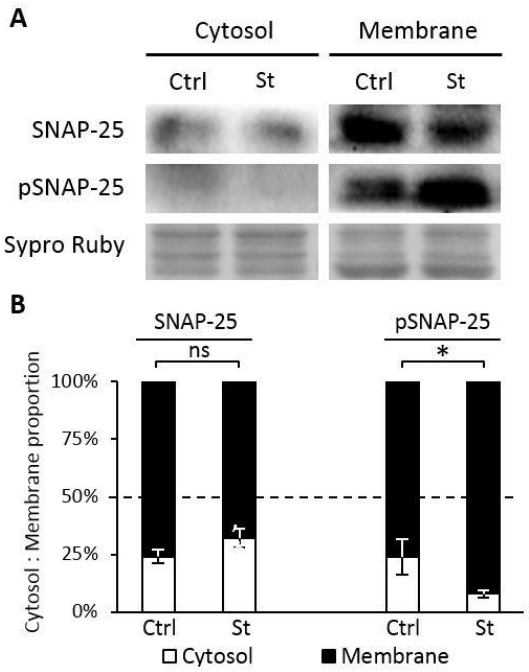

Figure 48. Synaptic activity increases pSNAP-25 levels in the membrane fraction of skeletal muscle. A) Western blot bands of membrane and cytosol distribution of SNAP-25 and pSNAP-25 both in basal and synaptic activity conditions (corresponding to a stimulated (*St*) treatment). **B)** Western blot bands of SNAP-25 and pSNAP-25 quantified as optical density corresponding to A. Results show that in synaptic activity condition SNAP-25 increases in the membrane fraction while total levels of SNAP-25 do not change. Data are mean percentage ± SEM, * $p < 0.05$ ($n = 5$). Values obtained from Western blot quantification have been normalized in relation with total protein in the membranes.

We analyzed pSNAP-25 and SNAP-25 along the time of stimulation (1, 10 and 30 min, 1Hz). Stimulation for 1 and 10 minutes did not modify the levels of SNAP-25 and their phosphorylated form (**figure 49**).

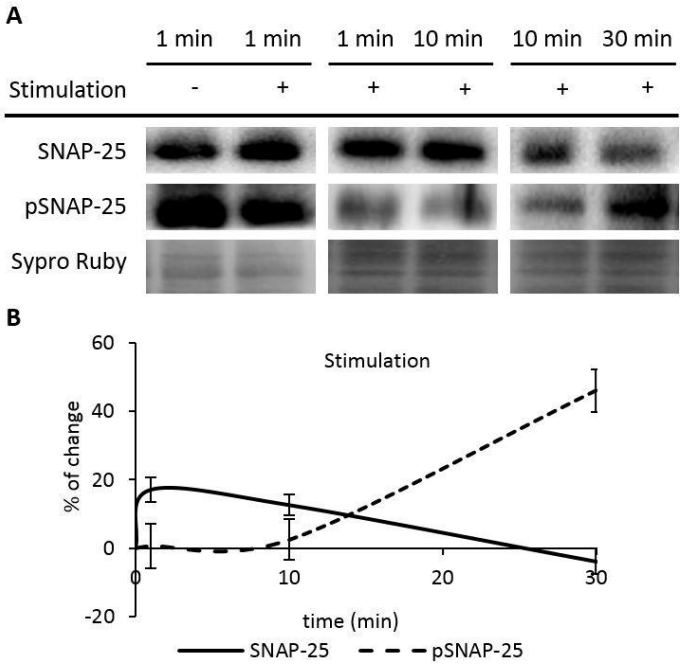

Figure 49. Time course of the modulation of SNAP-25 and pSNAP-25 by synaptic activity A) Western blot bands of SNAP-25 and pSNAP-25 at 1, 10 and 30 minutes after presynaptic stimulation treatment at 1 Hz. **B)** Western blot bands of SNAP-25 and pSNAP-25 quantified as optical density corresponding to A. Each time-point has been compared to its previous time-point. Presynaptic stimulation did not modify the SNAP-25 and pSNAP-25 level at 1 and 10 minutes. Data are mean percentage ± SEM, * $p < 0.05$ ($n = 5$). Values obtained from Western blot quantification have been normalized in relation with the total protein blotted in the membranes.

2.2. nPKCε but not cPKCβI modulates synaptic-induced pSNAP-25

SNAP-25 is a PKC substrate (Shimazaki et al., 1996; Risinger and Bennett, 1999) and we tested whether the two presynaptic exclusive isoforms of PKC, nPKCε and cPKCβI, are involved in its phosphorylation. Muscles were treated with the nPKCε-specific translocation inhibitor peptide, epsilon V1-2 (εV1-2; Johnson et al., 1996a), and to the cPKCβI-specific translocation inhibitor peptide, beta I V5-3 (βIV5-3; Liu et al. 1999; Zhang et al. 2015) to block the respective isoform activities in the muscle (Hurtado et al. 2017a; Obis et al. 2015a,b). Next, we determined how nPKCε and cPKCβI activities affect the level and the phosphorylation of SNAP-25 in basal conditions and after presynaptic stimulation.

Figure 50 shows that incubation for 30 minutes of the muscles with the peptide εV1-2 produced a significant decrease in SNAP-25 and pSNAP-25 indicating that, in basal conditions of the skeletal muscle, nPKCε upregulates SNAP-25 protein level and its phosphorylation. The ratio pSNAP-25/SNAP-25 in basal conditions was significantly increased (27.34 % ± 5.5; $p<0.05$) indicating that nPKCε has a tonic effect positively regulating pSNAP-25.

To link the effects of synaptic activity and nPKCε activity, we stimulated (1 Hz, 30 minutes) phrenic nerve of muscles previously incubated with the blocking peptide (100 µM, 30 minutes). We found a significant decrease in pSNAP-25 level (-27.53 % ± 7.23; $p<0.05$) without a change in the total SNAP-25 level (-8.37 % ± 5.22; $p>0.05$) (**Figure 50**). In concordance, the ratio pSNAP-25/SNAP-25 was significantly decreased (-20.91 % ± 4.96; $p<0.05$) indicating that nPKCε specifically enhances phosphorylation of SNAP-25 in conditions of increase of synaptic activity.

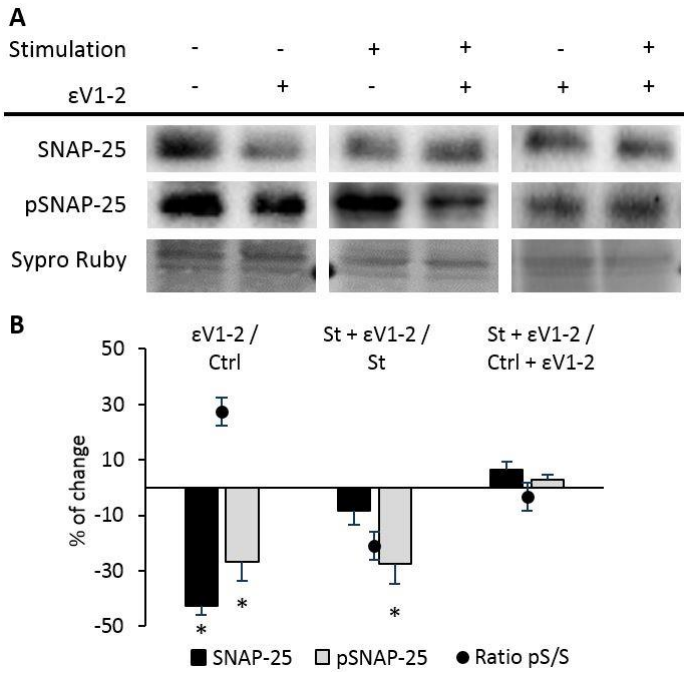

Figure 50. The nPKCε inhibitor εV1-2 peptide modulates SNAP-25 and pSNAP-25 levels under basal and synaptic activity conditions. A) Western blot bands of SNAP-25 and pSNAP-25 in skeletal muscle under basal and nerve stimulation conditions (1 Hz stimulation for 30 min) preincubated with the nPKCε inhibitor peptide εV1-2. **B)** Western blot bands of SNAP-25 and pSNAP-25 quantified as optical density corresponding to A. The analysis of the percentage of change values shows that under basal conditions both SNAP-25 and its phosphorylation significantly decrease in relation with the treatment with the inhibitory peptide (*εV1-2/Ctrl:* muscles in basal conditions versus preincubated with εV1-2 peptide). Moreover, in *St + εV1-2/ St* (synaptic activity compared with the εV1-2 peptide) condition, pSNAP-25 significantly decreases. Data are mean percentage ± SEM, * $p < 0.05$ ($n = 5$). Values obtained from Western blot quantification have been normalized in relation with the total protein blotted in the membranes.

Furthermore, to know whether nPKCε is responsible of the increase in SNAP-25 phosphorylation induced by the nerve stimulation we compared SNAP-25 and phosphoSNAP-25 protein levels in control and stimulated samples in which nPKCε had been blocked with the inhibitor peptide (*St + εV1-2 vs Ctrl + εV1-2*; **figure 50**). We found no significant change on SNAP-25 (6.4 % ± 3.11; $p>0.05$) nor pSNAP-25 levels (2.98 % ± 1.81; $p>0.05$). These results show that the inhibitor peptide completely avoids the phosphorylation induced by the synaptic activity

and emphasizes the specific role of nPKCε enhancing SNAP-25 phosphorylation in presence of synaptic activity.

Figure 51. A and B shows that in basal conditions, nPKCε is present mainly in the membrane and pnPKCε is almost equally distributed in the membrane and cytosol. Electrical stimulation did not change significantly this distribution (**figures 51.C and D**). Interestingly, when the total fraction of these proteins is analyzed synaptic activity without contraction reduces the levels of both nPKCε and pnPKCε, suggesting that in spite of this increased turnover, pnPKCε would be able to phosphorylate SNAP-25 (and also Munc18-1, see *Discussion* and **figures 31 and 50**).

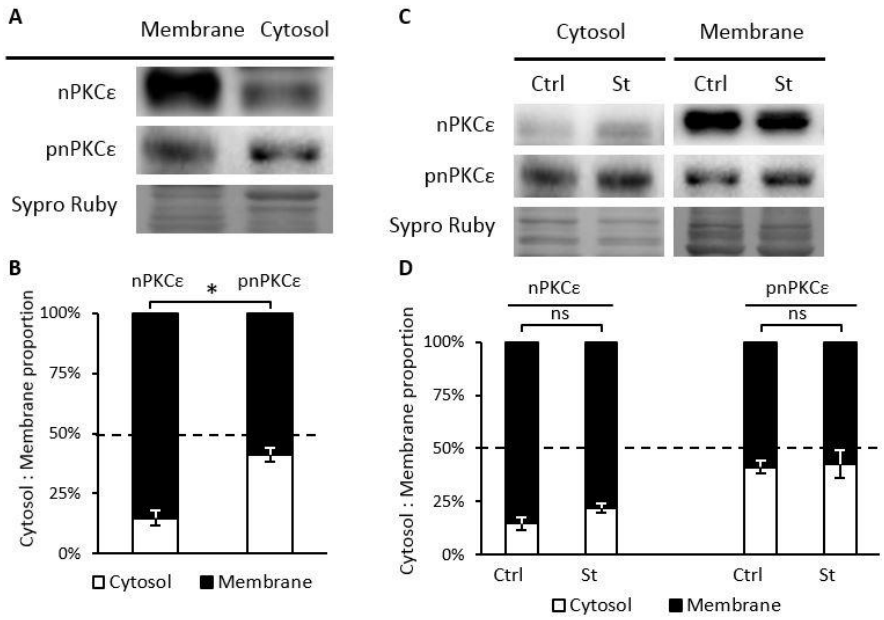

Figure 51. Membrane and cytosol distribution of nPKCε and pnPKCε under basal and synaptic activity conditions. A-C) Membrane and cytosol location of nPKCε and pnPKCε levels in basal conditions (A) and basal compared with synaptic activity conditions (C). **B-D)** Western blot bands of nPKCε and pnPKCε quantified as optical density corresponding to A and C, respectively. Results show that in basal conditions (B), nPKCε was essentially located in the membrane fraction while pnPKCε was equally located in both fractions. In synaptic activity condition (D) both nPKCε and pnPKCε did not change their distribution. Data are mean percentage ± SEM, * $p < 0.05$ ($n = 5$). Values obtained from Western blot quantification have been normalized in relation with the total protein blotted in the membranes.

We analyzed also the effect of blocking the membrane translocation of cPKCβI with the peptide βIV5-3 on SNAP-25 phosphorylation in the skeletal muscle. **Figure 52** shows that the peptide βIV5-3 did not change total SNAP-25 and pSNAP-25 in basal conditions (ratio pSNAP-25/SNAP-25: -13.82 % ± 5.31; $p>0.05$). Moreover, when the βIV5-3 is preincubated during synaptic activity neither pSNAP-25 nor SNAP-25 level were affected. In concordance, the ratio pSNAP-25/SNAP-25 remained unchanged (-11.19 % ± 6.1; $p>0.05$) indicating that cPKCβI isoform does not contributes to SNAP-25 phosphorylation during synaptic activity. As with nPKCε above, we compared SNAP-25 and pSNAP-25 protein levels in control and stimulated samples in which cPKCβI had been blocked with the inhibitor peptide (**figure 52**). We did not found any change in both SNAP-25 (5.2 % ± 3.3; $p>0.05$) and pSNAP-25 (9.36 % ± 8.75; $p>0.05$) level. This reinforces that cPKCβI activity is not necessary for the increase of SNAP-25 phosphorylation induced by the nerve stimulation. The results indicate that only nPKCε isoform contributes to positively regulate SNAP-25 phosphorylation during synaptic activity at the NMJ.

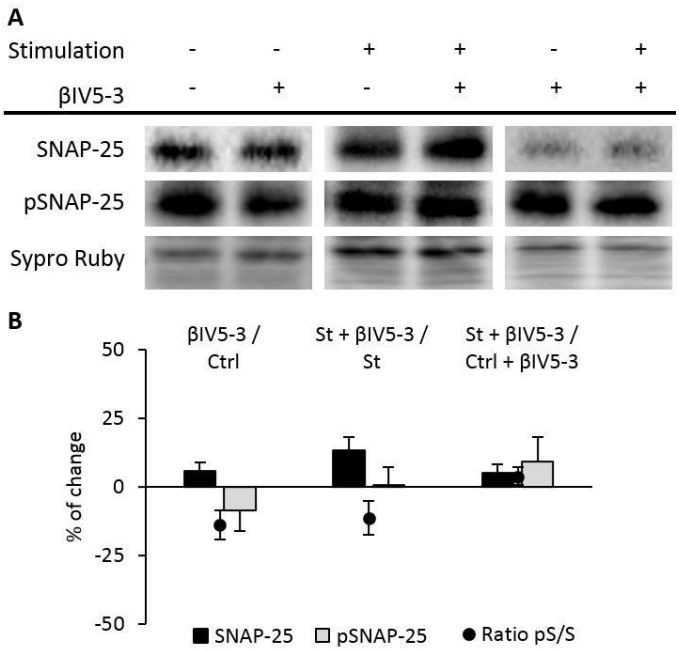

Figure 52. The cPKCβI inhibitor βIV5-3 peptide does not modulate SNAP-25 nor pSNAP-25 levels under basal and synaptic activity conditions. A) Western blot bands of SNAP-25 and pSNAP-25 in skeletal muscle under basal and nerve stimulation conditions (1 Hz stimulation for 30 min) preincubated with the cPKCβI inhibitor peptide βIV5-3. **B)** Western blot bands of SNAP-25 and pSNAP-25 quantified as optical density corresponding to A. The analysis of the percentage of change values shows that in any case cPKCβI modulates SNAP-25 nor its phosphorylation. Data are mean percentage ± SEM, * $p < 0.05$ ($n = 5$). Values obtained from Western blot quantification have been normalized in relation with total protein blotted in the membranes.

2.3. BDNF/TrkB pathway does not modulate pSNAP-25

As mentioned previously, we know that presynaptic activity enhances BDNF/TrkB signaling pathway to increase cPKCβI activity (Hurtado et al. 2017a) and decrease phosphorylation of nPKCε. To demonstrate whether the activation of TrkB is critical to affect pSNAP-25 levels, we selectively suppressed TrkB activity in electrically nerve-stimulated diaphragm muscles using a selective TrkB inhibitor. We used an anti-TrkB antibody (47/TrkB) which effectively inhibits BDNF binding to TrkB receptors (Balkowiec and Katz 2000). We measured resultant SNAP-25 and pSNAP-25 levels and found that in electrically stimulated muscles, TrkB blockade

did not result in a significant change (**figure 53**). In concordance, the ratio pSNAP-25/SNAP-25 remained the same (-6.5 % ± 7.71; p>0.05).

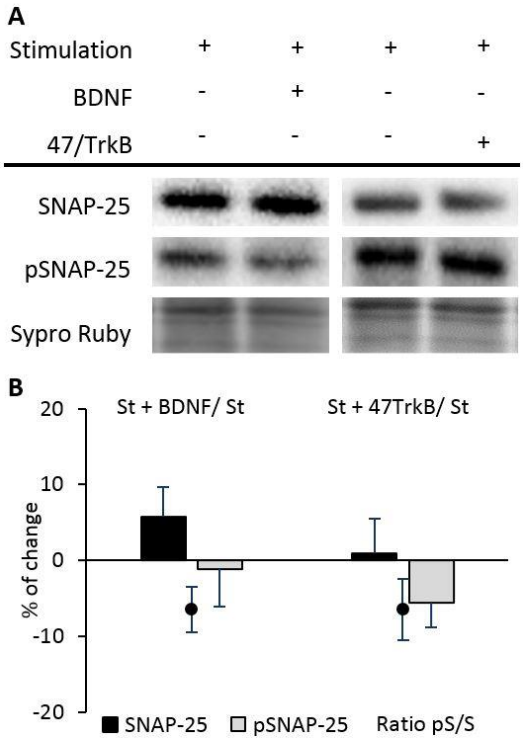

Figure 53. BDNF/TrkB signaling does not modulate SNAP-25 nor pSNAP-25 levels under synaptic activity conditions. A) Western blot bands of SNAP-25 and pSNAP-25 in skeletal muscle under presynaptic nerve stimulation treatment (1 Hz stimulation for 30 min) preincubated with exogenous BDNF and the sequestering antibody 47/TrkB respectively. **B)** Western blot bands of SNAP-25 and pSNAP-25 quantified as optical density corresponding to A. The analysis of the percentage of change values shows that neither SNAP-25 nor pSNAP-25 are modified after BDNF or 47/TrkB treatment. Data are mean percentage ± SEM, * $p < 0.05$ ($n = 5$). Values obtained from Western blot quantification have been normalized in relation with the total protein blotted in the membranes.

This result suggests that, during synaptic activity, TrkB is not mediating any modulation of the pSNAP-25 phosphorylation, which is produced during nerve stimulation. In concordance, preincubation with exogenous BDNF (10nM, 30 minutes) in nerve-stimulated muscles (*St*) did not modify the SNAP-25 and pSNAP-25 levels (**figure 53**). These results is in accordance with the idea that there is a

functional relation between TrkB and cPKCβI activity. In this case, none of the two molecules regulates SNAP-25 protein levels nor its phosphorylation. It is particularly noteworthy that, on the contrary, both molecules do exert a negative regulation on Munc18-1 phosphorylation (see *Discussion*).

In summary, our results indicate that the phosphorylation of SNAP-25 at the NMJ is increased in response to a signaling mechanism initiated with synaptic activity and directly mediated by nPKCε without the direct involvement of the cPKCβI and TrkB activities.

3. Effects of nerve-induced muscle contraction over SNAP-25 and their phosphorylation

3.1. Muscle contraction slightly downregulates pSNAP-25

It has been established previously that the presynaptic PKC isoforms ε and βI are differently regulated at the NMJ by nerve activity and by its resulting muscle activity (Besalduch et al. 2010; Hurtado et al. 2017a; Obis et al. 2015a). Specifically, muscle activity *per se* has a critical role in the enhancement of presynaptic nPKCε and cPKCβI protein levels through BDNF/TrkB signaling. Therefore, we next investigated the role of muscle contraction over SNAP-25 protein level and phosphorylation, and the relationship with these PKC isoforms.

Figure 54 shows that the electrical stimulation of synaptic inputs to the diaphragm muscle followed by the resulting muscle contraction (contrary to what happens in the condition of stimulation without contraction and showed previously) did not change the amount of SNAP-25 (1.92 % ± 6.9; $p>0.05$) and pSNAP-25 (-11.28 % ± 3.69; $p>0.05$). Interestingly, when the effect of muscle contraction was itself analyzed by comparing stimulated muscles with unaltered contraction (*St + Contraction*) versus stimulated muscles that were preincubated with μ-CgTx-GIIIB (*St*), (*Contraction* experiment in the figure, right columns), we found that the concurrence of muscle contraction with electrically stimulated

synaptic activity did not change SNAP-25 but significantly decreased its phosphorylated form levels (-33.35 % ± 5.38; $p<0.05$). In accordance, the resulting pSNAP-25/SNAP-25 ratio was unchanged (-17.92 % ± 7.28; $p>0.05$).

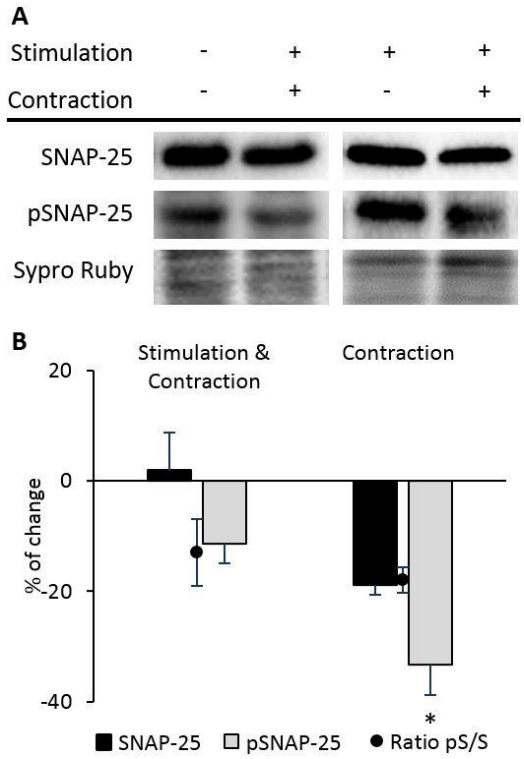

Figure 54. Muscle contraction downregulates pSNAP-25 levels in skeletal muscle. A) Western blot bands of SNAP-25 and pSNAP-25 from rat diaphragm submitted to electrical stimulation with contraction with or without contraction. **B)** Western blot bands of SNAP-25 and pSNAP-25 quantified as optical density corresponding to A. *Contraction* results showed a significant decrease of pSNAP-25. Data are mean percentage ± SEM, * $p < 0.05$ ($n = 5$). Values obtained from Western blot quantification have been normalized in relation with the total protein blotted in the membranes.

We next wanted to know whether muscle contraction changes the nerve-induced phosphorylation of SNAP-25 at short times of stimulation (**Figure 55**). Results show that 10 minutes of stimulation resulting in muscle contraction decreased SNAP-25 (-24.36 % ± 2.51; $p<0.05$) which, however, recovered the control value at 30 minutes. There was non-significant change in the level of pSNAP-25 at anytime. These results indicate that the concurrence of muscle contraction with electrically stimulated synaptic activity does not change phosphorylation of SNAP-25 over the time and respect of the control, but it decreases respect the *Stimulation* conditions at 30 minutes.

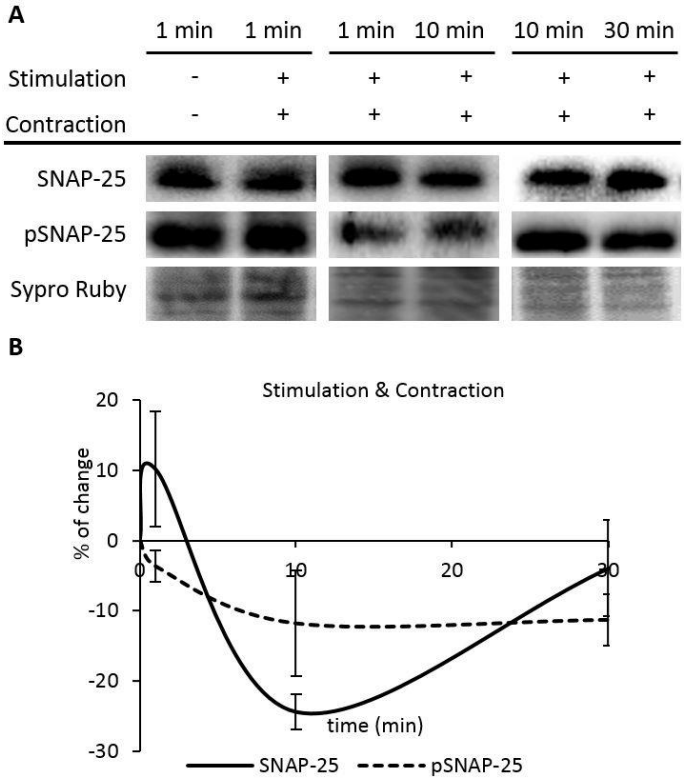

Figure 55. Time course of the modulation of SNAP-25 and pSNAP-25 by muscle contraction. A) Western blot bands of SNAP-25 and pSNAP-25 at 1, 10 and 30 minutes after presynaptic stimulation with contraction treatment at 1 Hz. **B)** Western blot bands of SNAP-25 and pSNAP-25 quantified as optical density corresponding to A. Each time-point has been compared to its previous one. Muscle contraction significantly decreased SNAP-25 at 10 minutes. Data are mean percentage ± SEM, * $p < 0.05$ ($n = 5$). Values obtained from Western blot quantification have been normalized in relation with the total protein blotted in the membranes.

3.2. nPKCε and cPKCβI promotes SNAP-25 phosphorylation in muscle contraction conditions

To test whether nPKCε is also related to SNAP-25 phosphorylation when nerve stimulation results in muscle contraction, we also analyzed pSNAP-25 level in electrical stimulated contracting muscles preincubated with the peptide εV1-2. We found a significant decrease in pSNAP-25 levels (-26.55 % ± 3.17; $p<0.05$) with unchanged levels of total SNAP-25 (9.07 % ± 3.4; $p>0.05$) (**figure 56**). In concordance, the ratio of pSNAP-25/SNAP-25 significantly decreased (-32.65 % ± 4.97; $p<0.05$). This result indicates that nPKCε positively regulates SNAP-25 phosphorylation in electrical stimulated contracting muscles similarly to the observed in stimulated muscles in which contraction is prevented.

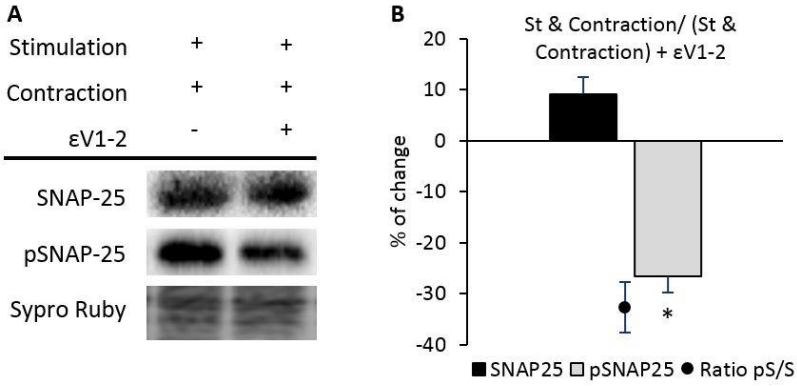

Figure 56. nPKCε modulates pSNAP-25 levels under synaptic activity with muscle contraction conditions. A) Western blot bands of SNAP-25 and pSNAP-25 in skeletal muscle under nerve stimulation conditions (1 Hz stimulation for 30 min) resulting in contraction preincubated with the nPKCε inhibitor peptide εV1-2. **B)** Western blot bands of SNAP-25 and pSNAP-25 quantified as optical density corresponding to A. The analysis of the percentage of change values shows that the ratio of pSNAP-25/SNAP-25 significantly decreases. Data are mean percentage ± SEM, * $p < 0.05$ ($n = 5$). Values obtained from Western blot quantification have been normalized in relation with total protein in the membranes.

When the βIV5-3 peptide was preincubated in muscles in which nerve stimulation resulted in muscle contraction, there was not any modification in SNAP-25 (7.62 % ± 3.3; p>0.05) nor pSNAP-25 level (-18.23 % ± 6.47; p>0.05) (**figure 57**). This result indicates that during the full activity of the NMJ, which includes muscle contraction, cPKCβI does not regulate pSNAP-25.

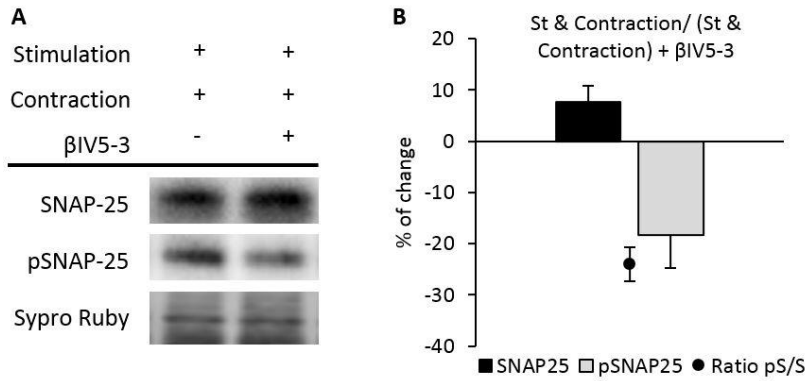

Figure 57. cPKCβI does not modulate neither SNAP-25 and pSNAP-25 levels under synaptic activity with muscle contraction. A) Western blot bands of SNAP-25 and pSNAP-25 in skeletal muscle under nerve stimulation conditions (1 Hz stimulation for 30 min) resulting in contraction preincubated with the cPKCβI inhibitor peptide βIV5-3. **B)** Western blot bands of SNAP-25 and pSNAP-25 quantified as optical density corresponding to A. The analysis of the percentage of change values shows that these proteins are not significantly modified. Data are mean percentage ± SEM, * $p < 0.05$ ($n = 5$). Values obtained from Western blot quantification have been normalized in relation with the total protein blotted in the membranes.

Altogether, the results show that nerve stimulation increases phosphorylation of SNAP-25 on Ser-187 and that the resulting nerve-induced muscle contraction is involved to returns it at basal condition levels. Moreover, nPKCε positively regulates SNAP-25 phosphorylation both in basal conditions and in synaptic activity conditions (with and without contraction). Finally, the cPKCβI isoform does not regulate SNAP-25 phosphorylation in any of the studied activity conditions.

3.3. BDNF/TrkB pathway does not modulate pSNAP-25 in muscle contraction conditions

Because muscle contraction is a key factor that regulates nPKCε and cPKCβI isoforms through the BDNF/TrkB pathway (Hurtado et al. 2017a; Obis et al. 2015a), we next analyzed the possible regulation of SNAP-25 and pSNAP-25 protein levels by the BDNF/TrkB signaling pathway. Blocking TrkB with 47/TrkB in the *Stimulation and Contraction* condition, did not change SNAP-25 (10.54 % ± 5.38; p>0.05) and pSNAP-25 (-11.31 % ± 4.07; p>0.05) (**figure 58**) indicating that endogenous BDNF does not affect SNAP-25 nor pSNAP-25 protein levels in this condition of electric stimulation. In concordance, exogenous BDNF in the *Stimulation and Contraction* condition did not change SNAP-25 (5.36 % ± 2.2; p>0.05) nor pSNAP-25 protein level (-14.53 % ± 5.25; p>0.05) with a resulting pSNAP-25/SNAP-25 ratio of -18.88 % ± 5.23; p>0.05 (**figure 58**). This result indicates that the BDNF/TrkB signaling is not regulating SNAP-25 nor its phosphorylation.

In summary, the phosphorylation of SNAP-25 at the NMJ is increased in response to a signaling mechanism initiated with synaptic activity (*St*) and directly mediated by nPKCε. cPKCβI and TrkB activities are not involved in this pathway. Moreover, the concurrence of muscle contraction intervenes to return to the basal condition of phosphorylation.

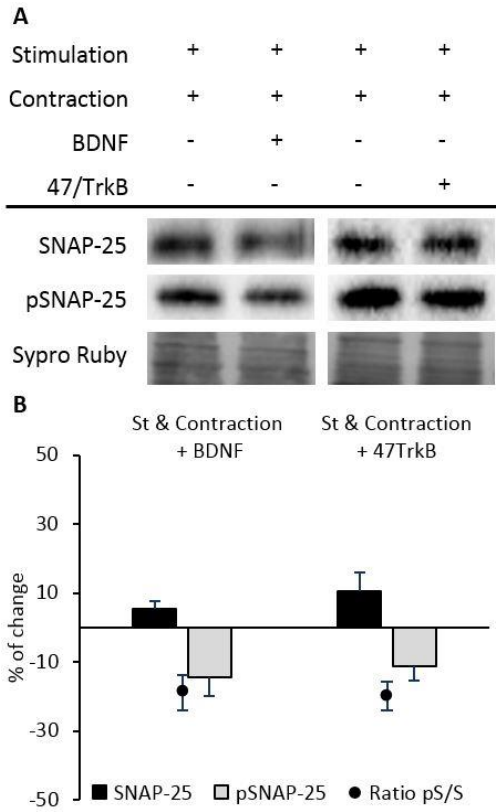

Figure 58. BDNF/TrkB signaling does not modulate neither SNAP-25 nor pSNAP-25 levels under synaptic activity with contraction conditions. A) Western blot bands of SNAP-25 and pSNAP-25 in skeletal muscle under presynaptic nerve stimulation with contraction treatment (1 Hz, 30 min) preincubated with exogenous BDNF and the sequestering antibody 47/TrkB respectively. **B)** Western blot bands of SNAP-25 and pSNAP-25 quantified as optical density corresponding to A. The analysis of the percentage of change values shows that neither of the treatments significantly modulate SNAP-25 nor its phosphorylation. Data are mean percentage ± SEM, * $p < 0.05$ ($n = 5$). Values obtained from Western blot quantification have been normalized in relation with the total protein blotted in the membranes.

UNIVERSITAT ROVIRA I VIRGILI
EFFECTS OF NEUROMUSCULAR ACTIVITY COUPLED TO BDNF/TRKB SIGNALING ON THE EXOCYTOTIC PROTEINS MUNC18-1 AND SNAP-25 THROUGH NPKCE AND CPKCSSI
Anna Simó Ollé

V. DISCUSSION

UNIVERSITAT ROVIRA I VIRGILI
EFFECTS OF NEUROMUSCULAR ACTIVITY COUPLED TO BDNF/TRKB SIGNALING ON THE EXOCYTOTIC PROTEINS MUNC18-1 AND SNAP-25 THROUGH NPKCE AND CPKCSSI
Anna Simó Ollé

CHAPTER I. SYNAPTIC ACTIVITY INDUCED BDNF/TrkB/PKC SIGNALING CONTROLS THE PHOSPHORYLATION OF MUNC18-1 IN THE SKELETAL MUSCLE

Munc18-1 knockout mice show complete loss of neurotransmitter release from synaptic vesicles throughout development and die immediately after birth (Verhage et al. 2000), demonstrating that Munc18-1 is essential for appropriate neurotransmitter secretion. No other protein related with exocytosis produces a comparably severe block of fusion when deleted. Munc18-1 is a neuron-specific member of the Sec1/Munc18 protein family that is involved in neurotransmitter release by binding tightly to Syntaxin 1. This binding holds it in a closed conformation and prevents the assembly of the ternary SNARE complex of the vesicular protein Synaptobrevin, the plasmalemma protein SNAP-25 and Syntaxin (Dulubova et al. 1999; Hata et al. 1993; Liu et al. 2004; Medine et al. 2007; Misura et al. 2000; Yang et al. 2000). Moreover, Munc18-1 functions as a chaperone by delivering Syntaxin 1 to the plasma membrane (Arunachalam et al. 2008; Han et al. 2009). Furthermore, Munc18-1 binds to the N-terminus of Syntaxin 1 ("open conformation"), to release it in a state that is primed for its interaction with the other SNARE proteins and allowing the formation of SNARE complex (Khvotchev et al. 2007; Shen et al. 2007; Smyth et al. 2010; Südhof and Rothman 2009). Furthermore, Munc18-1 also able to bind to the assembled SNARE complex (Dulubova et al. 2007; Rodkey et al. 2008; Shen et al. 2007; Xu et al. 2010). It has been proposed that whereas SNARE proteins force fusing membranes into close proximity, Munc18-1 riding on top of assembling SNARE complexes, may enable lipid mixing between the fusing membranes (Südhof, 2013).

Modification of the interaction between Munc18-1 and Syntaxin could therefore be an important mechanism for the regulation of synaptic vesicle exocytosis. However, how Munc18-1 proteins work together with SNARE complexes for fusion is still unclear.

In the neuromuscular system, evidence supports PKC signaling as a fundamental regulator of neuromuscular function. In particular, presynaptic protein phosphorylation by PKCs is an important mechanism that regulates transmitter release (Byrne and Kandel 1996; Catterall 1999; Numann et al. 1994; Santafé et al. 2005, 2006; Tomàs et al. 2014; West et al. 1991). Multiple studies show evidence that PKC phosphorylates several molecules of synaptic vesicle exocytotic apparatus and there is evidence that these PKC-mediated phosphorylations contribute directly to the regulation of the neurotransmitter release (Snyder et al. 2006). Munc18-1 is one of the PKC- substrates in the exocytotic apparatus phosphorylated on Ser-306 and Ser-313 *in vitro*. These phosphorylation events reduce the amount of Munc18-1 able to bind Syntaxin (Fujita et al., 1996). Cdk5 (cyclin-dependent kinase 5), a member of the Cdc2 family of cell division kinases, also phosphorylates Munc18-1 in threonine residue 574 (Fletcher et al., 1999) but it has been demonstrated that PKC is the main kinase for Munc18-1, and cdk5 has only a minor role (de Vries et al., 2000).

Although Munc18-1 is a target of PKC, there is not information about which PKC isoforms could be involved in the regulation of its phosphorylation and, even, no studies have been performed in the NMJ to corroborate the role of PKC in regulating phosphorylation of molecules of the core exocytic machinery. Because cPKCβI and nPKCε isoforms are exclusively located at the nerve terminal of the NMJ and are regulated by synaptic activity through the BDNF/TrkB signaling pathway (Besalduch et al. 2010; Hurtado et al. 2017a; Obis et al. 2015a), it could be suggested that one or both of these isoforms could regulate Munc18-1 phosphorylation in an activity-dependent way. Thus, in this study, we localized Munc18-1 at the neuromuscular synapse and we investigated the hypothesis that cPKCβI and nPKCε regulate Munc18-1 phosphorylation. The results demonstrate that phosphorylation of Munc18-1 at the NMJ is increased in response to a signaling mechanism initiated with synaptic activity and directly mediated by nPKCε. The cPKCβI and TrkB activities work to prevent this synaptic activity – induced Munc18-1 phosphorylation. Muscle contraction prevents Munc18-1

phosphorylation, when a continuous stimulation is performed. nPKCε, cPKCβI and TrkB activities enhance Munc18-1 phosphorylation in this condition, suggesting that contraction could regulate the nPKCε and cPKCβI and TrkB activities.

1. Munc18-1 and pMunc18-1 in the adult skeletal muscle: expression, location and regulation by calcium and PMA

1.1. Munc18-1 presence in the nerve terminal of the NMJ

Munc18-1 is distributed ubiquitously in mammalians (de Vries et al., 2000) due to its importance in neurotransmission, and its function suggests that it has a presynaptic location. Our immunohistochemical results confirm that at the NMJ. We immunolabeled muscles to colocalize Munc18-1 with proteins corresponding to identify elements of the NMJ (Syntaxin for the axon and presynaptic terminal, S-100 for the Schwann cell, and AChR for the postsynaptic membrane in the myocyte). As the results show, Munc18-1 is localized in the presynaptic element, over the postsynaptic gutters. There is no colocalization with the Schwann cell but there is a positive coincidence with Syntaxin (**figure 25**, inset), which confirms that Munc18-1 is present in the nerve terminal. It is also important to remark that in concrete areas there is a bigger immunosignal which may correspond to places close to the active zones where Syntaxin realizes its function with the help of Munc18-1. Also, the colocalization with Syntaxin is in accordance with the Munc18-1 function, which is implicated in the synaptic vesicle release when the nervous impulse arrives to the terminal button (Dulubova et al. 1999; Garcia et al. 1994; Pevsner et al. 1994; Yang et al. 2000).

1.2. Calcium and PMA promotes Munc18-1 phosphorylation

The PKC phosphorylation on Munc18-1 Ser-306 and Ser-313 has been determined to reduce the ability of Munc18-1 to bind to Syntaxin (Fujita et al., 1996). Later, it was demonstrated that phosphorylation on these sites occurs also in intact cells and was shown that phosphorylation of Ser-313 of Munc18-1 in

response of PKC activation leads to change in the kinetics of vesicle fusion and release (de Vries et al., 2000; Barclay et al., 2003). In relation with these facts, we used two antibodies against Munc18-1. One interacted with the protein around Tyr-157 and recognized the total amount of protein, the second one interacted with the residues 307-319 of Munc18-1 that includes Ser-313 but only recognized it in the phosphorylated form (anti-pMunc18-1). As it has been shown in the results section, we detected important amounts of Munc18-1 in brain and barely less in spinal cord. We also found no detectable phosphorylation of Munc18-1 in these tissues as previously reported (de Vries et al., 2000). Here, we describe for the first time to our knowledge the levels of Munc18-1 and pMunc18-1 in the skeletal muscle. Skeletal muscle shows high amounts of pMunc18-1 in basal conditions. In contrast to what happens in brain and spinal cord, pMunc18 level is markedly detected and this fact may mean a specific functional adaptation in muscle. As compared with the central nervous system synapses, the high number of synaptic vesicles released per impulse and thus, the high quantal content of the resultant postsynaptic potentials may be related with this presumed adaptation. Both Munc18-1 and pMunc18-1 are located mainly in the membrane fraction although they are also detected in the cytosol. This result indicates that, at basal conditions, there is a high portion of total and phosphorylated Munc18-1 attached to the membrane. This tendency may be linked to the SNARE complex once Munc18-1 has been released from Syntaxin after its phosphorylation. This result favours the hypothesis of the permanent assembly of Munc18-1 with the SNARE complex contributing to organize de docking-fusion sites (see Südhof 2013).

It was described in adrenal chromaffin cells that Munc18-1 is phosphorylated on Ser-313 in response of phorbol ester treatment, demonstrating that PKC is involved on it (Barclay et al., 2003). The increase of phosphorylated Munc18-1 that we found when stimulating PKCs with PMA proves that this family of serine/threonine kinases regulates phosphorylation of Munc18-1 also in the skeletal muscle and suggest that PKC is involved in neurotransmitter release at the NMJ probably through the phosphorylation of Munc18-1 protein. Although it has

been controversially suggested that the effects of phorbol esters on neurotransmission are due to Munc13 (Rhee et al., 2002), we now provide evidence that Munc18-1 is a key substrate to neurotransmission that is also affected by phorbol esters through PKC. Interestingly, PMA incubation also significantly increased Munc18-1 protein levels at the skeletal muscle being the ratio pMunc18-1/Munc18-1 the same than in basal conditions. This Munc18-1 increase also occurs in active stimulated muscles (see later) and suggest that PKC activation favours also the expression of the total protein in addition of their phosphorylation or, alternatively, Munc18-1 degradation could decrease.

Furthermore, because synaptic function is tightly linked with Ca^{2+} influx, we also studied the effect of different Ca^{2+} concentrations in phosphorylated Munc18-1 levels on Ser-313 in the NMJ. Results show that when calcium concentration is raised to 5mM, a dose that results in a higher level of transmitter release (Santafe et al. 2001, 2007), the ratio pMunc18-1/Munc18-1 was significantly increased. On the other hand, low calcium levels did not change the amount of phosphorylated protein but the ratio pMunc18-1/Munc18-1 was significantly decreased (there was a significant increase of total Munc18-1 protein levels). Further experiments are needed to better characterize the nerve-induced phosphorylation of Munc18-1 dependence on the influx of Ca^{2+}.

In conclusion, Munc18-1 is expressed and phosphorylated in basal conditions in the skeletal muscle with a predominant location in the membrane fraction. Furthermore, phosphorylation of Munc18-1 at Ser-313 occurs in response to pharmacologic PKC stimulus and changes in extracellular calcium. However, in these two last conditions, expression and phosphorylation are not regulated in the same direction. Although in these two conditions pMunc18-1 increases, PMA increases Munc18-1 whereas calcium decreases it. We think that the different effects of PMA and calcium over the PKC isoforms could explain this difference. PMA is able to stimulate all PKC isoforms in the regulatory domain resulting in the increase of expression and phosphorylation of Munc18-1. The increased calcium

inflow in high calcium media may enhance the activation of the calcium-dependent isoforms which may do not contribute directly to favour Munc18-1 expression in these conditions. In accordance, we found (**figure 24**) that in opposition with the outcome of high calcium, Munc18-1 expression is increased in low calcium media.

2. Synaptic activity modulates Munc18-1 and its phosphorylation through nPKCε and cPKCβI isoforms and BDNF/TrkB signaling pathway

2.1. Synaptic activity enhances Munc18-1 and its phosphorylation

When an action potential arrives at the presynaptic nerve terminal, the subsequent Ca^{2+} influx triggers the exocytotic fusion of synaptic vesicles containing neurotransmitter in the NMJ, which induces muscle contraction. Therefore, we investigated at the skeletal muscle whether synaptic activity regulates the phosphorylation of Munc18-1. Our results show that a moderate increase in the nerve activity (1 Hz, 30 minutes) significantly increases Munc18-1 and pMunc18-1 levels in the NMJ indicating that synaptic activity modulates phosphorylation of Munc18-1. This result is in concordance with previous one showing that depolarization of the nerve terminal in synaptosomes triggers Munc18-1 phosphorylation (de Vries et al., 2000). We also found that under nerve electrical stimulation pMunc18-1 is significantly decreased in the membrane fraction (**figure 27**), indicating that the increased amount of Munc18-1 phosphorylated after stimulation involves a disconnection of the molecule from the membrane. This fact can be related with the described release of Munc18-1 from Syntaxin after phosphorylation (de Vries et al., 2000; Cijsouw et al., 2014). However, we found also that in resting basal condition there is a particular high amount of pMunc18-1 attached to the membrane, supporting the notion of the permanent assembly of Munc18-1 with the SNARE complex to organize de docking-fusion sites (see Südhof, 2013). The release of pMunc18-1 from the membrane during the continuous activity may be related with the turnover of vesicles and related

molecules. The synaptic activity-induced increase of total levels of Munc18-1 could be explained by an increase of its synthesis or alternatively by a decrease in its degradation.

The data on the pMunc18-1 we obtained after 30 minutes of imposed synaptic activity (or those obtained with PMA incubation) can show the adaptative steady changes of a very rapid mechanism of vesicle movements. In fact, we show here that changes in pMunc18-1 cannot be observed at 1 minute of stimulation (60 stimuli), but can be revealed in the presence of inhibitors of phosphatases. This suggests that the balance phospho-dephosphorylation of Munc18-1 during synaptic activity is displaced in favour of accumulate the phosphorylated form. This indicates that phosphatase activity regulates Munc18-1 phosphorylation-dephosphorylation at short stimulation times whereas with continuous activity the level of pMunc18-1 continuously increases to be finally sustained for a long period. This effect would be related with a positive adaptive plasticity.

Our results show that although phosphorylation of Munc18-1 is markedly increased by electrically stimulated muscles, the ratio pMunc18-1/Munc18-1 is not significantly affected, similarly as it happens in PMA-stimulated muscles. As previously stated, this indicates the parallel increase of expression and phosphorylation in these two conditions. We found similar results in electrical nerve stimulated muscles and in muscles treated with PMA suggesting that Munc18-1 phosphorylation may be directly modulated by the increased PKC activity observed during synaptic activity. PKC has been involved since many years ago in the control of neurotransmitter release. In neurons, PKC regulates several different stages of the synaptic vesicle exocytotic process, suggesting that these multiple actions of PKC are mediated by phosphorylation of distinct protein targets. One of the exocytotic proteins identified as PKC substrate is Munc18-1 (Dulubova et al. 2007; Südhof and Rothman 2009; de Vries et al. 2000). Although there are several PKC isoforms differentially distributed at the NMJ (Besalduch et al. 2010, 2013; Hilgenberg and Miles 1995; Lanuza et al. 2000; Li et al. 2004; Obis

et al. 2015a; Perkins et al. 2001), nPKCε and cPKCβI are exclusively located in the nerve terminal of the NMJ, regulated by synaptic activity and involved in neurotransmitter release (Besalduch et al. 2010; Hurtado et al. 2017a; Obis et al. 2015a,b). Here we found that these two isoforms are involved in the phosphorylation of Munc18-1 incubating the muscles with the corresponding specific translocation inhibitor peptides, εV1-2 (Johnson et al., 1996a) and βIV5-3 (Liu et al. 1999; Zhang et al. 2015) to block the isoform activities.

2.2. nPKCε isoform enhances Munc18-1 phosphorylation both in basal and synaptic activity conditions

It has been showed that neurotransmission is modulated by PKCs that are typically activated by translocating to the membrane in their phosphorylated form (Gould and Newton 2008; Lanuza et al. 2014). It has been previously shown that Munc18-1 is a substrate for PKC and cyclin-dependent kinase 5 (Cdk5) *in vitro* (Fujita et al., 1996). Moreover, it is known that PKC is the principal kinase that modulates Munc18-1 pool, because Munc18-1 phosphorylation evoked by depolarization of the nerve terminals was Ca^{2+} dependent and was blocked by PKC-inhibitors while Cdk5- inhibitors had smaller effect (de Vries et al., 2000). Although there is evidence that PKC is the main kinase that phosphorylates Munc18-1, it is unknown which PKC isoform could be the one able to phosphorylate it. One of the aims of this study was to determine whether nPKCε isoform is involved in Munc18-1 phosphorylation. The motivation to investigate in this direction is that nPKCε is an isoform of the novel PKC family exclusively located in the nerve terminal of the NMJ and in brain (Chen and Tian 2011; Moraczewski et al. 2002; Obis et al. 2015a; Shirai et al. 2008) and, moreover, it is implicated in the neurotransmission mechanism (Obis et al. 2015a,b). Now, our results demonstrate that blocking the nPKCε with εV1-2, which inhibits the presence of pnPKCε in the synaptic membrane of the diaphragm muscle cells, heavily inhibited Munc18-1 phosphorylation indicating that nPKCε plays a key role in Munc18-1 phosphorylation not only in basal conditions but also under

stimulation (with and without contraction). Therefore, the effect of nPKCε over neurotransmission could be induced through Munc18-1 phosphorylation.

The present results emphasize the specific role of nPKCε enhancing Munc18-1 phosphorylation in presence of synaptic activity. Accordingly it was previously reported that pnPKCε significantly decreased in the same condition (Obis et al. 2015a) indicating that the nPKCε-induced increase of pMunc18-1 after synaptic activity is accompanied by a significant decrease of the total and phosphorylated nPKCε probably reflecting the well-known process of the downregulation of the PKC after its activation (Gould et al. 2009; Gould and Newton 2008; Kang et al. 2000; Lee et al. 1996; Lu et al. 1998). Moreover, it should be noted that nPKCε auto-phosphorylation is not induced by synaptic activity and that its decrease due to degradation does not affect its kinase function. It seems that there is a pool of signaling-competent nPKCε that is ready to phosphorylate the amount of substrate available at the start of the synaptic activity (and even at basal conditions).

2.3. cPKCβI isoform negatively modulates Munc18-1 phosphorylation during synaptic activity

cPKCβI is an isoform of the conventional PKC family that, as nPKCε is also located in the nerve terminal of the NMJ, is regulated by synaptic activity and involved in ACh release (Besalduch et al. 2010; Hurtado et al. 2017a). Here we demonstrate that the role of the cPKCβI isoform during synaptic activity contributes to reduce Munc18-1 phosphorylation. However and interestingly, cPKCβI activity seems also necessary for the increase of Munc18-1 phosphorylation induced by the nerve stimulation and positively modulated by nPKCε. As with nPKCε above, we compared Munc18-1 and pMunc18-1 protein levels in control and stimulated samples in which cPKCβI had been blocked with the corresponding inhibitor peptide (**figure 32**). We found a significant increase of Munc18-1 with a no significant change on pMunc18-1 level. This indicates that, in some way, cPKCβI activity is necessary for the increase of Munc18-1

phosphorylation induced by the nerve stimulation (**figure 32**, last column). There are several possible explanations to the best understanding of this complex situation. We observed that cPKCβI inhibits nPKCε both in the control (basal condition) and during electrical stimulation. Thus, it will be expected that the pMunc18-1 values were higher in both situations when cPKCβI is blocked with their inhibitor peptide because nPKCε could operate without the cPKCβI control. Thus, the values of pMunc18-1 may rise similarly in the control and in stimulated muscles without significant difference between them, which is in accordance with what we found.

We previously reported that pcPKCβI significantly increases in the membrane fraction while total cPKCβI is downregulated during synaptic activity (Hurtado et al. 2017a,b). This indicates that the synaptic activity induces cPKCβI phosphorylation and its activation, being functionally maintained in the membrane. Therefore, and in opposition with nPKCe phosphorylation, synaptic activity increases cPKCβI auto-phosphorylation suggesting that it promotes cPKCβI competence. In relation with the regulation of Munc18-1 phosphorylation, the synaptic activity-induced cPKCβI activity would promote a negative effect on pMunc18-1 protein level (not detected in basal conditions). Interestingly, Munc18-1 protein levels are influenced by cPKCβI activity. In particular, this isoform promotes Munc18-1 levels in basal conditions. However, synaptic activity can increase Munc18-1 without cPKCβI action, as stimulus without cPKCβI (in the presence of the peptide) keeps increasing Munc18-1 levels (**figure 32**, last column).

In summary, our results indicate that both, nPKCε and cPKCβI isoforms contribute to regulate Munc18-1 phosphorylation during synaptic activity at the NMJ, although cPKCβI and nPKCε work in opposite directions in relation with Munc18-1 phosphorylation. cPKCβI seems to reduce phosphorylation and nPKCε increases it. Therefore, a balance between the activities of the two isoforms can be a relevant cue in the regulation of the exocytotic apparatus. Moreover, our

results also show a mutual interdependence between the protein levels of these isoforms. Together, these findings demonstrate the mutual regulatory influence between nPKCε and cPKCβI. Thus, the hypothesis can be formulated on the existence of a mutual negative feedback between these two PKC isoforms to properly modulate relevant molecules of the exocytotic apparatus.

2.4. BDNF/TrkB pathway downregulates Munc18-1 phosphorylation during synaptic activity

BDNF is a molecule which has been identified as a product derived from the contraction of skeletal myocytes *in vitro* (Matthews et al., 2009). It is well accepted that, in the NMJ system, synaptic activity has a role in BDNF expression. It has been identified that basal synaptic activity is required to maintain BDNF levels (Gomez-Pinilla et al. 2002). Moreover, it has been demonstrated that exogenous BDNF is also able to influence synaptic plasticity (Schinder, 2000; Aguado, 2003). Altogether, it could be said that BDNF and TrkB signaling is a key regulator of the neuromuscular activity (Garcia et al. 2010; Gomez-Pinilla et al. 2002; Mantilla et al. 2004). Moreover, we recently described that synaptic activity enhances the BDNF/TrkB signaling pathway to increase cPKCβI activity (Hurtado et al. 2017a).

Therefore, here, we investigate the involvement of TrkB pathway in the regulation of the pMunc18-1 level. Our data show that during synaptic activity, a TrkB-mediated tonic effect (through endogenous BDNF) does not affect Munc18-1 protein levels though opposes to the pMunc18-1 increase that occurs in stimulated muscles. However, exogenous BDNF seems to positively regulate a moderate increase of Munc18-1 protein levels but does not affect their phosphorylation. Thus, results show that exogenous BDNF cannot affect Munc18-1 phosphorylation but endogenous BDNF could act through TrkB to negatively regulate phosphorylation of Munc18-1. It is possible that TrkB receptor sites are more accessible for the endogenous BDNF than for the BDNF exogenously applied through the media. Also, some saturation of the TrkB pathway by endogenous BDNF production (preventing additional effect of exogenous BDNF) cannot be

discarded. Interestingly, exogenous BDNF decreases also pMunc18-1 levels in basal conditions. Thus, it may be that in the resting state, there is not much endogenous BDNF production and the TrkB sites are free to exogenous BDNF access that promotes pMunc18-1 reduction similarly to the high endogenous BDNF (or NT-4 or both) production during imposed synaptic activity. In addition, we observed (Hurtado et al. 2017a; Obis et al. 2015a) that in active electrically stimulated muscles, that incubation with exogenous BDNF does not change de phosphorylation and activation of both cPKCβI and nPKCε. This is in accordance with the lack of effect of exogenous BDNF on pMunc18-1.

As stated, synaptic activity enhances the BDNF/TrkB pathway to increase cPKCβI activity (Hurtado et al. 2017a). We found here that, on the contrary, TrkB activity decreases phosphorylation of nPKCε. Because the TrkB activity also decrease pMunc18-1, results indicate that, in presynaptic stimulation conditions, pnPKCε activity and pMunc18-1 level are positively related with each other and negatively modulated by TrkB. Therefore, TrkB would enhance pcPKCβI activity to prevent the synaptic activity-induced Munc18-1 phosphorylation mediated by nPKCε.

3. Muscle contraction prevents Munc18-1 phosphorylation against the activity of nPKCε, cPKCβI and BDNF/TrkB

3.1. Muscle contraction prevents the synaptic activity-induced Munc18-1 phosphorylation

Nerve stimulation and synaptic activity results in the contraction of the muscle fiber. We next studied whether physiological synaptic activity (nerve stimulated with the resulting contraction) contributes to modulate in a different way pMunc18-1 levels at the NMJ. As stated, both, Munc18-1 and pMunc18-1 levels increase during continued synaptic activity lasting for 30 minutes. Contrarily, we found that muscle contraction in response to the nerve stimulus cancels out

the increase induced by synaptic activity. In fact, pMunc18-1 significantly decreases at 30 minutes. However, between 1-10 minutes pMunc18-1 increases with and without contraction pointing to the relevance of this phosphorylation to sustain neurotransmission. Thereafter, some adaptive change mediated by contraction seems to induce pMunc18-1 level decrease.

3.2. Both nPKCε and cPKCβI activity promote pMunc18-1 in muscle contraction conditions

It has been established previously that the presynaptic PKC isoforms ε and βI are differently regulated at the NMJ by nerve activity and by its resulting muscle activity (Besalduch et al. 2010; Hurtado et al. 2017a; Obis et al. 2015a). In particular, muscle activity *per se* has a critical role to enhance presynaptic nPKCε and cPKCβI protein levels. The present data show a complex change in the nPKCε, cPKCβI and Munc18-1 interactions when synaptic activity ends in muscle contraction. nPKCε positively regulates Munc18-1 phosphorylation in electrically stimulated contracting muscles similarly as the experiments with abolished contraction. In all cases, including the basal conditions, nPKCε makes this function. Also, in all cases, cPKCβI negatively regulates nPKCε phosphorylation. However, cPKCβI function shifts to increase pMunc18-1 after 30 minutes of stimulation, which is the opposite effect observed in stimulation without contraction.

3.3. BDNF/TrkB pathway modulates Munc18-1 phosphorylation 1 in muscle contraction conditions

Because muscle contraction regulates nPKCε and cPKCβI through the BDNF/TrkB pathway (Hurtado et al. 2017a; Obis et al. 2015a), we analyzed the regulation of Munc18-1 and pMunc18-1 levels by the BDNF/TrkB pathway when contraction occurs. We observed here that there is also a shift (similarly to that observed with the cPKCβI function) in the coupling of the endogenous BDNF-TrkB signaling (compared with the experiments with synaptic activity without contraction) to promote Munc18-1 phosphorylation in this case.

In summary, the results show that nerve stimulation increases phosphorylation of Munc18-1 on Ser-313 and that the resulting nerve-induced muscle contraction induces an important change that prevents the effect of nerve stimulation by itself on Munc18-1 and pMunc18-1 levels when a continuous stimulation is performed. Moreover, nPKCε positively regulates Munc18-1 phosphorylation both in basal conditions and in synaptic activity conditions (with and without contraction) being higher the effect of nPKCε in synaptic activity without contraction. The cPKCβI isoform negatively regulates pnPKCε phosphorylation activity in all the studied activity conditions. However, during the full activity of the NMJ that includes muscle contraction, the role of the cPKCβI shifts to increase pMunc18-1. BDNF/TrkB signaling has a similar effect than cPKCβI in all the activity conditions studied, suggesting the coordinated regulation of the two pathways.

Is thought-provoking the fact that when synaptic activity leads to muscle contraction Munc18-1 and pMunc18-1 levels are reduced if, at the same time, cPKCβI, nPKCε and the endogenous BDNF/TrkB pathway operate to increase pMunc18-1.

Surprisingly, exogenous BDNF significantly decreases pMunc18-1 and Munc18-1 protein levels in nerve-induced muscle contraction conditions, indicating that exogenous BDNF acts differentially than endogenous BDNF and suggesting the binding to a different receptor. The possibility exist that exogenous BDNF binds also to the $p75^{NTR}$ receptor with the result of a reduction of Munc18-1 and pMunc18-1. Endogenous BDNF may operate in part through $p75^{NTR}$ in the contraction condition. Although the interpretation of the data are very complex, we observed that in the experiments blocking TrkB with the antibody 47/TrkB, the total Munc18-1 does not depend of this receptor. Also, pcPKCβI does not affect Munc18-1 in synaptic activity condition (without contraction). Interestingly however, when contraction occurs, pcPKCβI strongly reduces Munc18-1 (**figure 34**) and it may be that as a consequence pMunc18-1 is also reduced finally. Thus, the

shift of pcPKCβI to reduce Munc18-1 protein levels during synaptic activity and muscle contraction, may be the key element that allows the final decrease of their phosphorylation which (at 30 minutes of the constant activity) would be considered as an adaptation. This effect seems to occur in parallel with the positive effects over Munc18-1 phosphorylation mediated by nPKCε, cPKCβI and the endogenous BDNF-TrkB pathway.

CHAPTER II. SNAP-25 PHOSPHORYLATION IS INDUCED BY SYNAPTIC ACTIVITY AND MEDIATED BY THE nPKCε ISOFORM AT THE NMJ

The three SNARE proteins (the vesicular SNARE protein Synaptobrevin and the plasma membrane SNARE proteins Syntaxin-1 and SNAP-25) form a *trans*-complex that involves a progressive zippering of the four-helical SNARE complex (Hanson et al., 1997). Zippering of trans-SNARE complexes forces the fusing membranes into close proximity, destabilizing their hydrophilic surfaces. Assembly of the full trans-SNARE complex together with the regulatory action of the SM protein Munc18-1 opens the fusion pore. Fusion pore expansion transforms the initial *trans*-SNARE complexes into *cis*-SNARE complexes that are then dissociated by NSF (which binds to SNARE complexes via SNAP adaptor proteins), completing the cycle (Fasshauer et al. 1998; Hanson et al. 1997; Südhof 2004; Sutton et al. 1998; Xu et al. 1999).

Thus, it is important the study of the phosphorylation of these proteins that regulate their interactions and formation of the SNARE/SM complex and exocytosis of neurotransmitters from the presynaptic components.

The main result of this study shows that the nPKCε isoform contributes to positively regulate SNAP-25 phosphorylation on Ser-187 during synaptic activity. Differing from the Munc18-1 regulation, TrkB receptor and cPKCβI activity do not modulate SNAP-25 protein level nor its phosphorylation. Thus, there exist critical differences between the regulatory Munc18-1 and the force generator SNAP-25 phosphorylation, which can contribute to explain their interaction in the SNARE/SM complex function.

1. SNAP-25 and pSNAP-25 in the adult skeletal muscle: regulation by calcium and PMA

2.1. Calcium negatively modulates SNAP-25 phosphorylation

It has been proposed that PKA phosphorylation of SNAP-25 at Thr-138 controls the size of the releasable vesicle pools, whereas PKC phosphorylation of SNAP-25 (Shimazaki et al., 1996; Kataoka et al., 2000) at Ser-187 is involved in regulating the fast vesicle pool refilling after it has been emptied during neurotransmission (Leenders and Sheng 2005; Nagy et al. 2002). The PKC phosphorylation site is in a region related with calcium-triggered exocytosis and changes within this region interfere with SNAP-25 interaction with the calcium sensor Synaptotagmin-1 (Zhang et al. 2002). Also, the level of phosphorylated SNAP-25 may change in response to elevated intracellular calcium concentration (Nagy et al., 2002). However, *trans*-SNARE complexes composed of ''open'' Syntaxin-1 and SNAP-25 exist in the membrane before Ca^{2+} triggers neurotransmitter release (Pertsinidis et al., 2013).

In our experiments changing the calcium concentration in the media, we observed that high calcium decreases both SNAP-25 and pSNAP-25 whereas low calcium decreases SNAP-25 and increases pSNAP-25. There is an inverse relation between extracellular calcium concentration and the level of SNAP-25 phosphorylation. There are several possible explanations. It may be that in the fast NMJ that secrete many quanta of ACh, and differently to what happens in chromaffin cells (Nagy et al., 2002), the presumed high calcium inflow would maintain low SNAP-25 phosphorylation as an adaptation to facilitate vesicular movements. Alternatively, the SNAP-25 and pSNAP-25 decrease may be attributed to an increased turnover and degradation because continued functioning in high calcium conditions. Nevertheless, the SNAP-25 behavior is opposed to that of the regulatory Munc18-1 because in high calcium Munc18-1 decrease and pMunc18-1 increase whereas in low calcium, Munc-18-1 increase and pMunc18-1 does no

change. These differences between Munc18-1 and SNAP-25 phosphorylation could be significant in relation with their interaction in the SNARE/SM complex formation. Modification of the interaction between SNAP-25 and Munc18-1 could be an important mechanism for the regulation of synaptic vesicle exocytosis.

2.2. PMA enhances SNAP-25 total levels

Because SNAP-25 is a PKC substrate (Shimazaki et al., 1996; Kataoka et al., 2000) we investigated in the NMJ the effect of the phorbol ester PMA, which previously we demonstrated that enhances ACh release and PKC at the NMJ (Besalduch et al. 2010; Lanuza et al. 2000, 2006, 2014; Santafé et al. 2005, 2006, 2009, 2014). Surprisingly we observed that PMA increases the total protein level of SNAP-25 but not the phosphorylated form. **Figure 44** shows more than a 75% of pSNAP-25 present in the membrane fraction in basal conditions similarly as it happens with other molecules of the SNARE/SM complex like Munc18-1. It could be hypothesized that pSNAP-25 has a rapid turnover, being the application of PMA able to maintain the phosphorylation through PKC, but not to increase it. Interestingly however, the pSNAP-25 behaviour after PMA treatment is (similarly as happens with extracellular calcium changes in the bath) opposed to that of the regulatory Munc18-1. PMA increases both total and phosphorylated Munc18-1. This highlights the different regulation of these molecules in the neuromuscular synapses. However, SNAP-25 has been clearly defined as a PKC target during the release process as showed by using phosphomimetic mutants of SNAP-25 expressed in chromaffin cells (Nagy et al., 2002). Overexpression of SNAP-25 mutants mimicking the phosphorylated state of Ser-187 accelerated vesicle recruitment after the emptying of the releasable vesicle pools (Nagy et al., 2002).

2. Synaptic activity and nPKCε increase SNAP-25 phosphorylation

We separated the effect of the presynaptic stimulation (and synaptic transmission) from the effect of the muscle cell contraction, by performing experiments in which contraction was inhibited using μ-CgTx-GIIIB (Obis et al.

2015a,b) that preserves the full functionalism of neurotransmission. We found that nerve stimulation increased pSNAP-25, mainly in the membrane fraction (roughly 90% of the phosphorylated molecule), without change the SNAP-25 levels. Moreover, we observed that at shorter times of stimulation (1 min and 10 min) the levels of these molecules does not change suggesting the occurrence of an adaptive process clearly observed at 30 minutes of induced activity.

All these data seems to indicate that the level of pSNAP-25 is high in the membrane in basal conditions, possibly sufficient to allow this function during the initial period of induced activity. In addition, non physiological stimulation of PKCs phosphorylation activity (PMA) does not lead to pSNAP-25 increase, suggesting that the existing amounts are sufficient, though the total SNAP-25 rises after 30 minutes. Moreover, our results indicate that high levels of exogenous calcium may lead to an increased use of pSNAP-25, which could cause its degradation. Finally, the synaptic activity of the NMJ increases the levels of SNAP-25 in the membrane after a relatively long adaptive period (30 minutes).

2.1. nPKCε enhances SNAP-25 phosphorylation in basal and synaptic activity conditions but cPKCβI does not

Because PMA does not increase pSNAP-25 in basal conditions, it seems that its presence in the membrane may be saturated and only continuous synaptic activity by nerve stimulation progressively increases it. Therefore, we investigated the possible PKC isoforms that tonically phosphorylate SNAP-25 both in basal conditions and during induced synaptic activity. Using specific translocation inhibitor peptides and therefore specifically blocking their activity, we studied the two isoforms of PKC that are located exclusively in the presynaptic component of the NMJ, nPKCε and cPKCβI (Hurtado et al. 2017a; Liu et al. 1999; Obis et al. 2015a,b; Zhang et al. 2015).

In relation with nPKCε, we observed that in basal conditions this isoform has a positive tonic effect regulating SNAP-25 because promotes expression and

phosphorylation. During synaptic activity, nPKCε specifically enhances also phosphorylation of SNAP-25 without change the SNAP-25 total amount. The inhibitor peptide εV1-2 completely avoids the phosphorylation induced by synaptic activity emphasizing the specific tonic role of nPKCε. Interestingly, in basal conditions, nPKCε is present mainly in the membrane and pnPKCε almost equally distributed in membrane and cytosol. Electrical stimulation did not change significantly this distribution. However, during synaptic activity, a significant reduction of both nPKCε and pnPKCε is seen (Obis et al. 2015a) suggesting an increased turnover of the kinase whereas doing its phosphorylation action. This may reflect the downregulation of the PKC after its activation (Gould et al. 2009; Gould and Newton 2008; Kang et al. 2000; Lee et al. 1996; Lu et al. 1998). Moreover, it should be noted that nPKCε auto-phosphorylation is not stimulated by synaptic activity and that its decrease due to degradation does not affect its kinase function.

pnPKCε phosphorylates both pSNAP-25 and pMunc18-1, but reduces the amount of Munc18-1 and does not change SNAP-25. Therefore, this isoform has an important involvement in regulating the SNARE/SM complex and exocytosis during synaptic activity.

In relation with cPKCβI, we observed that the specific translocation inhibitor peptide βIV5-3 did not change total SNAP-25 and pSNAP-25 both in basal conditions and during synaptic activity indicating that cPKCβI isoform does not contribute to SNAP-25 phosphorylation during synaptic activity. However, this isoform plays a relevant negative role in the phosphorylation of Munc18-1 by pnPKCε.

2.2. BDNF/TrkB signaling does not modulate nPKCε-mediated SNAP-25 phosphorylation

Presynaptic activity enhances BDNF/TrkB signaling to increase cPKCβI activity (Hurtado et al. 2017a) and decreases phosphorylation of nPKCε. We

investigated the possible involvement of this pathway on SNAP-25 phosphorylation by using the anti-TrkB antibody 47/TrkB or applying exogenous BDNF. In particular, we found that neither 47/TrkB nor exogenous BDNF could modify SNAP-25 and pSNAP-25 levels. In this case, none of the two molecules regulates SNAP-25 protein levels nor its phosphorylation. On the contrary, the BDNF/TrkB signaling exerts through downstream cPKCβI activity a negative regulation on Munc18-1 phosphorylation.

Our results show that pSNAP-25 does not depend of TrkB but this receptor effectively contributes to pnPKCε modulation. Thus, the pnPKCε regulation of pSNAP-25 could be independent of the regulation of TrkB on pnPKCε. In a near future, it might be interesting to consider the cooperation of another mechanism. Alternatively, it is important to note that the constitutive phosphorylation of SNAP-25 by pnPKCε may guarantee the continuous operation of this force-generation protein and the permanent refilling of the vesicular pools.

3. Muscle contraction decreases SNAP-25 phosphorylation dependent on synaptic activity

Muscle activity has a critical role to enhance presynaptic nPKCε and cPKCβI protein levels through a retrograde BDNF/TrkB signaling (Besalduch et al. 2010; Hurtado et al. 2017a; Obis et al. 2015a). In the present experiments we found that synaptic activity followed by muscle contraction does not change SNAP-25 phosphorylated level in a period of 30 minutes. Interestingly, muscle contraction *per se* is able to reduce the phosphorylation of SNAP-25 with respect to synaptic activity. In these conditions, nPKCε positively regulates SNAP-25 phosphorylation but cPKCβI does not, which in both cases is similar to the stimulated muscles in which contraction is preserved. The decrease in pSNAP-25 could be induced by a decrease of its phosphorylation (presumably through a decrease in nPKCε activity) or an increase of its dephosphorylation by phosphatases. Furthermore, BDNF/TrkB signaling does not regulate SNAP-25 nor

its phosphorylation in these conditions. These findings reinforce the suggestion of that the PKC phosphorylation of SNAP-25 seems less complex than the regulation of Munc18-1 phosphorylation.

In conclusion, the PKC phosphorylation of the force generator SNAP-25 protein seems a relatively simple process constitutively performed by the nPKCε isoform in basal and different synaptic activity conditions. This PKC isoform also guarantees the phosphorylation of the regulatory Munc18-1 protein. However in this case, a very complex regulation is mediated by at least TrkB and cPKCβI activity, which operate specifically in different conditions of imposed synaptic activity. In regard to SNAP-25, its phosphorylation is not regulated by TrkB nor cPKCβI in any activity conditions.

CONCLUDING REMARKS

This thesis describes, at the neuromuscular junction, the presence and regulation, by synaptic activity and muscle contraction, of Munc18-1 and SNAP-25, two PKC substrates of the synaptic vesicle exocytotic apparatus responsible to the regulation of neurotransmitter release. We demonstrate that both synaptic activity and muscle contraction contribute to regulate Munc18-1 and SNAP-25 phosphorylation and that the activities of two presynaptic PKC isoforms (nPKCε and cPKCβI) are involved closely related with the BDNF/TrkB signaling pathway.

The overall results of this thesis are summarized in **figure 59. A** is a representation of how nPKCε and cPKCβI modulate Munc18-1 and SNAP-25 under presynaptic stimulation without contraction. Presynaptic stimulation induces calcium influx, which can promotes the activation of cPKCβI. This isoform downregulates the constitutively active nPKCε. On the one hand, nPKCε phosphorylates Munc18-1 and SNAP-25. On the other hand, cPKCβI only inhibits Munc18-1 phosphorylation. BDNF/TrkB pathway (with a balanced ratio of TrkB.FL and TrkB.T1) enhances PKC action over Munc18-1, like the final result of synaptic

activity. In **B** is represented how nPKCε and cPKCβI modulate Munc18-1 and SNAP-25 under presynaptic stimulation with contraction. Muscle contraction induces the shift of cPKCβI isoform to upregulate Munc18-1 phosphorylation, maintaining the inhibition over nPKCε. Moreover, similarly to what happens in the presynaptic stimulation without contraction, SNAP-25 is not affected by cPKCβI. The final result of muscle contraction *per se* is to downregulate Munc18-1 and SNAP-25 phosphorylation to reach a basal state. Finally, TrkB functions to regulate this complex system through cPKCβI.

Thus, this thesis provides a mechanistic insight into how Munc18-1 and SNAP-25 phosphorylation is regulated contributing to achieve the extraordinary precision and plasticity of neurotransmission.

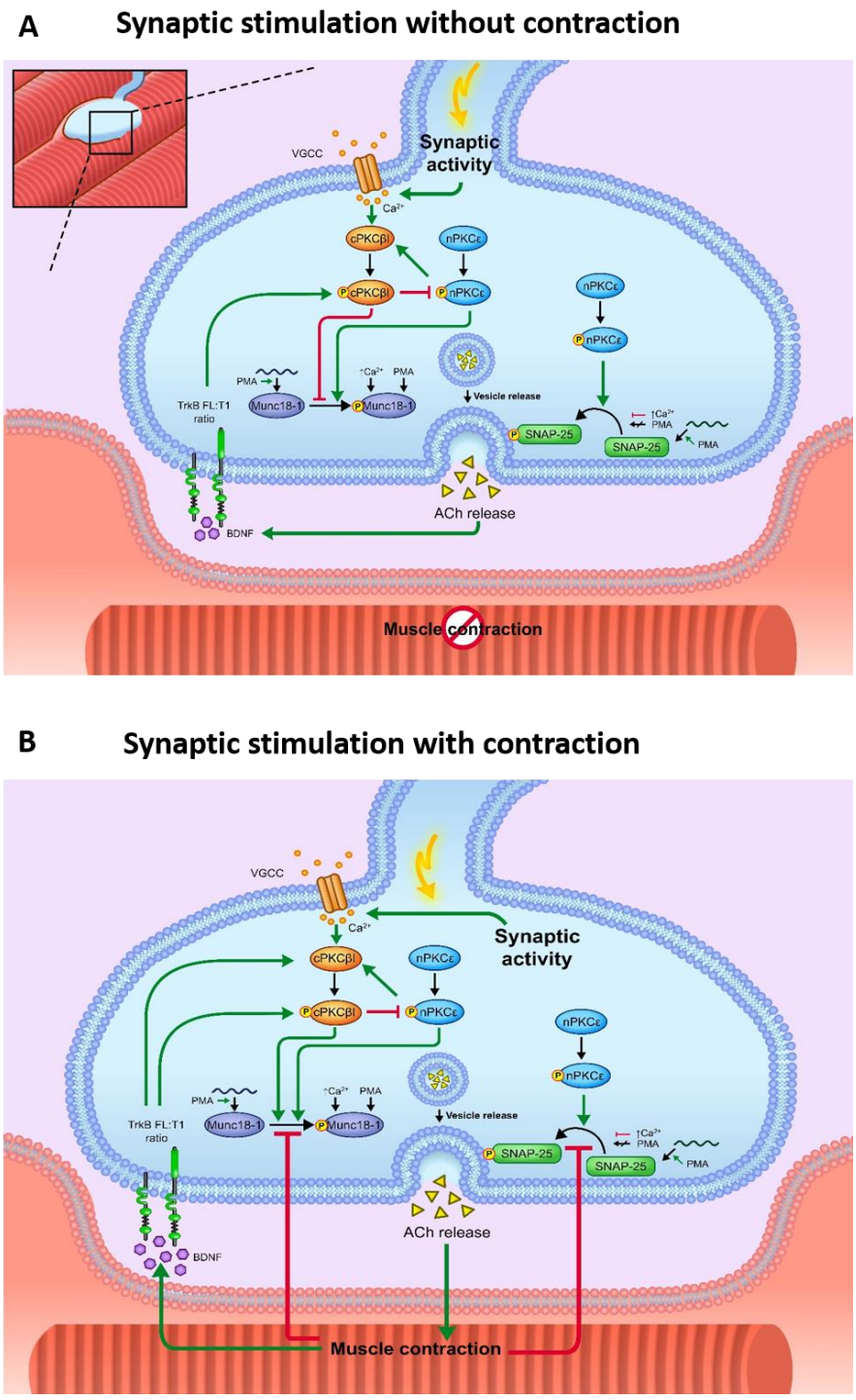

Figure 59. Summary of the results.

VI. CONCLUSIONS

UNIVERSITAT ROVIRA I VIRGILI
EFFECTS OF NEUROMUSCULAR ACTIVITY COUPLED TO BDNF/TRKB SIGNALING ON THE EXOCYTOTIC PROTEINS MUNC18-1 AND SNAP-25 THROUGH NPKCE AND CPKCSSI
Anna Simó Ollé

CONCLUSIONS

OBJECTIVE 1: To determine the expression, location and regulation by the PKC-activators calcium and PMA of Munc18-1 and SNAP-25 and their phosphorylated forms in the skeletal muscle.

- Muscle, spinal cord and brain have high amounts of Munc18-1, SNAP-25 and pSNAP-25, but pMunc18-1 is barely observed in brain and spinal cord tissue. In addition, both Munc18-1 and SNAP-25 are expressed and phosphorylated in basal conditions with a predominant location in the membrane fraction.

- Munc18-1 is present in the motor nerve terminals and absent in the Schwann and muscle cells.

- PMA increases both Munc18-1 and SNAP-25 total protein levels. Moreover, phosphorylation of Munc18-1 occurs in response to PMA, but SNAP-25 phosphorylation is not affected.

- In high calcium media, pMunc18-1 increases but pSNAP-25 decreases. In low calcium, pMunc18-1 does not change whereas pSNAP-25 increases.

OBJECTIVE 2: To determine whether the synaptic activity modulates Munc18-1, SNAP-25 and their phosphorylation levels in the skeletal muscle through nPKCε and cPKCβI isoforms and BDNF/TrkB signaling pathway.

- To determine whether presynaptic activity regulates Munc18-1, SNAP-25 and their phosphorylation levels.

  - Synaptic activity increases both Munc18-1 and pMunc18-1 and reduces pMunc18-1 in the membrane.

- Synaptic activity increases pSNAP-25 without affecting SNAP-25 total levels.

- Munc18-1 phosphorylation have a rapid increase from minute 1 to 10 and thereafter is maintained. In addition, the total level of Munc18-1 also increases steadily until reaching 30 minutes. In contrast, SNAP-25 phosphorylation increases after a continuous nerve-stimulation and total SNAP-25 levels do not change over time.

- Phosphatase activity regulates Munc18-1 phosphorylation-dephosphorylation at the beginning of stimulation (1 minute) and thereafter, pMunc18-1 increases and attains a steady value (10-30 minutes).

o To determine whether nPKCε and cPKCβI isoforms and their interaction regulate the phosphorylation of Munc18-1 and SNAP-25, related or not, with the presynaptic activity, and whether nPKCε and cPKCβI are interdependent.

- Both nPKCε and cPKCβI isoforms contribute to regulate pMunc18-1 during synaptic activity: nPKCε increases Munc18-1 phosphorylation while cPKCβI reduces it. Therefore, a balance between the activities of these two isoforms can be a relevant cue in the regulation of the exocytotic apparatus.

- SNAP-25 phosphorylation is positively modulated by nPKCε (in all basal and synaptic activity conditions) but cPKCβI does not regulate it in any activity condition.

- cPKCβI negatively regulates nPKCε phosphorylation and positively regulates nPKCε total levels both in basal and synaptic activity conditions. nPKCε isoform enhances cPKCβI without affecting pcPKCβI both in basal and synaptic activity conditions. Moreover, as a consequence of synaptic activity, pnPKCε enhances phosphorylation of Munc18-1 and cPKCβI

decreases it, maybe through the negative regulation of cPKCβI over pnPKCε.

- To determine whether BDNF/TrkB signaling pathway regulates the phosphorylation of Munc18-1 and SNAP-25 related with the synaptic activity.

  - BDNF/TrkB signaling negatively modulates pMunc18-1 level and pnPKCε activity.

  - BDNF/TrkB signaling enhances pcPKCβI action to prevent the synaptic activity-induced Munc18-1 phosphorylation mediated by nPKCε.

  - BDNF/TrkB and cPKCβI signaling does not affect pSNAP-25.

OBJECTIVE 3: To determine whether the synaptic activity resulting in muscle contraction has a repercussion on Munc18-1, SNAP-25 and their phosphorylation levels in the skeletal muscle through nPKCε and cPKCβI isoforms and BDNF/TrkB signaling pathway.

- To determine whether nerve-induced muscle contraction regulates Munc18-1, SNAP-25 and their phosphorylation levels.

  - Muscle contraction decreases the synaptic activity–induced Munc18-1 and SNAP-25 phosphorylation.

  - Complete neuromuscular activity prevents Munc18-1 phosphorylation only when continuous stimulation is performed over time but does not change the phosphorylation of SNAP-25.

- To determine whether nPKCε and cPKCβI isoforms regulate the phosphorylation of Munc18-1 and SNAP-25 under nerve-induced muscle contraction condition and the dependence between nPKCε and cPKCβI.

- Both nPKCε and cPKCβI isoforms positively regulate pMunc18-1 during muscle contraction.

- SNAP-25 phosphorylation is positively modulated by nPKCε but cPKCβI does not regulate it.

- cPKCβI negatively regulates nPKCε phosphorylation and positively regulates nPKCε total levels.

○ To determine whether BDNF/TrkB signaling pathway regulates the phosphorylation of Munc18-1 and SNAP-25 under nerve-induced muscle contraction condition.

- BDNF/TrkB signaling increases pMunc18-1 level and does not affect pSNAP-25.

- Muscle contraction prevents Munc18-1 phosphorylation against the activity of nPKCε, cPKCβI and BDNF/TrkB.

VII. REFERENCES

UNIVERSITAT ROVIRA I VIRGILI
EFFECTS OF NEUROMUSCULAR ACTIVITY COUPLED TO BDNF/TRKB SIGNALING ON THE EXOCYTOTIC PROTEINS MUNC18-1 AND SNAP-25 THROUGH NPKCE AND CPKCSSI
Anna Simó Ollé

Acheson A, Conover JC, Fandl JP, DeChiara TM, Russell M, Thadani A, Squinto SP, Yancopoulos GD, Lindsay RM (1995) A BDNF autocrine loop in adult sensory neurons prevents cell death. Nature 374:450–453.

Aguado F (2003) BDNF regulates spontaneous correlated activity at early developmental stages by increasing synaptogenesis and expression of the K+/Cl- co-transporter KCC2. Development 130:1267–1280.

Ahmari S E, Buchanan J SSJ (2000) Assembly of presynaptic active zones from cytoplasmic transport packets. Nat Neurosci 3:445–451.

Akita Y (2002) Protein kinase C-epsilon (PKC-epsilon): its unique structure and function. J Biochem 132:847–852.

Alabi A, Tsien R (2012) Synaptic vesicle pools and dynamics. Cold Spring Harb Perspect Biol 4:a013680.

Alabi A, Tsien R (2013) Perspectives on kiss-and-run: role in exocytosis, endocytosis, and neurotransmission. Annu Rev Physiol 75:393–422.

Alan R. Liss; MM Salpeter (1987) The vertebrate neuromuscular junction. Neurol Neurobiol 23 Alan R Liss, Inc, New York 2.

Angaut-Petit D, Molgo J, Connold AL, Faille L (1987) The levator auris longus muscle of the mouse: a convenient preparation for studies of short- and long-term presynaptic effects of drugs or toxins. Neurosci Lett 82:83–88.

Antal CE, Newton AC (2014) Tuning the signalling output of protein kinase C. Biochem Soc Trans 42:1477–1483.

Araç D, Chen X, Khant HA, Ubach J, Ludtke SJ, Kikkawa M, Johnson AE, Chiu W, Südhof TC, Rizo J (2006) Close membrane-membrane proximity induced by Ca(2+)-dependent multivalent binding of synaptotagmin-1 to phospholipids. Nat Struct Mol Biol 13:209–217.

Arenson MS (1989) Muscarinic inhibition of quantal transmitter release from the magnesium-paralysed frog sartorius muscle. Neuroscience 30:827–836.

Arunachalam L, Han L, Tassew NG, He Y, Wang L, Xie L, Fujita Y, Kwan E, Davletov B, Monnier PP, Gaisano HY, Sugita S (2008) Munc18-1 Is Critical for Plasma Membrane Localization of Syntaxin1 but Not of SNAP-25 in PC12 Cells. Mol Biol Cell 19:722–734.

Ashendel CL (1985) The phorbol ester receptor: a phospholipid-regulated protein kinase. Biochim Biophys Acta 822:219–242.

Atwal JK, Massie B, Miller FD, Kaplan DR (2000) The TrkB-Shc site signals neuronal survival and local axon growth via MEK and P13-kinase. Neuron 27:265–277.

Auld DS, Colomar A, Bélair E-L, Castonguay A, Pinard A, Rousse I, Thomas S, Robitaille R (n.d.) Modulation of neurotransmission by reciprocal synapse-glial interactions at the neuromuscular junction. J Neurocytol 32:1003–1015.

Auld DS, Robitaille R (2003) Perisynaptic Schwann cells at the neuromuscular junction: nerve- and activity-dependent contributions to synaptic efficacy, plasticity, and reinnervation. Neurosci 9:144–157.

Baker RW, Jeffrey PD, Zick M, Phillips BP, Wickner WT, Hughson FM (2015) A direct role for the Sec1/Munc18-family protein Vps33 as a template for SNARE assembly. Science (80-) 349.

Baldwin KM, Haddad F, Pandorf CE, Roy RR, Edgerton VR (2013) Alterations in muscle mass and contractile phenotype in response to unloading models: role of transcriptional/pretranslational mechanisms. Front Physiol 4:284.

Balkowiec A, Katz DM (2000a) Activity-Dependent Release of Endogenous Brain-Derived Neurotrophic Factor from Primary Sensory Neurons Detected by ELISA In Situ. J Neurosci 20.

Balkowiec A, Katz DM (2000b) Activity-dependent release of endogenous brain-derived neurotrophic factor from primary sensory neurons detected by ELISA in situ. J Neurosci 20:7417–7423.

Barclay JW, Craig TJ, Fisher RJ, Ciufo LF, Evans GJO, Morgan A, Burgoyne RD (2003) Phosphorylation of Munc18 by protein kinase C regulates the kinetics of exocytosis. J Biol Chem.

Barrett CF, Rittenhouse AR (2000) Modulation of N-type calcium channel activity by G-proteins and protein kinase C. J Gen Physiol 115:277–286.

Bazzi MD, Nelsestuen GL (1989) Differences in the effects of phorbol esters and diacylglycerols on protein kinase C. Biochemistry 28:9317–9323.

Bazzi MD, Nelsestuen GL (1990) Protein kinase C interaction with calcium: a phospholipid-dependent process. Biochemistry 29:7624–7630.

Becherer U, Rettig J (2006) Vesicle pools, docking, priming, and release. Cell Tissue Res 326:393–407.

Besalduch N, Lanuza MA, Garcia N, Obis T, Santafe MM, Tomàs M, Priego M, Tomàs J (2013) Cellular localization of the atypical isoforms of protein kinase C (aPKCζ/PKMζ and aPKCλ/ι) on the neuromuscular synapse. Neurosci Lett.

Besalduch N, Tomàs M, Santafé MM, Garcia N, Tomàs J, Lanuza MA (2010) Synaptic activity-related classical protein kinase C isoform localization in the adult rat neuromuscular synapse. J Comp Neurol.

Bhatheja K, Field J (2006) Schwann cells: origins and role in axonal maintenance and regeneration. Int J Biochem Cell Biol 38:1995–1999.

Biffo S, Offenhäuser N, Carter BD, Barde YA (1995) Selective binding and internalisation by truncated receptors restrict the availability of BDNF during development. Development 121:2461–2470.

Blum R, Konnerth A (2005) Neurotrophin-mediated rapid signaling in the central nervous system: mechanisms and functions. Physiology (Bethesda) 20:70–78.

Blumberg PM (1988) Protein kinase C as the receptor for the phorbol ester tumor promoters: sixth Rhoads memorial award lecture. Cancer Res 48:1–8.

Bock JB, Matern HT, Peden AA, Scheller RH (2001) A genomic perspective on membrane compartment organization. Nature 409:839–841.

Bodian D (1970) An electron microscopic characterization of classes of synaptic vesicles by means of controlled aldehyde fixation. J Cell Biol 44:115–124.

Bombardier JP, Munson M (2015) Three steps forward, two steps back: mechanistic insights into the assembly and disassembly of the SNARE complex. Curr Opin Chem Biol 29:66–71.

Bornancin F, Parker PJ (1996) Phosphorylation of threonine 638 critically controls the dephosphorylation and inactivation of protein kinase Calpha. Curr Biol 6:1114–1123.

Bothwell M (2016) Recent advances in understanding neurotrophin signaling. F1000Research 5.

Boyd A, Ciufo LF, Barclay JW, Graham ME, Haynes LP, Doherty MK, Riesen M, Burgoyne RD, Morgan A (2008) A Random Mutagenesis Approach to Isolate Dominant-Negative Yeast sec1 Mutants Reveals a Functional Role for Domain 3a in Yeast and Mammalian Sec1/Munc18 Proteins. Genetics 180.

Brigadski T, Hartmann M, Lessmann V (2005) Differential vesicular targeting and time course of synaptic secretion of the mammalian neurotrophins. J Neurosci 25:7601–7614.

Brose N (2008) For better or for worse: complexins regulate SNARE function and vesicle fusion. Traffic 9:1403–1413.

Brunger AT (2001) Structure of Proteins Involved in Synaptic Vesicle Fusion in Neurons. Annu Rev Biophys Biomol Struct 30:157–171.

Brunger AT (2005) Structure and function of SNARE and SNARE-interacting proteins. Q Rev Biophys 38:1.

Burns ME, Augustine GJ (1995) Synaptic structure and function: dynamic organization yields architectural precision. Cell 83:187–194.

Byrne JH, Kandel ER (1996) Presynaptic facilitation revisited: state and time dependence. J Neurosci 16:425–435.

Caccin P, Scorzeto M, Damiano N, Marin O, Megighian A, Montecucco C (2015) The synaptotagmin juxtamembrane domain is involved in neuroexocytosis. FEBS Open Bio 5:388–396.

Campanari M-L, García-Ayllón M-S, Ciura S, Sáez-Valero J, Kabashi E (2016) Neuromuscular Junction Impairment in Amyotrophic Lateral Sclerosis: Reassessing the Role of Acetylcholinesterase. Front Mol Neurosci.

Canossa M, Gärtner A, Campana G, Inagaki N, Thoenen H (2001) Regulated secretion of neurotrophins by metabotropic glutamate group I (mGluRI) and Trk receptor activation is mediated via phospholipase C signalling pathways. EMBO J 20:1640–1650.

Carr CM, Rizo J (2010) At the junction of SNARE and SM protein function. Curr Opin Cell Biol 22:488–495.

Castagna M, Takai Y, Kaibuchi K, Sano K, Kikkawa U, Nishizuka Y (1982) Direct activation of calcium-activated, phospholipid-dependent protein kinase by tumor-promoting phorbol esters. J Biol Chem 257:7847–7851.

Castonguay A, Lévesque S, Robitaille R (2001) Glial cells as active partners in synaptic functions. Prog Brain Res 132:227–240.

Catterall WA (1999) Interactions of presynaptic Ca2+ channels and snare proteins in neurotransmitter release. Ann N Y Acad Sci 868:144–159.

Caulfield MP (1993) Muscarinic receptors--characterization, coupling and function. Pharmacol Ther 58:319–379.

Cazorla M, Prémont J, Mann A, Girard N, Kellendonk C, Rognan D (2011) Identification of a low-molecular weight TrkB antagonist with anxiolytic and antidepressant activity in mice. J Clin Invest 121:1846–1857.

Chand KK, Lee KM, Schenning MP, Lavidis NA, Noakes PG (2015) Loss of β2-laminin alters calcium sensitivity and voltage-gated calcium channel maturation of neurotransmission at the neuromuscular junction. J Physiol 593:245–265.

Chao M V (2003) Neurotrophins and their receptors: a convergence point for many signalling pathways. Nat Rev Neurosci 4:299–309.

Chapman ER (2002) Synaptotagmin: a Ca(2+) sensor that triggers exocytosis? Nat Rev Mol Cell Biol 3:498–508.

Chapman ER (2008) How does synaptotagmin trigger neurotransmitter release? Annu Rev Biochem 77:615–641.

Chen X, Tomchick DR, Kovrigin E, Araç D, Machius M, Südhof TC, Rizo J (2002) Three-dimensional structure of the complexin/SNARE complex. Neuron 33:397–409.

Chen YA, Scales SJ, Patel SM, Doung YC, Scheller RH (1999) SNARE complex formation is

triggered by Ca2+ and drives membrane fusion. Cell 97:165–174.

Chen YA, Scheller RH (2001) SNARE-mediated membrane fusion. Nat Rev Mol Cell Biol 2:98–106.

Chen Y, Tian Q (2011) The role of protein kinase C epsilon in neural signal transduction and neurogenic diseases. Front Med 5:70–76.

Choi UB, Strop P, Vrljic M, Chu S, Brunger AT, Weninger KR (2010) Single-molecule FRET-derived model of the synaptotagmin 1-SNARE fusion complex. Nat Struct Mol Biol 17:318–324.

Choi UB, Zhao M, Zhang Y, Lai Y, Brunger AT, Südhof T, Reim K, Rosenmund C, Jahn R, Yoon T, Blanchard S, Mothes W (2016) Complexin induces a conformational change at the membrane-proximal C-terminal end of the SNARE complex. Elife 5:1308–1317.

Cijsouw T, Weber JP, Broeke JH, Broek JAC, Schut D, Kroon T, Saarloos I, Verhage M, Toonen RF (2014) Munc18-1 redistributes in nerve terminals in an activity- and PKC-dependent manner. J Cell Biol.

Cisterna BA, Cardozo C, Sáez JC (2014) Neuronal involvement in muscular atrophy. Front Cell Neurosci 8:405.

Correia-de-Sá P, Ribeiro JA (1994) Tonic adenosine A2A receptor activation modulates nicotinic autoreceptor function at the rat neuromuscular junction. Eur J Pharmacol 271:349–355.

Craig AM (1998) Activity and synaptic receptor targeting: the long view. Neuron 21:459–462.

Craig TJ, Evans GJO, Morgan A (2003) Physiological regulation of Munc18/nSec1 phosphorylation on serine-313. J Neurochem.

Dale HH, Feldberg W, Vogt M (1936) Release of acetylcholine at voluntary motor nerve endings. J Physiol 86:353–380.

Deák F, Xu Y, Chang W-P, Dulubova I, Khvotchev M, Liu X, Südhof TC, Rizo J (2009) Munc18-1 binding to the neuronal SNARE complex controls synaptic vesicle priming. J Cell Biol 184:751–764.

De Troyer A, Sampson M, Sigrist S, Macklem PT (1981) The diaphragm: two muscles. Science 213:237–238.

de Vries KJ, Geijtenbeek A, Brian EC, de Graan PN, Ghijsen WE, Verhage M (2000) Dynamics of munc18-1 phosphorylation/dephosphorylation in rat brain nerve terminals. Eur J Neurosci 12:385–390.

de Wit H, Walter AM, Milosevic I, Gulyás-Kovács A, Riedel D, Sørensen JB, Verhage M (2009) Synaptotagmin-1 docks secretory vesicles to syntaxin-1/SNAP-25 acceptor complexes. Cell 138:935–946.

Dechant G, Barde Y-A (2002) The neurotrophin receptor p75(NTR): novel functions and implications for diseases of the nervous system. Nat Neurosci 5:1131–1136.

Del Castillo J, Katz B (1954) Quantal components of the end-plate potential. J Physiol 124:560–573.

Denker A, Bethani I, Kröhnert K, Körber C, Horstmann H, Wilhelm BG, Barysch S V, Kuner T, Neher E, Rizzoli SO (2011) A small pool of vesicles maintains synaptic activity in vivo. Proc Natl Acad Sci U S A 108:17177–17182.

Dieni S, Matsumoto T, Dekkers M, Rauskolb S, Ionescu MS, Deogracias R, Gundelfinger ED, Kojima M, Nestel S, Frotscher M, Barde Y-A (2012) BDNF and its pro-peptide are stored in presynaptic dense core vesicles in brain neurons. J Cell Biol 196:775–788.

Dorsey SG et al. (2012) Genetic deletion of trkB.T1 increases neuromuscular function. Am J Physiol Cell Physiol 302:C141-53.

Du J, Feng L, Zaitsev E, Je H-S, Liu X-W, Lu B (2003) Regulation of TrkB receptor tyrosine kinase and its internalization by neuronal activity and Ca2+ influx. J Cell Biol 163:385–395.

Duclert A, Changeux JP (1995) Acetylcholine receptor gene expression at the developing neuromuscular junction. Physiol Rev 75:339–368.

Dulubova I, Khvotchev M, Liu S, Südhof TC, Rizo J (2007) Munc18-1 binds directly to the neuronal SNARE complex. Proc Natl Acad Sci U S A 104:2697–2702.

Dulubova I, Sugita S, Hill S, Hosaka M, Fernandez I, Südhof TC, Rizo J (1999) A conformational switch in syntaxin during exocytosis: role of munc18. EMBO J 18:4372–4382.

Dutil EM, Newton AC (2000) Dual role of pseudosubstrate in the coordinated regulation of protein kinase C by phosphorylation and diacylglycerol. J Biol Chem 275:10697–10701.

Dutil EM, Toker A, Newton AC (1998) Regulation of conventional protein kinase C isozymes by phosphoinositide-dependent kinase 1 (PDK-1). Curr Biol 8:1366–1375.

Eide FF, Vining ER, Eide BL, Zang K, Wang XY, Reichardt LF (1996) Naturally occurring truncated trkB receptors have dominant inhibitory effects on brain-derived neurotrophic factor signaling. J Neurosci 16:3123–3129.

Engel AG, Ohno K, Sine SM (2003) Congenital myasthenic syndromes: A diverse array of molecular targets. J Neurocytol 32:1017–1037.

Erzen I, Cvetko E, Obreza S, Angaut-Petit D (2000) Fiber types in the mouse levator auris longus muscle: a convenient preparation to study muscle and nerve plasticity. J Neurosci Res 59:692–697.

Falls DL, Rosen KM, Corfas G, Lane WS, Fischbach GD (1993) ARIA, a protein that stimulates

acetylcholine receptor synthesis, is a member of the neu ligand family. Cell 72:801–815.

Fasshauer D, Eliason WK, Brünger AT, Jahn R (1998) Identification of a minimal core of the synaptic SNARE complex sufficient for reversible assembly and disassembly. Biochemistry 37:10354–10362.

Favreau P, Le Gall F, Benoit E, Molgó J (1999) A review on conotoxins targeting ion channels and acetylcholine receptors of the vertebrate neuromuscular junction. Acta Physiol Pharmacol Ther Latinoam 49:257–267.

Feng Z, Ko C-P (2008) Schwann cells promote synaptogenesis at the neuromuscular junction via transforming growth factor-beta1. J Neurosci 28:9599–9609.

Fernandez I, Ubach J, Dulubova I, Zhang X, Südhof TC, Rizo J (1998) Three-dimensional structure of an evolutionarily conserved N-terminal domain of syntaxin 1A. Cell 94:841–849.

Fletcher AI, Shuang R, Giovannucci DR, Zhang L, Bittner MA, Stuenkel EL (1999) Regulation of exocytosis by cyclin-dependent kinase 5 via phosphorylation of Munc18. J Biol Chem 274:4027–4035.

Fotin A, Cheng Y, Sliz P, Grigorieff N, Harrison SC, Kirchhausen T, Walz T (2004) Molecular model for a complete clathrin lattice from electron cryomicroscopy. Nature 432:573–579.

Fotin A, Kirchhausen T, Grigorieff N, Harrison SC, Walz T, Cheng Y (2006) Structure determination of clathrin coats to subnanometer resolution by single particle cryo-electron microscopy. J Struct Biol 156:453–460.

Fujita Y, Sasaki T, Fukui K, Kotani H, Kimura T, Hata Y, Südhof TC, Scheller RH, Takai Y (1996) Phosphorylation of Munc-18/n-Sec1/rbSec1 by protein kinase C: its implication in regulating the interaction of Munc-18/n-Sec1/rbSec1 with syntaxin. J Biol Chem 271:7265–7268.

Ganguly DK, Das M (1979) Effects of oxotremorine demonstrate presynaptic muscarinic and dopaminergic receptors on motor nerve terminals. Nature 278:645–646.

Gao J, Hirata M, Mizokami A, Zhao J, Takahashi I, Takeuchi H, Hirata M (2016) Differential role of SNAP-25 phosphorylation by protein kinases A and C in the regulation of SNARE complex formation and exocytosis in PC12 cells. Cell Signal 28:425–437.

Gao T, Brognard J, Newton AC (2008) The phosphatase PHLPP controls the cellular levels of protein kinase C. J Biol Chem 283:6300–6311.

Garcia EP, Gatti E, Butler M, Burton J, De Camilli P (1994) A rat brain Sec1 homologue related to Rop and UNC18 interacts with syntaxin. Proc Natl Acad Sci U S A 91:2003–2007.

Garcia N, Priego M, Obis T, Santafe MM, Tomàs M, Besalduch N, Lanuza Ma, Tomàs J (2013)

Adenosine A1 and A2A receptor-mediated modulation of acetylcholine release in the mice neuromuscular junction. Eur J Neurosci.

Garcia N, Santafé MM, Salon I, Lanuza MA, Tomàs J (2005) Expression of muscarinic acetylcholine receptors (M1-, M2-, M3- and M4-type) in the neuromuscular junction of the newborn and adult rat. Histol Histopathol.

Garcia N, Tomas M, Santafe MM, Besalduch N, Lanuza MA, Tomas J (2010a) The Interaction between Tropomyosin-Related Kinase B Receptors and Presynaptic Muscarinic Receptors Modulates Transmitter Release in Adult Rodent Motor Nerve Terminals. J Neurosci 30:16514–16522.

Garcia N, Tomàs M, Santafé MM, Besalduch N, Lanuza MA, Tomàs J (2010b) The interaction between tropomyosin-related kinase B receptors and presynaptic muscarinic receptors modulates transmitter release in adult rodent motor nerve terminals. J Neurosci 30:16514–16522.

Gasnier B (2000) The loading of neurotransmitters into synaptic vesicles. Biochimie 82:327–337.

Genc O, Kochubey O, Toonen RF, Verhage M, Schneggenburger R (2014a) Munc18-1 is a dynamically regulated PKC target during short-term enhancement of transmitter release. Elife.

Genc O, Kochubey O, Toonen RF, Verhage M, Schneggenburger R (2014b) Munc18-1 is a dynamically regulated PKC target during short-term enhancement of transmitter release. Elife.

Gomez-Pinilla F, Hillman C (2013) The influence of exercise on cognitive abilities. Compr Physiol 3:403–428.

Gomez-Pinilla F, Vaynman S, Ying Z (2008) Brain-derived neurotrophic factor functions as a metabotrophin to mediate the effects of exercise on cognition. Eur J Neurosci 28:2278–2287.

Gomez-Pinilla F, Ying Z, Opazo P, Roy RR, Edgerton VR (2001) Differential regulation by exercise of BDNF and NT-3 in rat spinal cord and skeletal muscle. Eur J Neurosci 13:1078–1084.

Gomez-Pinilla F, Ying Z, Roy RR, Molteni R, Edgerton VR (2002) Voluntary exercise induces a BDNF-mediated mechanism that promotes neuroplasticity. J Neurophysiol 88:2187–2195.

Gomez-Pinilla F, Ying Z, Zhuang Y (2012) Brain and spinal cord interaction: protective effects of exercise prior to spinal cord injury. PLoS One 7:e32298.

Gonzalez M, Ruggiero FP, Chang Q, Shi YJ, Rich MM, Kraner S, Balice-Gordon RJ (1999) Disruption of Trkb-mediated signaling induces disassembly of postsynaptic receptor clusters at neuromuscular junctions. Neuron 24:567–583.

Gonzalo S, Greentree WK, Linder ME (1999) SNAP-25 is targeted to the plasma membrane through a novel membrane-binding domain. J Biol Chem 274:21313–21318.

Gould CM, Kannan N, Taylor SS, Newton AC (2009) The Chaperones Hsp90 and Cdc37 Mediate the Maturation and Stabilization of Protein Kinase C through a Conserved P XX P Motif in the C-terminal Tail. J Biol Chem 284:4921–4935.

Gould CM, Newton AC (2008) The life and death of protein kinase C. Curr Drug Targets 9:614–625.

Greenberg ME, Xu B, Lu B, Hempstead BL (2009) New insights in the biology of BDNF synthesis and release: implications in CNS function. J Neurosci 29:12764–12767.

Griffin JW, Thompson WJ (2008) Biology and pathology of nonmyelinating Schwann cells. Glia 56:1518–1531.

Guan R, Dai H, Rizo J (2008) Binding of the Munc13-1 MUN domain to membrane-anchored SNARE complexes. Biochemistry 47:1474–1481.

Gulyás-Kovács A, de Wit H, Milosevic I, Kochubey O, Toonen R, Klingauf J, Verhage M, Sørensen JB (2007) Munc18-1: sequential interactions with the fusion machinery stimulate vesicle docking and priming. J Neurosci 27:8676–8686.

Guo W, Sacher M, Barrowman J, Ferro-Novick S, Novick P (2000) Protein complexes in transport vesicle targeting. Trends Cell Biol 10:251–255.

Haapasalo A, Koponen E, Hoppe E, Wong G, Castrén E (2001) Truncated trkB.T1 is dominant negative inhibitor of trkB.TK+-mediated cell survival. Biochem Biophys Res Commun 280:1352–1358.

Han GA, Bin N-R, Kang S-YA, Han L, Sugita S (2013) Domain 3a of Munc18-1 plays a crucial role at the priming stage of exocytosis. J Cell Sci 126.

Han GA, Park S, Bin N-R, Jung CH, Kim B, Chandrasegaram P, Matsuda M, Riadi I, Han L, Sugita S (2014) A pivotal role for pro-335 in balancing the dual functions of Munc18-1 domain-3a in regulated exocytosis. J Biol Chem 289:33617–33628.

Han L, Jiang T, Han GA, Malintan NT, Xie L, Wang L, Tse FW, Gaisano HY, Collins BM, Meunier FA, Sugita S (2009) Rescue of Munc18-1 and -2 double knockdown reveals the essential functions of interaction between Munc18 and closed syntaxin in PC12 cells. Mol Biol Cell 20:4962–4975.

Hanson PI, Roth R, Morisaki H, Jahn R, Heuser JE (1997) Structure and conformational changes in NSF and its membrane receptor complexes visualized by quick-freeze/deep-etch electron microscopy. Cell 90:523–535.

Hansra G, Bornancin F, Whelan R, Hemmings BA, Parker PJ (1996) 12-O-Tetradecanoylphorbol-13-acetate-induced dephosphorylation of protein kinase Calpha correlates with the presence of a membrane-associated protein phosphatase 2A heterotrimer. J Biol Chem 271:32785–32788.

Harata N, Ryan TA, Smith SJ, Buchanan J, Tsien RW (2001) Visualizing recycling synaptic vesicles in hippocampal neurons by FM 1-43 photoconversion. Proc Natl Acad Sci U S A 98:12748–12753.

Hata Y, Slaughter CA, Südhof TC (1993) Synaptic vesicle fusion complex contains unc-18 homologue boundto syntaxin. Nature 366:347–351.

Hempstead BL (2006) Dissecting the diverse actions of pro- and mature neurotrophins. Curr Alzheimer Res 3:19–24.

Heuser JE, Reese TS (1973) Evidence for recycling of synaptic vesicle membrane during transmitter release at the frog neuromuscular junction. J Cell Biol 57:315–344.

Hilfiker S, Augustine GJ (1999) Regulation of synaptic vesicle fusion by protein kinase C. J Physiol 515 (Pt 1:1.

Hilfiker S, Pieribone VA, Nordstedt C, Greengard P, Czernik AJ (1999) Regulation of synaptotagmin I phosphorylation by multiple protein kinases. J Neurochem 73:921–932.

Hilgenberg L, Miles K (1995) Developmental regulation of a protein kinase C isoform localized in the neuromuscular junction. J Cell Sci 108 (Pt 1:51–61.

Hirsch NP (2007) Neuromuscular junction in health and disease. Br J Anaesth 99:132–138.

Hodgkin AL, Katz B (1949) The effect of sodium ions on the electrical activity of giant axon of the squid. J Physiol 108:37–77.

Hu S-H, Christie MP, Saez NJ, Latham CF, Jarrott R, Lua LHL, Collins BM, Martin JL (2011) Possible roles for Munc18-1 domain 3a and Syntaxin1 N-peptide and C-terminal anchor in SNARE complex formation. Proc Natl Acad Sci U S A 108:1040–1045.

Huang EJ, Reichardt LF (2001) Neurotrophins: roles in neuronal development and function. Annu Rev Neurosci 24:677–736.

Huang EJ, Reichardt LF (2003) Trk receptors: roles in neuronal signal transduction. Annu Rev Biochem 72:609–642.

Hui E, Johnson CP, Yao J, Dunning FM, Chapman ER (2009) Synaptotagmin-mediated bending of the target membrane is a critical step in Ca(2+)-regulated fusion. Cell 138:709–721.

Hurtado E, Cilleros V, Just L, Simó A, Nadal L, Tomas M, Garcia N, Lanuza MA, Tomas J (2017a) Synaptic Activity and Muscle Contraction Increases PDK1 and PKCbI Phosphorylation in the Presynaptic Membrane of the Neuromuscular Junction. Front Mol Neurosci.

Hurtado E, Cilleros V, Nadal L, Simó A, Obis T, Garcia N, Santafé MM, Tomàs M, Halievski K, Jordan CL, Lanuza MA, Tomàs J (2017b) Muscle Contraction Regulates BDNF/TrkB Signaling to Modulate Synaptic Function through Presynaptic cPKCα and cPKCβI.

Front Mol Neurosci 10:147.

Huxley HE (2004) Fifty years of muscle and the sliding filament hypothesis. Eur J Biochem 271:1403–1415.

Inoue M, Kishimoto A, Takai Y, Nishizuka Y (1977) Studies on a cyclic nucleotide-independent protein kinase and its proenzyme in mammalian tissues. II. Proenzyme and its activation by calcium-dependent protease from rat brain. J Biol Chem 252:7610–7616.

Jahn R, Fasshauer D (2012) Molecular machines governing exocytosis of synaptic vesicles. Nature 490:201–207.

Jahn R, Lang T, Südhof TC (2003) Membrane fusion. Cell 112:519–533.

Jahn R, Scheller RH (2006) SNAREs--engines for membrane fusion. Nat Rev Mol Cell Biol 7:631–643.

Jahn R, Südhof TC (1999) Membrane Fusion and Exocytosis. Annu Rev Biochem 68:863–911.

James DJ, Martin TFJ (2013) CAPS and Munc13: CATCHRs that SNARE Vesicles. Front Endocrinol (Lausanne) 4:187.

Jessell TM, Kandel ER (1993) Synaptic transmission: a bidirectional and self-modifiable form of cell-cell communication. Cell 72 Suppl:1–30.

Johnson JA, Gray MO, Chen C-H, Mochly-Rosen D (1996a) A Protein Kinase C Translocation Inhibitor as an Isozyme-selective Antagonist of Cardiac Function. J Biol Chem 271:24962–24966.

Johnson JA, Gray MO, Chen CH, Mochly-Rosen D (1996b) A protein kinase C translocation inhibitor as an isozyme-selective antagonist of cardiac function. J Biol Chem 271:24962–24966.

Jungbluth S, Bailey K, Barde YA (1994) Purification and characterisation of a brain-derived neurotrophic factor/neurotrophin-3 (BDNF/NT-3) heterodimer. Eur J Biochem 221:677–685.

Kaeser PS, Regehr WG (2014) Molecular mechanisms for synchronous, asynchronous, and spontaneous neurotransmitter release. Annu Rev Physiol 76:333–363.

Kaeser PS, Regehr WG (2017) The readily releasable pool of synaptic vesicles. Curr Opin Neurobiol 43:63–70.

Kandel, Eric R. Schwartz JH (2012) Principles of neural science.

Kang B-S, French OG, Sando JJ, Hahn CS (2000) Activation-dependent degradation of protein kinase Cη. Oncogene 19:4263–4272.

Kang H, Tian L, Mikesh M, Lichtman JW, Thompson WJ (2014) Terminal Schwann cells participate in neuromuscular synapse remodeling during reinnervation following nerve injury. J Neurosci 34:6323–6333.

Kataoka M, Kuwahara R, Iwasaki S, Shoji-Kasai Y, Takahashi M (2000) Nerve growth factor-induced phosphorylation of SNAP-25 in PC12 cells: a possible involvement in the regulation of SNAP-25 localization. J Neurochem 74:2058–2066.

Katayama N, Yamamori S, Fukaya M, Kobayashi S, Watanabe M, Takahashi M, Manabe T (2017) SNAP-25 phosphorylation at Ser187 regulates synaptic facilitation and short-term plasticity in an age-dependent manner. Sci Rep 7:7996.

Katz B (1996) Neural transmitter release: from quantal secretion to exocytosis and beyond. The Fenn Lecture. J Neurocytol 25:677–686.

Katz B, Miledi R (1967) The timing of calcium action during neuromuscular transmission. J Physiol 189:535–544.

Kazanietz MG, Barchi JJ, Omichinski JG, Blumberg PM (1995) Low affinity binding of phorbol esters to protein kinase C and its recombinant cysteine-rich region in the absence of phospholipids. J Biol Chem 270:14679–14684.

Keesey JC (2004) A history of treatments for myasthenia gravis. Semin Neurol 24:5–16.

Keranen LM, Dutil EM, Newton AC (1995) Protein kinase C is regulated in vivo by three functionally distinct phosphorylations. Curr Biol 5:1394–1403.

Kheifets V, Mochly-Rosen D (2007) Insight into intra- and inter-molecular interactions of PKC: design of specific modulators of kinase function. Pharmacol Res 55:467–476.

Khvotchev M, Dulubova I, Sun J, Dai H, Rizo J, Südhof TC (2007) Dual modes of Munc18-1/SNARE interactions are coupled by functionally critical binding to syntaxin-1 N terminus. J Neurosci 27:12147–12155.

Kim E, Sheng M (2004) PDZ domain proteins of synapses. Nat Rev Neurosci 5:771–781.

Kim J-Y, Choi B-K, Choi M-G, Kim S-A, Lai Y, Shin Y-K, Lee NK (2012) Solution single-vesicle assay reveals PIP2-mediated sequential actions of synaptotagmin-1 on SNAREs. EMBO J 31:2144–2155.

Kishino A, Ishige Y, Tatsuno T, Nakayama C, Noguchi H (1997) BDNF prevents and reverses adult rat motor neuron degeneration and induces axonal outgrowth. Exp Neurol 144:273–286.

Kloepper TH, Kienle CN, Fasshauer D (2007) An Elaborate Classification of SNARE Proteins Sheds Light on the Conservation of the Eukaryotic Endomembrane System. Mol Biol Cell 18:3463–3471.

Kolbeck R, Bartke I, Eberle W, Barde YA (1999) Brain-derived neurotrophic factor levels in the nervous system of wild-type and neurotrophin gene mutant mice. J Neurochem

72:1930–1938.

König B, DiNitto PA, Blumberg PM (1985) Stoichiometric binding of diacylglycerol to the phorbol ester receptor. J Cell Biochem 29:37–44.

Korogod N, Lou X, Schneggenburger R (2007) Posttetanic potentiation critically depends on an enhanced Ca2+ sensitivity of vesicle fusion mediated by presynaptic PKC. Proc Natl Acad Sci 104:15923–15928.

Kozlovsky Y, Chernomordik L V, Kozlov MM (2002) Lipid intermediates in membrane fusion: formation, structure, and decay of hemifusion diaphragm. Biophys J 83:2634–2651.

Krishnakumar SS, Radoff DT, Kümmel D, Giraudo CG, Li F, Khandan L, Baguley SW, Coleman J, Reinisch KM, Pincet F, Rothman JE (2011) A conformational switch in complexin is required for synaptotagmin to trigger synaptic fusion. Nat Struct Mol Biol 18:934–940.

Kulakowski SA, Parker SD, Personius KE (2011) Reduced TrkB expression results in precocious age-like changes in neuromuscular structure, neurotransmission, and muscle function. J Appl Physiol 111:844–852.

Kuromi H, Kidokoro Y (2003) Two synaptic vesicle pools, vesicle recruitment and replenishment of pools at the Drosophila neuromuscular junction. J Neurocytol 32:551–565.

Laemmli UK (1970) Cleavage of structural proteins during the assembly of the head of bacteriophage T4. Nature 227:680–685.

Lai Y, Shin Y-K (2012) The importance of an asymmetric distribution of acidic lipids for synaptotagmin 1 function as a Ca2+ sensor. Biochem J 443:223–229.

Lanuza M a, Li MX, Jia M, Kim S, Davenport R, Dunlap V, Nelson PG (2000) Protein kinase C-mediated changes in synaptic efficacy at the neuromuscular junction in vitro: the role of postsynaptic acetylcholine receptors. J Neurosci Res.

Lanuza MA, Garcia N, Santafe M, Nelson PG, Fenoll-Brunet MR, Tomas J (2001) Pertussis Toxin-Sensitive G-Protein and Protein Kinase C Activity are Involved in Normal Synapse Elimination in the Neonatal Rat Muscle. J Neurosci Res 63:330–340.

Lanuza MA, Gizaw R, Viloria A, González CM, Besalduch N, Dunlap V, Tomás J, Nelson PG (2006) Phosphorylation of the nicotinic acetylcholine receptor in myotube-cholinergic neuron cocultures. J Neurosci Res.

Lanuza MA, Santafe MM, Garcia N, Besalduch N, Tomàs M, Obis T, Priego M, Nelson PG, Tomàs J (2014) Protein kinase C isoforms at the neuromuscular junction: Localization and specific roles in neurotransmission and development. J Anat.

Lau CG, Takayasu Y, Rodenas-Ruano A, Paternain A V., Lerma J, Bennett MVL, Zukin RS (2010) SNAP-25 Is a Target of Protein Kinase C Phosphorylation Critical to NMDA Receptor Trafficking. J Neurosci 30:242–254.

Le Good JA, Ziegler WH, Parekh DB, Alessi DR, Cohen P, Parker PJ (1998) Protein kinase C isotypes controlled by phosphoinositide 3-kinase through the protein kinase PDK1. Science 281:2042–2045.

Lee H-K, Yang Y, Su Z, Hyeon C, Lee T-S, Lee H-W, Kweon D-H, Shin Y-K, Yoon T-Y (2010) Dynamic Ca2+-dependent stimulation of vesicle fusion by membrane-anchored synaptotagmin 1. Science 328:760–763.

Lee HW, Smith L, Pettit GR, Bingham Smith J (1996) Dephosphorylation of activated protein kinase C contributes to downregulation by bryostatin. Am J Physiol 271:C304-11.

Leenders AGM, Sheng Z-H (2005a) Modulation of neurotransmitter release by the second messenger-activated protein kinases: implications for presynaptic plasticity. Pharmacol Ther 105:69–84.

Leenders AGM, Sheng Z-H (2005b) Modulation of neurotransmitter release by the second messenger-activated protein kinases: Implications for presynaptic plasticity. Pharmacol Ther 105:69–84.

Li J-Y, Edelmann L, Jahn R, Dahlstriiml A (1996) Axonal Transport and Distribution of Synaptobrevin I and II in the Rat Peripheral Nervous System. J Neurosci 76:137–147.

Li M-X, Jia M, Yang L-X, Jiang H, Lanuza MA, Gonzalez CM, Nelson PG (2004) The role of the theta isoform of protein kinase C (PKC) in activity-dependent synapse elimination: evidence from the PKC theta knock-out mouse in vivo and in vitro. J Neurosci 24:3762–3769.

Lin RC, Scheller RH (2000) Mechanisms of synaptic vesicle exocytosis. Annu Rev Cell Dev Biol 16:19–49.

Lisman JE, Raghavachari S, Tsien RW (2007) The sequence of events that underlie quantal transmission at central glutamatergic synapses. Nat Rev Neurosci 8:597–609.

Littleton JT, Bellen HJ (1995) Presynaptic proteins involved in exocytosis in Drosophila melanogaster: a genetic analysis. Invert Neurosci 1:3–13.

Liu GS, Cohen M V., Mochly-Rosen D, Downey JM (1999) Protein Kinase C- ξ is Responsible for the Protection of Preconditioning in Rabbit Cardiomyocytes. J Mol Cell Cardiol 31:1937–1948.

Liu J, Ernst SA, Gladycheva SE, Lee YYF, Lentz SI, Ho CS, Li Q, Stuenkel EL (2004) Fluorescence resonance energy transfer reports properties of syntaxin1a interaction with Munc18-1 in vivo. J Biol Chem 279:55924–55936.

Lu B (2003) Pro-region of neurotrophins: role in synaptic modulation. Neuron 39:735–738.

Lu D, Yang H, Lenox RH, Raizada MK (1998) Regulation of angiotensin II-induced neuromodulation by MARCKS in brain neurons. J Cell Biol 142:217–227.

Luo JH, Kahn S, O'Driscoll K, Weinstein IB (1993) The regulatory domain of protein kinase C

beta 1 contains phosphatidylserine- and phorbol ester-dependent calcium binding activity. J Biol Chem 268:3715–3719.

Ma C, Li W, Xu Y, Rizo J (2011) Munc13 mediates the transition from the closed syntaxin-Munc18 complex to the SNARE complex. Nat Struct Mol Biol 18:542–549.

MacGillavry HD, Kerr JM, Blanpied TA (2011) Lateral organization of the postsynaptic density. Mol Cell Neurosci 48:321–331.

Maisonpierre PC, Le Beau MM, Espinosa R, Ip NY, Belluscio L, de la Monte SM, Squinto S, Furth ME, Yancopoulos GD (1991) Human and rat brain-derived neurotrophic factor and neurotrophin-3: gene structures, distributions, and chromosomal localizations. Genomics 10:558–568.

Majewski H, Iannazzo L (1998) Protein kinase C: a physiological mediator of enhanced transmitter output. Prog Neurobiol 55:463–475.

Mandolesi G, Vanni V, Cesa R, Grasselli G, Puglisi F, Cesare P, Strata P (2009) Distribution of the SNAP25 and SNAP23 synaptosomal-associated protein isoforms in rat cerebellar cortex. Neuroscience 164:1084–1096.

Mantilla CB, Ermilov LG (2012) The novel TrkB receptor agonist 7,8-dihydroxyflavone enhances neuromuscular transmission. Muscle Nerve 45:274–276.

Mantilla CB, Seven YB, Sieck GC (2014a) Convergence of Pattern Generator Outputs on a Common Mechanism of Diaphragm Motor Unit Recruitment. In: Progress in brain research, pp 309–329.

Mantilla CB, Stowe JM, Sieck DC, Ermilov LG, Greising SM, Zhang C, Shokat KM, Sieck GC (2014b) TrkB kinase activity maintains synaptic function and structural integrity at adult neuromuscular junctions. J Appl Physiol 117:910–920.

Mantilla CB, Zhan W-Z, Sieck GC (2004) Neurotrophins improve neuromuscular transmission in the adult rat diaphragm. Muscle Nerve 29:381–386.

Martyn JAJ, Fagerlund MJ, Eriksson LI (2009) Basic principles of neuromuscular transmission. Anaesthesia 64:1–9.

Matthews VB, Åström M-B, Chan MHS, Bruce CR, Krabbe KS, Prelovsek O, Åkerström T, Yfanti C, Broholm C, Mortensen OH, Penkowa M, Hojman P, Zankari A, Watt MJ, Bruunsgaard H, Pedersen BK, Febbraio MA (2009) Brain-derived neurotrophic factor is produced by skeletal muscle cells in response to contraction and enhances fat oxidation via activation of AMP-activated protein kinase. Diabetologia 52:1409–1418.

Medine CN, Rickman C, Chamberlain LH, Duncan RR (2007) Munc18-1 prevents the formation of ectopic SNARE complexes in living cells. J Cell Sci 120:4407–4415.

Middlemas DS, Lindberg RA, Hunter T (1991) trkB, a neural receptor protein-tyrosine kinase: evidence for a full-length and two truncated receptors. Mol Cell Biol 11:143–153.

Middlemas DS, Meisenhelder J, Hunter T (1994) Identification of TrkB autophosphorylation sites and evidence that phospholipase C-gamma 1 is a substrate of the TrkB receptor. J Biol Chem 269:5458–5466.

Miller TM, Heuser JE (1984) Endocytosis of synaptic vesicle membrane at the frog neuromuscular junction. J Cell Biol 98:685–698.

Milovanovic D, Jahn R (2015) Organization and dynamics of SNARE proteins in the presynaptic membrane. Front Physiol 6:89.

Misura KM, Scheller RH, Weis WI (2000) Three-dimensional structure of the neuronal-Sec1-syntaxin 1a complex. Nature 404:355–362.

Mitsui T, Ohshima H (2012) Theory of muscle contraction mechanism with -cooperative interaction among crossbridges. Biophysics (Oxf) 8:27–39.

Mohrmann R, de Wit H, Connell E, Pinheiro PS, Leese C, Bruns D, Davletov B, Verhage M, Sorensen JB (2013) Synaptotagmin Interaction with SNAP-25 Governs Vesicle Docking, Priming, and Fusion Triggering. J Neurosci 33:14417–14430.

Mohrmann R, Dhara M, Bruns D (2015) Complexins: small but capable. Cell Mol Life Sci 72:4221–4235.

Moraczewski J, Nowotniak A, Wróbel E, Castagna M, Gautron J, Martelly I (2002) Differential changes in protein kinase C associated with regeneration of rat extensor digitorum longus and soleus muscles. Int J Biochem Cell Biol 34:938–949.

Morgan A, Burgoyne RD, Barclay JW, Craig TJ, Prescott GR, Ciufo LF, Evans GJO, Graham ME (2005) Regulation of exocytosis by protein kinase C. Biochem Soc Trans 33:1341–1344.

Mosior M, McLaughlin S (1991) Peptides that mimic the pseudosubstrate region of protein kinase C bind to acidic lipids in membranes. Biophys J 60:149–159.

Mosior M, Newton AC (1995) Mechanism of interaction of protein kinase C with phorbol esters. Reversibility and nature of membrane association. J Biol Chem 270:25526–25533.

Mowla SJ, Farhadi HF, Pareek S, Atwal JK, Morris SJ, Seidah NG, Murphy RA (2001) Biosynthesis and post-translational processing of the precursor to brain-derived neurotrophic factor. J Biol Chem 276:12660–12666.

Munch AS, Kedar GH, van Weering JRT, Vazquez-Sanchez S, He E, André T, Braun T, Söllner TH, Verhage M, Sørensen JB (2016) Extension of Helix 12 in Munc18-1 Induces Vesicle Priming. J Neurosci 36.

Munson M, Chen X, Cocina AE, Schultz SM, Hughson FM (2000) Interactions within the yeast t-SNARE Sso1p that control SNARE complex assembly. Nat Struct Biol 7:894–902.

Murray LM, Talbot K, Gillingwater TH (2010) Review: neuromuscular synaptic vulnerability

in motor neurone disease: amyotrophic lateral sclerosis and spinal muscular atrophy. Neuropathol Appl Neurobiol 36:133–156.

Murthy VN, De Camilli P (2003) Cell biology of the presynaptic terminal. Annu Rev Neurosci 26:701–728.

Nadal L, Garcia N, Hurtado E, Simó A, Tomàs M, Lanuza MA, Cilleros V, Tomàs J (2017) Presynaptic Muscarinic Acetylcholine Receptors and TrkB Receptor Cooperate in the Elimination of Redundant Motor Nerve Terminals during Development. Front Aging Neurosci 9:24.

Nadal L, Garcia N, Hurtado E, Simó A, Tomàs M, Lanuza MA, Santafé M, Tomàs J (2016) Presynaptic muscarinic acetylcholine autoreceptors (M 1 , M 2 and M 4 subtypes), adenosine receptors (A 1 and A 2A) and tropomyosin-related kinase B receptor (TrkB) modulate the developmental synapse elimination process at the neuromuscular junction. Mol Brain 9.

Nagy G, Matti U, Nehring RB, Binz T, Rettig J, Neher E, Sørensen JB (2002) Protein kinase C-dependent phosphorylation of synaptosome-associated protein of 25 kDa at Ser187 potentiates vesicle recruitment. J Neurosci 22:9278–9286.

Neeper SA, Gómez-Pinilla F, Choi J, Cotman C (1995) Exercise and brain neurotrophins. Nature 373:109.

Neher E, Sakaba T (2008) Multiple Roles of Calcium Ions in the Regulation of Neurotransmitter Release. Neuron 59:861–872.

Newton AC (1993) Interaction of proteins with lipid headgroups: lessons from protein kinase C. Annu Rev Biophys Biomol Struct 22:1–25.

Newton AC (2001) Protein kinase C: structural and spatial regulation by phosphorylation, cofactors, and macromolecular interactions. Chem Rev 101:2353–2364.

Newton AC (2009) Lipid activation of protein kinases. J Lipid Res 50 Suppl:S266-71.

Nili U, de Wit H, Gulyas-Kovacs A, Toonen RF, Sørensen JB, Verhage M, Ashery U (2006) Munc18-1 phosphorylation by protein kinase C potentiates vesicle pool replenishment in bovine chromaffin cells. Neuroscience 143:487–500.

Nishizuka Y (1988) The molecular heterogeneity of protein kinase C and its implications for cellular regulation. Nature 334:661–665.

Numann R, Hauschka SD, Catterall WA, Scheuer T (1994) Modulation of skeletal muscle sodium channels in a satellite cell line by protein kinase C. J Neurosci 14:4226–4236.

Obis T, Besalduch N, Hurtado E, Nadal L, Santafe MM, Garcia N, Tomàs M, Priego M, Lanuza MA, Tomàs J (2015a) The novel protein kinase C epsilon isoform at the adult neuromuscular synapse: location, regulation by synaptic activity-dependent muscle contraction through TrkB signaling and coupling to ACh release. Mol Brain 8:8.

Obis T, Hurtado E, Nadal L, Tomàs M, Priego M, Simon A, Garcia N, Santafe MM, Lanuza MA, Tomàs J (2015b) The novel protein kinase C epsilon isoform modulates acetylcholine release in the rat neuromuscular junction. Mol Brain 8:80.

Ogata T (1988) Structure of motor endplates in the different fiber types of vertebrate skeletal muscles. Arch Histol Cytol.

Oliveira L, Costa AC, Noronha-Matos JB, Silva I, Cavalcante WLG, Timóteo MA, Corrado AP, Dal Belo CA, Ambiel CR, Alves-do-Prado W, Correia-de-Sá P (2015) Amplification of neuromuscular transmission by methylprednisolone involves activation of presynaptic facilitatory adenosine A2A receptors and redistribution of synaptic vesicles. Neuropharmacology 89:64–76.

Ono Y, Fujii T, Ogita K, Kikkawa U, Igarashi K, Nishizuka Y (1989) Protein kinase C zeta subspecies from rat brain: its structure, expression, and properties. Proc Natl Acad Sci U S A 86:3099–3103.

Oyler GA, Polli JW, Higgins GA, Wilson MC, Billingsley ML (1992) Distribution and expression of SNAP-25 immunoreactivity in rat brain, rat PC-12 cells and human SMS-KCNR neuroblastoma cells. Brain Res Dev Brain Res 65:133–146.

Padykula HA, Gauthier GF (1970) The ultrastructure of the neuromuscular junctions of mammalian red, white, and intermediate skeletal muscle fibers. J Cell Biol 46:27–41.

Palay SL, Palade GE (1955) The fine structure of neurons. J Biophys Biochem Cytol 1:69–88.

Pang PT, Teng HK, Zaitsev E, Woo NT, Sakata K, Zhen S, Teng KK, Yung W-H, Hempstead BL, Lu B (2004) Cleavage of proBDNF by tPA/plasmin is essential for long-term hippocampal plasticity. Science 306:487–491.

Parisotto D, Malsam J, Scheutzow A, Krause JM, Sollner TH (2012) SNAREpin Assembly by Munc18-1 Requires Previous Vesicle Docking by Synaptotagmin 1. J Biol Chem 287:31041–31049.

Parisotto D, Pfau M, Scheutzow A, Wild K, Mayer MP, Malsam J, Sinning I, Söllner TH (2014) An extended helical conformation in domain 3a of Munc18-1 provides a template for SNARE (soluble N-ethylmaleimide-sensitive factor attachment protein receptor) complex assembly. J Biol Chem 289:9639–9650.

Pattarawarapan M, Burgess K (2003) Molecular Basis of Neurotrophin−Receptor Interactions. J Med Chem 46:5277–5291.

Patton BL (2000) Laminins of the neuromuscular system. Microsc Res Tech 51:247–261.

Patton BL (2003) Basal lamina and the organization of neuromuscular synapses. J Neurocytol 32:883–903.

Perin MS, Brose N, Jahn R, Südhof TC (1991) Domain structure of synaptotagmin (p65). J Biol Chem 266:623–629.

Perkins GA, Wang L, Huang LJ, Humphries K, Yao VJ, Martone M, Deerinck TJ, Barraclough DM, Violin JD, Smith D, Newton A, Scott JD, Taylor SS, Ellisman MH (2001) PKA, PKC, and AKAP localization in and around the neuromuscular junction. BMC Neurosci 2:17.

Pertsinidis A, Mukherjee K, Sharma M, Pang ZP, Park SR, Zhang Y, Brunger AT, Südhof TC, Chu S (2013) Ultrahigh-resolution imaging reveals formation of neuronal SNARE/Munc18 complexes in situ. Proc Natl Acad Sci U S A 110:E2812-20.

Pevsner J, Hsu SC, Scheller RH (1994) n-Sec1: a neural-specific syntaxin-binding protein. Proc Natl Acad Sci U S A 91:1445–1449.

Pickering M, Jones JFX (2002) The diaphragm: two physiological muscles in one. J Anat 201:305–312.

Pitts EV, Potluri S, Hess DM, Balice-Gordon RJ (2006) Neurotrophin and Trk-mediated signaling in the neuromuscular system. Int Anesthesiol Clin 44:21–76.

Pobbati A V, Stein A, Fasshauer D (2006) N- to C-terminal SNARE complex assembly promotes rapid membrane fusion. Science (80-) 313:673–676.

Ponting CP, Parker PJ (1996) Extending the C2 domain family: C2s in PKCs delta, epsilon, eta, theta, phospholipases, GAPs, and perforin. Protein Sci 5:162–166.

Pozzi D, Condliffe S, Bozzi Y, Chikhladze M, Grumelli C, Proux-Gillardeaux V, Takahashi M, Franceschetti S, Verderio C, Matteoli M (2008) Activity-dependent phosphorylation of Ser187 is required for SNAP-25-negative modulation of neuronal voltage-gated calcium channels. Proc Natl Acad Sci U S A 105:323–328.

Puehringer D, Orel N, Lüningschrör P, Subramanian N, Herrmann T, Chao M V, Sendtner M (2013) EGF transactivation of Trk receptors regulates the migration of newborn cortical neurons. Nat Neurosci 16:407–415.

Quinn DM (1987) Acetylcholinesterase: enzyme structure, reaction dynamics, and virtual transition states. Chem Rev 87:955–979.

Radhakrishnan A, Stein A, Jahn R, Fasshauer D (2009) The Ca2+ affinity of synaptotagmin 1 is markedly increased by a specific interaction of its C2B domain with phosphatidylinositol 4,5-bisphosphate. J Biol Chem 284:25749–25760.

Rakowski RF, Gadsby DC, De Weer P (1989) Stoichiometry and voltage dependence of the sodium pump in voltage-clamped, internally dialyzed squid giant axon. J Gen Physiol 93:903–941.

Raptis A, Torrejón-Escribano B, Gómez de Aranda I, Blasi J (2005) Distribution of synaptobrevin/VAMP 1 and 2 in rat brain. J Chem Neuroanat 30:201–211.

Reichardt LF (2006) Neurotrophin-regulated signalling pathways. Philos Trans R Soc B Biol Sci 361:1545–1564.

Rhee JS, Betz A, Pyott S, Reim K, Varoqueaux F, Augustin I, Hesse D, Südhof TC, Takahashi

M, Rosenmund C, Brose N (2002) Beta phorbol ester- and diacylglycerol-induced augmentation of transmitter release is mediated by Munc13s and not by PKCs. Cell 108:121–133.

Richards DA, Guatimosim C, Rizzoli SO, Betz WJ (2003) Synaptic vesicle pools at the frog neuromuscular junction. Neuron 39:529–541.

Risinger C, Bennett MK (1999) Differential phosphorylation of syntaxin and synaptosome-associated protein of 25 kDa (SNAP-25) isoforms. J Neurochem 72:614–624.

Rizo J, Rosenmund C (2008) Synaptic vesicle fusion. Nat Struct Mol Biol 15:665–674.

Rizo J, Südhof TC (2002) Snares and Munc18 in synaptic vesicle fusion. Nat Rev Neurosci 3:641–653.

Rizo J, Südhof TC (2012) The membrane fusion enigma: SNAREs, Sec1/Munc18 proteins, and their accomplices--guilty as charged? Annu Rev Cell Dev Biol 28:279–308.

Rizo J, Udhof TC (2012) The Membrane Fusion Enigma: SNAREs, Sec1/Munc18 Proteins, and Their Accomplices—Guilty as Charged? Annu Rev Cell Dev Biol 28:279–308.

Rizo J, Xu J (2015) The Synaptic Vesicle Release Machinery. Annu Rev Biophys 44:339–367.

Rizzoli SO (2014) Synaptic vesicle recycling: steps and principles. EMBO J 33:788–822.

Rizzoli SO, Betz WJ (2005) Synaptic vesicle pools. Nat Rev Neurosci 6:57–69.

Rodkey TL, Liu S, Barry M, McNew JA (2008) Munc18a Scaffolds SNARE Assembly to Promote Membrane Fusion. Mol Biol Cell 19:5422–5434.

Rosato Siri MD, Uchitel OD (1999) Calcium channels coupled to neurotransmitter release at neonatal rat neuromuscular junctions. J Physiol 514 (Pt 2:533–540.

Rose CR, Blum R, Pichler B, Lepier A, Kafitz KW, Konnerth A (2003) Truncated TrkB-T1 mediates neurotrophin-evoked calcium signalling in glia cells. Nature 426:74–78.

Rossetto O, Pirazzini M, Montecucco C (2014) Botulinum neurotoxins: genetic, structural and mechanistic insights. Nat Rev Microbiol 12:535–549.

Rotundo RL (2003) Expression and localization of acetylcholinesterase at the neuromuscular junction. J Neurocytol 32:743–766.

Saheki Y, De Camilli P (2012) Synaptic Vesicle Endocytosis. Cold Spring Harb Perspect Biol 4:a005645–a005645.

Salpeter MM, Loring RH (1985) Nicotinic acetylcholine receptors in vertebrate muscle: properties, distribution and neural control. Prog Neurobiol 25:297–325.

Sanes JR, Lichtman JW (1999) Development of the Vertebrate Neuromuscular Junction.

Annu Rev Neurosci 22:389–442.

Sanes JR, Lichtman JW (2001) Development: Induction, assembly, maturation and maintenance of a postsynaptic apparatus. Nat Rev Neurosci 2:791–805.

Santafé M, Lanuza MA, Garcia N, Tomàs J (2006) Muscarinic autoreceptors modulate transmitter release through protein kinase C and protein kinase A in the rat motor nerve terminal. Eur J Neurosci 23:2048–2056.

Santafé MM, Garcia N, Lanuza MA, Tomàs J (2007a) Protein kinase C activity affects neurotransmitter release at polyinnervated neuromuscular synapses. J Neurosci Res.

Santafé MM, Garcia N, Lanuza MA, Tomàs M, Tomàs J (2009) Interaction between protein kinase C and protein kinase A can modulate transmitter release at the rat neuromuscular synapse. J Neurosci Res 87:683–690.

Santafé MM, Garcia N, Lanuza MA, Uchitel OD, Tomás J (2001) Calcium channels coupled to neurotransmitter release at dually innervated neuromuscular junctions in the newborn rat. Neuroscience.

Santafé MM, Garcia N, Tomàs M, Obis T, Lanuza MA, Besalduch N, Tomàs J (2014) The interaction between tropomyosin-related kinase B receptors and serine kinases modulates acetylcholine release in adult neuromuscular junctions. Neurosci Lett 561:171–175.

Santafé MM, Lanuza MA, Garcia N, Tomàs J (2005) Calcium inflow-dependent protein kinase C activity is involved in the modulation of transmitter release in the neuromuscular junction of the adult rat. Synapse 57:76–84.

Santafé MM, Lanuza MA, Garcia N, Tomàs M, Tomàs J (2007b) Coupling of presynaptic muscarinic autoreceptors to serine kinases in low and high release conditions on the rat motor nerve terminal. Neuroscience.

Santafe MM, Priego M, Obis T, Garcia N, Tomàs M, Lanuza MA, Tomàs J (2015) Adenosine receptors and muscarinic receptors cooperate in acetylcholine release modulation in the neuromuscular synapse. Eur J Neurosci.

Schechtman D, Mochly-Rosen D (2001) Adaptor proteins in protein kinase C-mediated signal transduction. Oncogene 20:6339–6347.

Schinder A (2000) The neurotrophin hypothesis for synaptic plasticity. Trends Neurosci 23:639–645.

Segal RA (2003) Selectivity in neurotrophin signaling: theme and variations. Annu Rev Neurosci 26:299–330.

Segal RA, Bhattacharyya A, Rua LA, Alberta JA, Stephens RM, Kaplan DR, Stiles CD (1996) Differential utilization of Trk autophosphorylation sites. J Biol Chem 271:20175–20181.

Seidah NG, Benjannet S, Pareek S, Chrétien M, Murphy RA (1996) Cellular processing of the neurotrophin precursors of NT3 and BDNF by the mammalian proprotein convertases. FEBS Lett 379:247–250.

Sharkey NA, Leach KL, Blumberg PM (1984) Competitive inhibition by diacylglycerol of specific phorbol ester binding. Proc Natl Acad Sci U S A 81:607–610.

Shen J, Tareste DC, Paumet F, Rothman JE, Melia TJ (2007) Selective Activation of Cognate SNAREpins by Sec1/Munc18 Proteins. Cell.

Shimazaki Y, Nishiki T, Omori A, Sekiguchi M, Kamata Y, Kozaki S, Takahashi M (1996) Phosphorylation of 25-kDa synaptosome-associated protein. Possible involvement in protein kinase C-mediated regulation of neurotransmitter release. J Biol Chem 271:14548–14553.

Shirai Y, Adachi N, Saito N (2008) Protein kinase Cepsilon: function in neurons. FEBS J 275:3988–3994.

Siksou L, Varoqueaux F, Pascual O, Triller A, Brose N, Marty S (2009) A common molecular basis for membrane docking and functional priming of synaptic vesicles. Eur J Neurosci 30:49–56.

Sine SM (2012) End-plate acetylcholine receptor: structure, mechanism, pharmacology, and disease. Physiol Rev 92:1189–1234.

Slater CR (2008) Reliability of neuromuscular transmission and how it is maintained. Handb Clin Neurol 91:27–101.

Smith IW, Mikesh M, Lee Y il, Thompson WJ (2013) Terminal Schwann cells participate in the competition underlying neuromuscular synapse elimination. J Neurosci 33:17724–17736.

Smyth AM, Duncan RR, Rickman C (2010) Munc18-1 and Syntaxin1: Unraveling the Interactions Between the Dynamic Duo. Cell Mol Neurobiol 30:1309–1313.

Snyder DA, Kelly ML, Woodbury DJ (2006) SNARE complex regulation by phosphorylation. Cell Biochem Biophys 45:111–123.

Sommerfeld MT, Schweigreiter R, Barde YA, Hoppe E (2000) Down-regulation of the neurotrophin receptor TrkB following ligand binding. Evidence for an involvement of the proteasome and differential regulation of TrkA and TrkB. J Biol Chem 275:8982–8990.

Sons MS, Verhage M, Plomp JJ (2003). Role of Munc18-1 in synaptic plasticity at the myasthenic neuromuscular junction. Ann N Y Acad Sci. 998:404-6.

Sørensen JB (2009) Conflicting Views on the Membrane Fusion Machinery and the Fusion Pore. Annu Rev Cell Dev Biol 25:513–537.

Sørensen JB, Nagy G, Varoqueaux F, Nehring RB, Brose N, Wilson MC, Neher E (2003)

Differential control of the releasable vesicle pools by SNAP-25 splice variants and SNAP-23. Cell 114:75–86.

Stebbins EG, Mochly-Rosen D (2001) Binding specificity for RACK1 resides in the V5 region of beta II protein kinase C. J Biol Chem 276:29644–29650.

Stein A, Weber G, Wahl MC, Jahn R (2009) Helical extension of the neuronal SNARE complex into the membrane. Nature 460:525–528.

Steinberg SF (2008) Structural basis of protein kinase C isoform function. Physiol Rev 88:1341–1378.

Stoilov P, Castren E, Stamm S (2002) Analysis of the Human TrkB Gene Genomic Organization Reveals Novel TrkB Isoforms, Unusual Gene Length, and Splicing Mechanism. Biochem Biophys Res Commun 290:1054–1065.

Südhof TC (2004) The synaptic vesicle cycle. Annu Rev Neurosci 27:509–547.

Südhof TC (2012) The presynaptic active zone. Neuron 75:11–25.

Südhof TC (2013) A molecular machine for neurotransmitter release: synaptotagmin and beyond. Nat Med 19:1227–1231.

Südhof TC, Rizo J (2011) Synaptic vesicle exocytosis. Cold Spring Harb Perspect Biol 3:a005637.

Südhof TC, Rothman JE (2009) Membrane fusion: grappling with SNARE and SM proteins. Science 323:474–477.

Sutton RB, Fasshauer D, Jahn R, Brunger AT (1998) Crystal structure of a SNARE complex involved in synaptic exocytosis at 2.4 A resolution. Nature 395:347–353.

Takai Y, Kishimoto A, Kikkawa U, Mori T, Nishizuka Y (1979) Unsaturated diacylglycerol as a possible messenger for the activation of calcium-activated, phospholipid-dependent protein kinase system. Biochem Biophys Res Commun 91:1218–1224.

Takamori S et al. (2006) Molecular Anatomy of a Trafficking Organelle. Cell 127:831–846.

Tanaka C, Nishizuka Y (1994) The protein kinase C family for neuronal signaling. Annu Rev Neurosci 17:551–567.

Terrian DM, White MK (1997) Phylogenetic analysis of membrane trafficking proteins: a family reunion and secondary structure predictions. Eur J Cell Biol 73:198–204.

Thomas SM, DeMarco M, D'Arcangelo G, Halegoua S, Brugge JS (1992) Ras is essential for nerve growth factor- and phorbol ester-induced tyrosine phosphorylation of MAP kinases. Cell 68:1031–1040.

Tomas J, Lanuza MA, Santafé M, Fenoll-Brunet MR, Garcia N (2000) Topological differences

along mammalian motor nerve terminals for spontaneous and alpha-bungarotoxin-induced sprouting. Histol Histopathol 15:43–52.

Tomàs J, Santafé MM, Garcia N, Lanuza MA, Tomàs M, Besalduch N, Obis T, Priego M, Hurtado E (2014) Presynaptic membrane receptors in acetylcholine release modulation in the neuromuscular synapse. J Neurosci Res.

Toonen RF, Verhage M (2007) Munc18-1 in secretion: lonely Munc joins SNARE team and takes control. Trends Neurosci 30:564–572.

Toonen RF, Wierda K, Sons MS, de Wit H, Cornelisse LN, Brussaard A, Plomp JJ, Verhage M. (2006) Munc18-1 expression levels control synapse recovery by regulating readily releasable pool size. Proc Natl Acad Sci U S A. 28;103(48):18332-7.

Trimbuch T, Rosenmund C (2016) Should I stop or should I go? The role of complexin in neurotransmitter release. Nat Rev Neurosci 17:118–125.

Tsuboi T, Fukuda M (2005) The C2B Domain of Rabphilin Directly Interacts with SNAP-25 and Regulates the Docking Step of Dense Core Vesicle Exocytosis in PC12 Cells. J Biol Chem 280:39253–39259.

Ultsch MH, Wiesmann C, Simmons LC, Henrich J, Yang M, Reilly D, Bass SH, de Vos AM (1999) Crystal structures of the neurotrophin-binding domain of TrkA, TrkB and TrkC. J Mol Biol 290:149–159.

Urbano FJ, Piedras-Renteria ES, Jun K, Shin H-S, Uchitel OD, Tsien RW (2003) Altered properties of quantal neurotransmitter release at endplates of mice lacking P/Q-type Ca2+ channels. Proc Natl Acad Sci 100:3491–3496.

Urfer R, Tsoulfas P, O'Connell L, Shelton DL, Parada LF, Presta LG (1995) An immunoglobulin-like domain determines the specificity of neurotrophin receptors. EMBO J 14:2795–2805.

van den Bogaart G, Thutupalli S, Risselada JH, Meyenberg K, Holt M, Riedel D, Diederichsen U, Herminghaus S, Grubmüller H, Jahn R (2011) Synaptotagmin-1 may be a distance regulator acting upstream of SNARE nucleation. Nat Struct Mol Biol 18:805–812.

van Praag H, Kempermann G, Gage FH (1999) Running increases cell proliferation and neurogenesis in the adult mouse dentate gyrus. Nat Neurosci 2:266–270.

Vaughan PF, Walker JH, Peers C (1998) The regulation of neurotransmitter secretion by protein kinase C. Mol Neurobiol 18:125–155.

Vaynman SS, Ying Z, Yin D, Gomez-Pinilla F (2006) Exercise differentially regulates synaptic proteins associated to the function of BDNF. Brain Res 1070:124–130.

Verhage M, Maia AS, Plomp JJ, Brussaard AB, Heeroma JH, Vermeer H, Toonen RF, Hammer RE, van den Berg TK, Missler M, Geuze HJ, Südhof TC (2000) Synaptic assembly of the brain in the absence of neurotransmitter secretion. Science 287:864–869.

Verhage M, Sørensen JB (2008) Vesicle docking in regulated exocytosis. Traffic 9:1414–1424.

Vetter ML, Martin-Zanca D, Parada LF, Bishop JM, Kaplan DR (1991) Nerve growth factor rapidly stimulates tyrosine phosphorylation of phospholipase C-gamma 1 by a kinase activity associated with the product of the trk protooncogene. Proc Natl Acad Sci U S A 88:5650–5654.

Wang T, Xie K, Lu B (1995) Neurotrophins promote maturation of developing neuromuscular synapses. J Neurosci 15:4796–4805.

Watanabe S, Liu Q, Davis MW, Hollopeter G, Thomas N, Jorgensen NB, Jorgensen EM (2013a) Ultrafast endocytosis at Caenorhabditis elegans neuromuscular junctions. Elife 2:e00723.

Watanabe S, Rost BR, Camacho-Pérez M, Davis MW, Söhl-Kielczynski B, Rosenmund C, Jorgensen EM (2013b) Ultrafast endocytosis at mouse hippocampal synapses. Nature 504:242–247.

Waters MG, Hughson FM (2000) Membrane tethering and fusion in the secretory and endocytic pathways. Traffic 1:588–597.

Watson FL, Porcionatto MA, Bhattacharyya A, Stiles CD, Segal RA (1999) TrkA glycosylation regulates receptor localization and activity. J Neurobiol 39:323–336.

Ways DK, Cook PP, Webster C, Parker PJ (1992) Effect of phorbol esters on protein kinase C-zeta. J Biol Chem 267:4799–4805.

Weber T, Zemelman B V, McNew JA, Westermann B, Gmachl M, Parlati F, Söllner TH, Rothman JE (1998) SNAREpins: minimal machinery for membrane fusion. Cell 92:759–772.

Weinberger A, Gerst JE (2004) Regulation of SNARE assembly by protein phosphorylation.

Weninger K, Bowen ME, Choi UB, Chu S, Brunger AT (2008) Accessory Proteins Stabilize the Acceptor Complex for Synaptobrevin, the 1:1 Syntaxin/SNAP-25 Complex. Structure 16:308–320.

West J, Numann R, Murphy B, Scheuer T, Catterall W (1991) A phosphorylation site in the Na+ channel required for modulation by protein kinase C. Science (80-) 254:866–868.

Wilhelm BG, Mandad S, Truckenbrodt S, Kröhnert K, Schäfer C, Rammner B, Koo SJ, Claßen GA, Krauss M, Haucke V, Urlaub H, Rizzoli SO (2014) Composition of isolated synaptic boutons reveals the amounts of vesicle trafficking proteins. Science 344:1023–1028.

Windisch JM, Auer B, Marksteiner R, Lang ME, Schneider R (1995) Specific neurotrophin binding to leucine-rich motif peptides of TrkA and TrkB. FEBS Lett 374:125–129.

Wood SJ, Slater CR (2001) Safety factor at the neuromuscular junction. Prog Neurobiol

64:393–429.

Wu-zhang AX, Newton AC (2013) Protein kinase C pharmacology: refining the toolbox. Biochem J 452:195–209.

Xu T, Rammner B, Margittai M, Artalejo AR, Neher E, Jahn R (1999) Inhibition of SNARE complex assembly differentially affects kinetic components of exocytosis. Cell 99:713–722.

Xu Y, Su L, Rizo J (2010) Binding of Munc18-1 to synaptobrevin and to the SNARE four-helix bundle. Biochemistry 49:1568–1576 Available at: http://www.pubmedcentral.nih.gov/articlerender.fcgi?artid=PMC2834481.

Xu Z-B, Chaudhary D, Olland S, Wolfrom S, Czerwinski R, Malakian K, Lin L, Stahl ML, Joseph-McCarthy D, Benander C, Fitz L, Greco R, Somers WS, Mosyak L (2004) Catalytic domain crystal structure of protein kinase C-theta (PKCtheta). J Biol Chem 279:50401–50409.

Xue M, Reim K, Chen X, Chao H-T, Deng H, Rizo J, Brose N, Rosenmund C (2007) Distinct domains of complexin I differentially regulate neurotransmitter release. Nat Struct Mol Biol 14:949–958.

Xue M, Stradomska A, Chen H, Brose N, Zhang W, Rosenmund C, Reim K (2008) Complexins facilitate neurotransmitter release at excitatory and inhibitory synapses in mammalian central nervous system. Proc Natl Acad Sci U S A 105:7875–7880.

Yang B, Steegmaier M, Gonzalez LC, Scheller RH (2000) nSec1 binds a closed conformation of syntaxin1A. J Cell Biol 148:247–252.

Yang X, Wang S, Sheng Y, Zhang M, Zou W, Wu L, Kang L, Rizo J, Zhang R, Xu T, Ma C (2015) Syntaxin opening by the MUN domain underlies the function of Munc13 in synaptic-vesicle priming. Nat Struct Mol Biol 22:547–554.

Yang Y, Craig TJ, Chen X, Ciufo LF, Takahashi M, Morgan A, Gillis KD (2007) Phosphomimetic mutation of Ser-187 of SNAP-25 increases both syntaxin binding and highly Ca2+-sensitive exocytosis. J Gen Physiol 129:233–244.

Yedovitzky M, Mochly-Rosen D, Johnson JA, Gray MO, Ron D, Abramovitch E, Cerasi E, Nesher R (1997) Translocation inhibitors define specificity of protein kinase C isoenzymes in pancreatic beta-cells. J Biol Chem 272:1417–1420.

Yoon T-Y, Lu X, Diao J, Lee S-M, Ha T, Shin Y-K (2008) Complexin and Ca2+ stimulate SNARE-mediated membrane fusion. Nat Struct Mol Biol 15:707–713.

Yoshihara M, Littleton JT (2002) Synaptotagmin I functions as a calcium sensor to synchronize neurotransmitter release. Neuron 36:897–908.

Zaccaro MC, Ivanisevic L, Perez P, Meakin SO, Saragovi HU (2001) p75 Co-receptors regulate ligand-dependent and ligand-independent Trk receptor activation, in part by altering Trk docking subdomains. J Biol Chem 276:31023–31029.

Zamponi GW, Bourinet E, Nelson D, Nargeot J, Snutch TP (1997) Crosstalk between G proteins and protein kinase C mediated by the calcium channel α1 subunit. Nature 385:442–446.

Zhang X, Kim-Miller MJ, Fukuda M, Kowalchyk JA, Martin TFJ (2002) Ca2+-dependent synaptotagmin binding to SNAP-25 is essential for Ca2+-triggered exocytosis. Neuron 34:599–611.

Zhang Y, Ying J, Jiang D, Chang Z, Li H, Zhang G, Gong S, Jiang X, Tao J (2015) Urotensin-II receptor stimulation of cardiac L-type Ca2+ channels requires the βγ subunits of Gi/o-protein and phosphatidylinositol 3-kinase-dependent protein kinase C β1 isoform. J Biol Chem 290:8644–8655.

Zhao L, Sheng A-L, Huang S-H, Yin Y-X, Chen B, Li X-Z, Zhang Y, Chen Z-Y (2009) Mechanism underlying activity-dependent insertion of TrkB into the neuronal surface. J Cell Sci 122:3123–3136.

Zhou L, McInnes J, Verstreken P (2014) Ultrafast synaptic endocytosis cycles to the center stage. Dev Cell 28:5–6.

Zoladz JA, Pilc A (2010) The effect of physical activity on the brain derived neurotrophic factor: from animal to human studies. J Physiol Pharmacol 61:533–541.

Zong Y, Jin R (2013) Structural mechanisms of the agrin-LRP4-MuSK signaling pathway in neuromuscular junction differentiation. Cell Mol life Sci 70:3077–3088.

UNIVERSITAT ROVIRA I VIRGILI
EFFECTS OF NEUROMUSCULAR ACTIVITY COUPLED TO BDNF/TRKB SIGNALING ON THE EXOCYTOTIC PROTEINS MUNC18-1 AND SNAP-25 THROUGH NPKCE AND CPKCSSI
Anna Simó Ollé

VIII. SCIENTIFIC CONTRIBUTIONS

UNIVERSITAT ROVIRA I VIRGILI
EFFECTS OF NEUROMUSCULAR ACTIVITY COUPLED TO BDNF/TRKB SIGNALING ON THE EXOCYTOTIC PROTEINS MUNC18-1 AND SNAP-25 THROUGH NPKCE AND CPKCSSI
Anna Simó Ollé

SCIENTIFIC ARTICLES

Scientific Articles belonging to this Doctoral Thesis:

Simó A, Hurtado E, Cilleros V, Just L, Nadal L, Tomàs M, Garcia N Lanuza MA, Tomàs J. (2017). "Synaptic activity induced BDNF/TrkB/PKC signalling controls the phosphorylation of the exocytotic protein Munc18-1 at the neuromuscular junction". Manuscript in preparation.

Simó A, Hurtado E, Cilleros V, Just L, Nadal L, Tomàs M, Garcia N Lanuza MA, Tomàs J. (2017). "Protein Kinase C phosphorylation of SNAP-25 on Ser-187 is induced by synaptic activity and is mediated by the nPKCε isoform". Manuscript in preparation.

Other scientific Articles:

Hurtado E, Cilleros V, Just L, **Simó A**, Nadal L, Tomàs M, Garcia N Lanuza MA, Tomàs J. (2017). "Synaptic activity and muscle contraction increases PDK1 and PKCβI phosphorylation in the presynaptic membrane of the neuromuscular junction". Frontiers in Molecular Neuroscience. DOI: 10.3389/fnmol.2017.00270.

Hurtado E, Cilleros V, Nadal L, **Simó A**, Obis T, Garcia N, Santafé MM, Tomàs M, Halievski K, Jordan C, Lanuza MA, Tomàs J. (2017). "Muscle contraction regulates BDNF/TrkB signaling to retrogradely modulate synaptic function through presynaptic cPKCα and cPKCβI". Frontiers in Molecular Neuroscience. DOI: 10.3389/fnmol.2017.00147.

Tomàs J, Garcia N, Lanuza MA, Nadal L, Tomàs M, Hurtado E, Cilleros V, **Simó A**. (2017). Membrane receptor-induced changes of the protein kinases A and C activity may play a leading role in promoting developmental synapse elimination at the neuromuscular junction. Frontiers in Molecular Neuroscience. DOI: 10.3389/fnmol.2017.00255.

Tomàs J, Garcia N, Lanuza MA, Santafé MM, Tomàs M, Nadal L, Hurtado E, **Simó A**, Cilleros V. (2017). "Presynaptic membrane receptors modulate ACh release, axonal competition and synapse elimination during neuromuscular junction development". Frontiers in Molecular Neuroscience, DOI: 10.3389/fnmol.2017.00132.

Nadal L, Garcia N, Hurtado E, **Simó A**, Tomàs M, Lanuza MA, Cilleros V, Tomàs J. (2017). "Presynaptic muscarinic acetylcholine receptors and TrkB receptor cooperate in the elimination of redundant motor nerve terminals during development". Frontiers in Aging Neuroscience, 9:24. DOI: 10.3389/fnagi.2017.00024.

Nadal L, Garcia N, Hurtado E, **Simó A**, Tomàs M, Lanuza MA, Cilleros V, Tomàs J. (2017). "Synergistic action of presynaptic muscarinic acetylcholine receptors and adenosine receptors in developmental axonal competition at the neuromuscular junction". Developmental Neuroscience, DOI: 10.1159/000458437.

Nadal L, Garcia N, Hurtado E, **Simó A**, Tomàs M, Lanuza MA, Santafé MM, Tomàs J. (2016). "Presynaptic muscarinic acetylcholine autoreceptors (M1, M2 and M4 subtypes), adenosine receptors (A1 and A2A) and tropomyosin-related kinase B receptor (TrkB) modulate the developmental synapse elimination process at the neuromuscular junction". Molecular Brain, 23;9(1):67. DOI: 10.1186/s13041-016-0248-9.

Obis T, Hurtado E, Nadal N, Tomàs M, **Simón A**, Garcia N, Santafé MM, Lanuza MA, Tomàs J. (2015). "The novel protein kinase C epsilon isoform modulates acetylcholine release in the rat neuromuscular junction". Molecular Brain, 8(1):80. DOI: 10.1186/s13041-015-0171-5.

PARTICIPATION IN NATIONAL AND INTERNATIONAL CONGRESSES

Congress: 17th National Congress of the Spanish Society for Neuroscience (SENC).

Date and Place: 27-30 September 2017; Alicante (Spain).

Authors: Anna Simó, Erica Hurtado, Víctor Cilleros, Laia Just, Laura Nadal, Manel Santafé, Marta Tomàs, Neus Garcia, Maria Angel Lanuza and Josep Tomàs.

Title: nPKCε and cPKCβI modulate the synaptic activity induced phosphorylation of the exocytotic protein Munc18-1 at the adult neuromuscular junction.

Format: Poster.

Congress: 17th National Congress of the Spanish Society for Neuroscience (SENC).

Date and Place: 27-30 September 2017; Alicante (Spain).

Authors: Erica Hurtado, Laia Just, Víctor Cilleros, **Anna Simó**, Laura Nadal, Olivier Biondi, Frédéric Charbonnier, Neus Garcia, Maria Angel Lanuza, and Josep Tomàs.

Title: Physical exercise improves BDNF/TrkB/PKCβI signaling pathway in a mouse model of amyotrophic lateral sclerosis.

Format: Poster.

Congress: 17th National Congress of the Spanish Society for Neuroscience (SENC).

Date and Place: 27-30 September 2017; Alicante (Spain).

Authors: Víctor Cilleros, Erica Hurtado, **Anna Simó**, Laia Just, Laura Nadal, Manel Santafé, Marta Tomàs, Neus Garcia, Maria Angel Lanuza, Josep Tomàs.

Title: PKA and PKC isoforms are differentially modulated by M1 and M2 muscarinic autoreceptor subtypes to influence SNAP25 and Munc18-1 phosphorylation in the neuromuscular synapse.

Format: Poster.

Congress: X Symposium of Neurobiology.

Date and Place: 6-7 October 2016; Barcelona (Spain).

Authors: Anna Simó, Erica Hurtado, Víctor Cilleros, Laura Nadal, Neus Garcia, Manel Santafé, Marta Tomàs, Maria Angel Lanuza and Josep Tomàs.

Title: BDNF-TrkB-PKC signaling modulated by synaptic activity controls the phosphorylation of the exocytotic proteins Munc18-1 and SNAP25 at the neuromuscular junction.

Format: Poster.

Congress: X Symposium of Neurobiology.

Date and Place: 6-7 October 2016; Barcelona (Spain).

Authors: Erica Hurtado, Víctor Cilleros, Laura Nadal, Teresa Obis, **Anna Simó**, Neus Garcia, Manel Santafé, Marta Tomàs, Maria Angel Lanuza and Josep Tomàs.

Title: Synaptic activity-modulated BDNF-TrkB pathway enhances presynaptic cPKCβI to control neuromuscular synaptic function.

Format: Poster.

Congress: X Symposium of Neurobiology.

Date and Place: 6-7 October 2016; Barcelona (Spain).

Authors: Víctor Cilleros, Erica Hurtado, Laura Nadal, Teresa Obis, **Anna Simó**, Neus Garcia, Manel Santafé, Marta Tomàs, Maria Angel Lanuza and Josep Tomàs.

Title: Synaptic activity-modulated BDNF-TrkB pathway enhances presynaptic cPKCβI to control neuromuscular synaptic function.

Format: Oral communication (Víctor Cilleros)

Congress: X Symposium of Neurobiology.

Date and Place: 6-7 October 2016; Barcelona (Spain).

Authors: Laura Nadal, Neus Garcia, Erica Hurtado, **Anna Simó**, Víctor Cilleros, Laia Just, Marta Tomàs, Maria Angel Lanuza, Manel Santafé, and Josep Tomàs.

Title: Adenosine receptors, mAChRs and TrkB modulate the developmental synapse elimination process at the neuromuscular junction.

Format: Poster.

Congress: 10th FENS Forum of Neuroscience.

Date and Place: 2-6 July 2016; Copenhagen (Denmark).

Authors: Anna Simó, Erica Hurtado, Víctor Cilleros, Laura Nadal, Neus Garcia, Manel Santafé, Marta Tomàs, Maria Angel Lanuza and Josep Tomàs.

Title: BDNF-TrkB-PKC signaling modulated by synaptic activity controls the phosphorylation of the exocytotic proteins Munc18-1 and SNAP25 at the neuromuscular junction.

Format: Poster

Congress: 10th FENS Forum of Neuroscience.

Date and Place: 2-6 July 2016; Copenhagen (Denmark).

Authors: Erica Hurtado, Víctor Cilleros, Laura Nadal, Teresa Obis, **Anna Simó**, Neus Garcia, Manel Santafé, Marta Tomàs, Maria Angel Lanuza and Josep Tomàs.

Title: Synaptic activity-modulated BDNF-TrkB pathway enhances presynaptic cPKCβI to control neuromuscular synaptic function.

Format: Poster.

Congress: 10th FENS Forum of Neuroscience.

Date and Place: 2-6 July 2016; Copenhagen (Denmark).

Authors: Laura Nadal, Neus Garcia, Erica Hurtado, **Anna Simó**, Víctor Cilleros, Marta Tomàs, Maria Angel Lanuza, Manel Santafé, and Josep Tomàs.

Title: Muscarinic acetylcholine autoreceptors, adenosine receptors and tropomyosin-related kinase B receptor (TrkB) cooperate in the developmental axonal loss and synapse elimination process at the neuromuscular junction.

Format: Poster.

Congress: Society for Neuroscience (SfN)

Date and Place: 17-21 October 2015; Chicago (USA).

Authors: Maria Angel Lanuza, Erica Hurtado, Laura Nadal, Teresa Obis, **Anna Simó**, Víctor Cilleros, Neus Garcia, Manel M. Santafé, Marta Tomàs, Josep Tomàs.

Title: BDNF and TrkB are regulated by both pre- and postsynaptic activity and enhance presynaptic cPKC-betaI to modulate neuromuscular synaptic function.

Format: Poster.

Congress: 16th National Congress of the Spanish Society for Neuroscience (SENC).

Date and Place: 23-25 September 2015; Granada (Spain).

Authors: Anna Simó, Erica Hurtado, Laura Nadal, Víctor Cilleros, Neus Garcia, Manel Santafé, Marta Tomàs, Maria Angel Lanuza, and Josep Tomàs.

Title: Synaptic activity and PKC-TrkB signaling modulates the phosphorylation of the exocytotic proteins SNAP-25 and Munc18-1 at adult neuromuscular junction.

Format: Poster.

Congress: 16th National Congress of the Spanish Society for Neuroscience (SENC).

Date and Place: 23-25 September 2015; Granada (Spain).

Authors: Erica Hurtado, Laura Nadal, Teresa Obis, **Anna Simó**, Víctor Cilleros, Neus Garcia, Manel Santafé, Marta Tomàs, Maria Angel Lanuza, and Josep Tomàs.

Title: BDNF and TrkB are regulated by both pre- and postsynaptic activity and enhance presynaptic cPKCβI to modulate neuromuscular synaptic function.

Format: Poster.

Congress: 16th National Congress of the Spanish Society for Neuroscience (SENC).

Date and Place: 23-25 September 2015; Granada (Spain).

Authors: Laura Nadal, Neus Garcia, Erica Hurtado, **Anna Simó**, Marta Tomàs, Maria Angel Lanuza, Manel Santafé, and Josep Tomàs.

Title: Presynaptic muscarinic acetylcholine autoreceptors (M_1, M_2 and M_4 subtypes) modulate the developmental synapse elimination process on the neuromuscular junction.

Format: Poster.

UNIVERSITAT ROVIRA I VIRGILI
EFFECTS OF NEUROMUSCULAR ACTIVITY COUPLED TO BDNF/TRKB SIGNALING ON THE EXOCYTOTIC PROTEINS MUNC18-1 AND SNAP-25 THROUGH NPKCE AND CPKCSSI
Anna Simó Ollé

UNIVERSITAT ROVIRA I VIRGILI
EFFECTS OF NEUROMUSCULAR ACTIVITY COUPLED TO BDNF/TRKB SIGNALING ON THE EXOCYTOTIC PROTEINS MUNC18-1 AND SNAP-25 THROUGH NPKCE AND CPKCSSI
Anna Simó Ollé

UNIVERSITAT
ROVIRA i VIRGILI